DTIC FILE COPY

(1)

SECURITY CLASSIFICATION OF THIS PAGE

REPORT DOCUMENTATION PAGE

Form Approved OMB No. 0704-0188

AD-A221 272

1b. RESTRICTIVE MARKINGS
NONE

3. DISTRIBUTION/AVAILABILITY OF REPORT
APPROVED FOR PUBLIC RELEASE; DISTRIBUTION UNLIMITED.

4. PERFORMING ORGANIZATION REPORT NUMBER(S)

5. MONITORING ORGANIZATION REPORT NUMBER(S)
AFIT/CI/CIA-90-002

6a. NAME OF PERFORMING ORGANIZATION
AFIT STUDENT AT Rochester Institute of Technology

6b. OFFICE SYMBOL (If applicable)

7a. NAME OF MONITORING ORGANIZATION
AFIT/CIA

6c. ADDRESS (City, State, and ZIP Code)

7b. ADDRESS (City, State, and ZIP Code)
Wright-Patterson AFB OH 45433-6583

8a. NAME OF FUNDING/SPONSORING ORGANIZATION

8b. OFFICE SYMBOL (If applicable)

9. PROCUREMENT INSTRUMENT IDENTIFICATION NUMBER

8c. ADDRESS (City, State, and ZIP Code)

10. SOURCE OF FUNDING NUMBERS

PROGRAM ELEMENT NO.	PROJECT NO.	TASK NO.	WORK UNIT ACCESSION NO.

11. TITLE (Include Security Classification) (UNCLASSIFIED)
Fourier Image Synthesis and Slope Spectrum Analysis of Deepwater, Windwave Scenes Viewed at Brewster's Angle

12. PERSONAL AUTHOR(S)
Jan Arthur North

13a. TYPE OF REPORT
THESIS/~~DISSERTATION~~

13b. TIME COVERED
FROM ________ TO ______

14. DATE OF REPORT (Year, Month, Day)
1990

15. PAGE COUNT
291

16. SUPPLEMENTARY NOTATION
APPROVED FOR PUBLIC RELEASE IAW AFR 190-1
ERNEST A. HAYGOOD, 1st Lt, USAF
Executive Officer, Civilian Institution Programs

17. COSATI CODES

FIELD	GROUP	SUB-GROUP

18. SUBJECT TERMS (Continue on reverse if necessary and identify by block number)

19. ABSTRACT (Continue on reverse if necessary and identify by block number)

DTIC
ELECTE
APR 25 1990
S B D

90 04 23 072

20. DISTRIBUTION/AVAILABILITY OF ABSTRACT
☒ UNCLASSIFIED/UNLIMITED ☐ SAME AS RPT. ☐ DTIC USERS

21. ABSTRACT SECURITY CLASSIFICATION
UNCLASSIFIED

22a. NAME OF RESPONSIBLE INDIVIDUAL
ERNEST A. HAYGOOD, 1st Lt, USAF

22b. TELEPHONE (Include Area Code)
(513) 255-2259

22c. OFFICE SYMBOL
AFIT/CI

DD Form 1473, JUN 86 Previous editions are obsolete.

SECURITY CLASSIFICATION OF THIS PAGE

FOURIER IMAGE SYNTHESIS AND SLOPE SPECTRUM ANALYSIS OF DEEPWATER, WIND-WAVE SCENES VIEWED AT BREWSTER'S ANGLE

BY

JAN ARTHUR NORTH
CAPTAIN USAF

B.A. LAWRENCE UNIVERSITY of WISCONSIN

(1978)

A thesis submitted in partial fulfillment
of the requirements for the degree of
Master of Science in the Center for
Imaging Science in the College of
Graphic Arts and Photography of the
Rochester Institute of Technology

8 December 1989

Signature of the Author Jan A. North
Capt. Jan A. North, M.S. Candidate

Accepted by Mehdi Vaez-Iravani
Dr. Mehdi Vaez-Iravani, Coordinator, M.S. Degree Program

COLLEGE OF GRAPHIC ARTS AND PHOTOGRAPHY
ROCHESTER INSTITUTE OF TECHNOLOGY
ROCHESTER, NEW YORK

CERTIFICATE OF APPROVAL

M.S. DEGREE THESIS

The M.S. Degree Thesis of Jan A. North
has been examined and approved
by the thesis committee as satisfactory
for the thesis requirement for the
Master of Science degree

Roger Easton
Dr. Roger Easton, Thesis Advisor

Dr. John Schott, Committee Member

Carl Salvaggio
Mr. Carl Salvaggio, Committee Member

08 December 1989
Date

FOURIER IMAGE SYNTHESIS AND SLOPE SPECTRUM ANALYSIS OF DEEPWATER, WIND-WAVE SCENES VIEWED AT BREWSTER'S ANGLE

BY

JAN A. NORTH
CAPTAIN USAF

Submitted to the
Center for Imaging Science
in partial fulfillment of the requirements
for the Master of Science Degree
at the Rochester Institute of Technology

ABSTRACT

A semi-empirical model for the Fourier synthesis of deepwater, wind-wave scenes has been constructed for the analysis of water-wave slope spectra. The main simplifying assumptions of this model are 1) fully-developed wind-wave surfaces are quasi-homogeneous, quasi-stationary and are therefore treatable by Fourier methods, 2) the subsurface is both optically and mechanically deep, and 3) the small range of spectral wave components defines a fetch-limited, small-amplitude condition. A nonlinear transformation of wave slope to reflected and refracted radiance in both horizontal and vertical polarizations was effected under the special conditions of Brewster-angle viewing under clear skies at a spectral wavelength of 460 nanometers. Seventy two syntheses were varied with ~~respect to six~~ distinct solar positions, four ~~distinct~~ wind directions, and three distinct wind velocities.

The synthetic wave scenes were analyzed via the forward Fourier transformation and their radiance magnitude spectra were compared with the original slope magnitude spectra of the initial synthesis in order to estimate the effects of the nonlinear radiance transformation on the recovery of the wave slope spectrum from imagery. Within the boundaries of this study, it was determined that 1) the limited results of Chapman and Irani [1981] have been generally verified, 2) the existence of an optimal imaging geometry for slope spectrum estimation is indicated, and 3) the presence of subresolution wave slopes creates a significant effect on wave slope spectra derived from imagery.

Theses. (ghd)

DEDICATION

To Kathy, Hollie and Janson

TABLE OF CONTENTS

1.0 INTRODUCTION.................................... 1

1.1 Introduction to Wind-Driven Water Waves...... 6

1.2 Image Synthesis of Water-Wave Scenes......... 11

1.3 Image Analysis of Water-Wave Scenes.......... 18

1.4 Review of Pertinent Literature.............. 24

2.0 METHODS.. 36

2.1 Radiometric Model for Image Synthesis........ 45

2.2 Fourier Synthesis of Wind-Wave Surfaces...... 49

2.3 Synthesis of Skydome Downwelling Radiance.... 69

2.4 Synthesis of Subsurface Upwelling Radiance... 77

2.5 Synthesis of Reflected Skydome Radiance...... 87

2.6 Synthesis of Refracted Subsurface Radiance... 105

2.7 Generation of Synthetic Radiance Imagery..... 108

2.8 Slope Spectrum Analysis of Synthetic Images.. 112

3.0 RESULTS and DISCUSSION......................... 117

3.1 Discussion of D_0 Results................... 118

3.2 Discussion of D_1 Results................... 130

4.0 CONCLUSION..................................... 135

5.0 REFERENCES..................................... 139

APPENDICES

Appendix I - D_1 Results..................... A-1

Appendix II - D_0 Results.................... A-26

Appendix III - FORTRAN 77 Code.............. A-63

1.0 INTRODUCTION

The intent of this study is twofold:

1) The first goal is to construct a reasonable linear model to describe the interaction of wind-driven water waves with the two primary sources of natural illumination: the down-welling sun and sky radiance (of which a fraction is reflected in the direction of an overhead observer) and the up-welling back-scattered subsurface radiance (of which a fraction is refracted in the direction of an overhead observer). This linear model will be used to create synthetic scenes of wind-driven water waves and derive their radiance magnitude spectra.

2) The second goal is to analyze the spatial radiance distribution of the synthetic wave scenes with respect to sun position, wind direction, wind velocity, polarization, and sub-resolution slope variance in order to compare the magnitudes of error that arise from the treatment of the radiance image magnitude spectrum as a linearizable reconstruction of the slope magnitude spectrum of the imaged water surface.

This study is essentially an amplification and extension of

the work of Chapman and Irani [1981].

In the 1950s, the two unrelated fields of oceanography and photographic science both experienced a minor renaissance with the introduction of the concepts of stochastic processes and power spectral analysis that were first applied in communications engineering [Blackman & Tukey, 1958]. Power spectral analysis provided a powerful analytical tool to photographic science for evaluating image quality; likewise, power spectral analysis provided a linear, statistical mechanism to oceanography for evaluating the large number of deterministic theories concerning the development, propagation, and decay of water waves [Kinsman, 1965]. An excerpt of a letter from the oceanographer, Dr. Walter Munk, to Drs. Blackman and Tukey gives an indication of beneficial results that were obtained with the new methods:

> "...we were able to discover in the general wave record a very weak low-frequency peak which would surely have escaped our attention without spectral analysis. This peak, it turns out, is almost certainly due to a swell from the Indian Ocean, 10,000 miles distant. Physical dimensions are: 1 mm high, a kilometer long." [Blackman & Tukey, 1958]

Oceanographers had previously developed a number of photographic techniques to capture and optically analyze large amounts of high-resolution, two-dimensional (2D) spatial

information about water-wave surface structure [Hulburt, 1934; Barber,1949,1954; Cox & Munk,1954a,b; Schooley,1954; Pierson,1960]. It was not until the advent of the digital computer and the implementation of the digital Fast Fourier Transform (FFT) that oceanography was able to efficiently analyze the wave scene into its spectral components and derive the directional 2D spectrum for elevation and slope [Kinsman,1965; Pierson & Stacy,1973]. The current study is a continuation of existing research which analyzes digital images of water waves through digital simulations.

The current study builds upon the work of Chapman and Irani [1981]. They, in turn, extended the work of Stilwell [1969; Stilwell & Pilon,1974] and Kasevich [1975; Kasevich et al.,1971,1972] in an attempt to quantify the parametric nonlinearities that may exist between the slope magnitude spectrum of the water surface and the radiance magnitude spectrum of the water surface image - as a linearizable reconstruction of the slope magnitude spectrum of the actual water surface. The current study reconstructs the synthetic model of Chapman and Irani with some selected modifications and enhancements:

1) no sensor or path radiance model is introduced as the

intent of this study is to estimate only the effects of wave and illumination geometry on the nonlinear transformation of slope to radiance,

2) a correlation model is introduced to provide a conservative spatial filter for synthesizing the effects of sub-resolution wave-slope variance on the image spatial radiance distribution,

3) a subsurface upwelling refracted radiance model is introduced to provide an additional nonlinear element to the analysis and to more adequately model the slope spectra obtained from visible images,

4) the zenith angle of observation is set at the Brewster angle (relative to mean sea surface) in order to define the extent to which the nonlinear transformation is affected by vertically polarized radiance added by the variance of wave slopes, and

5) the analysis of normalized difference spectra is introduced in order to provide a more direct correspondence with the analysis of slope variance as calculated from integrated power spectra.

The remainder of the Introduction is organized into four sub-chapters:

Chapter 1.1 introduces the topic of wind-generated waves, with emphasis on the small nonlinearities that must be considered.

Chapter 1.2 is an overview of the development of realistic syntheses of water-wave scenes, with emphasis on synthetic radiance imagery.

Chapter 1.3 is an overview of the development of image analysis of water-wave scenes, with emphasis on wave-slope spectrum analysis.

Chapter 1.4 is a review of the pertinent research which precedes the current study, with emphasis on the development of the first-order theory. Extracts from the introductory analysis of Kasevich [1975] and Stilwell [1969] are presented, followed by an overview of both the simulation experiment of Chapman and Irani [1981] and the experimental design of the current study.

1.1 Introduction to Wind-Driven Water Waves

Fully three quarters of the planet is covered with a layer of water; except for the rare instances of sustained windlessness where the surface is smooth and specular, the water surface is disturbed by the addition of directional friction energy applied by wind passing over the surface. (Tides, Coriolis-force waves, earthquake-generated waves, and other very-long-period waves are not considered here.) Up to some maximum wind velocity, the disturbed surface remains analytic (infinitely differentiable) and can be described as a quasi-stationary, pseudo-Gaussian process [Kinsman,1965] with an approximate power elevation spectrum.

Figure 1.1:1 illustrates Dr. Kinsman's relative estimation of the power elevation spectrum describing the energy contained in the surface waves of the oceans. Note that energy, L^2, is proportional to $|\text{elevation}|^2$.

The nonlinearities of real water-wave surfaces can be attributed to four dominant factors [Kinsman,1965; LeMehaute,1976]:

First, wind energy is added to the water in a directional

and time-variant manner. Cox and Munk [1954a,b] found the wave-slope distribution to be nearly Gaussian, as would be expected for a continuous wideband spectrum. However, the cross-wind distribution of slopes is symmetric and the along-wind distribution is slightly skewed so that the most probable wave slope is directed upwind, a result they attributed to directional wind stress.

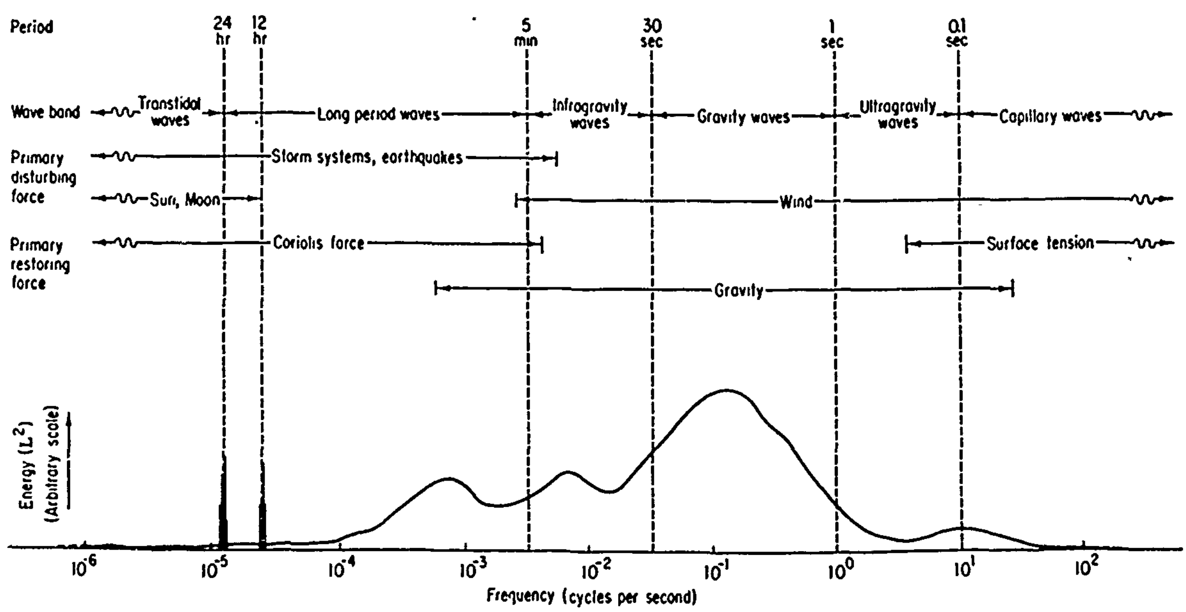

FIGURE 1.1:1. Schematic representation of the energy contained in the surface waves of the oceans - in fact, a guess at the power spectrum. (from Kinsman,1965)

Second, both gravitational and molecular forces act on material water waves to inhibit random generation of very-large-elevation waves and, in the derivative, random generation of very steep wave slopes. Also, the natural

propagation state of a high-amplitude, narrowband water wave is cycloidal rather than sinusoidal, i.e. with elongated flat troughs and shorter peaked crests. This cycloidal form diminishes as the sea state increases and spectral wave-component energy is transferred over a wider band of wave-numbers, but it does not disappear. Therefore, the wave surface is pseudo-Gaussian in that the elevation and slope distributions exhibit a slight kurtosis (peakedness) and a truncation of the large-variance components. Cox and Munk correlated their results with a Gram-Charlier representation of a Gaussian distribution to account for this slight skew-ness and kurtosis.

Figure 1.1:2 illustrates the cross-wind and along-wind distributions of wave slopes (from Cox & Munk,1954b).
Note that the curves are normalized to equal areas.

Third, there is a nonlinear transfer of wave energy from the high-frequency components of the wave spectrum to the low-frequency components as a function of time, fetch, and sea state. As previously mentioned, there is some maximum wind velocity beyond which the water surface acquires excessive energy, which leads to instability and a consequent loss of analytic structure. A familiar manifestation is white-

capping of the waves. Up to this point of fully-developed sea state, the effect of wind energy is to generate small-amplitude capillary waves which tend to become dampened by surface tension and which impart energy to the lower-frequency waves upon which they are riding. In 1847, Stokes [1880] defined the maximum wave slope which each wave component could attain before it became unstable; each spectral component transferred energy to lower frequencies until saturation; if the lower regime was saturated, whitecapping resulted. Within the range of gravity waves, the maximum wave slope is approximately 1/7. For capillary waves, the maximum wave slope can approach 1/1. Chapter 2.2 will illustrate the fact that the greater part of the slope variance from a fully-developed wind-wave surface is due to capillary waves.

Fourth, water waves refract in the presence of subsurface obstacles just as light refract in the presence of media with differing refractive indices. Refractive nonlinearities appear only when the ratio of wavelength to depth becomes large. As long as the deepwater condition is satisfied (i.e. the longest wavelength under consideration is small relative to depth) the wave surface remains linear with respect to subsurface refraction.

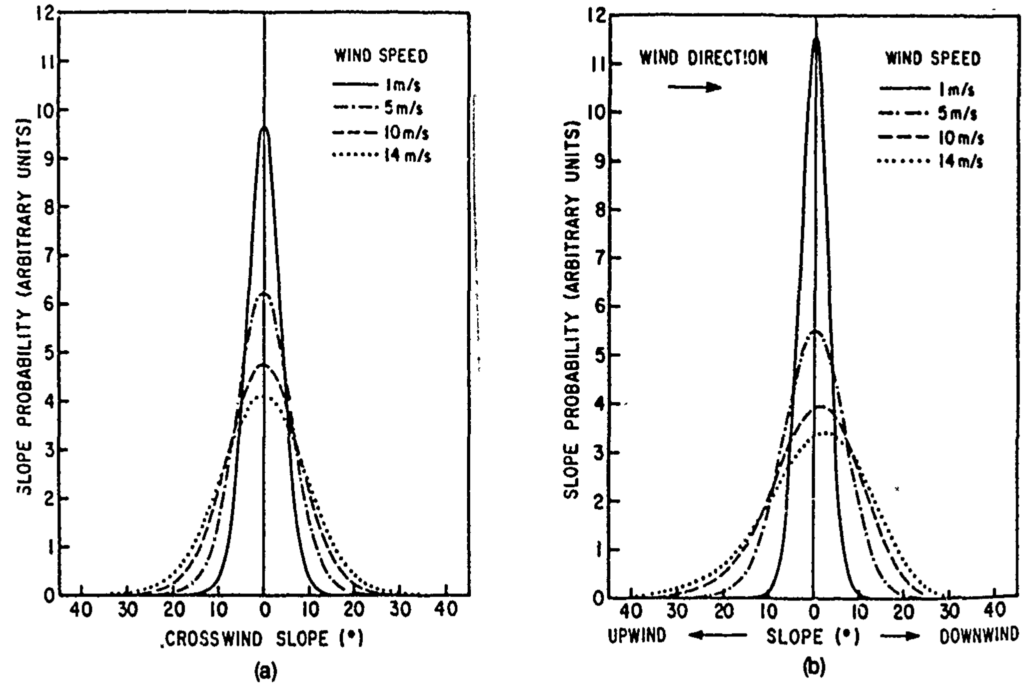

FIGURE 1.1:2. Facet slope-angle (beta) distribution probability for a wind-roughened sea, computed for various wind speeds by means of the Cox & Munk probability function. (from Sidran,1981)

In sum, a linear model for a synthetic water surface would most accurately describe infinite-fetch, fully developed wind waves propagating over deep water and with steady homogeneous winds blowing in a constant direction at velocities well below the point of spectral saturation. The predominant discrepancy of a linear model is that the lack of directional skew allows a 180-degree ambiguity in the direction of wind propagation.

1.2 Image Synthesis of Water-Wave Scenes

An Overview

The subject of image synthesis is best introduced by Upson:

> "Within computer graphics and animation, two major sub-disciplines have developed: graphics for entertainment or artistic purposes, and graphics for scientific or technical purposes. Computer scientists working on entertainment applications have emphasized the correct visual representation of natural phenomena and have developed ad hoc physical simulations to accomplish this. Computational scientists working in the physical sciences have devoted their efforts to the underlying physics for simulating phenomena, with little emphasis on the visual representation.
>
> In recent years these two approaches have begun to reach the limits of their ability to work without each other. The realism required in entertainment animation is beyond that obtainable without physically realistic models. Similarly, numerical simulations in the physical sciences are complex to the point of being incomprehensible without visual representations." [Upson,1987]

Progress in the image synthesis of natural phenomena is occurring within three overlapping lines of research:

1) geometric models which provide a more accurate model of natural texture and shape,

2) illumination models which provide a more accurate model of the physical interaction between light and matter, and

3) temporal models which provide a more accurate model of the equations of motion for natural systems.

Most research devoted to the realistic synthesis of water-wave scenes has occurred within the last decade as part of the general interest in rendering of complex natural phenomena by computer. Early artistic renderings concentrated on generating low oblique scenes with realistic surface texture but with little attention to correct illumination effects. Early scientific renderings concentrated on the generation of near-nadir scenes with correct radiometry in order to simulate remotely sensed oceanographic imagery having low spatial resolution.

Whitted [1980] created one of the earliest attempts at rendering water waves in his film "The Compleat Angler". The ripples on a flat pool surface were generated by 'bump mapping', where the surface normal was perturbed by a single sinusoidal function. Bump mapping was first introduced by Blinn [1978]. Information International used a similar technique with cycloidal waveforms to create a leader for Pyramid Films [1981]. Perlin [1985] amplified this technique by using 20 superimposed cycloidal waveforms, each radiating from randomly selected centers. The characteristic limitation of bump mapping is that the actual surface is flat; there is no change in surface height to correspond to the perturbation of a local normal vector.

Schacter [1980] developed a scalar texture model for realtime image generation of waves, using sums of three or fewer long-crested, narrowband noise waveforms. This stochastic geometric model was intended for realtime image synthesis of a variety of textured surfaces or random fields with no regard to the physics of surface-light interaction. Norton et al.[1982] employed frequency-limited (or 'clamped') analytical functions for the same purpose.

Max [1981] used a vectorized ray-tracing algorithm on a Cray-1 supercomputer to model optical reflection on water waves for use in a color animation film "Carla's Island". The wave-surface height field was modeled by superimposed traveling sine waves. Each ray was constrained to reflect off the water at most two times before it proceeded to other scene elements. However, no effort was made to accurately model the attenuated spectral radiance of the synthetic scene; a geometric rule-of-thumb approach was used to compute each pixel based on a weighted average of 'sun color' and 'sky color' that were input from an RGB (Red-Green-Blue) translation table.

In 1985, Ts'o and Barsky [1987] applied the Stokes

model of the sea surface and generated height fields by fitting beta-splines with parameters that yielded symmetric waves. This model simulated directional refraction of water waves due to interaction with the ocean floor. Peachey [1986] similarly implemented the Stokes model as a height field but used quadric surfaces to create asymmetry. This synthesis also used a particle-system model to simulate the effects of surf spray on a beach but without the effect of directional refraction. Peachey gave some thought to surface reflection of skylight but ultimately assumed a Lambertian approximation for rough surfaces in the calculation of pixel brightness. Fournier and Reeves [1986] reviewed the work of the previous authors and produced a Gerstner wave model that incorporated a wind field and a stochastic element to perturb the wave model in addition to the previously noted features. Even in this final product, reflection is simulated by a one-level ray trace with selective filtering of the RGB color 'spectrum'.

Fractal and sequential Markov-chain synthesis techniques have been developed to simulate the texture of many natural surfaces including ocean waves [Mandelbrot,1977, 1988; Gagalowicz & Ma,1985; Monne et al.,1981]. In general, these techniques are considered to produce poor synthetic

water-wave images. The main objection to the surfaces generated by these processes is that they are not continuously differentiable. The surface normal vector at a point can only be approximated via a neighborhood average. However, it is interesting to note (in the context of wave surfaces) that the mathematician Karl Weierstrass developed the first fractal function by describing an infinite series of superimposed harmonic sinusoids:

$$f(t) = (1)COS(w*t)+(1/a)COS(b*w*t)+(1/a^2)COS(b^2*w*t)+\ldots ,$$

to yield a series representation of a continuous yet non-differentiable function. In this particular case, the fractal dimension d = LN(a)/LN(b).

Mastin et al.[1987] recognized the inadequacy of the fractal model for ocean scenes and instead treated water surfaces as filtered white-noise processes. For his filter, Mastin used a modified Pierson-Moskowitz, temporal-domain, elevation power spectrum for fully-developed, wind-driven seas. A white-noise surface was filtered in the frequency domain and then inverse-Fourier-transformed to create the synthesized wave image. The surfaces were animated by varying the phase of the frequency components between each

frame, based on the dispersion relation between phase velocity and wave frequency. Mastin employed a simple illumination model to render the scenes but indicated that "incorporation of Fresnel's law into the reflectance model would probably enhance image quality."

Borrego and Machado [1985] used essentially the same filter technique as Mastin but with a Pierson-Neumann spectrum. They wrote their images to photographic film and then analyzed the film via the optical Fourier transformation and optical cross-correlation in order to compare synthetic results with real photographs of the sea. They did not use any illumination model - density values on film corresponded to surface height - since their analysis was only a first-order approximation.

Attempts to combine a water-wave surface model with correct radiometry are fewer in number:

Chapman and Irani [1981] attempted to quantify the error magnitudes associated with linearizing the relationship between the spatial frequency spectrum of an image and the slope spectrum of the actual water surface. Their radiometric model, though incomplete, is the most comprehen-

sive found within this survey. It will be described in detail in the Methods section as their combined model provides the point of departure for the current study.

Wilf and Manor [1984] applied the Chapman and Irani model to a restricted case: the simulation of water-wave images in the far infrared. They simplified their model with the assumption of a Forward Looking Infra-Red (FLIR) sensor having limited spatial resolution and sensitivity. Schwartz and [illegible]on [unpublished] and Masuda et al. [1988] also limited the[illegible] models to the far infrared with the intent of simulating th angular effect of emissivity on sea temperature variation due to wind-roughened water.

It is apparent from this overview that the field of image synthesis, with emphasis on rendering of water waves, is less than a decade old. The integration of radiometry within these syntheses has occurred infrequently and for a limited objective in each instance.

1.3 Image Analysis of Water-Wave Scenes

An Overview

In 1925, Schumacher made oblique stereo-pairs from a ship with the intent of measuring the variability of wave heights. The utility of this method was severely limited due to many factors: 1) the camera baseline was restricted to the length of the ship; 2) waves in the foreground obstructed waves in the background; 3) backsides of waves were not visible; and 4) there was a lack of 'ground' control on open seas for height determination - the errors are especially pronounced from an oblique perspective [Pos,1988].

In 1933, Hulburt [1934] made polarized and unpolarized oblique photographs of sun glitter on sea waves to measure the polarization of light at sea with respect to surface roughness, sun angle, and weather conditions. Because the widths of glitter patterns correlate to the maximum slope of the sea surface, Hulburt was able to demonstrate that waves in the North Atlantic varied from 15 degrees inclination when winds were blowing at 3 knots up to 25 degrees inclination at 18 knots.

Sawyer [1949] mounted a Sonne strip camera on a fast

low-flying airplane to photograph narrow strips of the sea surface and measure the directional spectrum of the waves. The field of view was too narrow to capture significant amounts of surface data orthogonal to the flightline. The accuracy of the spectral estimate decreased with the angle from the flightline.

Also in 1949, Barber [1949,1954] analyzed single photographs of sea surfaces to determine wave direction but he was unable to determine the two-dimensional (2D) spectrum due to the computing limitations of the time. At this point, it became apparent that an essential requirement for future analysis of water-wave surfaces was to have near-vertical, high-resolution, high-contrast images covering large areas. The intent was to photographically capture significant information about the largest range of spatial frequency components without perspective distortion or hidden surface detail. It also became apparent that the analysis of large amounts of spatial information required the power of a digital computer.

In 1951, Cox and Munk [1954a,b] measured the wave-slope distributions of the sea surface from aerial photographs of sun-glitter patterns. They computed the distribution from

the measured variation of radiance within a glitter pattern instead of computing maxima from the pattern boundaries as done by Hulburt. Four cameras were flown from a single airplane at altitudes of 2000 feet, with two used as imagers and two used as radiometers. Their image analysis was quite sophisticated; it accounted for sun diameter, angular reflectivity, lens falloff, film sensitivity, exposure calibration, and ultimately provided a first-order relationship between film density and directional wave-slope probability.

In 1953, Schooley [1954] performed a simplified version of the Cox and Munk experiment by taking flash photographs of a river surface from a 45-foot bridge elevation at night. The main limitation of his experiment was the probable inhomogeneity of the water surface due to limited fetch and the presence of surrounding obstacles.

In 1954, medium-altitude (3000 ft) stereophotography was employed by Marks and Ronne [1955] to generate stereopairs of sea surfaces. Two airplanes carried radio-synchronized cameras and a surface ship acted as 'ground' control in the photographs. Elevations were photogrammetrically measured at discrete points and the sampled elevation array was then auto-correlated (the sampling distance determined

the desired spectral resolution). This experiment marks the first recorded use of a digital computer to calculate the directional 2D spectra of water waves. The work of Cote et al. [1960] enhanced this basic technique. More recent stereophotogrammetric efforts include Holthuijsen [1983a,b] and Pos et al. [1988]. Elements of this later work include methods to render the water opaque so that a more exact calculation of the height field can be made.

During the 1950s and early 1960s, Longuet-Higgins [1952-1962; Cartwright & Longuet-Higgins,1956] elaborated on the results of Cox and Munk to formulate the statistical theory of patterns, paths, number, frequency, and distributions of specular reflection points on randomly moving surfaces. Stilwell [1969; Stilwell & Pilon,1974] correlated the statistics of sea-surface images to the wave-slope statistics of the actual sea surface. Under the assumptions of uniform sky radiance, optimized viewing geometry, and small surface slopes, Stilwell derived the relationship between the film transmittance of an imaged surface point and the range component of the wave slope at that surface point. He further demonstrated a linearizable relationship between the spatial image spectrum and the imaged surface slope spectrum. Kasevich [1975] extended Stilwell's model

to second order to develop an optimization criterion for the relationship. Chapman and Irani [1981] took this work one step further by applying a synthetic model and executing a limited quantification of the error magnitudes associated with the parametric dependence of this linear model. This work will be further detailed in Chapter 1.4.

Sheres [1980] developed a novel technique for remotely sensing surface-flow velocities based on imagery of monochromatic wavetrains of known frequency (such as those generated by a motor boat) propagating over the region of interest. His work demonstrated that the wavelength and direction of two different wavetrains generated all the required information to calculate surface flows. Gotwols and Irani [1980] developed a similar technique to determine the phase velocity of short gravity waves.

Exotic sensors using LASER [Palm et al.,1977; Schau, 1978; Abshire & McGarry,1987] and LIDAR [Weinman,1988] have been used to extract directional spectra and surface backscatter data at higher wavenumbers (i.e. the capillary wave regime). Synthetic Aperture Radar (SAR) imagery has been used to estimate spectra, phase velocities, and propagation directions at lower wavenumbers (i.e. the gravity wave re-

gime) [Monaldo & Lyzenga,1986; Monaldo & Kasevich,1982; Carlson,1984]. Also, Long Wave Infrared (LWIR) sensors have been used to calculate spatial spectra of ocean-surface temperature [Saunders,1967,1968; McLeish,1970].

Lybanon [1985] reported on the implementation of an automated image-analysis system by the U.S. Naval Ocean Research & Development Activity (NORDA). The Interactive Digital Satellite Image Processing System, or IDSIPS, can automatically derive the sea-surface slope statistics from sun-glitter images through analysis of the imaging geometry. As a late example of the practical application of water-surface spectra determination, Fisher [1986] analyzed four sun-glitter images taken from the space shuttle Challenger (STS-41G) to locate acoustically important oceanographic features in support of hydro-acoustical sensor placement.

It is apparent from this overview that, in six decades, the methods of water-surface imaging have moved from surface ships to airplanes to satellites and spacecraft. Likewise, the measurement and analysis of the resulting imagery have undergone a corresponding increase in computational power and sophistication.

1.4 Review of Pertinent Literature

A comprehensive review would include the work of Stilwell and Pilon [1974], and Kasevich et al. [1971,1972]. The emphasis of this earlier work is on the analysis of coherent optical processing techniques as applied to photographic emulsions of wave scenes. Kasevich [1975] provides a general introduction to the first-order theory subsequent to the development of his approximate geometric-optics second-order theory to estimate the optimum viewing geometry for the obtainment of reasonable spectra. Stilwell [1969] provides additional development of image analysis with respect to the law of Malus subsequent to performing an optical analysis to derive directional energy spectra. Only the first-order theory is reviewed here; a review of the second-order theory is beyond the scope of this study since the theory of Kasevich assumes simplified approximations for both Fresnel reflectivity and sky radiance distributions. However, the most general results of the second-order theory can be compared, with caution, to the results of this study. Any second-order theory that is developed for this geometric problem loses definiteness because the spatial distributions for natural radiance are independent; no general solution can be specified [Stilwell,1969]. This is the prime motiva-

tion for the simulation and analysis of geometric effects through empirical models.

Review of Kasevich [1975]

The essential requirement for the determination of slope spectra from wave images is to have the spatial modulation of the image be proportional to the wave profile. Kasevich uses the example of a transparency with film exposure, E, defined over its linear region by

$$E(y) = [f_0(y)^{(-gamma/2)}]*[1+f(y)/f_0(y)]^{(-gamma/2)} \qquad [1.4:1]$$

where

$$E(y) = f_0(y) + f(y), \qquad [1.4:2]$$

and

gamma = the film gamma,

such that

$f_0(y)$ = the mean exposure on film,

and

$f(y)$ = the exposure modulation due to scattering of radiance from specular wave-slope facets.

This example is given for a two-dimensional case.

If $f_0(y) >> f(y)$, then Equation [1.4:1] can be expanded

in a binomial series to yield the approximation

$$E(y) \cong [f_0(y)^{(-gamma/2)}]*[1-(gamma/2)*f(y)/f_0(y)]. \qquad [1.4:3]$$

The estimation of the slope spectrum from the forward Fourier transform of the image requires that f(y) be linear with respect to the wave slope dz/dy, where z is the surface elevation. This condition can only be approximately satisfied because of the nonlinearity of 1) the spatial radiance distributions found in nature, 2) the Fresnel reflectivity variation with respect to incidence angle, and 3) the refraction of upwelling subsurface radiance in the direction of the observer.

Review of Stilwell [1969]

For a small wave-slope angle beta, the small-angle approximation is:

$$beta = ATAN(dz/dy) \cong dz/dy, \qquad [1.4:4]$$

where beta is the fundamental parameter for extracting wave-slope spectra from imagery. The law of Malus defines the radiance observed at azimuth angle theta as a simple function of Fresnel reflectivity and incident radiance:

L_o(theta,beta,omega) = L(mu)*R(omega), [1.4:5]

where

L_o(theta,beta,omega) = the observed reflected radiance,

L(mu) = the incident radiance to be reflected,

R(omega) = the Fresnel reflectivity (for any arbitrary polarization),

theta = the zenith angle of observation,

beta = the slope of the reflecting surface,

mu = the zenith angle of the incident radiance,

and

omega = the angle of incidence,

such that

omega = theta - beta [1.4:6]

and

mu = omega - beta. [1.4:7]

Figure 1.4:1 illustrates the angular relations in two dimensions.

The variation of observed radiance with respect to a change of surface slope dbeta at some point is

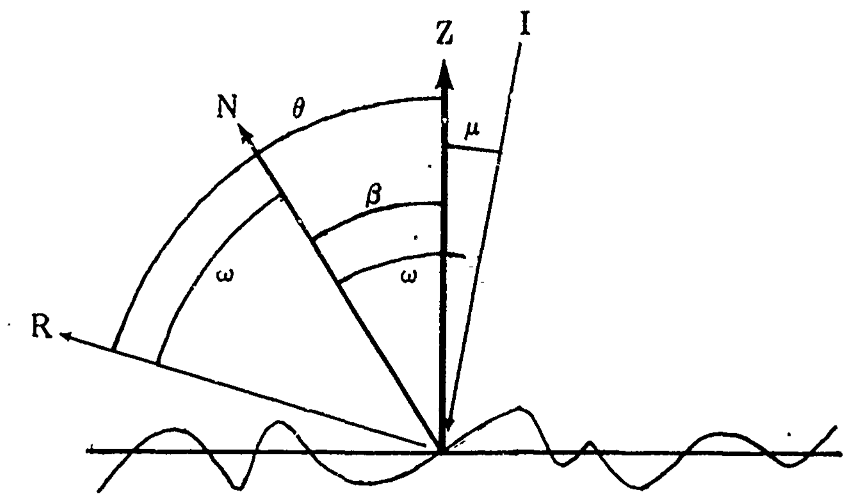

FIGURE 1.4:1. Angular relations for the 2D case.

$$\frac{dL(theta)}{dbeta} = \frac{dL(mu)}{dmu}*R(omega)*\frac{dmu}{dbeta}$$

$$+ L(mu)*\frac{dR(omega)}{domega}*\frac{domega}{dbeta}. \qquad [1.4:8]$$

If beta is a small angle and

$$omega \cong mu, \qquad [1.4:9]$$

then

$$\frac{dL(theta)}{dbeta} = [L'(mu)*R(omega)$$

$$+ L(mu)*R'(omega)]*\frac{domega}{dbeta}], \qquad [1.4:10]$$

where the prime (') denotes the first derivative with respect to the argument. With the assumption that the water surface remains analytic, the small-angle linear approxima-

tion holds in the Fourier transform for wave-slope angles (beta) up to at least 30 degrees [Stilwell,1969].

Review of Chapman and Irani [1981]

The intent of the work of Chapman and Irani was to quantify the parametric dependencies of errors inherent in linearly relating a wave-slope magnitude spectrum to the corresponding radiance image magnitude spectrum. Their approach was to simulate radiance images of sea-like surfaces in two dimensions. Their simulation utilized models of the sea surface, the sky radiance distribution, and the non-linear transfer function that transforms surface slope to radiance. They determined that the two-dimensional simulation was computationally expensive so only a small number of geometries were investigated. However, they initially used a simpler one-dimensional model of a ±15-degree sinusoidal surface propagating in a single direction along the sensor field in order to survey various imaging geometries for potential synthesis and analysis in two dimensions.

Figure 1.4:2 illustrates the two-dimensional methodology for image synthesis and error analysis used by Chapman and Irani. This methodology is described in detail in Chapters 2.1 through 2.8.

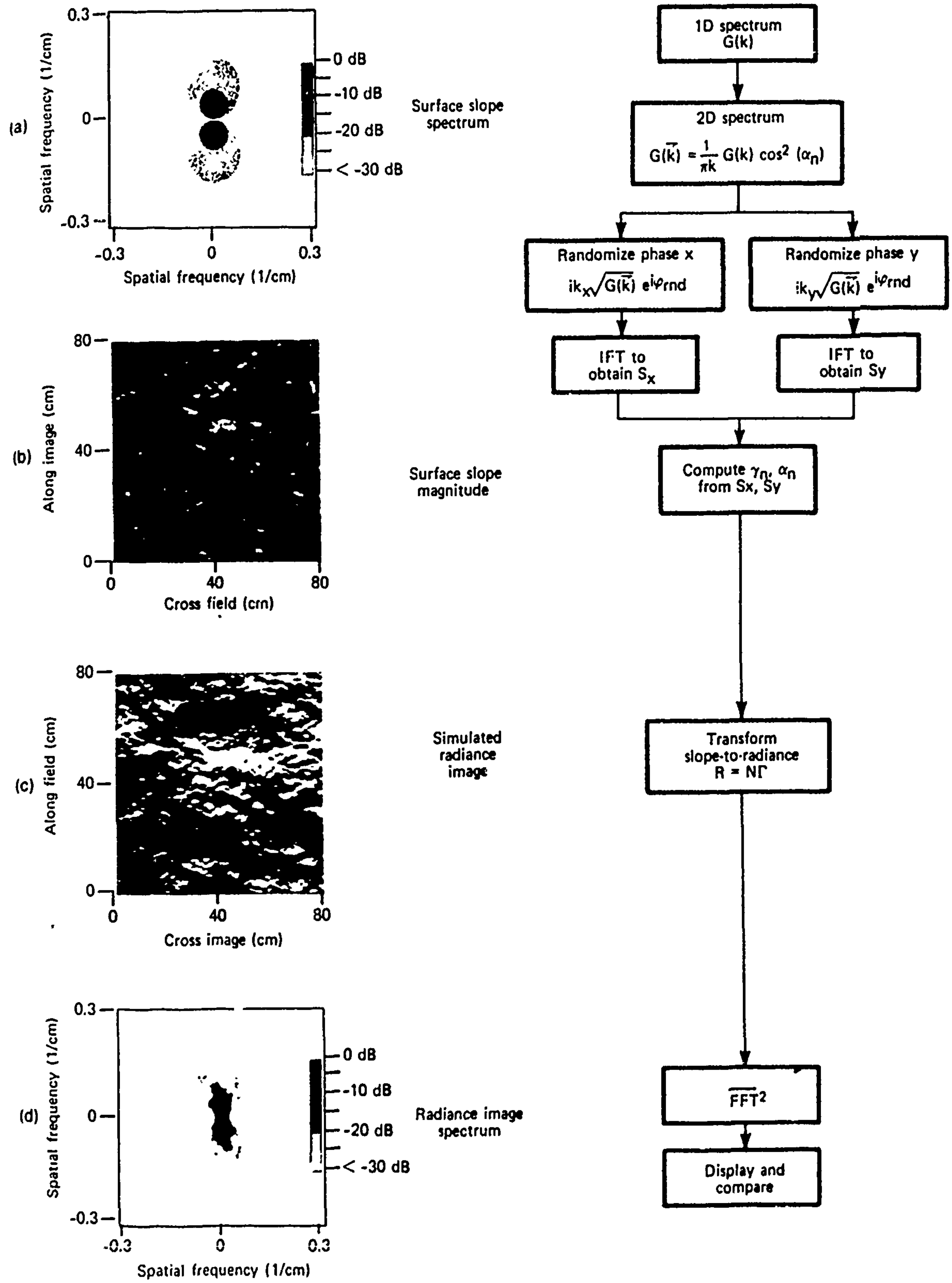

FIGURE 1.4:2. Methodology of error estimation in two dimensions. (from Chapman & Irani,1981)

Chapman and Irani used two figures of merit derived from signal analysis to describe the nonlinearity of the slope-to-radiance transformation. The first figure of merit is the ratio of the fundamental component to the DC component which they termed the contrast of the wave image. The second figure of merit is the square root of the power in the upper harmonics divided by the power in the fundamental, which they termed the Total Harmonic Distortion (THD) of the wave image. An optimal imaging geometry for measuring slope statistics would maximize contrast and minimize THD, based upon their terminology. These figures of merit were computed for the results of their one-dimensional model. To quote Chapman and Irani:

> "...these figures of merit do not represent realistic contrasts or distortion statistics for sea surface imaging because the distribution of slopes over a sinusoid differs substantially from the approximately Gaussian distribution of sea surface slopes." [Chapman & Irani, 1981]

Their initial results indicated that the figures of merit showed a substantial, asymmetric dependence on slope azimuth for certain geometries and may misrepresent the utility of a particular geometry.

Chapman and Irani then applied their two-dimensional synthesis and analysis to six selected geometries with the

intent of evaluating the azimuthal dependence of their figures of merit. Their two-dimensional results indicated that 1) nonlinearity is largely independent of wavenumber, 2) nonlinearity remains relatively low (error < 3 dB) over a relatively wide range of azimuth (100-120 degrees) around the sensor azimuth, and 3) nonlinearities increase within 30-40 degrees of the cross-field direction.

Experimental Design of the Current Study

As earlier stated, the current study is essentially an amplification and extension of Chapman and Irani as developed from a proposed statement of work:

> "An exhaustive evaluation of our radiance modulation model would involve: 1) simulating the geometry of a surface area; 2) transforming that surface geometry into an image using a particular set of optical conditions; 3) estimating the slope spectrum of the simulated surface and the spectrum of the image; 4) repeating steps 1-3 for all other possible imaging geometries; and 5) comparing each image spectrum with the corresponding slope spectrum to obtain estimates of the error arising from nonlinearity. This, in fact, is impractical because there are a large number of parameters to be varied, and, for any set of these parameters, the error computation involves a large number of operations." [Chapman & Irani, 1981]

The intent of this study is to develop and execute a test design which provides a minimal yet optimal set of parameters to both verify the limited results of Chapman and

Irani and to complete a more detailed parametric surface exploration.

For their two-dimensional analysis, the experimental design of Chapman and Irani was of the order 1x3x2 factors relative to the current study, which is of the order 3x4x6 factors:

Wind Friction Velocity - 12.0, 36.0, and 60.0 cm/sec versus 12.0 cm/sec. These three velocities define the envelope of the linear wind-wave model.

Wind Azimuth - +90:-90, +45:-135, 0:180, and -45:135 degrees (with ambiguity) versus +90:-90, +30:-120, and 0:180 degrees (with ambiguity).

Sun Position - (0,0), (0,53.2), (45,53.2), (90,53.2), (135,53.2), and (180,53.2), where the coordinates are (azimuth angle, zenith angle) in degrees, versus (90,45) and (135,45).

The experimental design of the current study spans the complete range of azimuthal geometries in increments of 45 degrees.

The zenith angle of observation for the current study model is set at the mean Brewster angle (53.2 degrees at 460 nm) (versus 60.0 degrees at 800 nm in the Chapman and Irani model) so that the effect of vertically polarized radiance due to wave-slope deviations from the mean surface can be compared with the observed horizontally polarized radiance. Only the horizontally polarized radiance was computed in the Chapman and Irani study.

In addition, the effect of upwelling subsurface radiance is incorporated into the current study model in order to estimate the effect that refracted radiance may have on the nonlinearity of the reconstructed slope spectrum.

Also, the effect of sub-resolution wave slopes is incorporated into the current study model in order to account for the spatially filtered wave-slope spectrum that exists beyond the maximum sampling frequency of the model.

Figure 1.4:3 illustrates the differences between the two studies, based on the combinations of synthetic imaging geometries that are analyzed in two dimensions.

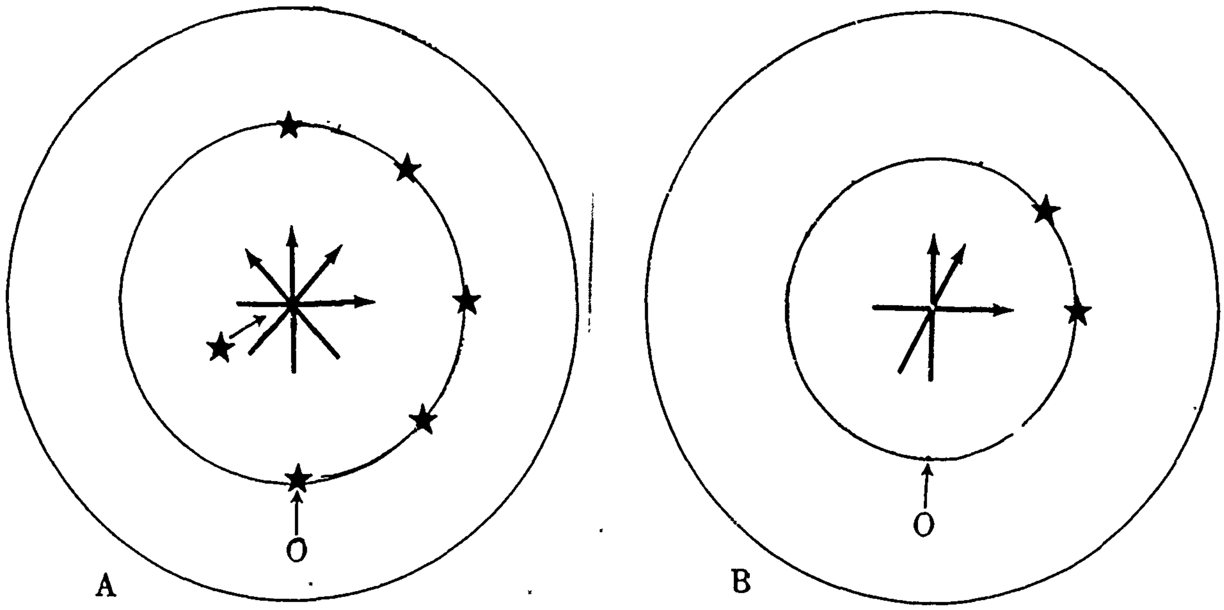

FIGURES 1.4:3(a) & (b). 2D imaging geometries used in the current study (a) versus the Chapman and Irani study (b).

In summation, the experimental design for the current study requires the analysis of 72 distinct synthetic imaging combinations versus 6 combinations in the previous study. The analysis of these synthetic results will provide more complete information on the geometric effects of slope spectrum reconstruction than the simplified one-dimensional analysis in the previous work of Chapman and Irani [1981].

2.0 METHODS

Overview

The current study model uses a two-dimensional Pierson-Stacy elevation power spectrum to create a synthetic wind-wave-slope surface that conforms to the results of a number of statistical studies [Cox & Munk,1954a,b; Longuet-Higgins, 1957; Pierson & Stacy,1973]. Downwelling skydome (solar and skylight) radiance for clear skies and upwelling subsurface radiance for clear, deep water are both synthetically created from analytic models. These synthetic radiance distributions are decomposed into their polarized components.

The synthetic radiance image is generated by first calculating the surface-slope distribution of the synthesized water surface and then applying the law of Malus to linearly map the radiance distributions, the polarized Fresnel reflection coefficients, and the surface projection coefficients to the surface-slope distributions to compute the reflected and refracted polarized radiance from each sample area in the direction of observation.

Figure 2.0:1 illustrates the methodology for image synthesis and error analysis used in the current study.

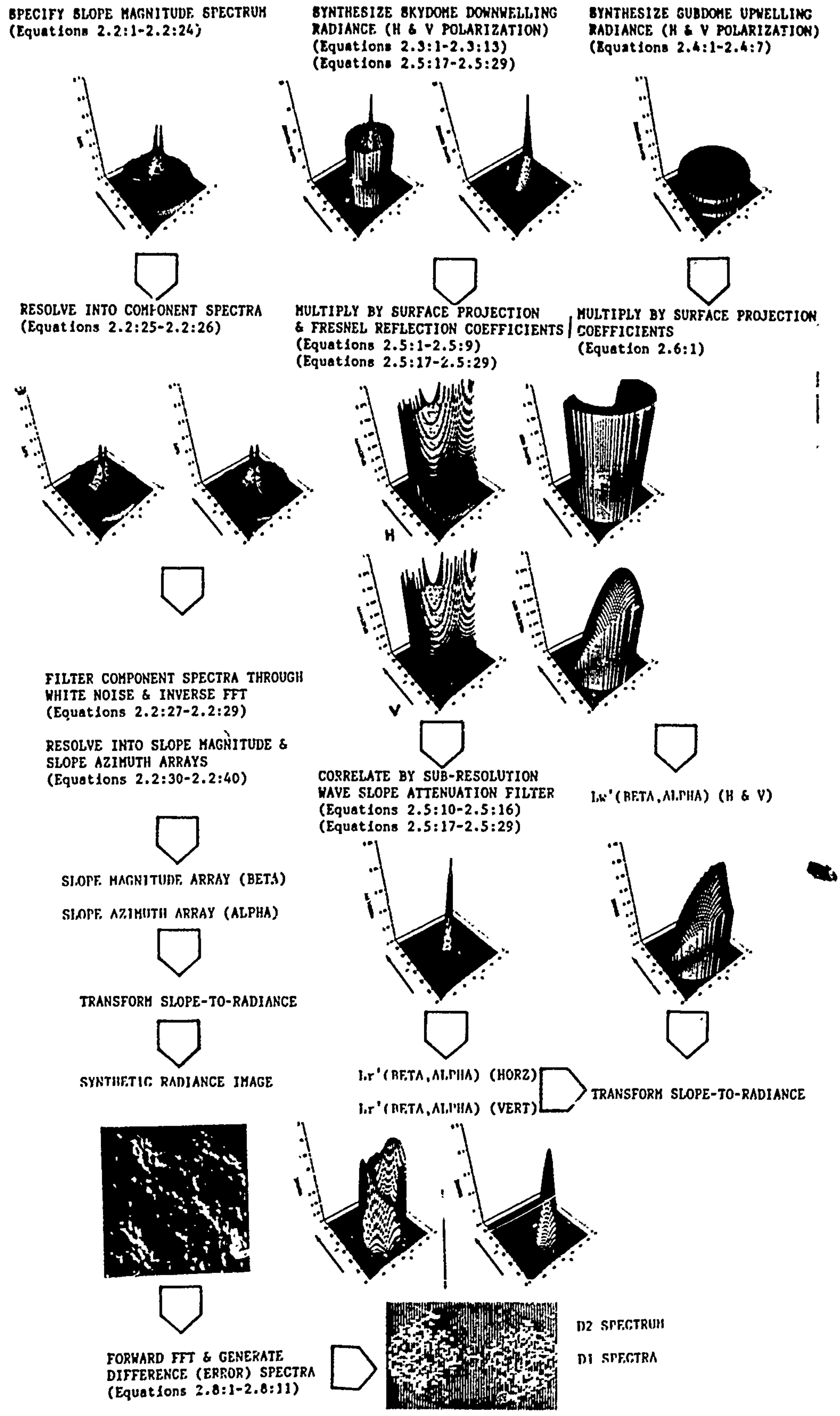

FIGURE 2.0:1. Schematic methodology of the current study.

Chapman and Irani [1981], in their error computations of the linear estimation of surface-slope spectra from image spectra, assumed that the nonlinearity of the slope-to-radiance transfer function was the principal source of error. They did note other possible sources of error but chose not to incorporate them in their study. The current study attempts to include those sources of variation which are directly or indirectly attributable to the geometric effect of water surfaces on the modulation of observed radiance:

1) Perspective Distortion
2) Variation of the Sensor Response Function
3) Spatial and Spectral Filtering

No sensor model is implied in this synthesis other than the existence of a spatial Nyquist frequency and a geometric location for a viewpoint. Chapman and Irani stated "we assume digital processing techniques are used so that perspective distortion and trends in the response function over the field of measurement can be removed prior to obtaining the image spectra" and "we assume that the optical modulation transfer function of the camera adequately filters the surface radiance spectrum and thereby eliminates aliasing errors." This synthesis does, however, incorporate a corre-

lation model to account for the spatially filtered, high-frequency wave-slope spectrum that exists beyond the maximum spatial sampling frequency.

4) Upwelling Radiant Energy

5) Scattered Radiant Energy

No atmospheric model is implied in this synthesis. However, a model for subsurface absorption and scattering is incorporated, providing radiance variation due to refraction of upwelling surface radiance by surface waves. The model of Chapman and Irani assumed that the surface is viewed 15-60 degrees from nadir so that surface reflection predominates. Also, they assumed that their camera was viewing through clear air and sensing in the near-infrared region so that the effects of path radiance and refracted subsurface radiance could be ignored.

6) Wave Shadows

The work of both Saunders [1967] and Goodell [1971] was reviewed in regard to potential models which compensate for wave shadowing or "hiding". The current linear model, as developed, adequately incorporates the effect described by Goodell for the established zenith angle of observation, the mean Brewster angle. To quote Goodell:

"Facets with small tilts, although more probable, reflect only small portions of the sky. Facets with greater tilts, although less probable, reflect much larger sky portions from higher up. Eventually the [G]aussian slope distribution allows only vanishingly small contributions from wave slopes so that the average contribution seems to come from sky elevations of [approximately 30 degrees, for an oblique observation looking below the horizon]. Thus, masking need not be postulated in order to explain the apparent 15-degree sea slope effect." [Goodell,1971]

Figure 2.0:2 illustrates the effect modeled by Goodell.

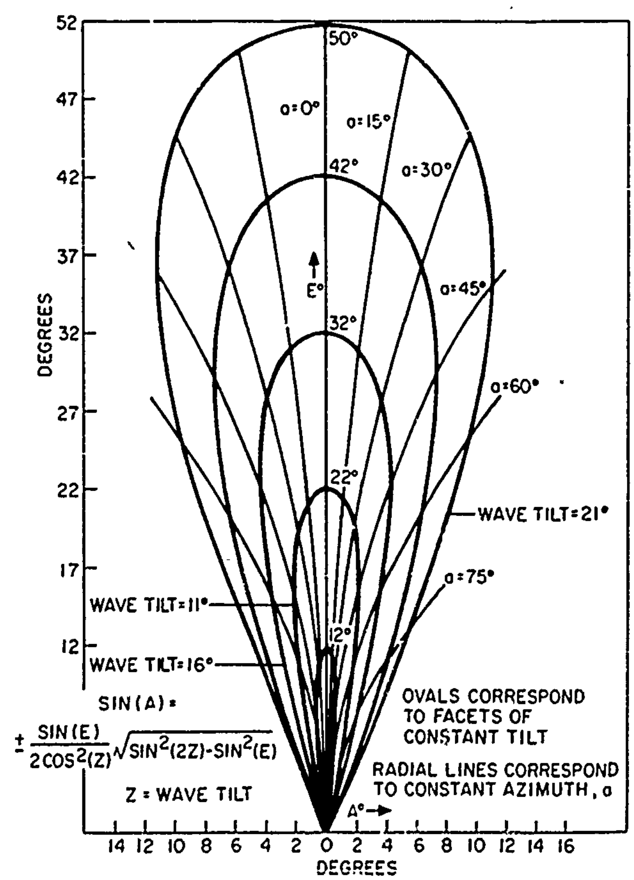

FIGURE 2.0:2. Sky portions reflected to an observer on the ocean surface, looking at the horizon. (from Goodell,1971)

Although the effect is apparently reversed for near-zenith-viewing imagery, the modeling approach is the same for any angle of observation. In Figure 2.0:2, the slope distribution is mapped to sky coordinates; in the current study model, skydome radiance is mapped to slope coordinates.

It is intuitive that the effects of wave shadowing diminish as the observation point approaches zenith. Because the majority of wave slopes are less than 30 degrees, the effect of wave shadowing on Brewster-angle-viewing imagery (53.2 degrees from zenith) is assumed to be insignificant.

7) Multiple Reflections

Only an elaborate Monte Carlo simulation or multiple-ray-tracing model could account for multiple reflections, simulations which are beyond the scope of this linear-model study. The assumption for this synthesis is that the probability of multiple reflections in near-nadir imagery is negligible.

Definition of Model Terms

The following list is a brief glossary of the terms used in the synthetic image model. These terms are formally defined in Chapters 2.1 through 2.8.

alpha = azimuth angle to (wind-wave) surface normal

beta = zenith angle to (wind-wave) surface normal

D_0 = scalar squared difference (error), integrated over both wavenumber (k) and azimuth (phi)

$D_1(k)$ = 1D difference (error) spectrum with respect to wavenumber (k), integrated over azimuth (phi)

$D_1(phi)$ = 1D difference (error) spectrum with respect to azimuth (phi), integrated over wavenumber (k)

$D_2(k_x,k_y)$ = 2D difference (error) spectrum

H = horizontally polarized fraction of radiance

H0(x,y) = horizontally polarized, reflected & refracted synthetic radiance image

H1(x,y) = horizontally polarized, reflected synthetic radiance image

H3(x,y) = H1(x,y) without the incorporation of sub-resolution wave-slope model

I = 3D incident radiance vector

k = dummy variable for scalar wavenumber

$k_{x,y}$ = scalar wavenumber relative to spatial coordinate axes

K = 2D vector wavenumber = (k_x, k_y)

L_g = reflected radiance due to sun glitter

L_p = atmospheric path radiance

L_r = total reflected sky (+ sun) radiance = $L_s + L_g$

L_{ref} = reference Lsky radiance at zenith

L_s = reflected radiance due to skylight

L_{sky} = downwelling radiance from sky (including sun)

L_u = upwelling radiance above water surface = $L_r + L_w$

L_w = upwelling subsurface refracted radiance above surface

L0(x,y) = total (unpolarized) reflected & refracted synthetic radiance image

L1(x,y) = total (unpolarized) reflected synthetic radiance image

$m_{x,y}(x,y)$ = (wind-wave) slope component arrays

mu = zenith angle to reflecting sky element

mu_0 = angle from sun to sky element

$M_{x,y}(k_x,k_y)$ = (wind-wave) slope-component magnitude spectra

nu = azimuth angle to reflecting sky element

nu_0 = angle between vector parallel to direction of polarization and projection of vector to surface plane

$N(k_x,k_y)$ = synthetic image radiance magnitude spectrum

N = 3D surface normal vector

omega = angle of incidence

phi = azimuth angle to point of observation (180 deg)

= dummy variable for azimuth angle

phi_0 = azimuth angle to sun

psi = multiplicative depolarization factor

$P_{2D}(k_x,k_y)$ = (wind-wave) elevation power spectrum

Pr(beta,alpha) = (wind-wave) slope probability distribution

R(omega) = Fresnel reflectivity (arbitrary polarization)

R_0 = unpolarized Fresnel reflectivity at normal incidence

R = 3D reflected radiance vector

$S_{2D}(k_x,k_y)$ = (wind-wave) slope power spectrum

$S_{x,y}(k_x,k_y)$ = (wind-wave) slope-component power spectra

theta = zenith angle to point of observation (53.2 deg)

$theta_0$ = zenith angle to sun

T_a = atmospheric transmittance

T_w = transmittance through water

v_{fric} = friction velocity of wind at water surface

v_{1950} = velocity of wind at height z=1950 cm above surface

V = vertically polarized fraction of radiance

$WGN(k_x,k_y)$ = white-noise spectrum

wind_az = azimuth angle to dominant wind direction (with 180-degree ambiguity)

x,y = spatial coordinates

z = height above mean water surface

2.1 Radiometric Model for Image Synthesis

The total radiance reaching an overhead radiometric sensor be can defined by,

$$L_{tot} = (L_u * T_a) + L_p, \qquad [2.1:1]$$

where

L_u = the spectral upwelling radiance just above the water surface in direction of the sensor,

T_a = the transmittance of the intervening atmosphere between the water surface and the sensor,

and

L_p = the spectral path radiance due to light scattered in the direction of the sensor by the intervening atmosphere.

In general, L_p is much larger than L_u across the visible and infrared spectrum. The estimation of of L_p must be accurate within 1% in order to estimate L_u within 10%. This is known as the 'atmospheric correction problem' and is a well-defined subject of research. However, this synthesis does not include an atmospheric model since it is the variation of L_u with respect to several independent geometries that is the object of study. Therefore, this synthetic model will assume a perfectly non-absorbing, non-scattering atmosphere

and will set $T_a = 1.0$ and $L_p = 0.0$. This simplification reduces the radiometric equation to:

$$L_{tot} = (L_u * 1.0) + 0.0 = L_u \qquad [2.1.2]$$

for the duration of this study. More sophisticated models may vary T_a and L_p and may include a sensor model for spectral/spatial/temporal attenuation and distortion as well. An alternative perspective on this study is to consider that the model creates a synthetic radiant object rather than an image since no part of an imaging chain (including the intervening atmosphere) is modeled; we are interested only in the spatial effects of the water surface on the reflected/ refracted radiance in the direction of a hypothetical distant sensor.

The above surface radiance L_u can be decomposed into three terms,

$$L_u = L_g + L_s + L_w, \qquad [2.1:3]$$

where

L_g = the above-surface radiance due to reflected sunlight (commonly known as sun glitter),

L_s = the above-surface radiance due to reflected skylight,

and

L_w = the above-surface radiance due to subsurface upwelling radiance propagating across the water surface.

Most oceanographic imaging has been directed at estimating L_w, as this term conveys information about water color and the factors which affect water color (non-aqueous constituents and water temperature, to name a few). For this reason, the large radiance due to glitter L_g has been generally avoided by the judicious selection of a minimizing geometry. However, reflected skylight L_s cannot be geometrically avoided; instead, L_s has usually been considered to be constant by assuming that a uniformly radiant skydome reflecting off a uniformly rough water surface yields an approximately Lambertian condition. This is one of the few instances where poor spatial resolution can be used to advantage. The reflected skylight term is then usually collected with the path radiance term:

$$\begin{aligned} L_{tot} &= L_w{*}T_a + (L_s{*}T_a + L_g{*}T_a + L_p) \\ &= L_w{*}T_a + (L_s{*}T_a + 0.0 \quad + L_p) \\ &= L_w{*}T_a + (L_p{}') \qquad [2.1:4] \end{aligned}$$

Thus, estimation of L_w has typically been reduced to cal-

culating T_a and L_p' and applying a linear atmospheric correction.

This synthetic model does not assume that L_w is the pre-eminent datum to collect: for information about the surface geometry, it is important to establish a relation between L_u and surface slope. In this context, the reflected radiance terms, L_g and L_s, are re-collected under the common term,

$$L_r = L_g + L_s \qquad [2.1:5]$$

where

L_r = the above-surface spectral radiance due to the reflected skydome, since, as the surface varies its slope, the surface normal vector points to the skydome independent of the position of the sun on the skydome.

In this study, an optimal imaging geometry provides for the accurate estimation of the slope magnitude spectrum over the broadest range of possible water-surface slope spectra. The general approach to this estimation is to maximize the spatial contrast of L_r and either minimize or correct for the spatial variation of L_w.

2.2 Fourier Synthesis of Wind-Wave Surfaces

The geometric model for Fourier synthesis of wave-slope surfaces closely follows the model of Chapman and Irani [1981] with one exception: the often substantial slope variance that exists above the spatial Nyquist frequency is calculated and the radiometric effect of this sub-resolution slope variance is introduced within the illumination models.

Specification of a 1D Elevation Power Spectrum

The first step is to specify a 1D wave elevation power spectrum. Several spectra were previously cited: Pierson-Neumann [Borrego & Machado,1985; Pierson-Moskowitz [Mastin et al.,1987], and modified Pierson-Stacy [Chapman & Irani, 1981]. For this study, the original 1D Pierson-Stacy power spectrum is employed for two reasons: 1) the spectral scale is spatial wavenumber [radians per centimeter or just /cm] and 2) Pierson and Stacy [1973] went into great detail in their report to attempt to correlate their spectrum with the empirical results of other researchers, including the Cox and Munk [1954a,b] photographic study.

The equations of the 1D wave elevation power spectrum P(k) come directly from Pierson and Stacy [1973]. P(k) is

defined over five spectral regions:

P_1 = the gravity wave-gravity equilibrium spectral range,

$$P_1(k) = (a/2*k^3)*EXP(-b*g^2/(v_{1950}{}^4*k^2))$$

$$\text{for } 0 < k < k_1, \qquad [2.2:1]$$

P_2 = the Kitaigorodskii spectral range,

$$P_2(k) = a/(2*SQRT(k_1)*k^{2.5})$$

$$\text{for } k_1 < k < k_2, \qquad [2.2:2]$$

P_3 = the Leykin-Rosenberg spectral range,

$$P_3(k) = (a*d)/(2*(k_3{}^P)*(k^{3-P}))$$

$$\text{for } k_2 < k < k_3, \qquad [2.2:3]$$

P_4 = the capillary spectral range,

$$P_4(k) = (a*d)/(2*k^3)$$

$$\text{for } k_3 < k < k_{nu}, \qquad [2.2:4]$$

and

P_5 = the Cox viscous cut-off range,

$$P_5(k) = (E/(nu*g))*v_{fric}{}^3*k_{max}{}^6/k^9$$

$$\text{for } k_{nu} < k < \text{infinity}, \qquad [2.2:5]$$

where

$$d = (1.274 + (0.0268*v_{fric}) + (6.03E-5*v_{fric}^2))^2, \quad [2.2:6]$$

$$k_1 = (k2*v_{min}^2)/v_{fric}^2, \quad [2.2:7]$$

$$k_{nu} = (0.5756*SQRT(v_{fric})*k_{max})/(d^{1/6}), \quad [2.2:8]$$

and

$$p = LOG(d/(v_{fric}/v_{min}))/LOG(k_3/k_2), \quad [2.2:9]$$

such that

$a = 0.0081$ = the Phillips constant [unitless],

$b = 0.74$ [unitless],

$E/(nu*g) = 1.473E-4$ [unitless],

$g = 980.0$ = the acceleration of gravity [cm/sec^2],

$k_2 = 0.359$ [rad/cm],

$k_3 = 0.942$ [rad/cm],

$k_{max} = 3.63$ [rad/cm]

$v_{min} = 12.0$ [cm/sec] = the minimum friction velocity defined by the Pierson-Stacy model,

v_{1950} = the wind velocity at 1950 cm above water level [cm/sec], and

v_{fric} = the wind friction velocity at the water surface (i.e. $z = 0$ cm).

v_{fric} and the wind velocity v [cm/sec] at height z [cm] have an empirical correspondence under the assumption of a neutrally stratified atmosphere:

$$v(z) = (v_{fric}/0.4)*LN(z/z_0) \qquad [2.2:10]$$

and

$$z_0 = (0.684/v_{fric}) + (4.28E\text{-}5*v_{fric}^2) - 0.0443 \qquad [2.2:11]$$

Values for v_{fric}, v_{1950}, as well as v_{250}, v_{1000}, and v_{1250} are interpolated from values tabulated by Pierson and Stacy. (Refer to V_DATA.DAT input data file in Appendix III.)

Figure 2.2:1 graphs k*P(k) versus LOG10(k) for friction velocities of 12.0, 36.0, and 60.0 cm/sec, to illustrate of the effect of wind velocity on the character of the elevation power spectrum. Note that most of the power is located in the gravity wavenumber region, i.e. below k = 0.002/cm. The curve for 12.0 cm/sec has a maximum value of 30.0 cm^2.

Specification of a 2D Directional Spreading Function

The 2D power spectrum is created via a directional spreading factor D(k,phi) that attenuates the 1D spectrum at the azimuth angle phi from the upwind/downwind directions:

$$P_{2D}(k,phi) = P(k)*D(k,phi) \qquad [2.2:12]$$

The equations of the 1D wave elevation power spectrum P(k)

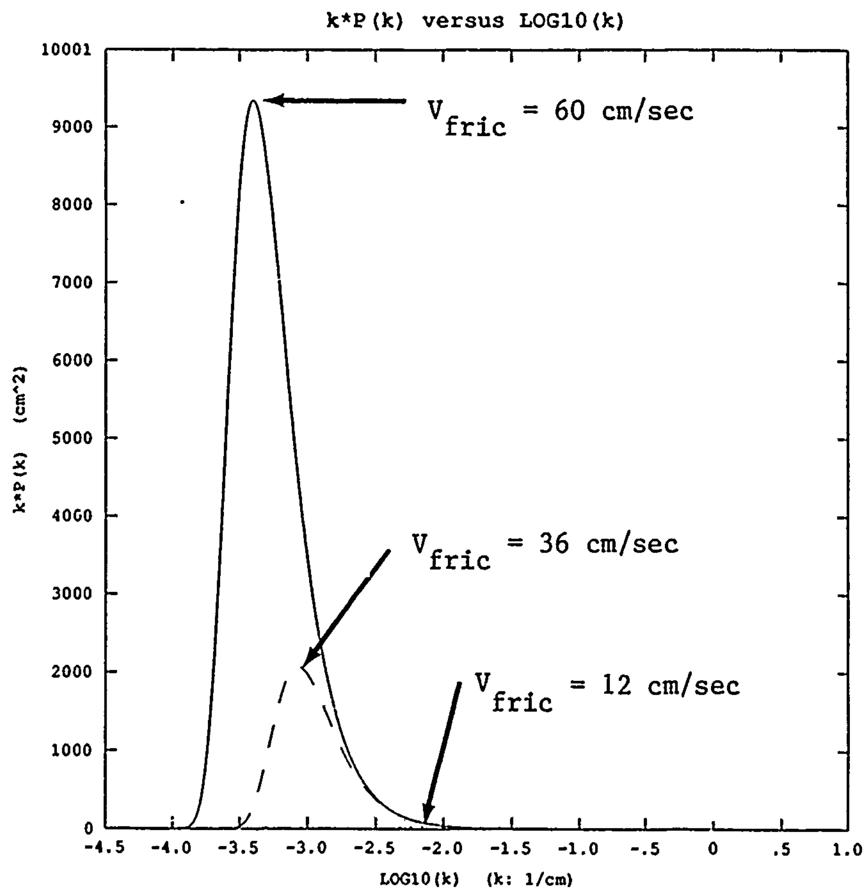

FIGURE 2.2:1. The Pierson-Stacy 1D elevation power spectrum k*P(k) versus LOG10(k).

come directly from Pierson and Stacy [1973] with a small modification to allow rotation of the 2D spectra relative to the wind azimuth wind_az.

The directional spreading function is defined:

D(k,phi,wind_az) = (A*(1-B)) + (B*C) [2.2:13]

where

$A = (8/(3*pi))*(D^2),$ [2.2:14]

$B = EXP(-g^2/(2*k^2*v_{1950}{}^4)),$ [2.2:15]

and

$C = (A*D+0.5)/pi$ [2.2:16]

such that

$D = COS(wind\_az-phi).$ [2.2:17]

Creation of the Slope-Component Spectra

The third step is to derive the two slope-component spectra from the scalar power spectrum. The 2D spectrum must first be normalized by k over the range of wavenumber:

$P_{2D}'(k,phi) = P(k)*D(k,phi)/k$ [2.2:18]

since

$P(k) = \int P_{2D}'(k,phi)*k*dphi = \int P_{2D}(k,phi)*dphi.$ [2.2:19]

The two slope-component spectra are obtained by multiplying the scalar 2D elevation spectrum by the squares of the orthogonal components of the wave vector $\vec{K}$ that are aligned with the image coordinate system (x,y):

The slope power spectrum is

$S(k,phi) = k^2*P_{2D}'(k,phi),$ [2.2:20]

which leads to

$$S_x(k_x,k_y) = k_x^2*P_{2D}'(k,phi) = k_x^2*P_{2D}'(k_x,k_y) \qquad [2.2:21]$$

and

$$S_y(k_x,k_y) = k_y^2*P_{2D}'(k,phi) = k_y^2*P_{2D}'(k_x,k_y), \qquad [2.2:22]$$

since

$$|K| = SQRT(k_x^2 + k_y^2) = k \qquad [2.2:23]$$

and

$$\begin{aligned} P_{2D}'(K)*dK &= P_{2D}(k_x,k_y)*k*dk \\ &= P_{2D}(k*COS(phi),k*SIN(phi))*k*dK \\ &= P_{2D}(k,phi)*k*dkdphi \\ &= P_{2D}'(k,phi)*dkdphi. \qquad [2.2:24] \end{aligned}$$

The square roots of the slope-component power spectra yield the corresponding slope-component magnitude spectra, which are used as filters when generating the synthetic slope arrays:

$$M_x(k_x,k_y) = SQRT(S_x(k_x,k_y)) \qquad [2.2:25]$$

and

$$M_y(k_x,k_y) = SQRT(S_y(k_x,k_y)). \qquad [2.2:26]$$

Creation of a Frequency-Domain White Noise Image

The fourth step is to create a scalar matrix of spatial white noise, i.e. uniformly distributed, uncorrelated random

values with unit magnitudes ranging between +pi and -pi. The Fourier transform of this matrix yields a complex phase matrix with conjugate symmetry about its central ordinate:

$$\mathcal{F}^{+1}[wgn(x,y)] = WGN(k_x,k_y) \qquad [2.2:27]$$

Frequency-Domain Filtering and Back Transformation

WGN is filtered by M_x and M_y in the frequency domain to create the two complex Fourier transforms of the synthesized wave-slope components. The inverse Fourier transform yields the two slope-component arrays:

$$m_x(x,y) = \mathcal{F}^{-1}[M_x(k_x,k_y)*WGN(k_x,k_y)] \qquad [2.2:28]$$

and

$$m_y(x,y) = \mathcal{F}^{-1}[M_y(k_x,k_y)*WGN(k_x,k_y)]. \qquad [2.2:29]$$

Both m_x and m_y are real scalar arrays of slope components because of the conjugate symmetry.

Conversion to Slope Magnitude and Slope Azimuth

The fifth and final step is to convert the two slope-component arrays into a slope magnitude array beta(x,y) and a slope azimuth array alpha(x,y), where beta is the maximum

slope at the coordinate (x,y) and alpha is the azimuth angle to the direction of beta. The angles alpha and beta are related to m_x and m_y by the geometric relations:

$$TAN(m_x) = TAN(beta)*COS(alpha) \qquad [2.2:30]$$

and

$$TAN(m_y) = TAN(beta)*SIN(alpha). \qquad [2.2:31]$$

Therefore, the maximum slope magnitude of an array facet is

$$beta = ATAN\ [TAN(m_x)^2 + TAN(m_y)^2] \qquad [2.2:32]$$

and the azimuth angle in the direction of the maximum slope is

$$alpha = ATAN\ [TAN(m_y)/TAN(m_x)]. \qquad [2.2:33]$$

Figures 2.2:2 through 2.2:4 illustrate the 2D Pierson-Stacy elevation magnitude spectra for friction velocities of 12.0, 36.0, and 60.0 cm/sec, respectively. The spectra are oriented with wind azimuth = -45 deg (or +135 deg with ambiguity).

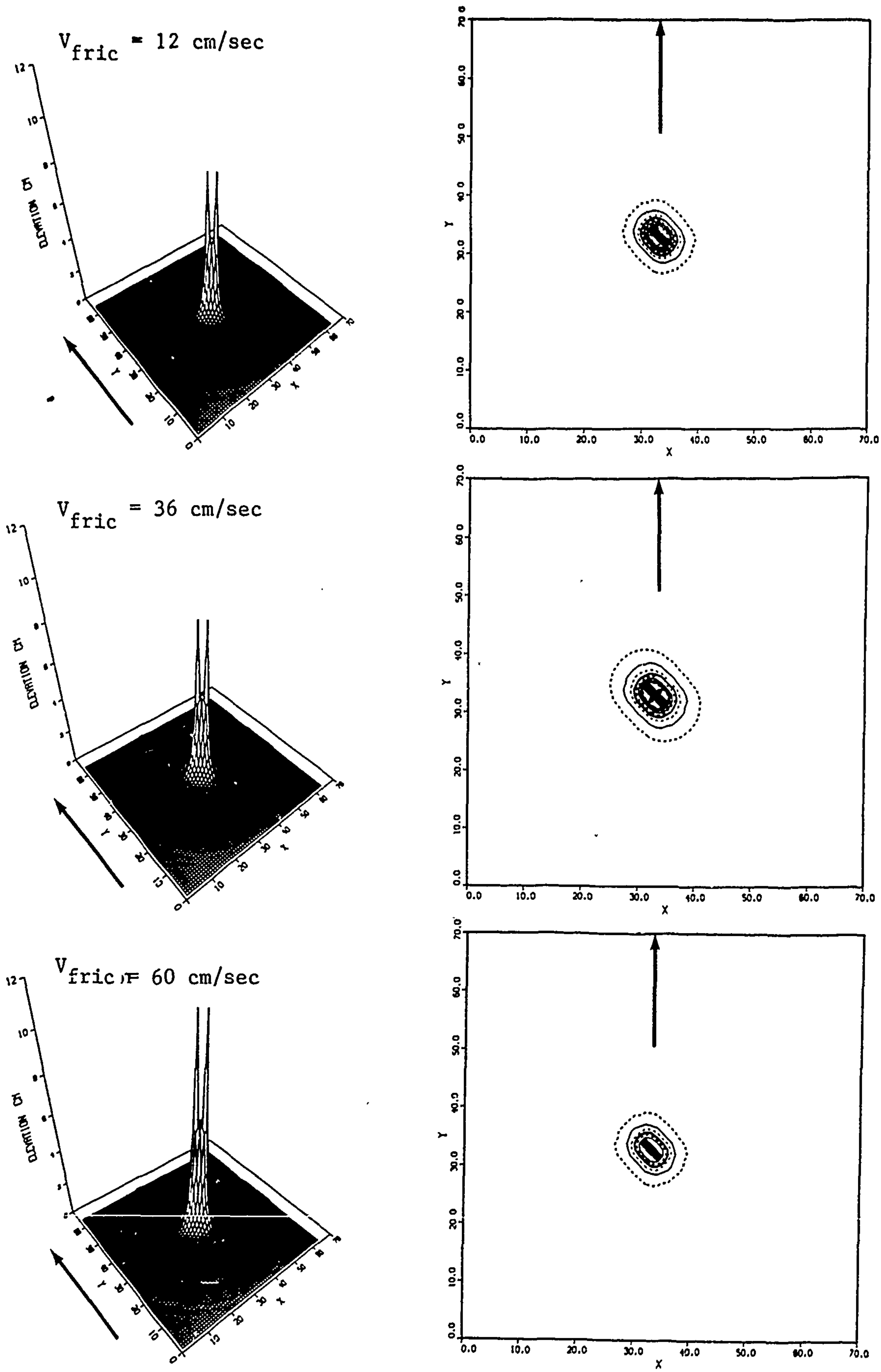

FIGURES 2.2:2-4. Elevation magnitude spectra, $\sqrt{P(k_x,k_y)}$.

Figures 2.2:5 through 2.2:7 illustrate the 2D Pierson-Stacy slope magnitude spectra for friction velocities of 12.0, 36.0, and 60.0 cm/sec, respectively. The spectra are oriented with wind azimuth = -45 deg (or 135 deg with ambiguity).

Figures 2.2:8 through 2.2:10 illustrate the x-components of the above slope spectra. Figures 2.2:11 through 2.2:13 illustrate the y-component slope spectra. The spectra are oriented with wind azimuth = -45 deg (or 135 deg with ambiguity).

Figures 2.2:14 through 2.2:16 illustrate the sample slope distributions Pr(beta,alpha) for synthetic realizations using the above slope spectra. The spectra are oriented with wind azimuth = -45 deg (or 135 deg with ambiguity).

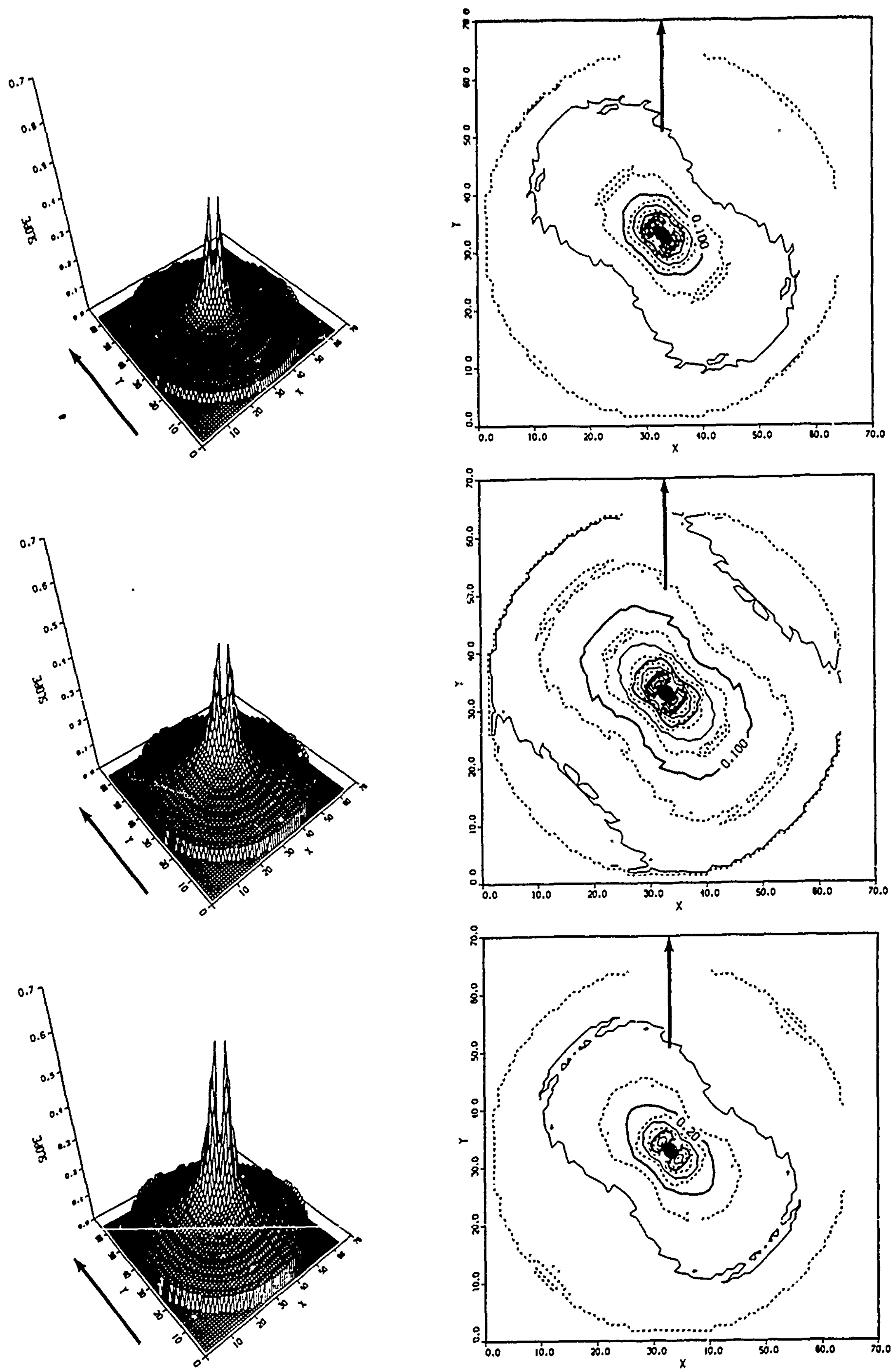

FIGURES 2.2:5-7. Slope magnitude spectra, $M_0(k_x, k_y)$.

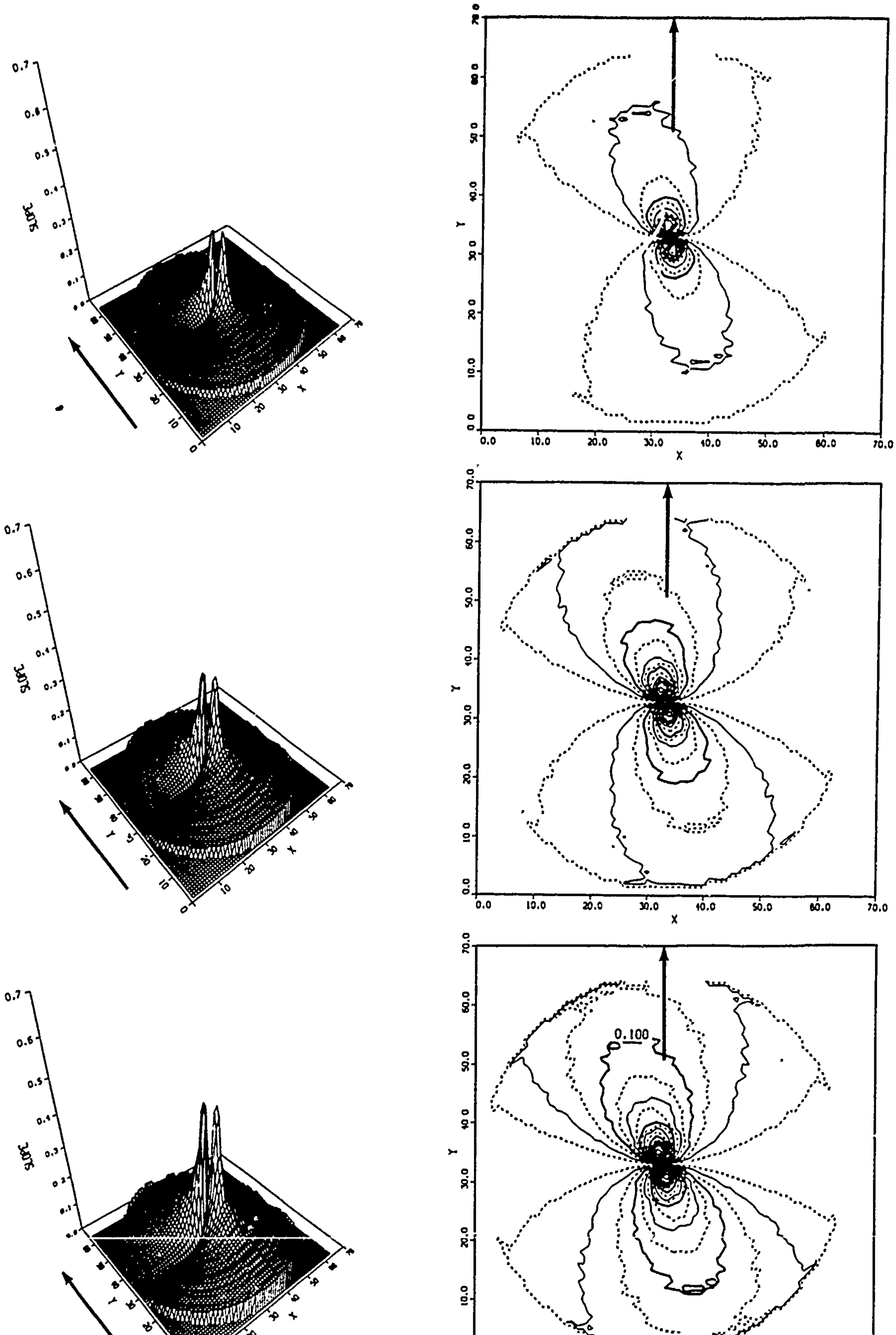

FIGURES 2.2:8-10. X-components of slope magnitude spectra.

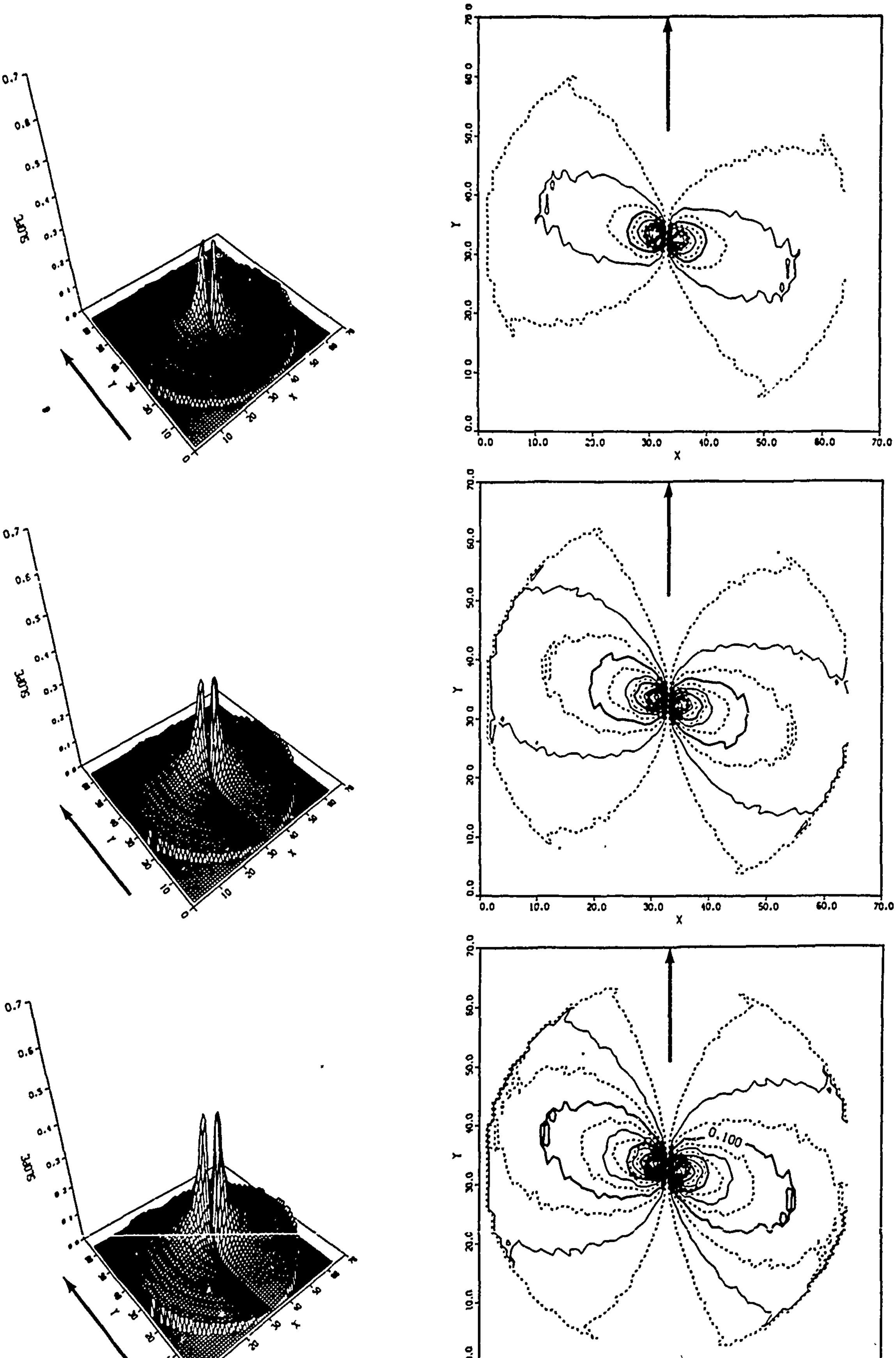

FIGURES 2.2:11-13. Y-components of slope magnitude spectra.

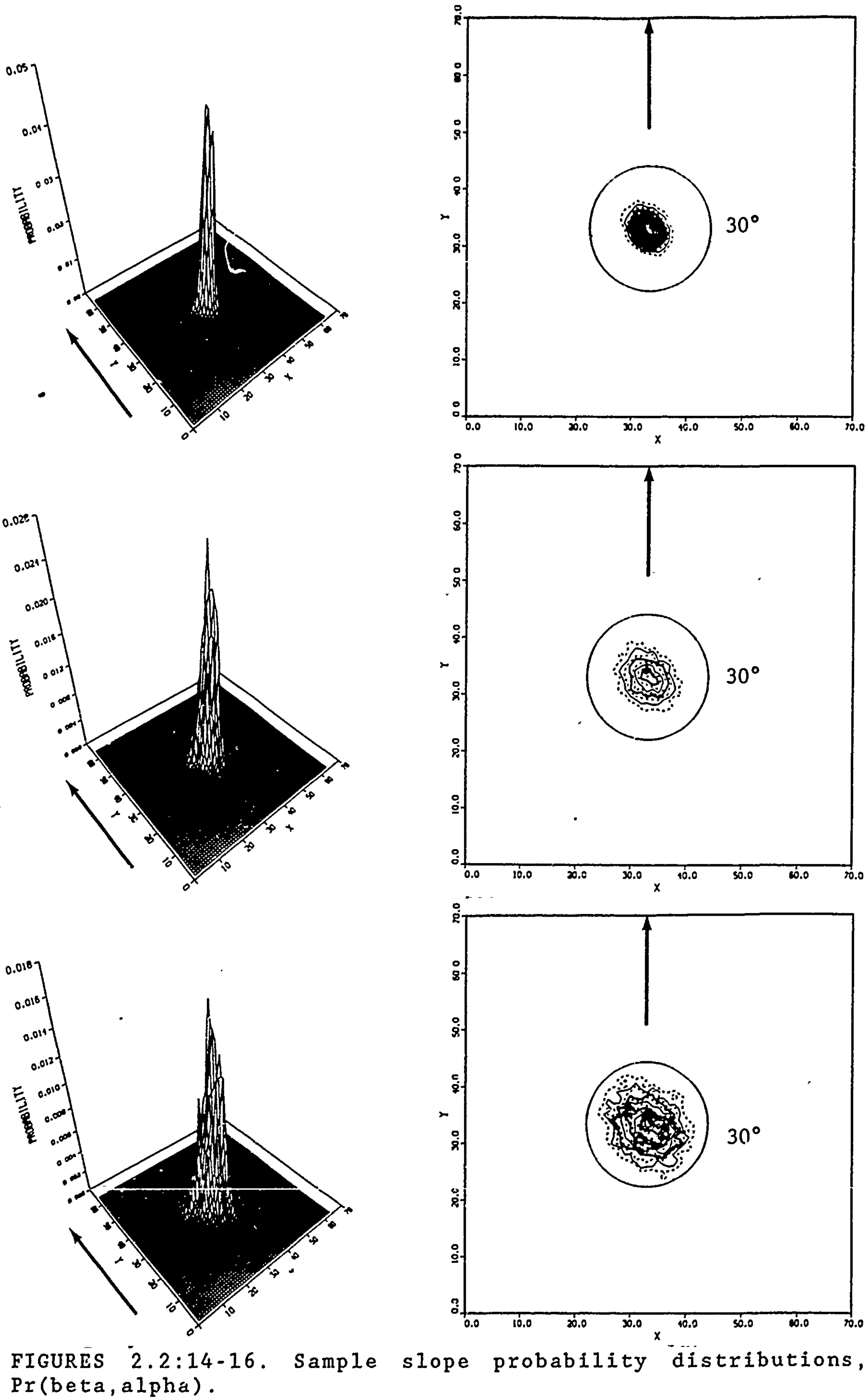

FIGURES 2.2:14-16. Sample slope probability distributions, Pr(beta,alpha).

Calculation of Total and Component Slope Variance

The slope variance is calculated from the 1D slope power spectrum for a specified range of wavenumber:

$$VAR(k1,k2) = \int_{k1}^{k2} S(k)*dk = \int_{k1}^{k2} k*S(k)*dLN(k) \qquad [2.2:34]$$

The unresolved (i.e. both x- and y-components combined) slope variance is calculated from the 2D slope power spectrum for a specified range of wavenumber:

$$VAR(k1,k2) = \iint_{\vec{k1}}^{\vec{k2}} S(k,phi)*dkdphi = \iint_{\vec{k1}}^{\vec{k2}} S(k_x,k_y)*dk_x dk_y \qquad [2.2:35]$$

Likewise, the x-component and y-component slope variance can be calculated by substituting S_x or S_y for S in Equation [2.2:35].

The 2D distribution of slopes in the downwind and crosswind directions correlate well with the results of Cox and Munk [1954a,b] and this is one measure of the adequacy of the Pierson-Stacy model. However, Pierson and Stacy [1973] suggest that the optical system used by Cox and Munk acted as a high-frequency spatial filter on the reflected

radiance from the sea surface. Pierson and Stacy concluded that the calculation of variance from the integration of their power spectrum over k and phi yielded variances which fit reasonably well with the Cox and Munk model when they imposed an upper bound of k = 1.2 radians per centimeter. This corresponds to a wavelength of 5.24 centimeters. To maintain consistency between the results of two previous efforts, this model assumes a maximum spatial frequency of k = 1.2 radians per centimeter.

Figure 2.2:17 graphs k*S(k) versus LOG(k) for three friction velocities, 12.0, 36.0, and 60.0 cm/sec. This graph has the interesting property that the area under the curve equals the total variance and the area between two wavenumbers equals the fraction of the total variance between the two wavenumbers, as specified in Equation [2.2:34]. The wavenumber range sampled by the current study model is located between the two vertical lines.

Figure 2.2:18 graphs the fractional and total slope variance over the friction velocity range from 12.0 to 60.0 cm/sec. The lower line represents the integration of variance up to k1 = 0.0375/cm. k1 is the fundamental spatial frequency for

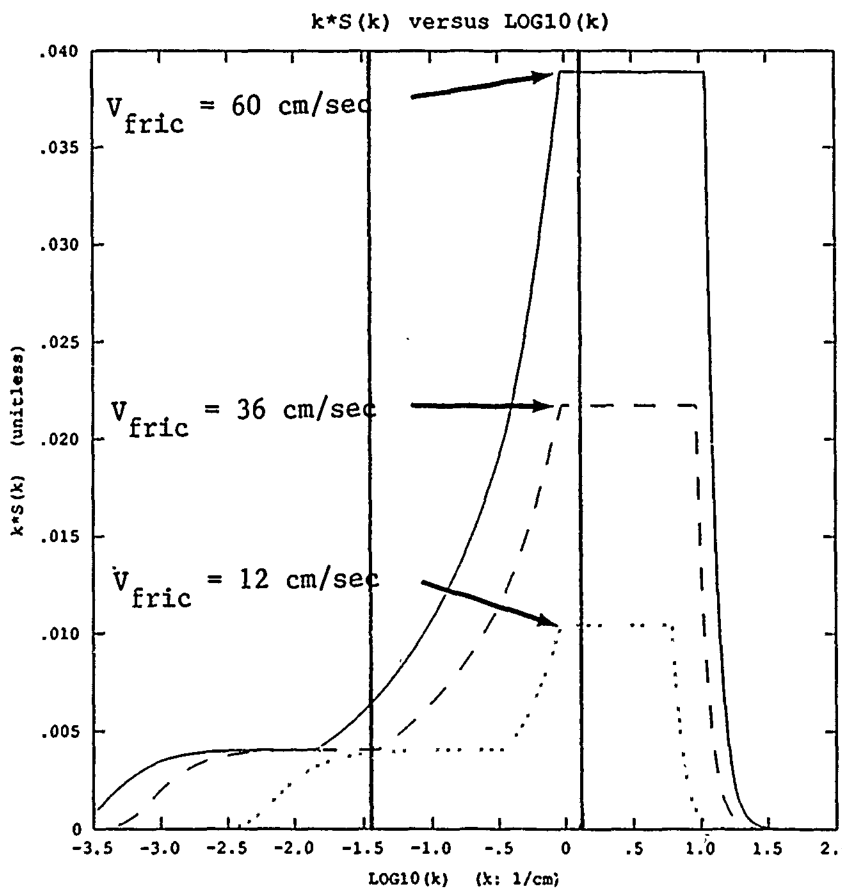

FIGURE 2.2:17. The 1D Pierson-Stacy slope power spectrum k*S(k) versus LOG10(k).

the current study model, that is

$$k1 = kmax/(n/2) = (1.2/cm)/(64/2) = 0.0375/cm \qquad [2.2:36]$$

The middle line represents the integration of variance up to k2 = 1.2/cm = kmax. kmax is the maximum spatial frequency

for the current study model. The upper line represents the integration of variance over the entire range of wavenumber. The points represent the measurements of Cox and Munk [1954b].

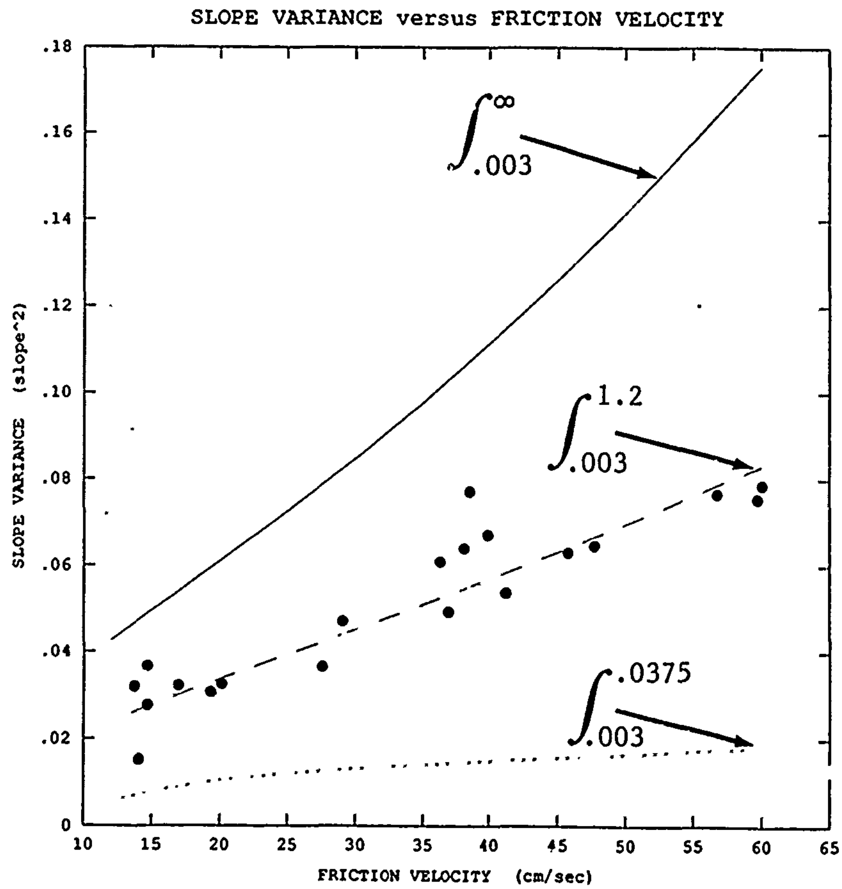

FIGURE 2.2:18. Slope Variance versus Friction Velocity.

Figures 2.2:1, 2.2:17, and 2.2:18 are identical in magnitude to Figures 8.3, 8.4, and 9.1 of Pierson and Stacy [1973]. Note that there is a large fraction of the total slope

variance above $k = 1.2/\text{cm}$. For this and preceding studies, this fraction represents the sub-resolution slope variance; its effect on the spatial attentuation of the reflected and refracted radiance will be introduced into this study by a correlation filter model described in Chapter 2.5.

2.3 Synthesis of Skydome Downwelling Radiance

Chapman & Irani Model

Chapman and Irani [1981] incorporated a combination of the modified clear-sky luminance model of Hopkinson [1954] and the pure Rayleigh-scattering polarization model. The analytic Hopkinson model is defined:

$$L_{sky}(mu,nu) = L_{ref} * A * B \qquad [2.3:1]$$

where

$L_{sky}(mu,nu)$ = the downwelling radiance at skydome coordinates (mu,nu),

mu = the zenith angle to the skydome location [0:+90 deg],

nu = the azimuth angle to the skydome location [-180:+180 deg],

$L_{ref} = L_{sky}(0,0)$ = the reference radiance at zenith, [2.3:2]

$$A = (1+COS(mu_0)^2)/(1-COS(mu_0)^2), \qquad [2.3:3]$$

$$B = 1-EXP(-0.32*SEC(mu)), \qquad [2.3:4]$$

and

$$COS(mu_0) = COS(theta_0)*COS(mu) + SIN(theta_0)*SIN(mu)*COS(nu-phi_0) \qquad [2.3:5]$$

such that

mu_0 = the angle from the sun to a sky element,

$theta_0$ = the zenith angle to the sun,

and

phi_0 = the azimuth angle to the sun.

Hopkinson's model was one of the earlier responses to a 1953 CIE proposal to establish a standard, analytic clear-sky radiance distribution to serve as a basis for daylight factor calculations. A broadband telephotometer was modified to measure the integrated radiance over a 5-degree Instantaneous Field Of View (IFOV). The actual measurements used in this model were made under the clear blue skies of Stockholm (approximately 60 degrees North latitude).

Current Study Model

This study uses the current CIE standard, analytic clear-sky radiance distribution [CIE,1973] for the sole reason that it is a current, accepted standard:

$L_{sky}(mu,nu) = L_{ref} * A * B / C$ [2.3:6]

where

$A = 0.91 + 10*EXP(-3*mu_0) + 0.45*COS(mu_0)^2$, [2.3:7]

$B = 1 - EXP(-0.32/COS(mu))$, [2.3:8]

and

$C = 0.274*(0.91+10*EXP(-3*theta_0)+0.45*COS(theta_0)^2$. [2.3:9]

All other parameters are as previously defined. Although

both the CIE model and the Hopkinson model provide broadband spectral radiance values, the results from the CIE model must be used with caution when applied to the narrowband spectral radiance in the vicinity of the peak solar spectral radiance, particularly in the vicinity of 460 nanometers. Chapman and Irani [1981] applied the Hopkinson model to their model requirement for a near-infrared narrowband distribution and noted that "measurements of sky radiance which we have made show [L_{ref}] varies more than a factor of 3 for apparently clear skies."

This study requires only a reasonable relative spatial distribution of radiance and does not attempt to acquire absolute radiance values. Therefore, the convention used in this study sets the value of L_{ref} such that the radiance at the solar location is equal to 100.0 in arbitrary units of radiance. All other radiance values can be expressed as a relative percentage of the total radiance in the vicinity of the sun.

Figures 2.3:1 and 2.3:2 illustrate two of the 11 synthetic total skydome radiance distributions used in this study, for a solar azimuth of -45 degrees and solar zenith angles of 0.0 and 53.2 degrees, respectively. The arrows in these

(and following) figures point to zero azimuth.

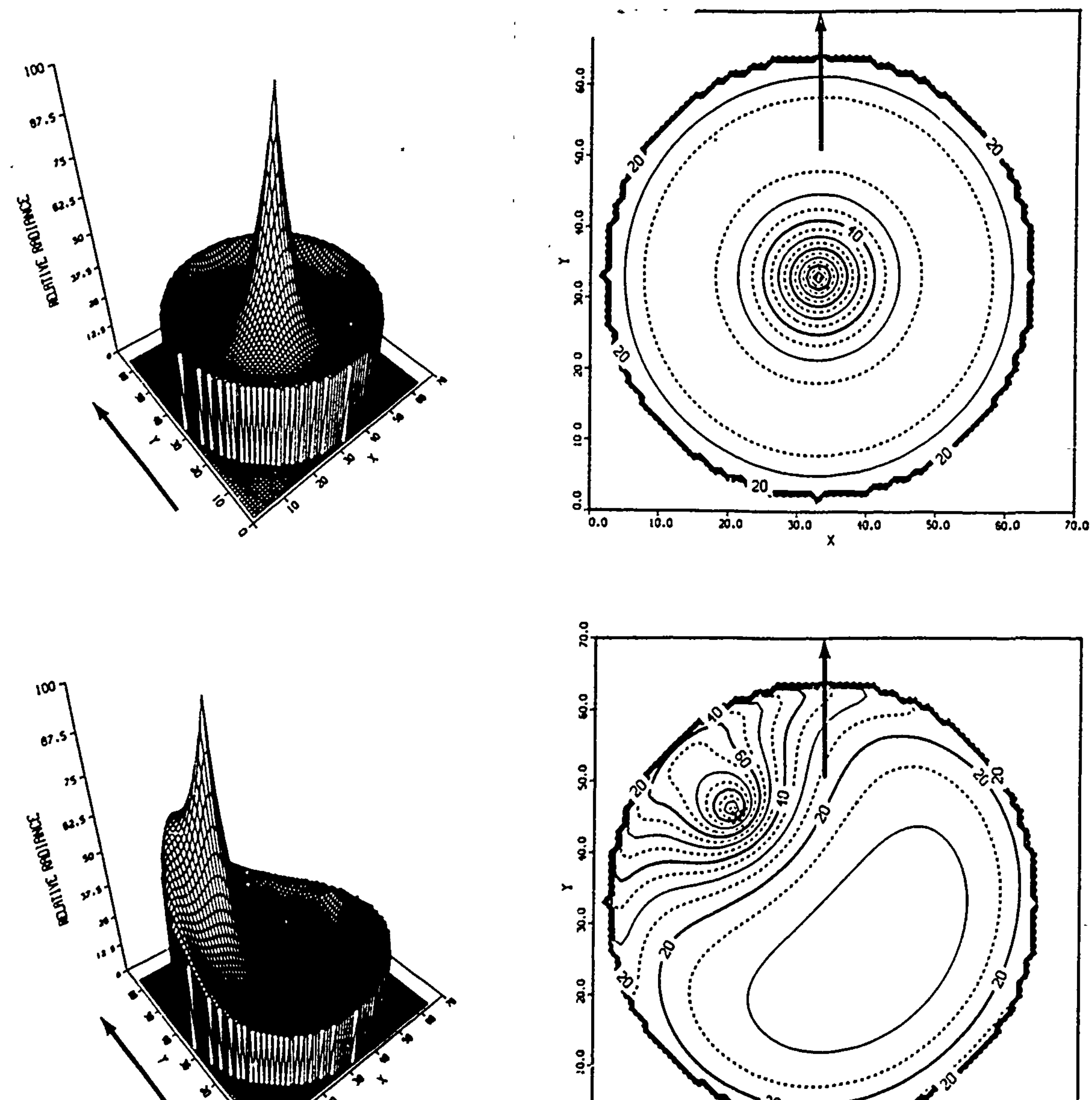

FIGURES 2.3:1-2. Synthetic skydome radiances distributions.

Polarized Rayleigh Scattering Model

The fraction of the unpolarized solar radiance that is horizontally polarized by Rayleigh scattering in the atmosphere is defined:

$$H = 0.5*(1-psi)+psi*COS(nu_0)^2 \qquad [2.3:10]$$

where

$$psi = 0.94*(1-COS(mu_0)^2)/(1+COS(mu_0)^2), \qquad [2.3:11]$$

and

$$nu_0 = ACOS[SIN(theta)*COS(theta_0) - SIN(theta_0)*COS(theta)*COS(phi-phi_0)/SIN(mu_0)]. \qquad [2.3:12]$$

Likewise, the fraction of the unpolarized solar radiance that is vertically polarized by Rayleigh scattering in the atmosphere is defined:

$$V = 0.5*(1-psi)+psi*(1-COS(nu_0)^2). \qquad [2.3:13]$$

All other parameters are as previously defined: nu_0 is the angle between the vector parallel to the direction of polarization and the projection of that vector onto the surface coordinate plane. psi includes the multiplicative depolarization term defined by Coulson [1975] to account for anisotropy of scattering.

Figures 2.3:3 and 2.3:4 illustrate the horizontally polarized component of the total radiance distributions illustrated in Figures 2.3:1 and 2.3:2.

Figures 2.3:5 and 2.3:6 illustrate the vertically polarized component of the total radiance distributions illustrated in Figures 2.3:1 and 2.3:2.

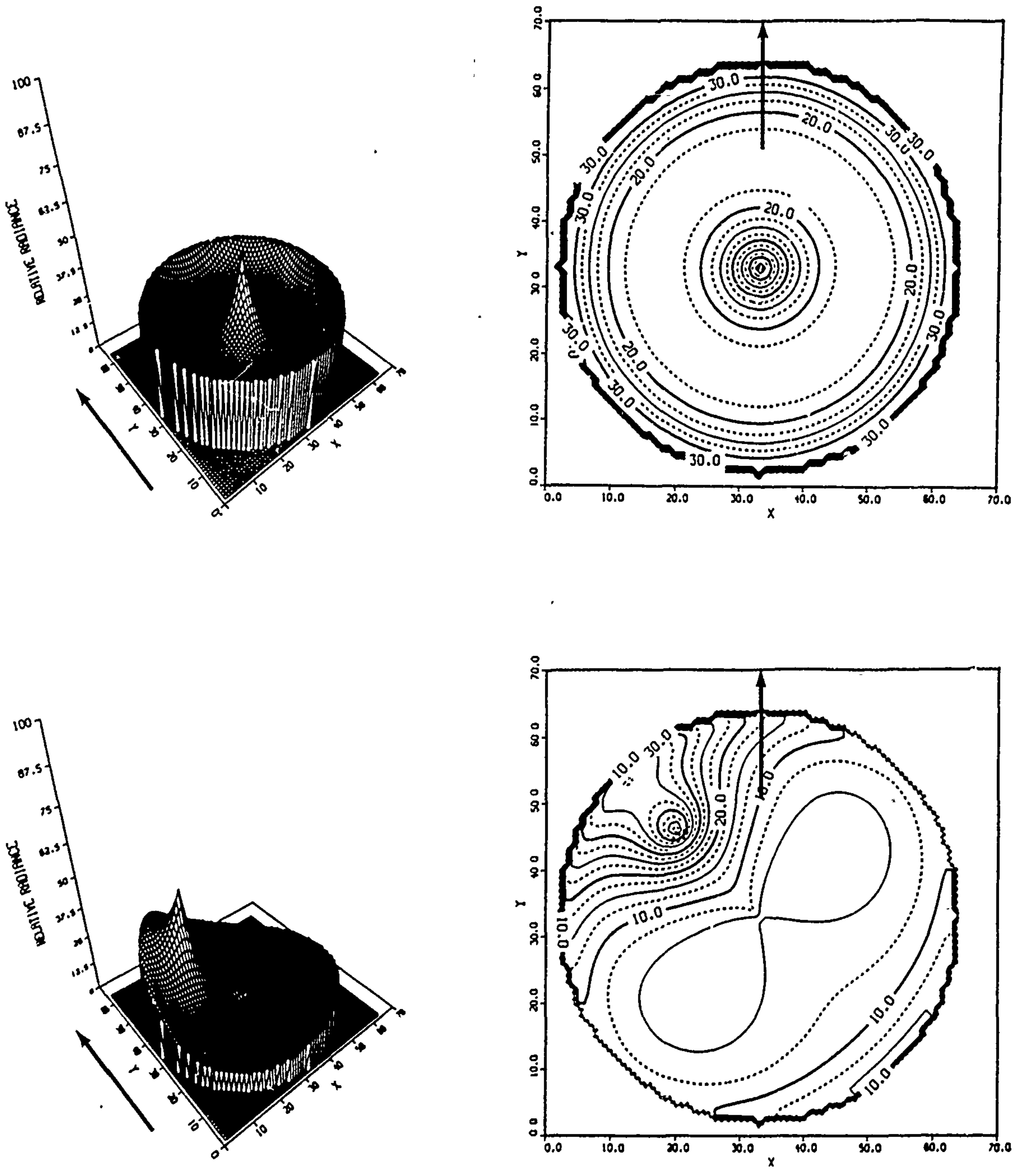

FIGURES 2.3:3-4. Horizontally polarized radiance components.

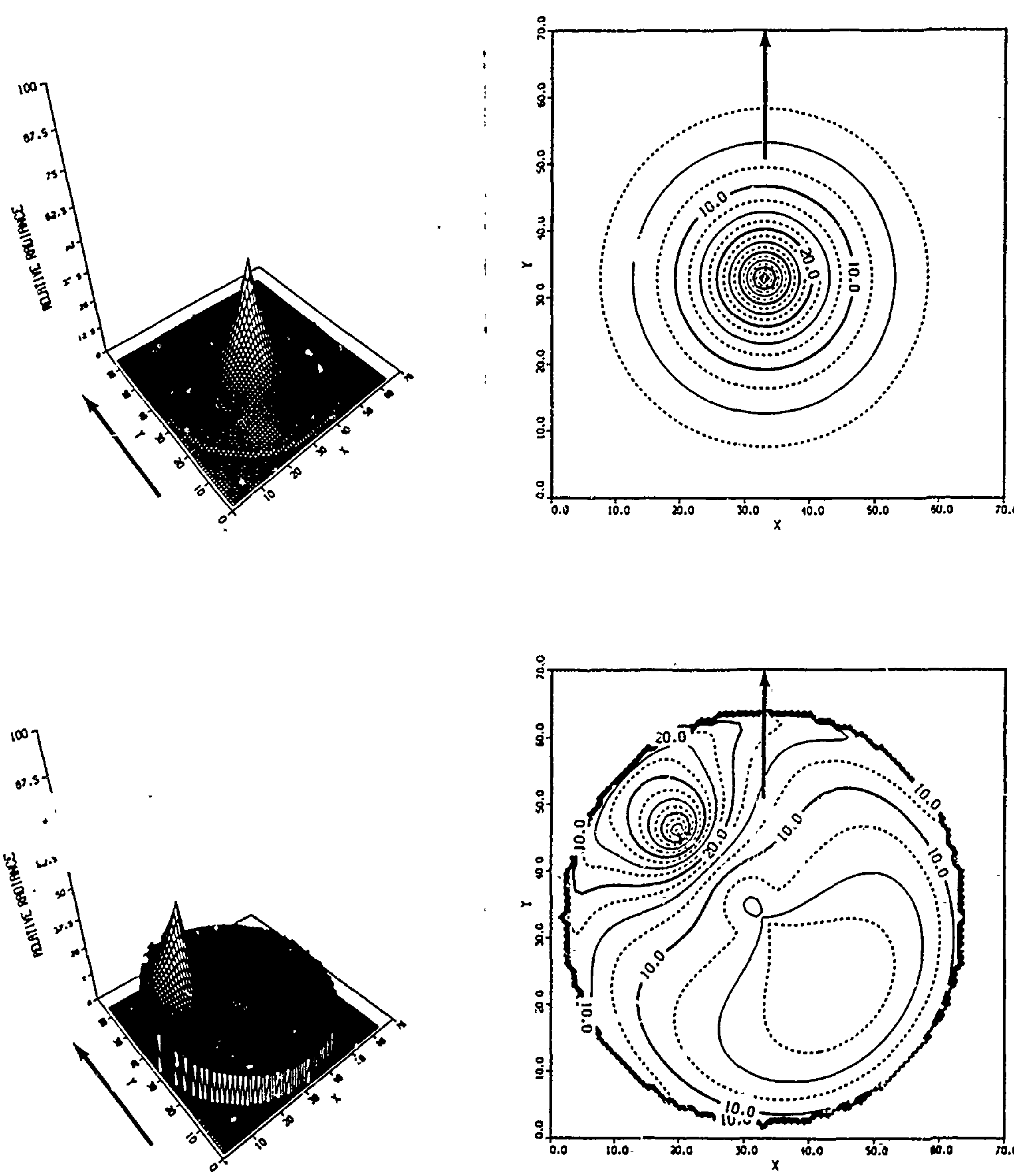

FIGURES 2.3:5-6. Vertically polarized radiance components.

2.4 Synthesis of Subsurface Upwelling Radiance

Introduction

Existing linear or linearizable models for subsurface upwelling radiance employ one or more limiting assumptions:

1) the existence of a flat water surface,

2) an homogeneous subsurface profile,

3) a single-scattering approximation (i.e. clear or shallow water),

4) direct solar illumination only, and/or

5) diffuse sky illumination only [Aas,1987; Gordon et al., 1975; Gordon & McCluney,1975; Philpot,1987; Zaneveld,1982].

The minimum subsurface model for this synthesis must assume an homogeneous deepwater subsurface profile in order to simplify several radiometric and mechanical considerations:

1) the bottom is not visible and therefore not a radiometric factor,

2) surface waves do not mechanically refract (as they would in shallow water) and impart energy to the bottom,

3) the interaction of wave energy with subsurface waters is sufficient to make the inherent optical properties of the subsurface homogeneous at all radiometrically significant

depths, and

4) the subsurface is homogeneous to a sufficient optical depth in order to assume that the subsurface hemispheric radiance distribution (the 'subdome') is spatially invariant with respect to the image sample area of the water surface, i.e. the model assumes that each image sample area on the water surface 'sees' the same subsurface radiance distribution.

The calculation of upwelling subsurface radiance in the presence of a non-smooth water surface is complicated by several factors:

1) attenuation and refraction of the above-surface downwelling radiance by the rough water surface,

2) absorption and back-scattering (single or multiple) of the below-surface downwelling radiance due to the inherent optical properties of the water and its constituents,

3) attenuation and refraction of the below-surface upwelling radiance by the rough water surface, and

4) localized total internal reflection of the below-surface upwelling radiance where the angle between the surface normal vector and the upwelling radiance vector exceeds the critical angle (48.8 degrees at 460 nanometers).

A complete synthetic model for upwelling subsurface radiance would fully accommodate its parametric dependence on the four inherent optical properties of natural waters [Gordon et al.,1975]:

a = the absorption coefficient,

b = the scattering coefficient,

c = the attenuation coefficient, and

B(theta) = the volume-scattering coefficient,

with the following inter-relations:

c = b + a , and

$$b = 2*pi* \int_{0}^{pi} B(theta)*SIN(theta)*dtheta.$$

Two nonlinear integrations would be applied to accommodate attenuation of a non-flat water surface. The first integration would angularly distribute the refracted downwelling surface radiance based upon the slope distribution of the total surface area of the image. The second integration would angularly distribute the refracted upwelling subsurface radiance based upon the individual slope distribution of each image sample area.

In essence, at least three independent nonlinear operations would be required to compute the subsurface upwelling radiance; one intermediate operation for the single-scattering model. The only successful technique that can adequately model this level of complexity (and higher) is a Monte Carlo simulation [Plass & Kattawar,1969], a method which is beyond the scope of this study.

Chapman & Irani Model

No subsurface model was defined by Chapman and Irani [1981] because they included the assumption of spectral sensing in the infrared where transmittance through water approaches zero.

Current Study Model

The approach for this study is to employ the results of previous Monte Carlo simulations as ad hoc analytic models. Results have been published by Plass, Kattawar and Guinn [1975,1976] and will be used with the following assumptions:

1) the results are valid in a narrowband spectral region centered at 460 nanometers (which is near the wavelength of maximum transparency for clear water),

2) the optical depth tau of water is 10 at this wavelength,

3) the bottom layer has unit absorption, and

4) the results are valid over a broad band of wind velocities centered at 1030 cm/sec (measured at a height of 1950 cm). (This is equivalent to a friction velocity of 36 cm/sec for an homogeneous wind profile.)

Figures 2.4:1 through 2.4:5 illustrate the Monte Carlo results of Plass, Kattawar and Guinn [1976] for solar zenith angles of 0, 15, 32, 57, and 80 degrees, respectively.

The upwelling subsurface radiance observed just above the surface is given the following approximate analytic expression relative to L_{ref}, the reference sky radiance at zenith:

L_w(beta,alpha) = L_{ref}*R_0*C*(1+COS(A*beta)^2)/2.0 [2.4:1]

where

L_w(beta,alpha) = the upwelling subsurface radiance observed at the wave-slope coordinates (beta,alpha),

beta = the maximum wave-slope angle [0:+90 deg],

alpha = the azimuth angle to the wave-slope angle beta [-180:+180 deg],

L_{ref} = L_{sky}(0,0) = the reference radiance at zenith, [2.4:2]

R_0 = 0.0208 = the unpolarized Fresnel reflectivity at normal

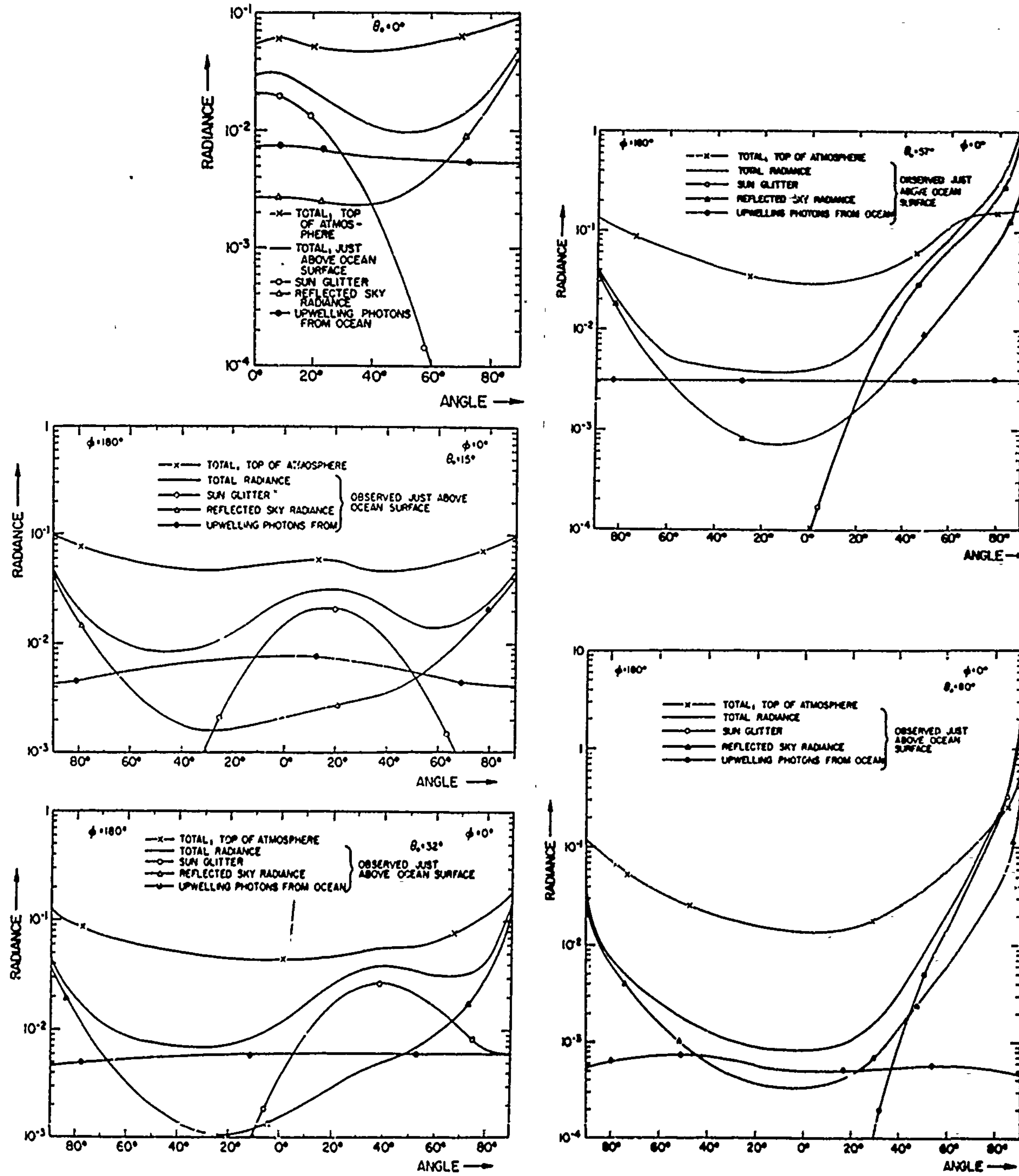

FIGURES 2.4:1-5. Monte Carlo scattering results. (from Plass, Kattawar & Guinn,1976)

incidence at 460 nanometers, [2.4:3]

$C = 0.32*10^{B}$, [2.4:4]

$A = COS(theta_0)^2$, [2.4:5]

and

$B = SIN(1.1*theta_0)^{SQRT(3)}$ [2.4:6]

such that

$theta_0$ = the zenith angle to the sun.

Note that this model has no dependence on phi_0, the azimuth angle of the sun.

Again, this study requires only a reasonable relative spatial distribution of radiance and does not attempt to compute absolute radiance values. Therefore, the value of L_{ref} is set such that the radiance at the solar location is equal to 100.0 in arbitrary units of radiance. All other radiance values can then be expressed as a percentage of the total radiance in the vicinity of the sun.

Figures 2.4:6 and 2.4:7 illustrate the two synthetic total subdome radiance distributions for solar zenith angles of 0.0 and 53.2 degrees, respectively.

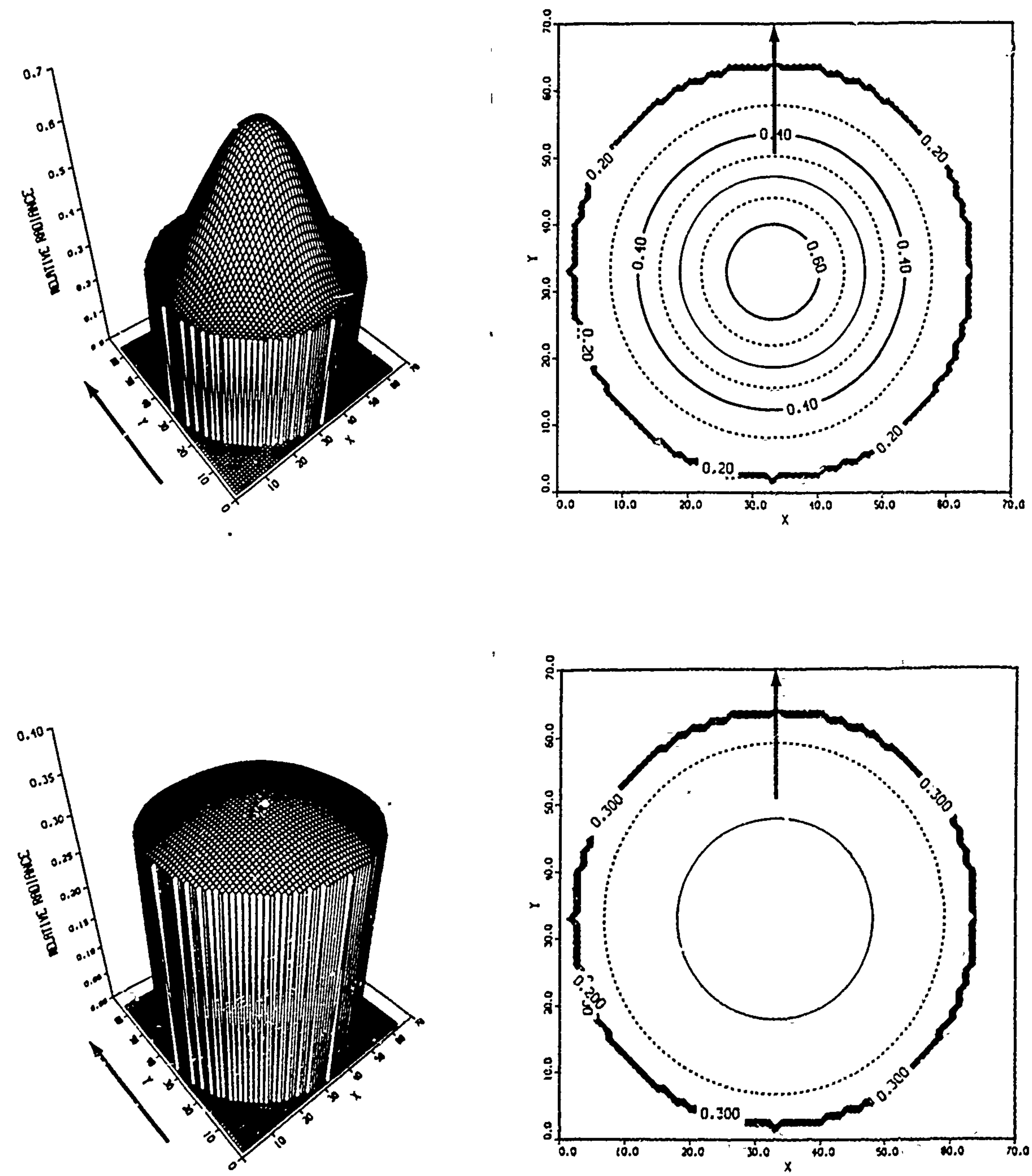

FIGURES 2.4:6-7. Synthetic subdome radiance distributions.

Depolarized Random Scattering Model

Both Beckmann and Spizzichino [1963] and Konnen [1985] give evidence that the effect of rough water surfaces on the propagation of polarized downwelling radiance through the surface is a depolarization, either through multiple reflections or turbulent refraction. Therefore, this model will assume equal fractions of horizontally and vertically polarized radiance:

$$H = V = 0.5 \qquad [2.4:7]$$

Figures 2.4:8 and 2.4:9 illustrate the identical horizontally and vertically polarized components of the total upwelling subsurface (subdome) radiance distributions illustrated in Figures 2.4:6 and 2.4:7.

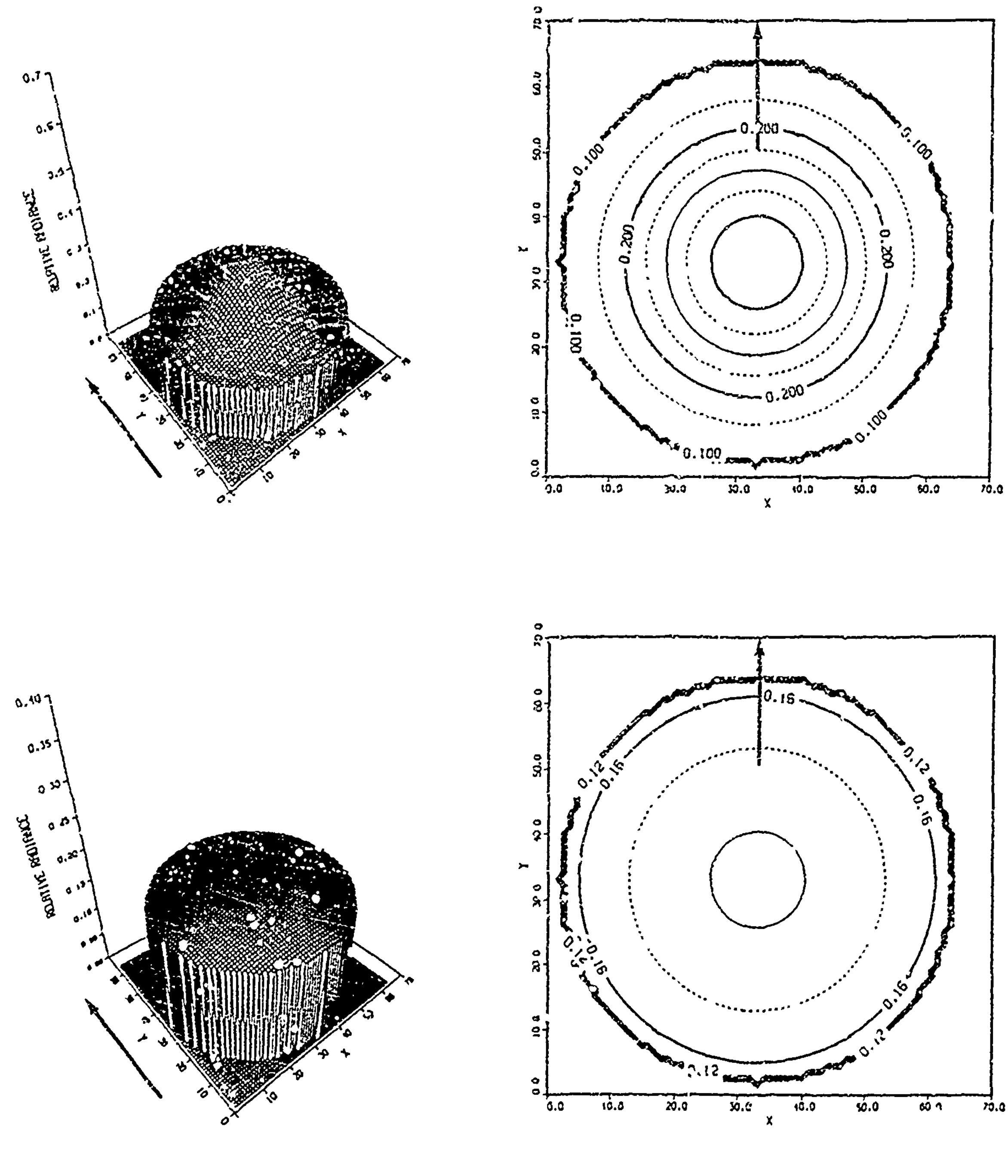

FIGURES 2.4:8-9. Horizontally and vertically polarized components of the synthetic subdome radiance distributions.

2.5 Synthesis of Reflected Skydome Radiance

Chapman & Irani Model

Chapman and Irani [1981] incorporated a variant of the law of Malus into their calculation of reflected skydome radiance:

$$L_r = R*L_{sky}, \qquad [5.2:1]$$

where

R = the Fresnel reflectivity (for arbitrary polarization),

and

L_{sky} = the sky radiance (for arbitrary polarization).

Their paper does not indicate whether the attenuation due to surface-slope projection was incorporated in their model.

Current Study Model

The radiance reflected from the water surface is calculated by the same method used by Cox and Munk [1954a] and Saunders [1967]:

Consider a small specular facet of the sea surface with area dA that is inclined from the zenith by the angle beta. The projection of the facet onto a horizontal surface is

$dA_h = dA*COS(beta)$. [2.5:2]

Likewise, the actual area of the sloping facet is

$dA = dA_h*SEC(beta)$. [2.5:3]

The projection of the actual facet area onto a plane normal to the incident radiance is

$dA_i = dA*COS(omega) = dA*COS(theta-beta)$

$= dAh*SEC(beta)*COS(omega)$, [2.5:4]

where

omega = the angle of incidence,

and

theta = the zenith angle of reflection.

Consider the probability distribution for surface slopes:

$Pr(beta,alpha) = Pr(s_x,s_y) = Pr(dz/dx,dz/dy)$ [2.5:5]

where

alpha = the azimuth angle to maximum slope angle beta,

and

dz/dx,dz/dy = the slope components unique to beta and alpha such that

$dA_h = dx*dy$, [2.5:6]

$$\mathrm{TAN}(s_x) = \mathrm{TAN}(dz/dx) = \mathrm{TAN}(beta)*\mathrm{COS}(alpha), \qquad [2.5:7]$$

and

$$\mathrm{TAN}(s_y) = \mathrm{TAN}(dz/dy) = \mathrm{TAN}(beta)*\mathrm{SIN}(alpha). \qquad [2.5:8]$$

The projection of the reflected radiance normal to the plane of reflection can then be defined in surface-slope coordinates (beta,alpha) for any small, specular surface facet of slope = beta(alpha):

$$L_r'(beta,alpha) = L_r(beta,alpha)*\mathrm{COS}(theta)$$

$$= R(omega)*L_{sky}(mu,nu)*\mathrm{COS}(omega)*\mathrm{SEC}(beta), \qquad [2.5:9]$$

where

R(omega) = the Fresnel reflectivity of the water facet (for arbitrary polarization),

and

$L_{sky}(mu,nu)$ = the incident radiance of the skydome from the direction (mu,nu) that is reflected normal to the defined plane of reflection (theta = 53.2 deg, phi = 180 deg) for both polarizations. (The calculation of the incident vector coordinates from the reflection and surface normal vector coordinates is defined at the end of this chapter.)

The mean reflection radiance perceived by an observer at the reflection coordinates is similarly defined:

$$\langle L' \rangle = \langle L_r \rangle * COS(theta)$$
$$= \int\int R(omega)*L_{sky}(beta,alpha)*Pr(beta,alpha) *COS(omega)*SEC(beta)*dbetadalpha \qquad [2.5:10]$$

over the full distribution of surface slopes. This value, combined with the small contribution due to refraction, is computed as the central ordinate of the radiance magnitude spectrum, M(0,0), as an ensemble average of spectra. Because the reflection vector (i.e. line of sight) is fixed with respect to the other geometries, L_r can be linearly mapped to surface-slope coordinates (beta,alpha) once the skydome radiance distribution is uniquely determined.

Figure 2.5:1 illustrates the mapping of the function, SEC (beta), to the surface-slope coordinates (beta,alpha). For this illustration, the function was truncated at SEC(60 deg) for values of beta greater than 60 degrees. Note also that the function is not computed for values of beta where
(omega - mu) = (theta - omega) > 90 degrees,
i.e. the regions where surface slopes are not visible with respect to the line of sight.

Figure 2.5:2 illustrates the mapping of the function, COS (omega), to the surface-slope coordinates (beta,alpha).

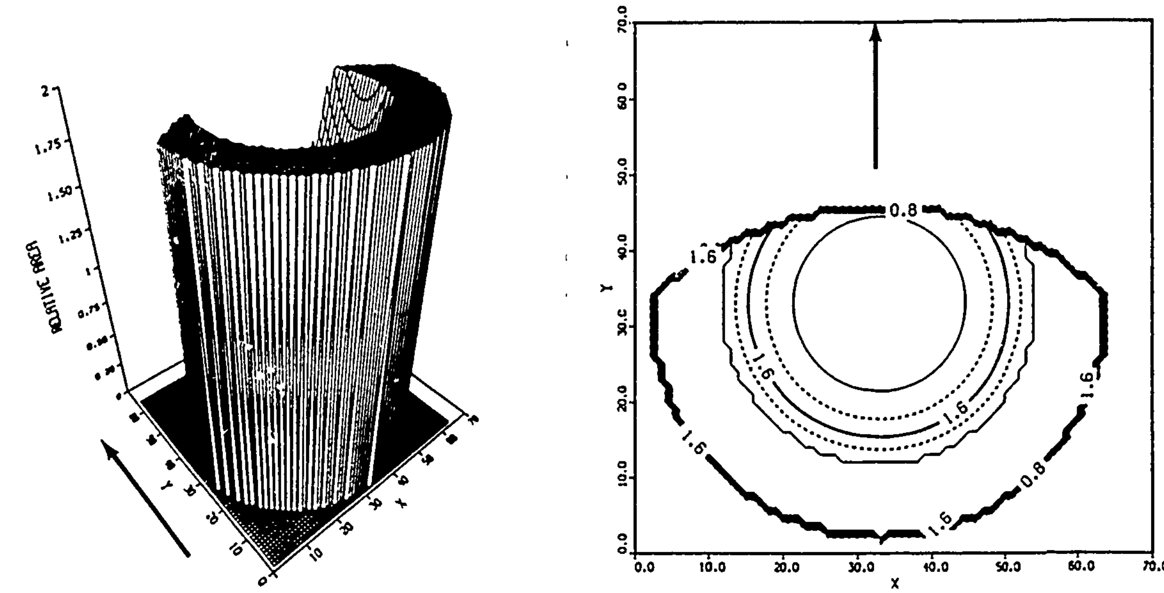

FIGURE 2.5:1. Map of SEC(beta) to coordinates (beta,alpha).

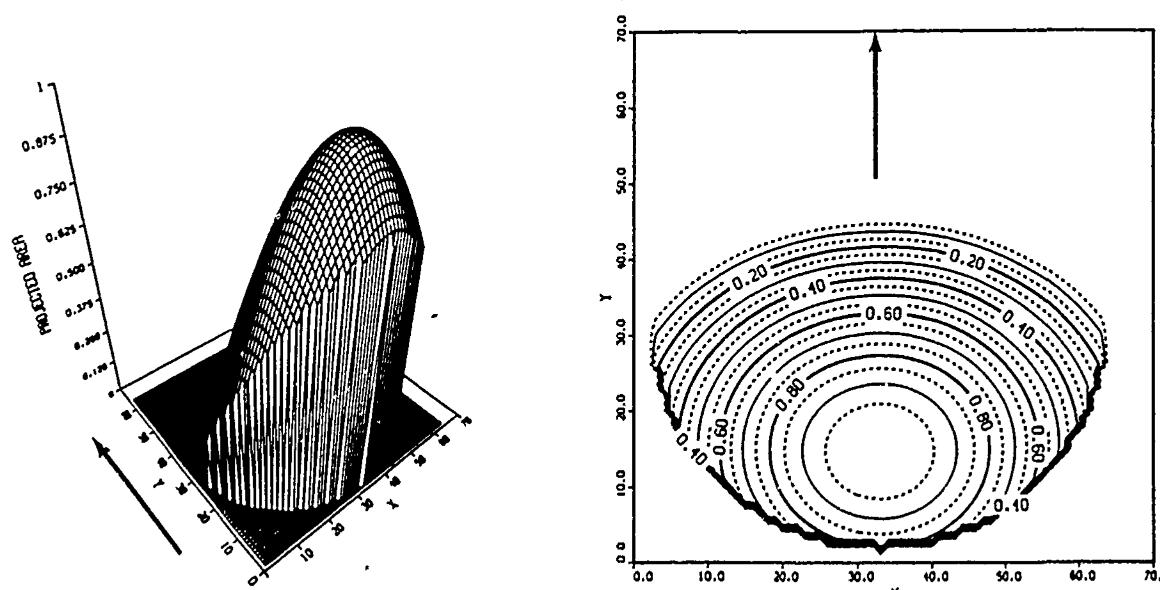

FIGURE 2.5:2. Map of COS(omega) to coordinates (beta,alpha).

Figures 2.5:3 and 2.5:4 illustrate the mapping of Fresnel reflectivity, R(omega), to surface-slope coordinates (beta,alpha) for horizontal and vertical polarizations, respectively.

Figures 2.5:5 and 2.5:6 illustrate the mapping of skydome radiance, L_{sky}(mu,nu), to surface-slope coordinates (beta, alpha) for horizontal and vertical polarization, respectively. The solar zenith angle $theta_0$ in this example is 0 degrees. The original L_{sky} distributions in skydome coordinates (mu,nu) are illustrated in Figures 2.3:3 and 2.3:4.

Figures 2.5:7 and 2.5:8 illustrate the mapping of the reflected skydome radiance, L_r', to the surface-slope coordinates (beta,alpha) for horizontal and vertical polarization, ··vely. The solar zenith angle $theta_0$ in this example is 0 degrees.

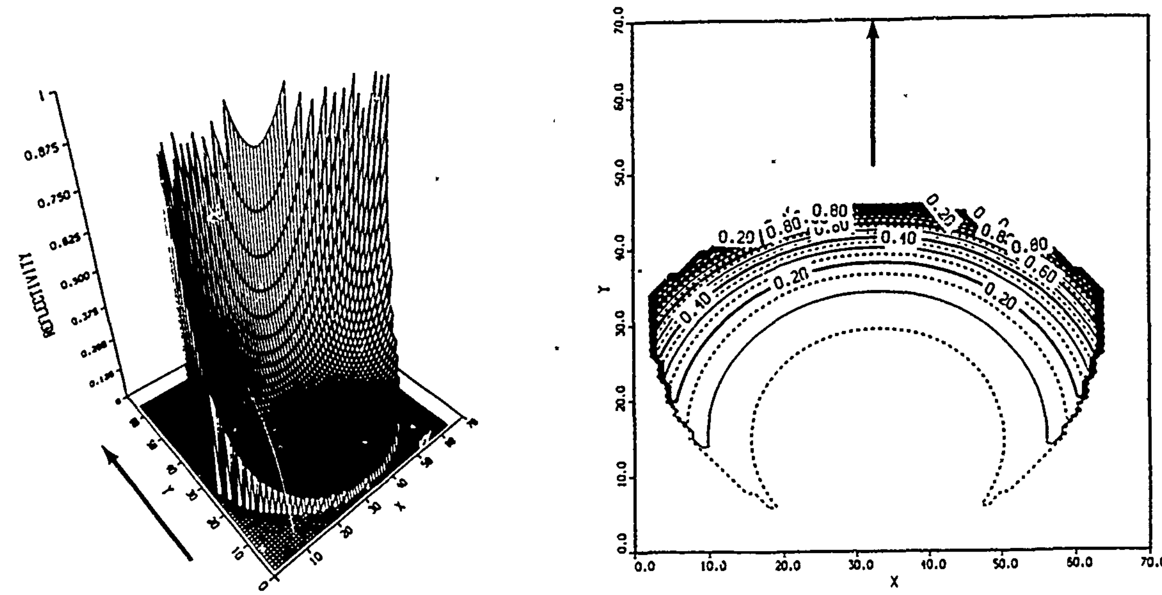

FIGURE 2.5:3. Map of Fresnel reflectivity, R(omega), to coordinates (beta,alpha) for horizontal polarization.

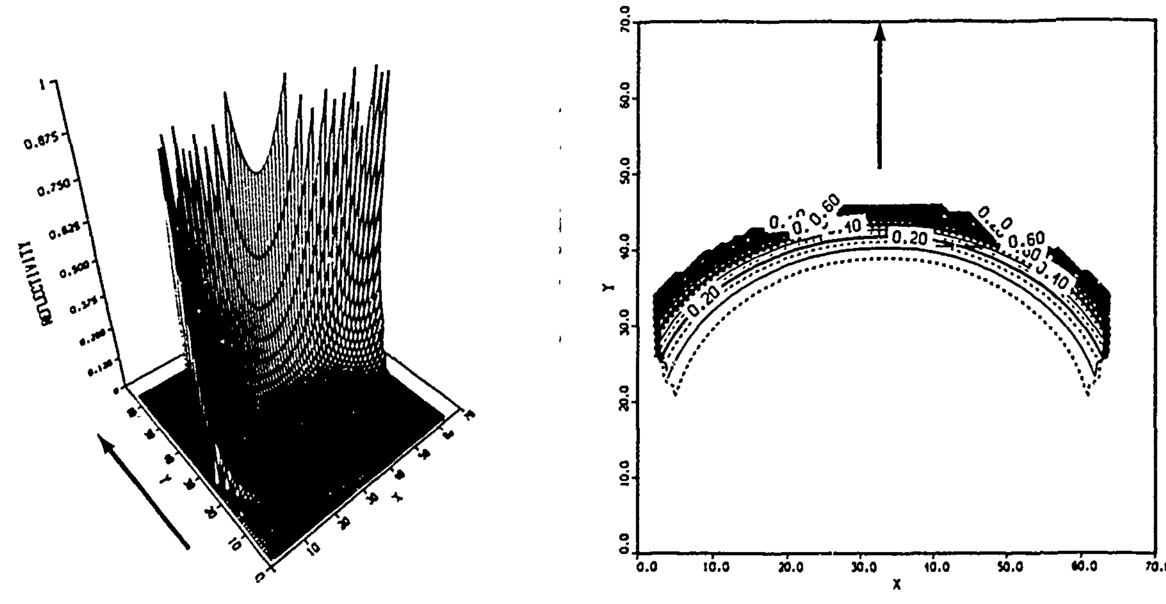

FIGURE 2.5:4. Map of Fresnel reflectivity, R(omega), to coordinates (beta,alpha) for vertical polarization.

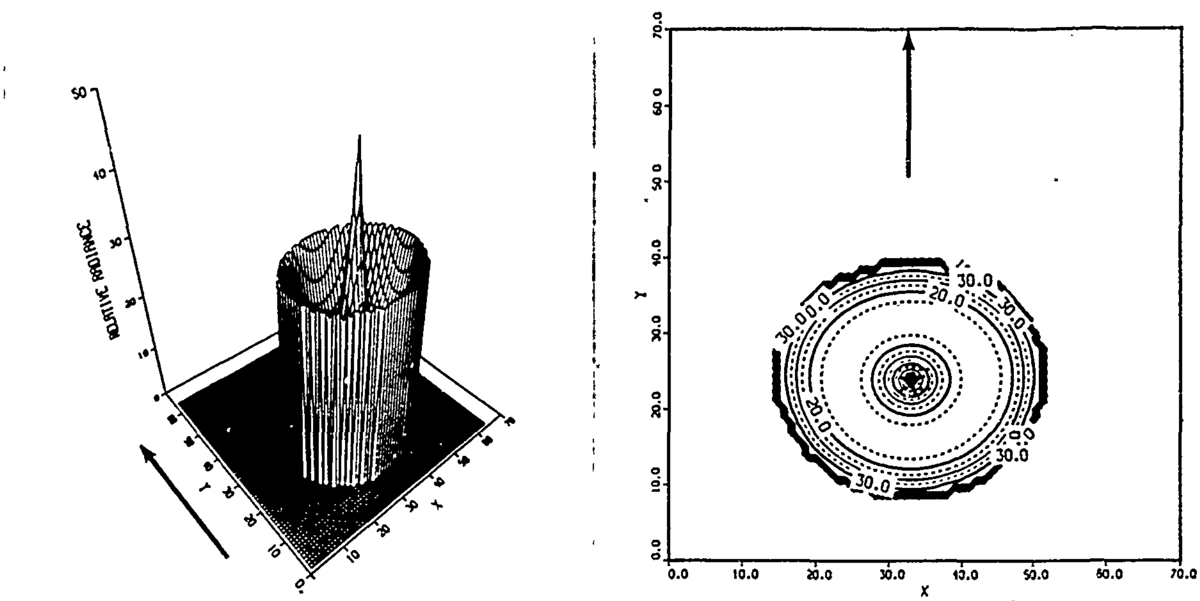

FIGURE 2.5:5. Map of skydome radiance, L_{skv}(mu,nu), to coordinates (beta,alpha) for horizontal polarization.

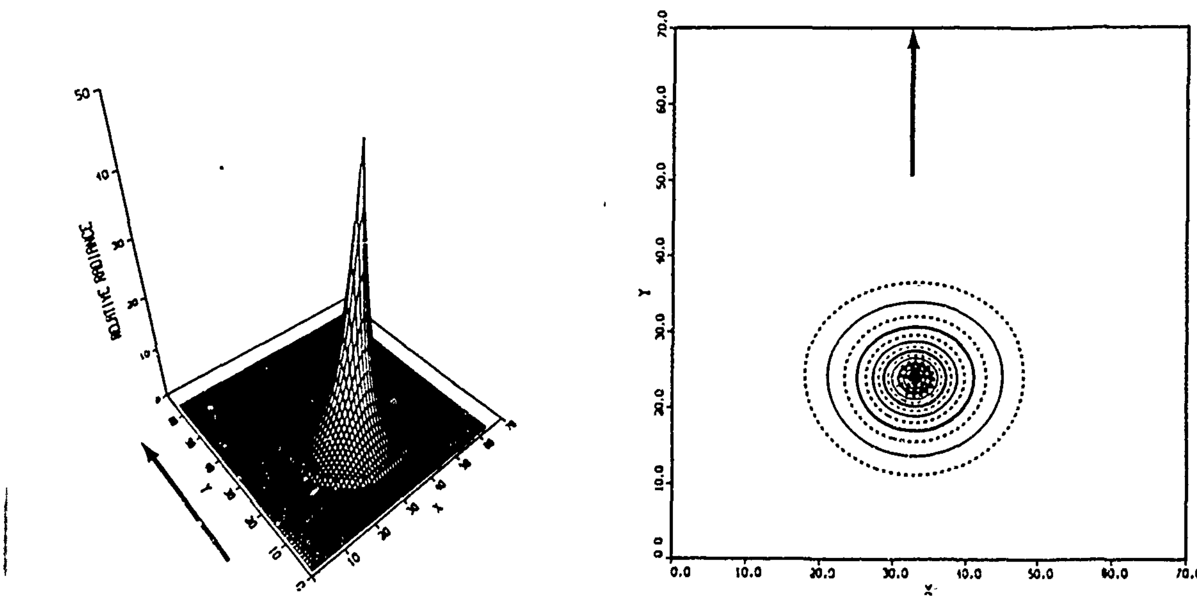

FIGURE 2.5:6. Map of skydome radiance, L_{sky}(mu,nu), to coordinates (beta,alpha) for vertical polarization.

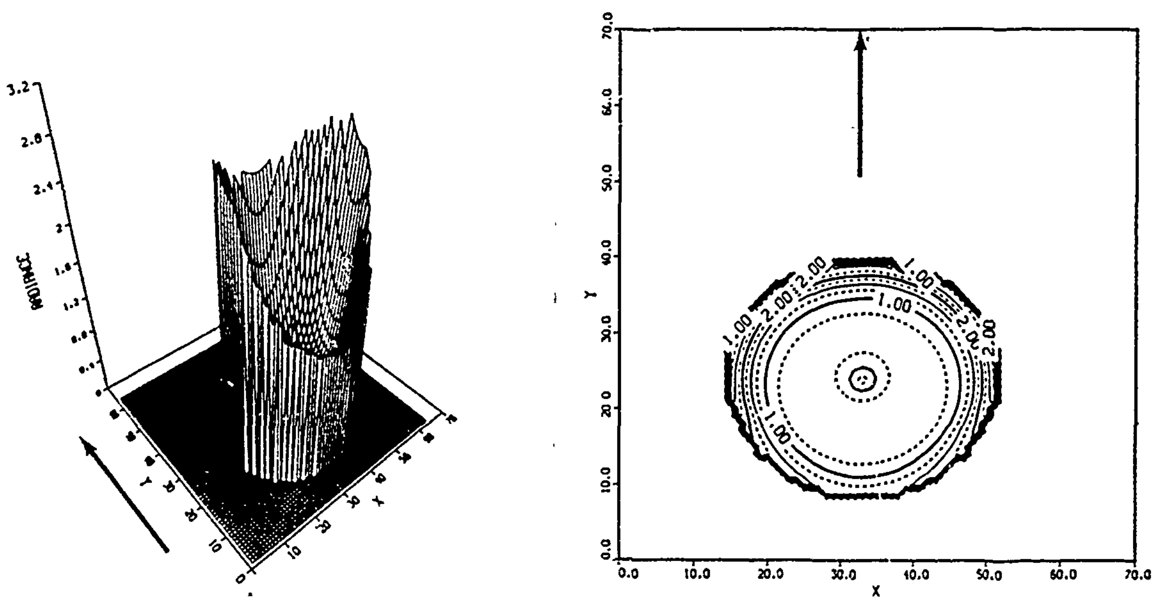

FIGURE 2.5:7. Map of reflected skydome radiance, L_r', to coordinates (beta,alpha) for horizontal polarization.

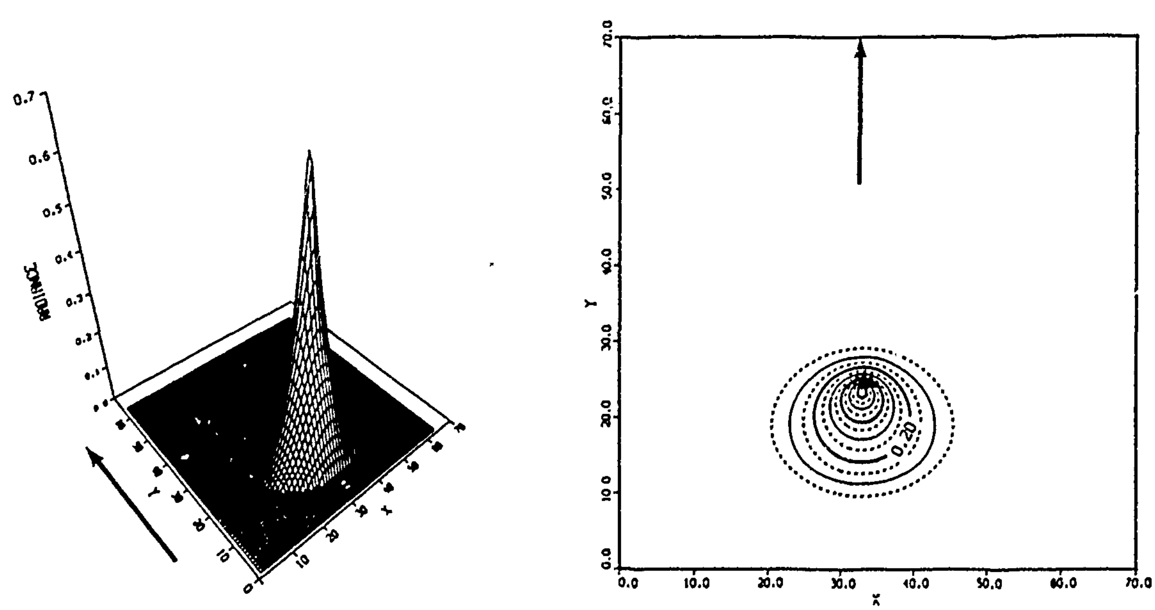

FIGURE 2.5:8. Map of reflected skydome radiance, L_r', to coordinates (beta,alpha) for vertical polarization.

Correlation of Sub-Resolution Wave-Slope Variance

The maximum wavenumber of the current study model is kmax = 1.2 per centimeter to coincide with the results of other studies [Cox & Munk,1954a,b; Pierson & Stacy, 1973]. This corresponds to a sample surface area of

$$A_h = 2.6 \text{ cm} \times 2.6 \text{ cm} = 6.76 \text{ cm}^2 \qquad [2.5:11]$$

which is defined in the literature as the Cox-Munk window.

Because slope spectra (cite Figure 2.2:13) reveal significant slope energy between k = 1.2/cm and k = 30.0/cm, it is important to model the effect of this sub-resolution variance on the reconstruction of wave-slope spectra. However, it is unreasonable to synthesize large surfaces with sampling windows of the order $A_h = 1.0 \text{ mm}^2$, as required to consider k = 30 per centimeter. Previous investigators [Chapman & Irani,1981; Wilf & Manor,1984; Schwartz & Hon, unpub.] all employed the Kirchoff approximation for reflection from rough surfaces [Kajiya,1985; Beckmann & Spizzichino,1963], which essentially replaces a rough surface facet by its mean tangent plane. This approximation is valid only if the rough sub-resolution surface is of low curvature. However, for wind-driven water-wave surfaces, it

is exactly the spectral region above k > 1.0 per centimeter where all the spectral energy of curvature exists.

Figure 2.5:9 illustrates $k^3*S(k)$ versus k, the curvature power spectrum (after Pierson & Stacy, 1973). It is apparent that the Kirchoff approximation is not optimum for this particular circumstance.

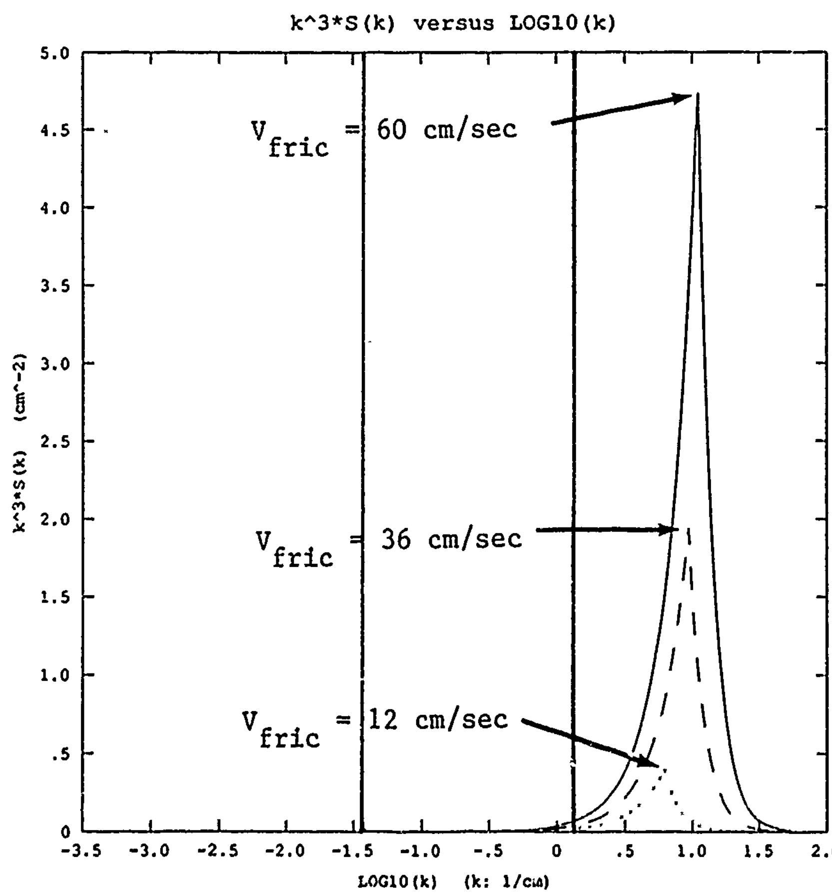

FIGURE 2.5:9. The 1D Pierson-Stacy curvature power spectrum $k^3*S(k)$ versus LOG10(k).

Current Study Model

To quote Stilwell and Pilon:

> "The subresolution waves, especially those in the capillary regime, can have significant slopes. Since they are unresolved on the film, the intensity variations of the sky are partially smoothed. This effect can be observed by examining the reflection of a cloud in a ruffled water surface. As a result the small waves can smooth the sky luminance distribution and allow the use of photographic procedures on days in which the sky is far from a monotonic luminance function. Contingent only on the distribution of sub-resolution waves being homogeneous, the effective luminance distributions may extend the environmental conditions under which optical transforms are useful." [Stilwell & Pilon,1974]

An alternative method, then, for introducing the effect of sub-resolution wave slopes is to assume an homogeneous distribution and use it as a correlation filter to smooth the reflected skydome radiance. The correlation is nonlinear if executed in reflected skydome coordinates (mu,nu). However, a linear correlation is possible if executed in surface slope coordinates (beta,alpha).

The unresolved directional wave-slope variance for the wavenumber range k > 1.2/cm is calculated directly from the Pierson-Stacy model. A directional bivariate normal Gaussian distribution is calculated as a function of along-wind slope variance, cross-wind slope variance, and wind azimuth:

$$Pr'(beta,alpha) = EXP(-(L^2+M^2)/2)/(2*pi*DEV_A*DEV_C), \quad [2.5:12]$$

where

$$L = TAN(beta)*COS(wind\_az-alpha)/DEV_A, \quad [2.5:13]$$

and

$$M = TAN(beta)*SIN(wind\_az-alpha)/DEV_C, \quad [2.5:14]$$

such that

DEV_A = SQRT(along-wind slope variance),

DEV_C = SQRT(cross-wind slope variance),

and

wind_az = the wind azimuth (with 180-degree ambiguity).

The directional distribution of sub-resolution wave slopes, Pr'(beta,alpha), is then correlated with the reflected sky-dome radiance, L_r'(beta,alpha),

$$L_r''(beta,alpha) = \int\int L_r'(b,a)*Pr'(b-beta,a-alpha)*dadb$$
$$= L_r'(beta,alpha) \star\star Pr'(beta,alpha), \quad [2.5:15]$$

which follows directly from Equations [2.5:9] and [2.5:10]. (The ★ ★ denotes the double correlation operation.)

Note that because the sub-resolution wave-slope distribution is assumed to be both homogeneous and symmetric about its central ordinate, Equation [2.5:15] could also be implement-

ed as a double convolution operation:

$$L_r''(\text{beta,alpha}) = L_r'(\text{beta,alpha}) \bigstar\bigstar \, Pr'(\text{beta,alpha})$$
$$= Lr'(\text{beta,alpha}) \bullet\bullet \, Pr'(\text{beta,alpha}). \qquad [2.5:16]$$

Figure 2.5:10 is the sub-resolution wave-slope distribution for a friction velocity of 12.0 cm/sec and a wind azimuth of -45 deg (or +135 deg with ambiguity).

Figures 2.5:11 and 2.5:12 illustrate the correlation of Lr', the reflected skydome radiance (Figures 2.5:7 and 2.5:8), with Pr', the sub-resolution wave-slope distribution.

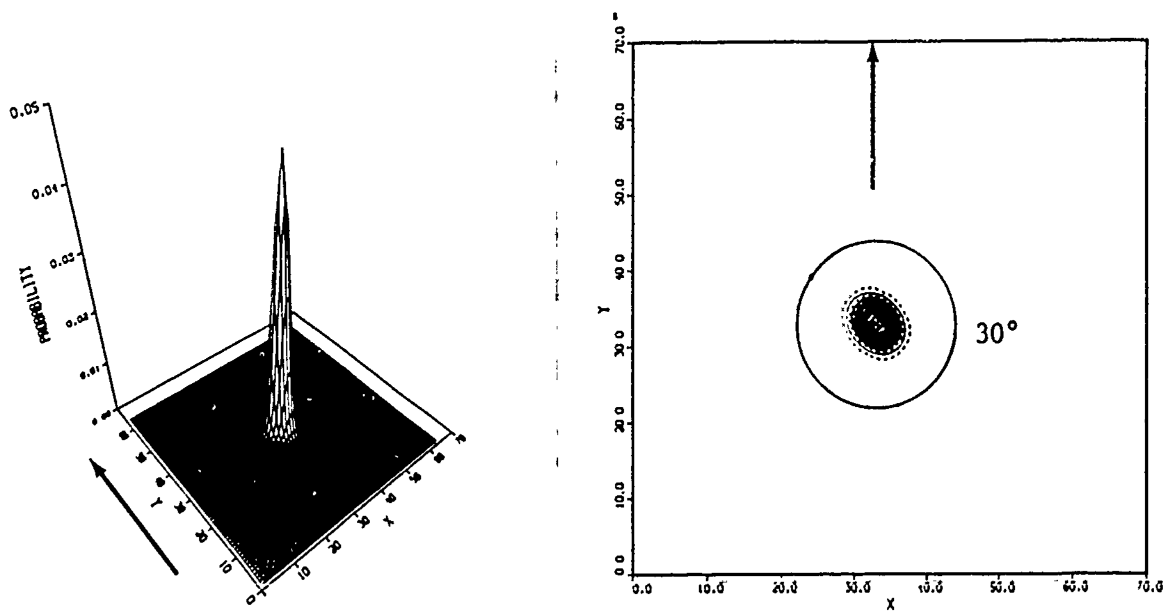

FIGURE 2.5:10. Sub-resolution wave-slope distribution Pr' for v_{fric} = 12.0 cm/sec and wind_az = -45 deg.

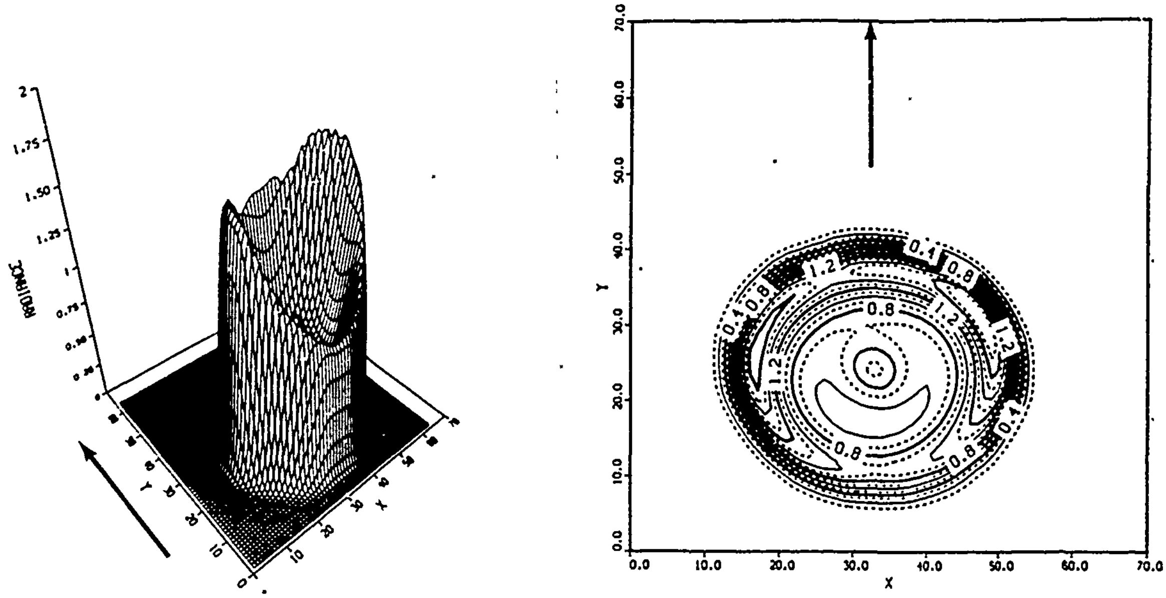

FIGURE 2.5:11. Effect of correlation of L_r' with sub-resolution wave-slope distribution Pr' (horizontal polarization).

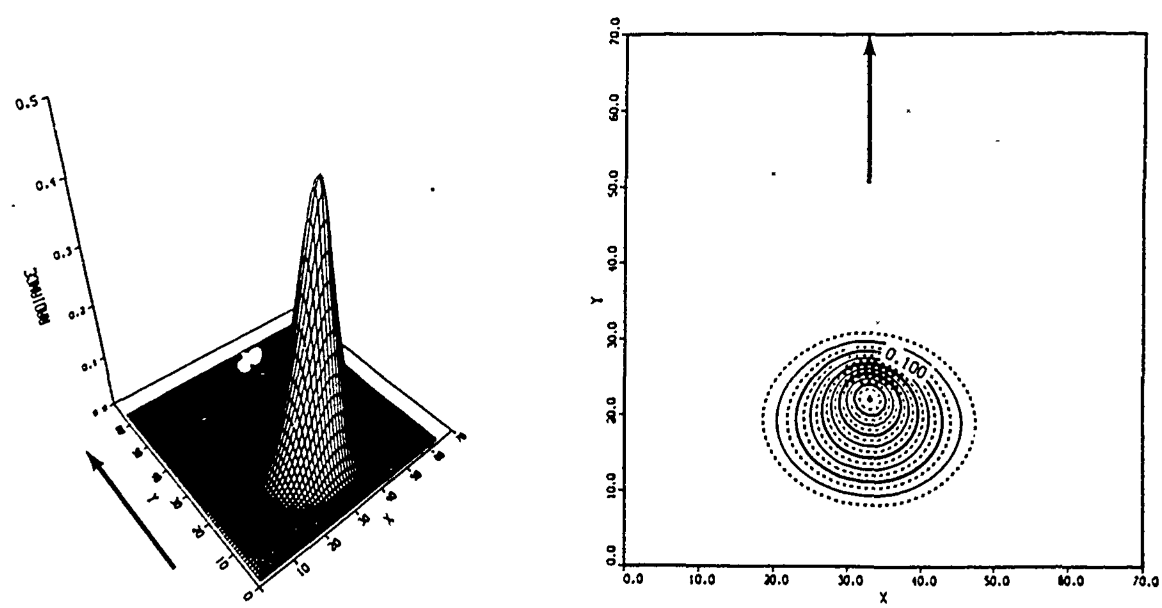

FIGURE 2.5:12. Effect of correlation of L_r' with sub-resolution wave-slope distribution Pr' (vertical polarization).

Calculation of Reflection Angular Coordinates

The angular coordinates that describe the ray path due to reflection can be calculated if two of three vectors (the surface normal vector N, the incident vector I, and the reflection vector R) are known.

Figure 2.5:13 illustrates the geometric relations and nomenclature for the current study model.

The reflection vector is fixed in this model. The observer is located at an azimuth angle phi of 180 degrees and zenith angle theta of 53.2 degrees (the Brewster angle) relative to the point of observation. The reflection vector R can be resolved into its unit vector coordinates in (x,y,z) space:

R_x = SIN(theta)*COS(180 deg), [2.5:17]

R_y = SIN(theta)*SIN(180 deg), [2.5:18]

and

R_z = COS(theta). [2.5:19]

The surface normal vector N and the incident vector I can be similarly resolved:

N_x = SIN(beta)*COS(alpha), [2.5:20]

$$N_y = SIN(beta)*SIN(alpha), \quad [2.5:21]$$

and

$$N_z = COS(beta); \quad [2.5:22]$$

$$R_x = SIN(mu)*COS(nu), \quad [2.5:23]$$

$$R_y = SIN(mu)*SIN(nu), \quad [2.5:24]$$

and

$$R_z = COS(mu). \quad [2.5:25]$$

Because the vector N must be in the plane containing I and R and because it must also bisect the angle between I and R, the following equations have unique solutions:

$$IN = RN = COS(omega), \quad [2.5:26]$$

$$IR = COS(2*omega), \quad [2.5:27]$$

$$N = (R - I)/(2*COS(omega), \quad [2.5:28]$$

and

$$R = N*2*COS(omega) - I. \quad [2.5:29]$$

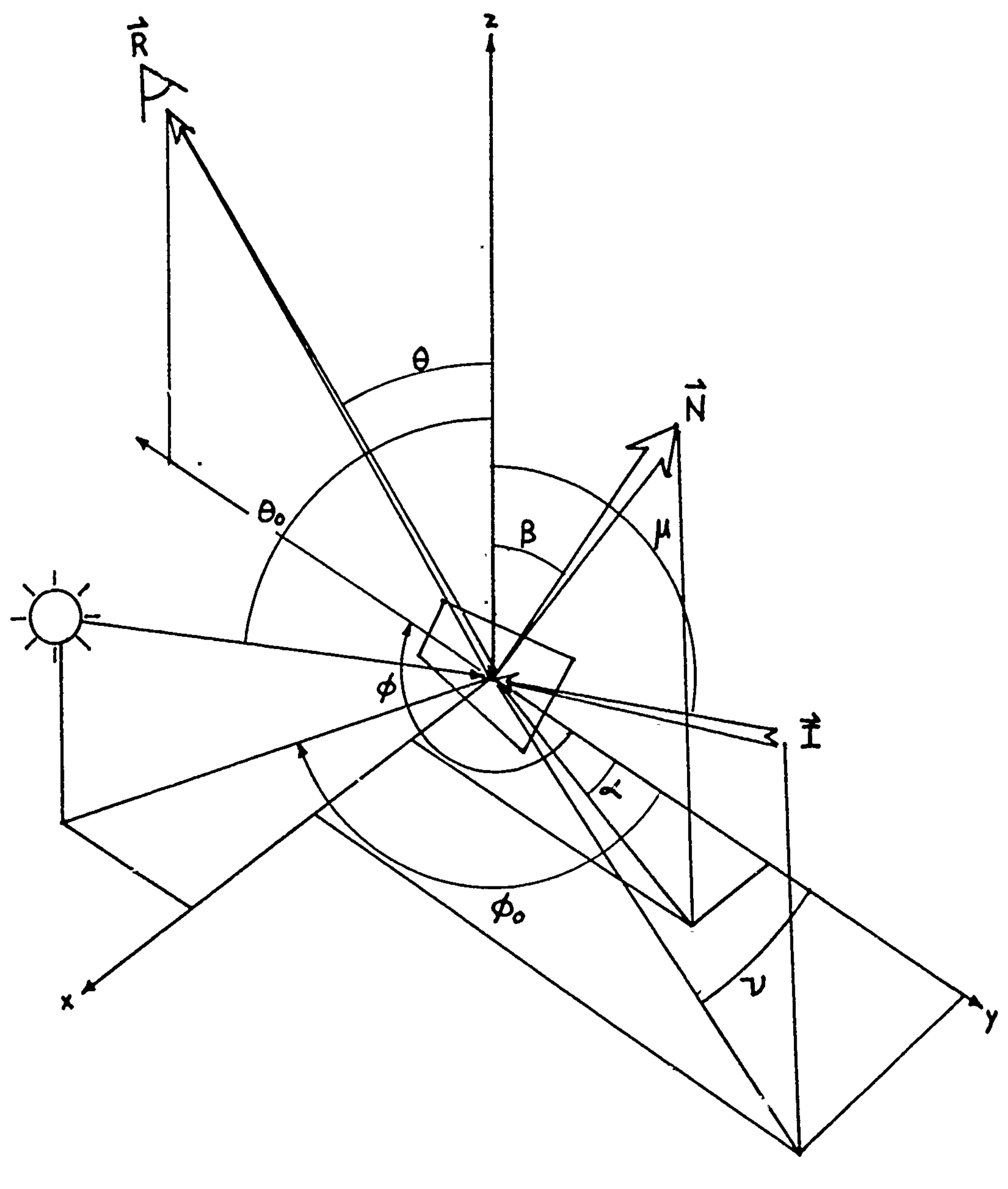

FIGURE 2.5:13. 3D geometric relations and nomenclature for the current study model.

2.6 Synthesis of Refracted Subsurface Radiance

Chapman & Irani Model

No refracted subsurface radiance model was defined by Chapman and Irani [1981] because they included the assumption of spectral viewing in the infrared where the transmittance of water approaches zero.

Current Study Model

As defined in Chapter 2.4, the upwelling subsurface radiance model of Plass et al. [1976] provides the radiance just above the ocean surface as a function of zenith angle of observation. Therefore, no angular refraction model is required. Only attenuation due to surface projection (as described in Chapter 2.5) needs to be considered:

The projection of the refracted radiance normal to the plane of observation can be defined, in surface-slope coordinates (beta,alpha) for any small, specular surface facet of slope:

L_w'(beta,alpha) = L_w(beta,alpha)*COS(omega)*SEC(beta)[2.6:1]

where

L_w(beta,alpha) = the refracted subsurface radiance observed at wave-slope coordinates (beta,alpha),

and

omega is as previously defined.

Figure 2.6:1 illustrates the mapping of L_w', the refracted subsurface radiance, to the surface-slope coordinates (beta, alpha) for identical horizontal and vertical polarizations, respectively. The solar zenith angle in this example is 0 degrees. The original unattenuated upwelling subsurface radiance distribution, L_w, is illustrated in Figure 2.4:8. Note that the the function, SEC(beta), was truncated for values of beta greater than 60 degrees (as in Figure 2.5:1), in order to maintain the scale of the illustration.

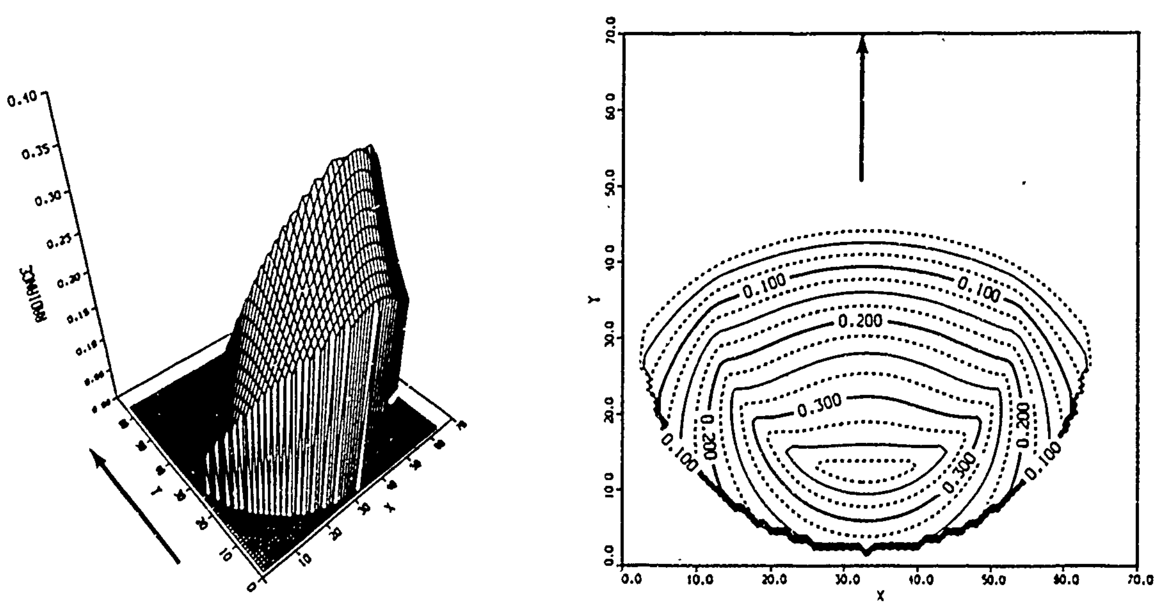

FIGURE 2.6:1. Map of refracted subsurface radiance, L_w', to coordinates (beta,alpha) for both polarizations.

Correlation of Sub-Resolution Wave-Slope Variance

No correlation of the refracted radiance is required for the current study model since the Monte Carlo simulation of Plass et al. [1976] has already incorporated the effect of wave slopes.

2.7 Generation of Synthetic Radiance Imagery

The integrated current study model can generate any combination of these synthetic radiance conditions:

1) Horizontal, Vertical polarization, or Both (unpolarized),
2) Reflected, Refracted radiance, or Both, and
3) Sub-resolution wave-slope attenuation (On or Off).

Because of Brewster-angle viewing relative to the mean sea surface, an initial assumption of the current study is that the effect of vertically polarized radiance is at a minimum and a comparison of horizontally polarized radiance spectra with unpolarized radiance spectra is sufficient to demonstrate the effect of vertical polarization. A second assumption is that the effect of upwelling subsurface refracted radiance is small relative to reflected radiance and a comparison of reflected radiance spectra with combined (reflected + refracted) radiance spectra is sufficient to demonstrate the effect of refracted radiance. A third assumption is that horizontally polarized, reflected radiance spectra synthesized without the sub-resolution wave-slope correlation filter will emulate the synthetic results of Chapman and Irani [1981].

The following radiance images (and their magnitude spectra) are synthesized in support of the current study:

H1(x,y) = Horizontally polarized, reflected radiance image,

L1(x,y) = Total (unpolarized), reflected radiance image,

H0(x,y) = Horizontally polarized, reflected and refracted radiance image,

L0(x,y) = Total (unpolarized), reflected and refracted radiance image, and

H3(x,y) = H1(x,y) without the incorporation of the sub-resolution wave-slope correlation filter model.

The following pages illustrate individual realizations of synthetic images that were generated in support of the current study. All examples are L0 images with contrasts normalized relative to a discrete 32-level gray scale: black corresponds to zero radiance and white corresponds to the maximum pixel radiance of the image. Only these examples are discrete: the actual syntheses are real scalar arrays.

Figures 2.7:1 through 2.7:3 illustrate synthetic images generated by filtering the same white noise array with slope spectra for v_{fric} = 12.0, 36.0, and 60.0 cm/sec, respectively. wind_az = 135 deg (-45 deg) and sun is at zenith.

FIGURE 2.7:1. LO image.

v_{fric} = 12.0 cm/sec
Max pixel radiance LO = 1.526
Avg pixel radiance H1 = 0.578
Avg pixel radiance H3 = 0.528
Avg pixel radiance V1 = 0.032
Avg pixel radiance L1 = 0.610
Avg pixel radiance H2 = 0.106
Avg pixel radiance V2 = 0.106
Avg pixel radiance L2 = 0.212
Avg pixel radiance H0 = 0.684
Avg pixel radiance V0 = 0.138
Avg pixel radiance LO = 0.822

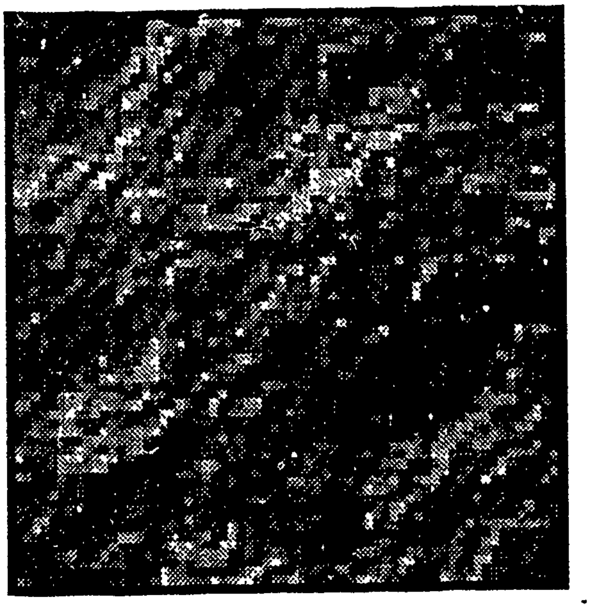

FIGURE 2.7:2. LO image.

v_{fric} = 36.0 cm/sec
Max pixel radiance LO = 1.894
Avg pixel radiance H1 = 0.602
Avg pixel radiance H3 = 0.564
Avg pixel radiance V1 = 0.050
Avg pixel radiance L1 = 0.652
Avg pixel radiance H2 = 0.105
Avg pixel radiance V2 = 0.105
Avg pixel radiance L2 = 0.210
Avg pixel radiance H0 = 0.707
Avg pixel radiance V0 = 0.155
Avg pixel radiance LO = 0.862

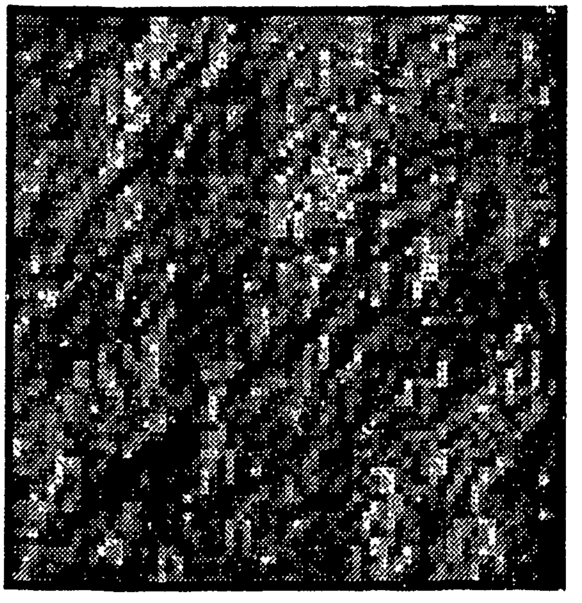

FIGURE 2.7:3. LO image.

v_{fric} = 60.0 cm/sec
Max pixel radiance LO = 1.737
Avg pixel radiance H1 = 0.579
Avg pixel radiance H3 = 0.574
Avg pixel radiance V1 = 0.054
Avg pixel radiance L1 = 0.633
Avg pixel radiance H2 = 0.105
Avg pixel radiance V2 = 0.105
Avg pixel radiance L2 = 0.210
Avg pixel radiance H0 = 0.684
Avg pixel radiance V0 = 0.159
Avg pixel radiance LO = 0.843

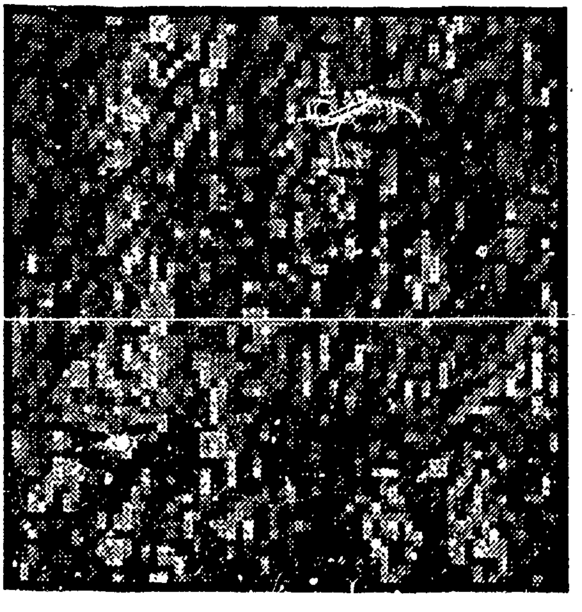

The synthetic image in Figure 2.7:4 is a different synthetic realization (i.e. different white noise spectrum) using the same parameters as Figure 2.7:1. Note both the similarity of the image and its statistics to that of Figure 2.7:1.

FIGURE 2.7:4. LO image.

v_{fric} = 12.0 cm/sec
Max pixel radiance LO = 1.523
Avg pixel radiance H1 = 0.578
Avg pixel radiance H3 = 0.526
Avg pixel radiance V1 = 0.031
Avg pixel radiance L1 = 0.609
Avg pixel radiance H2 = 0.106
Avg pixel radiance V2 = 0.106
Avg pixel radiance L2 = 0.212
Avg pixel radiance H0 = 0.684
Avg pixel radiance V0 = 0.137
Avg pixel radiance LO = 0.821

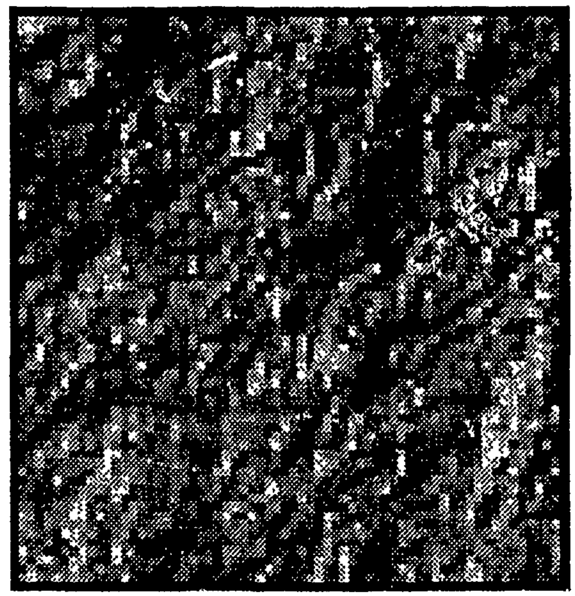

The final example in Figure 2.7:5 has v_{fric} = 60.0 cm/sec and wind_az is now 0 degrees.

FIGURE 2.7:5. LO image.

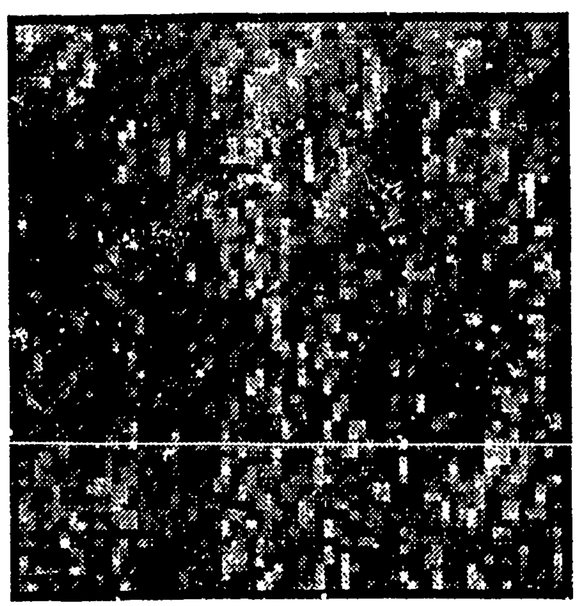

2.8 Slope Spectra Analysis of Synthetic Images

Analysis of slope spectra involves several related figures of merit that are all based upon the difference in slope spectral response between the original slope magnitude spectra used in the synthesis and the final synthetic image magnitude spectra resulting from the nonlinear transformation of wave slope to radiance. These figures of merit can be correlated to either wave slope variance or the difference in wave slope variance.

The first figure of merit is the 2D difference (or error) spectrum $D_2(k,phi)$. An ensemble average of four independent spectral realizations of the same synthetic geometry is calculated and the fundamental component $N'(0,0)$ (that represents the mean image radiance) is then removed.

$$N'(k,phi) = \sum_{i=1}^{4} N_i(k,phi) \qquad [2.8:1]$$

$$N''(k,phi) = N'(k,phi) - N'(0,0) \qquad [2.8:2]$$

where

N = the magnitude spectrum of the synthetic radiance image,

k = wavenumber,

and

phi = azimuth angle.

The modified image magnitude spectrum, N"(k,phi), is normalized so that the peak response matches the peak response of the original slope magnitude spectrum M_0(k,phi). The motivation is to provide a scaled difference (error) spectrum to illustrate the nonlinearity in slope spectral response of N_{norm}(k, phi) relative to M_0(k,phi) over the domains of wavenumber and azimuth.

$$N_{norm}(k,phi) = N"(k,phi)/MAX(M_0(k,phi) \qquad [2.8:3]$$

$$D_2(k,phi) = M_0(k,phi) - N_{norm}(k,phi) \qquad [2.8:4]$$

Note that coordinates k and phi are specified here for the consistency of this discussion only. The actual arrays used in this study are specified by rectangular spatial frequency (wavenumber) coordinates (k_x,k_y) such that

$$D_2(k_x,k_y) = D_2(k*COS(phi),k*SIN(phi)). \qquad [2.8:5]$$

The second and third figures of merit are the 1D squared difference (error) spectra D_1(k) and D_1(phi). The motiva-

tion is to provide a scaled 1D variance spectrum to illustrate the nonlinearity in spectral response of $N_{norm}(k)$ relative to $M_0(k)$ over the domain of wavenumber only, and of $N_{norm}(phi)$ relative to $M_0(phi)$ over the domain of azimuth.

$$D_1(k) = \int |D_2(k,phi)|^2 * dphi \qquad [2.8:6]$$

$$D_1(phi) = \int |D_2(k,phi)|^2 * dk \qquad [2.8:7]$$

The fourth figure of merit is the squared integrated value of the difference (error) in slope spectral response D_0. The 2D difference (error) spectrum $D_2(k,phi)$ is integrated with respect to both azimuth phi and wavenumber k. The motivation is to provide a single number to describe the nonlinearity in slope spectral response in the calculation of the variance of N_{norm}, i.e. the estimate of the variance of M_0, relative to the actual slope variance of the original (input) spectrum.

$$D_0 = \int\int |D_2(k,phi)|^2 * dkdphi. \qquad [2.8:8]$$

The cross-wind and along-wind squared differences are also calculated:

$$D_{0c} = \int\int |D_2(k,phi)*SIN(wind\_az-phi)|^2*dkdphi, \qquad [2.8:9]$$

and

$$D_{0a} = \int\int |D_2(k,phi)*COS(wind\_az-phi)|^2*dkdphi. \qquad [2.8:10]$$

These figures of merit are determined for each of four differentially polarized variations of the same synthetic image:

H1(x,y) - Horizontally polarized, reflected radiance image,

L1(x,y) - Total (unpolarized), reflected radiance image,

H0(x,y) - Horizontally polarized, reflected and refracted radiance image,

L0(x,y) - Total (unpolarized), reflected and refracted radiance image, and

H3(x,y) - H1(x,y) without the incorporation of the sub-resolution wave-slope correlation filter model,

where

$$N_{ji}(k_x,k_y) = \left| \mathcal{F}^{-1} IM_i(x,y) \right|$$

for IM=H1,L1,H0,L0,H3 and i=1-4. [2.8:11]

Because of the large number of spectra to be processed, the Results will include only the D1 and D0 data.

Figure 2.8:1 illustrates a typical 2D difference spectrum $D_2(k_x, k_y)$ for a single synthetic realization of image H1, where wind azimuth is 0 degrees, the sun is at zenith, and the wind friction velocity is 12.0 cm/sec. Note that this example is an 'alphascale' representation, where 'a - z' corresponds to increasing negative scaled values and 'A - Z' corresponds to increasing positive scaled values. Blanks correspond to near-zero deviations (errors) between spectra.

FIGURE 2.8:1. 2D difference (error) spectrum, $D_2(k_x, k_y)$.

3.0 RESULTS AND DISCUSSION

The D_1 results (slope variance versus wavenumber; slope variance versus azimuth) are listed in Appendix I. These results provide the most graphic illustration of the wave-slope error generated by the parametric variation of wind azimuth, solar position and wind velocity. The D_0 results (partial and total integrated slope variance) are listed in Appendix II. The D_2 difference (error) spectra (from which the D_1 and D_0 results are derived) are not included with this report to avoid cumbersome detail (i.e. 360 graphic examples of three-dimensional difference/error spectra).

3.1 Discussion of D_0 Results

Please refer to the D_0 results in Appendix II.

Parametric Variation of Mean Radiance

The mean radiance reflected/refracted in the direction of observation is the central ordinate of the forward Fourier transform of the radiance image and is calculated for each imaging geometry and for each of five polarized radiance conditions:

H1 - reflected horizontal radiance,

L1 - reflected total (horizontal + vertical) radiance,

H0 - reflected & refracted horizontal radiance,

L0 - reflected & refracted total radiance, and

H3 - reflected horizontal radiance without the sub-resolution wave-slope model (essentially a reconstruction of the Chapman & Irani synthesis.)

H3 will be compared with H1 as an examination of the effect of sub-resolution wave slopes on model results.

As expected, the following conditions are observed:

1) The mean radiance is maximum when the imaging geometry favors specular reflection of the sun, i.e. the solar position is azimuth angle $phi_0 = 0.0$ deg and zenith angle $theta_0 = 53.2$ deg (denoted $(phi_0, theta_0)$ for the remainder of this discussion). The second highest mean radiance is observed where the sun is at zenith (i.e (0,0)). Mean radiance decreases as sun azimuth varies from 0 degrees.

2) Under the conditions of maximum solar reflection and $v_{fric} = 12.0$ cm/sec, the slightly disturbed water surface yields a mean radiance of approximately 1.98 for L0 (averaged over the four wind azimuths). This value compares favorably with the theoretical L0 value of 2.62 when the surface is a totally flat, specular surface. Mean radiance drops to 1.75 when $v_{fric} = 36.0$ cm/sec and drops to 1.50 when $v_{fric} = 60.0$ cm/sec. As the surface becomes rougher, the probability of reflecting facets having zero slope decreases and less of the direct solar radiance is reflected.

3) Under the conditions of maximum solar reflection and $v_{fric} = 60.0$ cm/sec, mean radiance is highest (1.57 for L0) when the dominant wind azimuth wind_az is orthogonal to the plane of reflection and lowest (1.45 for L0) when wind_az is parallel to the plane of reflection. As the surface becomes

rougher due to wind, the slope distribution increases its spread along the azimuthal plane of the wind defined by wind_az. When wind_az is orthogonal to the plane of reflection, there is a greater probability that a facet will reflect radiance from the skydome near the plane of reflection than when wind_az is parallel to the plane. With the sun located in this plane, the probability that a facet will reflect radiance from the vicinity of the sun is greater when wind_az is orthogonal. This effect can be observed, to a lesser degree, for all sun orientations in the plane of reflection. The effect diminishes as v_{fric} decreases because of the lower directional attenuation of the dominant low-frequency waves.

Demonstration of Statistical Model Stability

Comparisons of symmetric test cases with three different solar geometries provide an indication of the statistical stability of the complete model.

TABLE 3.1:1. Symmetric test cases and their parameters.

	Comparison 1	Comparison 2	Comparison 3	v_{fric}
	12 and 24	07 and 19	11 and 23	12 cm/sec
	60 and 72	55 and 67	59 and 71	36 cm/sec
	36 and 48	31 and 43	35 and 47	60 cm/sec
Sun Coord	(0,53.2)	(0,0)	(180,53.2)	

The three sets of test cases have mirror symmetry with respect to observation: the sun is in the plane of reflection (phi_0 = 0 or 180 deg) but the dominant wind azimuths wind_az for the comparison cases are directed 45 degrees away from the the plane of reflection and differ in sign only. The respective test cases should demonstrate similar statistics based on the ensemble average of the magnitude spectra of the four synthetic scenes within each test case.

TABLE 3.1:2. Comparison of mean radiances between symmetric geometries.

	Comparison of symmetric test cases					
Condition	12 vs	24	60 vs	72	36 vs	48
H1	1.7183	1.7183	1.4580	1.4629	1.2105	1.2145
L1	1.7740	1.7739	1.5352	1.5404	1.2886	1.2929
H0	1.8241	1.8241	1.5635	1.5682	1.3155	1.3196
L0	1.9855	1.9854	1.7461	1.7511	1.4987	1.5030
Avg Diff	± 0.0027 %		± 0.3145 %		± 0.3147 %	
Condition	07 vs	19	55 vs	67	31 vs	43
H1	0.9664	0.9649	1.0081	1.0093	0.9621	0.9645
L1	0.9760	0.9742	1.0300	1.0304	0.9966	0.9977
H0	1.1519	1.1503	1.1918	1.1928	1.1436	1.1459
L0	1.3469	1.3451	1.3975	1.3974	1.3596	1.3606
Avg Diff	± 0.1530 %		± 0.0622 %		± 0.1583 %	
Condition	11 vs	23	59 vs	71	35 vs	47
H1	0.4582	0.4577	0.4607	0.4619	0.4223	0.4237
L1	0.4674	0.4668	0.4788	0.4800	0.4456	0.4470
H0	0.5640	0.5635	0.5661	0.5672	0.5274	0.5288
L0	0.6790	0.6784	0.6897	0.6907	0.6558	0.6571
Avg Diff	± 0.1036 %		± 0.2121 %		± 0.2766 %	

Mean radiances (the ensemble DC components) are similar to within ± 0.32% among all comparisons. There does not appear

to be any correlation between average percent difference and solar geometry even though the mean radiance diminishes as the geometry moves away from maximum solar reflection.

The ensemble fundamental components differ more than expected and this is an indication that a larger ensemble may be one additional requirement for statistical stability.

TABLE 3.1:3. Comparison of fundamental components between symmetric geometries.

	Comparison of symmetric test cases					
Condition	12 vs	24	60 vs	72	36 vs	48
H1	0.0359	0.0315	0.0243	0.0220	0.0183	0.0167
L1	0.0400	0.0374	0.0269	0.0245	0.0194	0.0177
H0	0.0347	0.0320	0.0229	0.0206	0.0170	0.0158
L0	0.0376	0.0350	0.0241	0.0218	0.0169	0.0159
Avg Diff	± 8.3628 %		± 9.4935 %		± 7.6205 %	
Condition	07 vs	19	55 vs	67	31 vs	43
H1	0.0216	0.0225	0.0120	0.0126	0.0060	0.0060
L1	0.0211	0.0223	0.0106	0.0114	0.0048	0.0048
H0	0.0194	0.0204	0.0094	0.0099	0.0058	0.0056
L0	0.0168	0.0180	0.0056	0.0061	0.0104	0.0086
Avg Diff	± 5.2375 %		± 6.2567 %		± 5.1890 %	
Condition	11 vs	23	59 vs	71	35 vs	47
H1	0.0124	0.0126	0.0083	0.0085	0.0051	0.0048
L1	0.0135	0.0138	0.0091	0.0094	0.0052	0.0049
H0	0.0112	0.0115	0.0069	0.0069	0.0040	0.0038
L0	0.0111	0.0114	0.0063	0.0063	0.0032	0.0032
Avg Diff	± 2.2504 %		± 1.3861 %		± 4.1629 %	

For these three geometries, the fundamental components are similar to within ± 10% among all comparisons. This may be a poor choice of imaging geometry for statistical validation

because the contrast ratios (fundamental/DC components) are not the highest among the full set of test cases. The main consideration that applies to these particular geometries is that a nearly saturated image (i.e a very high DC component relative to the remainder of the spatial spectrum) skews the confidence of spectral estimation in favor of the DC component, a parameter which has an expected value of zero in the slope spectral estimate, i.e. the water surface is expected to have a mean slope of zero. However, there does appear to be a correlation between a decrease in the mean radiance with a decrease in the average percent difference (and therefore increased statistical confidence) in the fundamental components. A fundamental consideration for this method is to determine an optimal geometry which removes spectral energy from the DC component and distributes it across the rest of the spatial spectrum with the intent of increasing the statistical stability of the non-DC portion of the spectrum.

Correlation of Contrast Ratio with Slope Variance

As explained in the Methods section, the DC component of the radiance image magnitude spectrum is removed and the remaining image spectrum is normalized with respect to the input slope magnitude spectrum M_0 by a geometric scaling

factor between the peak slope components. The difference between the two spectra is then defined as the error, or difference, spectrum. Integration of the squared error over both wavenumber and azimuth yields the D_0 results, the total slope variance due to errors/differences between the two spectra.

The contrast of the wave image was defined by Chapman and Irani as the ratio of the fundamental component to the DC component and was used as a figure of merit in their error analysis. A comparison of the contrast ratio of the image spectrum with the resulting integrated squared deviation (variance) from its difference spectrum demonstrates a good correlation between high contrast and low error. A simple matrix is presented, where the contrasts of the images for each geometry (with the exception of H3) are ranked from 1 to 4 (high contrast to low contrast) and the corresponding D_0 results are likewise ranked from 1 to 4 (low to high error).

TABLE 3.1:4. Rank correlation matrices for contrast ratio vs. slope variance.

v_{fric} = 60.0 cm/sec

		CONTRAST 1	2	3	4
V	1	22	1	1	0
A	2	1	18	3	2
R	3	1	3	14	6
	4	0	2	6	16

v_{fric} = 36.0 cm/sec

		CONTRAST 1	2	3	4
V	1	17	1	0	6
A	2	1	14	8	1
R	3	1	7	13	3
	4	5	2	3	14

v_{fric} = 12.0 cm/sec

		CONTRAST 1	2	3	4
V	1	9	4	5	6
A	2	2	10	6	6
R	3	4	9	6	5
	4	9	1	7	7

The above results display a high correlation at v_{fric} = 60.0 cm/sec and increasing loss of correlation as v_{fric} decreases. This can be explained as a result of decreasing statistical confidence and increasing ambiguity among contrast values and D_0 values. For v_{fric} = 60.0 cm/sec, the differences between contrast ratios and D_0 values are generally on the order of ±10%; for v_{fric} = 36.0 cm/sec, the differences are often less than ±5%; for v_{fric} = 12.0 cm/sec, the dif-

ferences are often less than $\pm 1\%$. With the assumptions 1) that the fundamental component (the numerator of the contrast ratio) has an average model error tolerance of $\pm 6\%$ (based on the analysis of Table 3.1:3) and 2) the corresponding D_0 value may have a similar tolerance, it is reasonable to consider that the confidence of unambiguous rank-ordering should decrease for values at and below $v_{fric} = 36.0$ cm/sec.

Determination of Optimal Imaging Geometry

Figure 3.1:1 provides a graphic comparison of the D_0 values for each geometry. The intent of this comparison is to determine those imaging geometries which provide the lowest integrated squared errors (slope variance) for all sampled variations of dominant wind azimuth wind_az and friction velocity v_{fric}.

Within this limited sample space, the unambiguous selection for optimal imaging of wind-wave slopes is a geometry which requires the sun to be directed 135 degrees away from the azimuth of reflection (i.e. observation) or, by complement, 45 degrees away from the solar azimuth of maximum specular reflection. The D_0 results for this geometry are generally lowest for all polarized conditions.

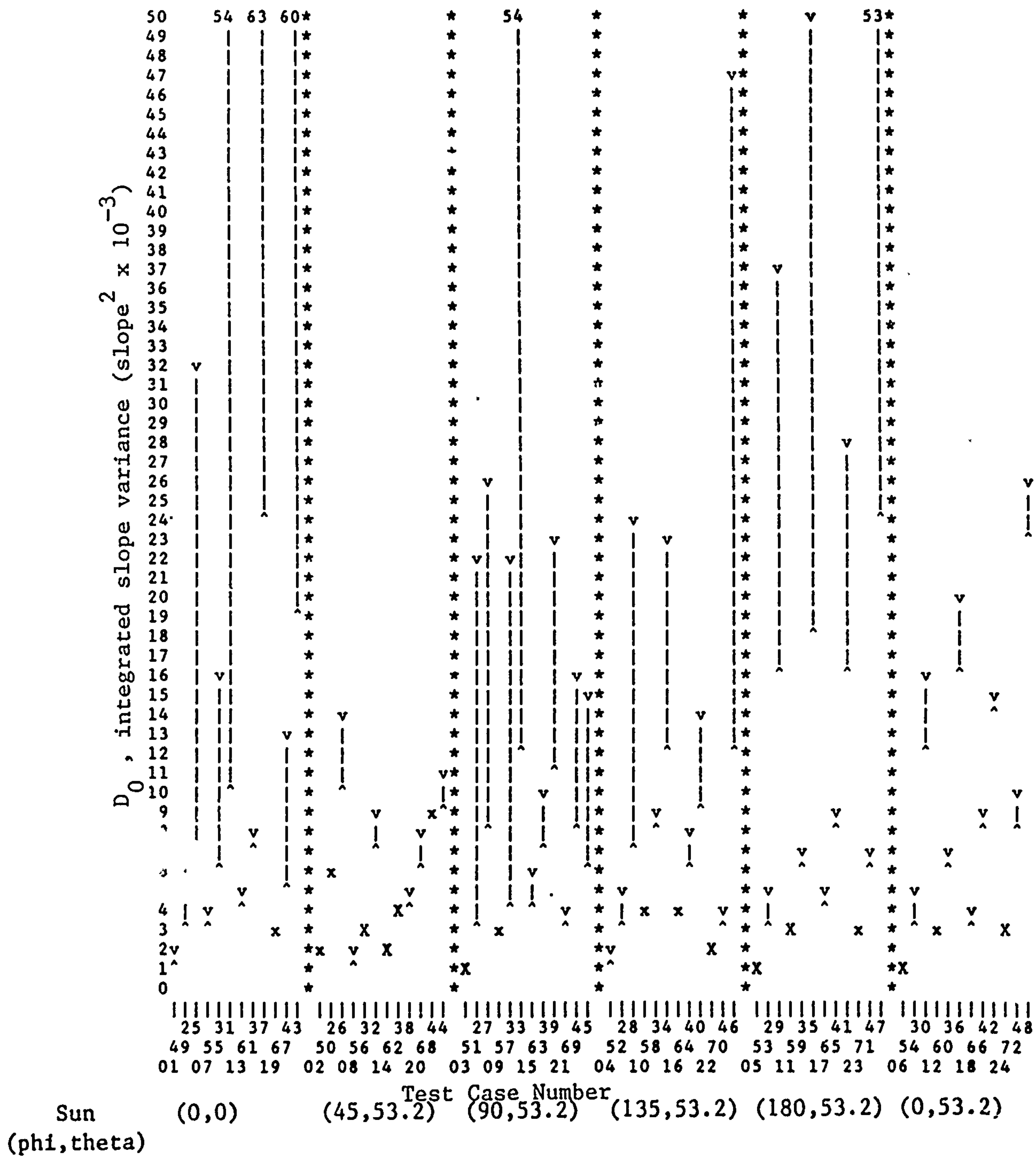

FIGURE 3.1:1. Range of slope variance ($error^2$) versus test case number (slope variance expressed as $slope^2$) x 10^{-3}).

The second choice of imaging geometry places the sun at the position of maximum specular reflection but this is an ambiguous selection because other geometries provide lower D_0 results for particular values of wind_az and v_{fric}.

This result, from two-dimensional analysis of the current study model, is in full agreement with the results of the one-dimensional survey of Chapman and Irani [1981] and demonstrates a secondary validation of their approach.

Effect of Subsurface Refraction on Slope Variance

The following conditions are observed:

1) The effect of refraction on slope variance is minimal when contrast ratios are high relative to the set of all test cases. It was expected that the additional nonlinearity created by refraction in the transformation of slope to radiance would consistently generate higher slope variances in H0 and L0 relative to H1 and L1. However, the stronger correlation between contrast and slope variance tends to swamp any effect created by subsurface refraction.

2) As expected, the effects of refraction are most noticeable when the sun is furthest away from point of maximum

specular reflection, i.e. when the proportion of refracted radiance relative to reflected radiance is largest. In these test cases, the contrast ratios approach a minimum among all test cases and the slope variances approach a maximum. The large differences between H1 and H0 and between L1 and L0 confirm that the decrease in contrast and increase in slope variance are both due to the effect of refraction on the minimum reflection cases.

Effect of Polarization on Slope Variance

A comparison of H1 with L1 indicates no apparent correlation between polarization and slope variance. Again, the stronger correlation between contrast and slope variance tends to swamp any effect created by differences in polarization. It was expected that the decrease in mean radiance from L1 to H1 would be offset by an increase in contrast and consequent decrease in slope variance. No such effect was discernible among this small sample. Because of Brewster-angle viewing, the effect due to the addition of vertically polarized radiance should be at a minimum among all observation geometries.

3.2 Discussion of D_1 Results

Please refer to the graphic D_1 results (slope variance versus wavenumber; slope variance versus azimuth) in Appendix I. Note that the slope variance for H1 is plotted as a solid line; L0 is plotted as a dashed line; H3 is plotted as a dotted line.

Slope Error as a Function of Wavenumber

The following conditions are observed:

1) For v_{fric} = 12.0 cm/sec, the major source of slope error occurs in the vicinity of the dominant, low-spatial-frequency peak centered near k = 0.12 rad/cm.

2) With the sole exception of the optimal imaging geometry (as determined in Chapter 3.1), the higher-spatial-frequency slope errors increase relative to the error peak near k = 0.12 rad/cm as v_{fric} increases.

3) With the sole exception of the optimal imaging geometry, the higher spatial frequencies (above k = 0.12 rad/cm) are the dominant source of slope error at v_{fric} = 60.0 cm/sec.

4) At the optimal imaging geometry, the major source of slope error remains in the vicinity of the dominant, low-spatial-frequency peak centered near $k = 0.12$ rad/cm for all values of v_{fric}.

5) At the optimal imaging geometry (and at the geometry of maximum solar reflection), the plots of H1 and L0 (as well as the unplotted L1 and H0 data) closely approximate each other within the set of test cases. The same plots within the other imaging geometries tend to approximate each other at $v_{fric} = 12.0$ cm/sec and then deviate from each other at higher values of v_{fric}.

Variation of H3 with Respect to Wavenumber

H3 represents the results based on the model of Chapman and Irani where no sub-resolution wave-slope model is incorporated. H1 represents results based upon the inclusion of a radiance attenuation model to add the effect of sub-resolution wave slopes on scene radiance.

The following conditions are observed:

1) H3 does not demonstrate a good correlation with any of the model parmeters as a function of wavenumber. Within the

limited scope of this experiment, H3 appears to be independent of the model parameters as a function of wavenumber.

2) As expected, H3 maps most closely with H1 when v_{fric} = 12.0 cm/sec. The correlation filter that is used to attenuate radiance as a function of the sub-resolution wave-slope distribution provides a nearly impulse response at v_{fric} = 12.0 cm/sec than at higher values of V_{fric} and the resulting difference between the H1 and H3 radiance models is slight.

3) Within the constraint of optimal imaging geometry, H3 maps closely to H1, L1, H0, and L0 when v_{fric} = 12.0 cm/sec but deviates significantly at higher values of v_{fric}. The most general trend to note is that the slope error associated with H3 becomes much larger relative to the other four radiance conditions as wavenumber increases.

4) Within the constraint of maximum solar reflection geometry, H3 maps closely to H1, L1, H0 and L0 at higher values of v_{fric} but deviates when v_{fric} = 12.0 cm/sec. This effect is opposite to that observed in 3) above.

The demonstrated independence of H3 as a function of wavenumber is also in agreement with the results of Chapman

and Irani. However, the significant result to note is that the other four radiance conditions do demonstrate a definite correlation with wavenumber at the optimal imaging geometry. This correlation is also exhibited in the geometry of maximum solar reflection, although to a lesser degree.

Slope Error as a Function of Azimuth

The following conditions are observed:

1) There is a definite azimuthal dependence between slope variance and the parameters of solar azimuth and dominant wind azimuth. This dependence is most readily observable in the two most optimal imaging geometries.

2) When v_{fric} = 12.0 cm/sec and wind_az is in the plane of reflection, a dominant error lobe is observable which has an orientation within 20 degrees of the azimuth orthogonal to the sun position. A minor error lobe is observable in the azimuthal plane of the sun, i.e. approximately orthogonal to the dominant lobe.

3) When v_{fric} = 12.0 cm/sec and wind_az is varied, the error lobes redistribute so that the dominant errors angularly skew toward the plane of the dominant wind azimuth.

4) As v_{fric} increases, the error lobes tend to angularly spread out so that the dominant errors redistribute between the solar azimuth and the dominant wind azimuth.

Variation of H3 with Respect to Azimuth

The following conditions are observed:

1) The H3 results follow the general trends outlined in Chapter 3.2 above. As discussed with respect to wavenumber, H3 maps closely to the results of the other four radiance conditions when $v_{fric} = 12.0$ cm/sec.

2) Where H3 deviates significantly from the other four conditions, the additional slope error is observed to align with the plane of the solar azimuth. This result is most noticeable within the two most optimal geometries.

The demonstrated dependence of H3 as a function of azimuth is also in general agreement with the limited results of Chapman and Irani. However, the results for H1, L1, H0, and L0 demonstrate a more consistent correlation with the variation of model parameters.

4.0 CONCLUSION

The results of the current study have established three main conclusions: 1) the limited results of Chapman and Irani [1981] have been generally verified, 2) the existence of an optimal imaging geometry for slope spectrum estimation is indicated, and 3) the enhanced model, incorporating the effects of sub-resolution wave slopes and subsurface refraction on observed radiance, demonstrates a significant effect on wave-slope spectra derived from imagery.

The most conclusive result is the analytic determination of the region containing an optimal geometry for the estimation of wave-slope spectra from imagery under the specified conditions of this study. Through the use of an integrated set of analytic models, the variation of a limited number of parameters has predicted the magnitude of slope variation as a function of azimuth and wavenumber. These predictions exceed the capability of a deterministic second-order theory. While this study has been directed toward a generalization of the Chapman and Irani study, the generalized model requires a more complete exploration of the parametric surface.

Suggestions for Further Research

There are several potential directions for further research which will build upon this study. The types of research fall into two main categories: 1) comparison of the analytic model with empirical data derived from a physical experiment and 2) refinement and extension of the parametric surface exploration of the analytic model.

Physical Experiment

It is obvious that an analytic model requires empirical results to verify its predictions. However, the complexity of this model and its limited utility presumes that the real world problem has an even higher level of complexity. The requirement still exists for the execution of a controlled experiment to calibrate the various techniques that attempt to measure the two-dimensional elevation/slope spectra of large water surfaces under natural conditions.

Refinement of the Analytic Model

The current study verified the limited results of Chapman and Irani [1981] and amplified their method to execute an only slightly larger exploration of the paramet-

ric surface. There are many assumptions in this model which remain to be tested through a vigorous exploration of the currently unvaried parameters:

sample size and kmax

ensemble size

radiant wavelength and index of refraction

zenith angle of observation

Also, other analytic functions await comparison with the current analytic model and with existing empirical data:

input elevation spectrum

clear sky versus cloudy sky radiance

clear water versus turbid water refraction

sub-resolution wave-slope distributions

- Gram-Charlier versus Gaussian

A secondary (and more vigorous) approach to the simulation of wave shadowing could also be explored: the elevation power spectrum is available for the generation of synthetic height arrays which can be used to modify the radiance distributions at each surface element. A comparison of the current synthesis with this nonlinear masking technique and with real imagery could potentially verify the utility of the current synthesis at increasingly larger zenith angles of observation.

Additionally, a refined exploration of the current parameter set might establish an even more optimal imaging geometry. The results of the current study have placed the new point of departure at a solar azimuth angle 45 degrees from the point of maximum specular reflection. Small variations of solar azimuth and solar zenith angle from this point may isolate the ideal image geometry for slope spectrum estimation.

Finally, the method of analysis can be more robust. The current study deviates from the Chapman and Irani study with respect to the choice of figures of merit. However, the current study is consistent with the earlier study with respect to the implied assumption that the output radiance magnitude spectrum should be compared with the undecomposed slope magnitude spectrum. There is evidence [Stilwell,1969; Kasevich,1975] that the x-component slope magnitude spectrum alone or a linear combination of the two slope-component magnitude spectra may yield a more accurate synthetic representation of the radiance magnitude spectrum. A more detailed analysis, using results from the current study model, could verify this theory and provide a more accurate tool for the estimation of wave-slope spectra from imagery.

5.0 REFERENCES

Aas, E., "Two-stream irradiance model for deep waters", in Applied Optics, 26(11), pp 2095-2101, 1987.

Abshire, J.B. & J.F. McGarry, "Two-color short-pulse laser altimeter measurements of ocean surface backscatter", in Applied Optics, 26(7), pp 1304-1310, 1987.

Barber, N.F., "A diffraction analysis of a photograph of the sea", in Nature, 164(4168), pp 485, 1949.

Barber, N.F., "Finding the direction of travel of sea waves", in Nature, 174(4440), pp 1048-1050, 1954.

Beckmann, P. & A. Spizzichino, The Scattering of Electromagnetic Waves from Rough Surfaces, Macmillan Company, New York, 1963.

Blackman, R.B. & J.W. Tukey, The Measurement of Power Spectra From The Point Of View Of Communications Engineering, Dover Publications, Inc., New York, 1959.

Blinn, J.F., "Simulation of Wrinkled Surfaces", in ACM Computer Graphics (Proceedings of ACM SIGGRAPH 78), pp 286-292, 1978.

Borrego, J.A. & M.A. Machado, "Optical analysis of a simulated image of the sea surface", in Applied Optics, 24(7), pp 1064-1072, 1985.

Carlson, G.E., "Estimation of ocean wave wavenumber and propagation direction from limited synthetic aperture radar data", in IEEE Transactions on Geoscience and Remote Sensing, GE-22(6), pp 609-614, 1984.

Cartwright, D.E. & M.S. Longuet-Higgins, "The statistical distribution of the maxima of a random function", in Proceedings of the Royal Society, A237(1209), pp 212-232, 1956.

Chapman, R.D. & G.B. Irani, "Errors in estimating slope spectra from wave images", in Applied Optics, 20(20), pp 3645-3652, 1981.

CIE Technical Committee 4.2, "Standardization of luminance distribution on clear skies", in CIE Publication #22, Comission International de l'Eclairaze, Paris, 1973.

Cote, L.J., J.O. Davies, W. Marks, R.J. McCough, E. Mehr, W.J. Pierson, J.F. Ropek, G. Stephenson & R.C. Vetter, "The directional spectrum of a wind-generated sea as determined from data obtained by the stereo wave observation project", in Meteorological Papers, NYU College of Engineering, 2(6), 1960.

Coulson, K.L., Solar and Terrestrial Radiation, Academic Press, New York, 1975.

Cox, C.S. & W.H. Munk, "Measurement of the roughness of the sea surface from photographs of the sun's glitter", in Journal of the Optical Society of America, 44(11), pp 838-850, 1954a.

Cox, C.S. & W.H. Munk, "Statistics of the sea surface derived from sun glitter", in Journal of Marine Research, 13(2), pp 198-227, 1954b.

Cox, C.S., "Measurements of slopes of high-frequency wind waves", in Journal of Marine Research, 16(3), pp 199-225, 1958.

Fisher, M.G., Oceanographic Analysis of Sun Glint Images Taken on Space Shuttle Mission STS 41-G, M.S. Thesis, Naval Postgraduate School, 1986.

Fournier, A. & W.T. Reeves, "A simple model of ocean waves", in ACM Computer Graphics (Proceedings of ACM SIGGRAPH 86), pp 75-84, 1986.

Gagalowicz, A. & S.D. Ma, "Sequential synthesis of natural textures", in Computer Vision, Graphics, And Image Processing, 30, pp 289-315, 1985.

Goodell, J.B., "The appearance of the sea reflected sky", in Applied Optics, 10, pp 223-225, 1971.

Gordon, H.R., O.B. Brown & M.M. Jacobs, "Computed relationship between the inherent and apparent optical properties of a flat homogeneous ocean", in Applied Optics, 14(2), pp 417-427, 1975.

Gordon, H.R. & W.R. McCluney, "Estimation of the depth of sunlight penetration in the sea for remote sensing", in Applied Optics, 14(2), pp 413-416, 1975.

Gotwols, B.L. & G.B. Irani, "Optical determination of the phase velocity of short gravity waves", in Journal of Geophysical Research, 85(C7), pp 3964-3970, 1980.

Gotwols, B.L. & G.B. Irani, "Charge-coupled device camera system for remotely measuring the dynamics of ocean waves", in Applied Optics, 21(5), pp 851-860, 1982.

Hale, G.M. & M.R. Querry, "Optical constants of water in the 200-nanometer to 200-micrometer wavelength region", in Applied Optics, 12(3), pp 555-563, 1973.

Hasselmann, D.E., M. Dunckel & J.A. Ewing, "Dirctional wave spectra observed during JONSWAP 1973", in Journal of Physical Oceanography, 10, pp 1264-1280, 1980.

Hopkinson, R.G., "Measurements of sky luminance distribution at Stockholm", in Journal of the Optical Society of America, 44(6), pp 455-459, 1954.

Holthuijsen, L.H., "Observations of the directional distribution of ocean-wave energy in fetch limited conditions", in Journal of Physical Oceanography, 13(2), pp 191-207, 1983a.

Holthuijsen, L.H., "Stereophotography of ocean waves", in Applied Ocean Research, 5(4), pp 204-209, 1983b.

Hulburt, E.O., "The polarization of light at sea", in Journal of the Optical Society of America, 24, pp 35-42, 1934.

Kasevich, R.S., C.H. Tang & S.W. Henriksen, "Energy spectra of sea waves for photographic interpretation", in Proceedings of the Seventh International Symposium on Remote Sensing of the Environment, pp 607-624, University of Michigan, Ann Arbor, 1971.

Kasevich, R.S., C.H. Tang & S.W. Henriksen, "Analysis and optical processing of sea photographs for energy spectra", in IEEE Transactions on Geoscience and Electronics, GE-10(1), pp 51-58, 1972.

Kasevich, R.S., "Directional wave spectra from daylight scattering", in Journal of Geophysical Research, 80 (33), pp 4535-4541, 1975.

Kajiya, J.T., "Anisotropic reflection models", in ACM Computer Graphics, 19(3), pp 15-21, 1985.

Keller, W.C. & B.L. Gotwols, "Two-dimensional optical measurement of wave slope", in Applied Optics, 22(22), pp 3476-3478, 1983.

Kinsman, B., Wind Waves: their generation and propagation on the ocean surface, Prentice Hall, Englewood Cliffs NJ, 1965.

Komen, G.J., S. Hasselmann & K. Hasselmann, "On the existence of a fully developed wind-sea spectrum", in American Meteorological Society, 14, pp 1271-1285, 1984.

Konnen, G.P., Polarized light in Nature, Cambridge University Press, Cambridge England, 1985.

LeMehaute, B., An Introduction to Hydrodynamics & Water Waves, Springer-Verlag, New York NY, 1976.

Longuet-Higgins, M.S., "On the statistical distribution of the heights of sea waves", in Journal of Marine Research, 11(3), pp 245-266, 1952.

Longuet-Higgins, M.S., "Statistical properties of a moving wave-form", in Proceedings of the Cambridge Philosophical Society, 52(2), pp 234-245, 1956.

Longuet-Higgins, M.S., "The statistical analysis of a random moving surface", in Philisophical Transactions of the Royal Society, A249(966), pp 321-387, 1957.

Longuet-Higgins, M.S., "On the interval between sucessive zeros of a random function", in Proceedings of the Royal Society, A246, pp 99-118, 1958.

Longuet-Higgins, M.S., "Reflection and refraction at a random moving specular point", Parts I, II, & III in Journal of the Optical Society of America, 50(9), pp 838-856, 1960.

Longuet-Higgins, M.S., "The directional spectrum of ocean waves, and processes of wave generation", in Proceedings of the Royal Society, A265(1322), pp 286-315, 1962.

Lybanon, M., "Ocean Wave Slope Statistics from Automated Analysis of Sun Glitter Photographs", NORDA Report 103, 1985.

Mandelbrot, B.B., Fractals: Form, Chance, and Dimension, Freeman, San Francisco CA, 1977.

Mandelbrot, B.B., The Fractal Geometry of Nature, Freeman, San Francisco CA, 1982.

Marks, W., "The use of a filter to sort out directions in a short-crested sea surface", in Transactions of the American Geophysical Union, 35(5), pp 758-766, 1954.

Marks, W. & F.C. Ronne, "Aerial stereo-photography and ocean waves", in Photogrammetric Engineering & Remote Sensing, 21, pp 107-110, 1955.

Mastin, G.A., P.A. Watterberg & J.F. Mareda, "Fourier synthesis of ocean scenes", in IEEE Computer Graphics & Applications, 7(3), pp 16-23, 1987.

Masuda, K., T. Takashima & Y. Takayama, "Emissivity of pure and sea waters for the model sea surface in the infrared window region", in Remote Sensing of Environment, 24, pp 313-329, 1988.

Maul, G.A., Introduction To Satellite Oceanography, Martinus Nijhoff Publishers, Dordrecht Netherlands, 1985.

Max, N.L., "Vectorized procedural models for natural terrain: waves and islands in the sunset", in ACM Computer Graphics (Proceedings of ACM SIGGRAPH 81), pp 317-324, 1981.

McLeish, W., "Spatial spectra of ocean surface temperature", in Journal of Geophysical Research, 75(33), pp 6872-6877, 1970.

Monaldo, F.M. & R.S. Kasevich, "Optical determination of short-wave modulation by long ocean gravity waves", in IEEE Transactions on Geoscience and Remote Sensing, GE-20(3), pp 254-259, 1982.

Monaldo, F.M. & D.R. Lyzenga, "On the estimation of wave slope- and height-variance spectra from SAR imagery", in IEEE Transactions on Geoscience and Remote Sensing, GE-24(4), pp 543-551, 1986.

Monne, J., F. Schmitt & D. Massaloux, "Bidimensional texture synthesis by Markov chains", in Computer Graphics and Image Processing, 17, pp 1-23, 1981.

Neumann, G. & W.J. Pierson, Principles of Physical Oceanography, Prentice-Hall, Englewood Cliffs NJ, 1966.

Norton, A., A.P. Rockwood & P.T. Skolmoski, "Clamping: A method of anti-aliasing textured surfaces by bandwidth limiting in object space", in ACM Computer Graphics (Proceedings of ACM SIGGRAPH 82), pp 1-8, 1982.

Palm, C.S., R.C. Anderson & A.M. Reece, "Laser probe for measuring 2-D wave slope spectra of ocean wave capillary waves", in Applied Optics, 16(4), pp 1074-1081, 1977.

Peachey, D.R., "Modeling waves and surf", in ACM Computer Graphics (Proceedings of ACM SIGGRAPH 86), pp 65-73, 1986.

Perlin, K., "An image synthesizer", in ACM Computer Graphics (Proceedings of ACM SIGGRAPH 85), pp 287-296, 1985.

Philpot, W.D., "Radiative transfer in stratified waters: a single-scattering approximation for irradiance", in Applied Optics, 26(19), pp 4123-4132, 1987.

Pierson, W.J. & W. Marks, "The power spectrum analysis of ocean wave records", in Transactions of the American Geophysical Union, 33(6), pp 834-844, 1952.

Pierson, W.J. & L. Moskowitz, "A proposed spectral form for fully developed wind seas based on the similarity theory of S. A. Kiyaigorodskii", in Journal of Geophysical Research, 69, pp 5181-5190, 1964.

Pierson, W.J., Jr. & R.A. Stacy, "The elevation, slope, and curvature spectra of a wind roughened sea surface", NASA Contractor Report 2247, 1973.

Plass, G.N. & G.W. Kattawar, "Radiative transfer in an atmosphere-ocean system", in Applied Optics, 8(2), pp 455-466, 1969.

Plass, G.N. & G.W. Kattawar, "Monte Carlo calculations of radiative transfer in the earth's atmosphere-ocean system: I. flux in the atmosphere and ocean", in Journal of Physical Oceanography, 2, pp 139-145, 1972.

Plass, G.N., G.W. Kattawar & J.A. Guinn, Jr., "Radiative transfer in the earth's atmosphere and ocean: infuence of ocean waves", in Applied Optics, 14(8), pp 1924-1936, 1975.

Plass, G.N., G.W. Kattawar & J.A. Guinn, Jr., "Radiance distribution over a ruffled sea: contributions from glitter, sky, and ocean", in Applied Optics, 15(12), pp 3161-3165, 1976.

Pos, J.D., L.P. Adams & F.A. Kilner, "Synoptic wave height and pattern measurements in laboratory wave basins using close-range photogrammetry", in Photogrammetric Engineering and Remote Sensing, 54(12), pp 1749-1756, 1988.

Powell, W.M. & G.L. Clarke, "The reflection and absorption of daylight at the surface of the sea", in Journal of the Optical Society of America, 26, pp 111-120, 1936.

Pyramid Films, Inc., Pyramid Catalogue, Santa Monica CA, 1981.

Ray, P.S., "Broadband complex refractive indices of ice and water", in Applied Optics, 11(8), pp 1836-1844, 1972.

Robinson, I.S., Satellite Oceanography, an introduction for oceanographers and remote-sensing scientists, Ellis Horwood Limited, West Sussex England, 1985.

Saunders, P.M., "Shadowing on the ocean and the existence of the horizon", in Journal of Geophysical Research, 72 (18), pp 4643-4649, 1967.

Saunders, P.M., "Radiance of sea and sky in the infrared window 800-1200 cm^{-1}", in Journal of the Optical Society of America, 58(5), pp 645-652, 1968

Sawyer, D.W., "Preliminary report on the determination of water surface profiles", U.S. Naval Photographic Interpretation Center Report 103-49, 1949.

Schacter, B.J., "Long-crested wave models", in Computer Graphics and Image Processing, 12(3), pp 187-201, 1980.

Schau, H.C., "Measurement of capillary wave slopes on the ocean" in Applied Optics, 17(1), pp 15-17, 1978.

Schooley, A.H., "A simple method for measuring the statistical distribution of water wave surfaces", in Journal of the Optical Society of America, 44(1), pp 37-40, 1954.

Schwartz, I.B. & D. Hon, "Emissivity as a function of surface roughness: a computer model", NRL Report (unpublished).

Sheres, D., Remote Synoptic Surface Flow Measurements In Small Bodies Of Water, Ph.D. Dissertation, University of California, San Diego, 1980.

Sheres, D., "Remote and synoptic water-wave measurements by aerial photography: a model, experimental results, and an application", in IEEE Journal of Oceanic Engineering, OE-6(2), pp 63-69, 1981.

Sidran, M., "Broadband reflectance and emissivity of specular and rough water surfaces", in Applied Optics, 20 (18), pp 3176-3183, 1981.

Spitzer, D. & D. Arief, "Relationship between the sky radiance reflected at the sea surface and the downwelling irradiance", in Applied Optics, 22(3), pp 378-379, 1983.

Stewart, R.H., Methods of Satellite Oceanography, University of California Press, Berkeley & Los Angeles CA, 1985.

Stilwell, D., Jr., "Directional energy spectra of the sea from photographs", in Journal of Geophysical Research, 74(8), pp 1974-1986, 1969.

Stilwell, D. & R.O. Pilon, "Directional spectra of surface waves from photographs", in Journal of Geophysical Research, 79(9), pp 1277-1284, 1974.

Stokes, G.G., "On the theory of oscillatory waves", in <u>Mathematical and Physical Papers of the Cambridge Philosophical Society</u>, Vol I, pp 197-229, Cambridge University Press, London, 1880.

Stotts, L.B. & S. Karp, "Wave slope statistics derived from optical radiance measurements below the sea surface", in Applied Optics, 21(6), pp 978-981, 1982.

Ts'o, P.Y. & B.A. Barsky, "Modeling and rendering waves: wave-tracing using beta-splines and reflective and refractive texture mapping", in ACM Transactions on Graphics, 6(3), pp 191-214, 1987.

Upson, C., "The physical simulation and visual representation of natural phenomena", in ACM Computer Graphics (Proceedings of ACM SIGGRAPH 87), pp 335-336, 1987.

Weinman, J.A., "Derivation of atmospheric extinction profiles and wind speed over the ocean from a satellite-borne lidar", in Applied Optics, 27(19), pp 3994-4001, 1988.

Whitted, T., "An improved illumination model for shaded display", in Communications of the ACM, 23(6), pp 343-349, 1980.

Wilf, I. & Y. Manor, "Simulation of sea surface images in the infrared", in Applied Optics, 23(18), pp 3174-3180, 1984.

Wu, J., "Slope and curvature distributions of wind-disturbed water surface", in Journal of the Optical Society of America, 61(7), pp 852-858, 1971.

Wu, J., "Effects of long waves on wind boundary layer and on ripple slope statistics", in Journal of Geophysical Research, 82(9), pp 1359-1362, 1977.

Zaneveld, J.R.V., "Remotely sensed reflectance and its dependence on vertical structure: a theoretical derivation", in Applied Optics, 21(22), pp 4146-4150, 1982.

APPENDIX I - D_1 Results

The two-dimensional graphic results for the 72 combinations of solar position, dominant wind azimuth, and wind friction velocity are presented in Appendix I. Each page presents the graphic variation of wind friction velocity for a single combination of solar position and dominant wind azimuth:

v_{fric} = 12.0 cm/sec (Slope Variance versus Wavenumber)
(Slope Variance versus Azimuth)

v_{fric} = 36.0 cm/sec (Slope Variance versus Wavenumber)
(Slope Variance versus Azimuth)

v_{fric} = 60.0 cm/sec (S_.pe Variance versus Wavenumber)
(Slope Variance versus Azimuth)

Each set of four pages presents the graphic variation of dominant wind velocity wind_az for a single solar position:

First Page	wind_az = 0 deg	(or 180 deg with ambiguity)
Second Page	wind_az = 45 deg	(or -135 deg with ambiguity)
Third Page	wind_az = 90 deg	(or - 90 deg with ambiguity)
Fourth Page	wind_Az = 135 deg	(or - 45 deg with ambiguity)

The graphic variation for the six solar positions is then presented in the following order:

First Set	phi_0 = 0 deg	$theta_0$ = 0.0 deg
Second Set	phi_0 = 45 deg	$theta_0$ = 53.2 deg
Third Set	phi_0 = 90 deg	$theta_0$ = 53.2 deg
Fourth Set	phi_0 = 135 deg	$theta_0$ = 53.2 deg
Fifth Set	phi_0 = 180 deg	$theta_0$ = 53.2 deg
Sixth Set	phi_0 = 0 deg	$theta_0$ = 53.2 deg

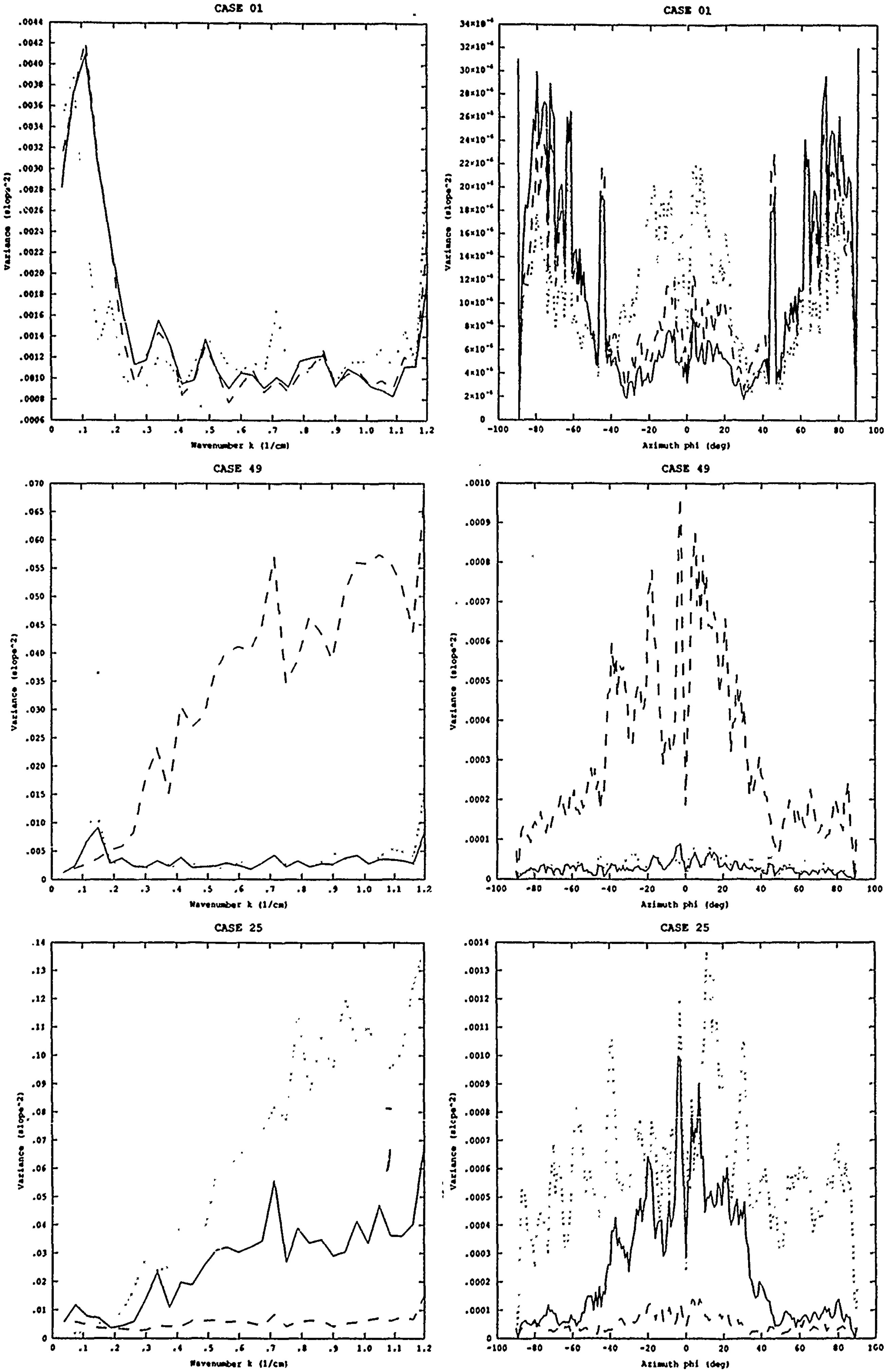
CASE 01
Variance (slope^2)
Wavenumber k (1/cm)
CASE 01
Variance (slope^2)
Azimuth phi (deg)
CASE 49
Variance (slope^2)
Wavenumber k (1/cm)
CASE 49
Variance (slope^2)
Azimuth phi (deg)
CASE 25
Variance (slope^2)
Wavenumber k (1/cm)
CASE 25
Variance (slope^2)
Azimuth phi (deg)

CASE 07

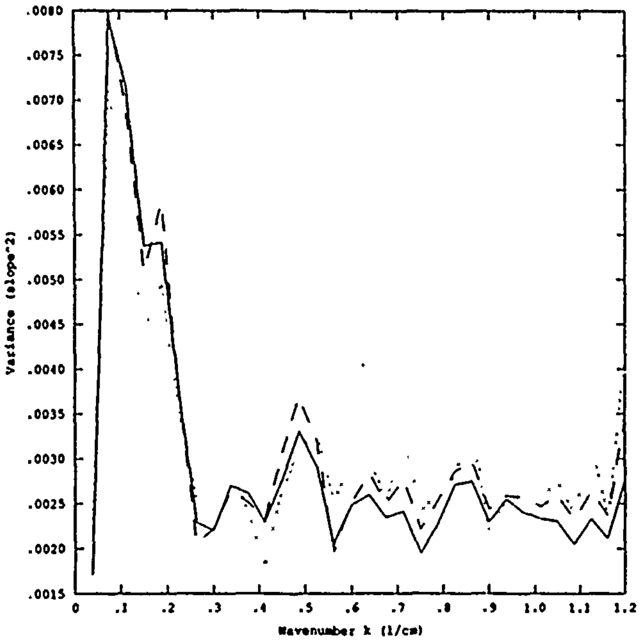

CASE 07

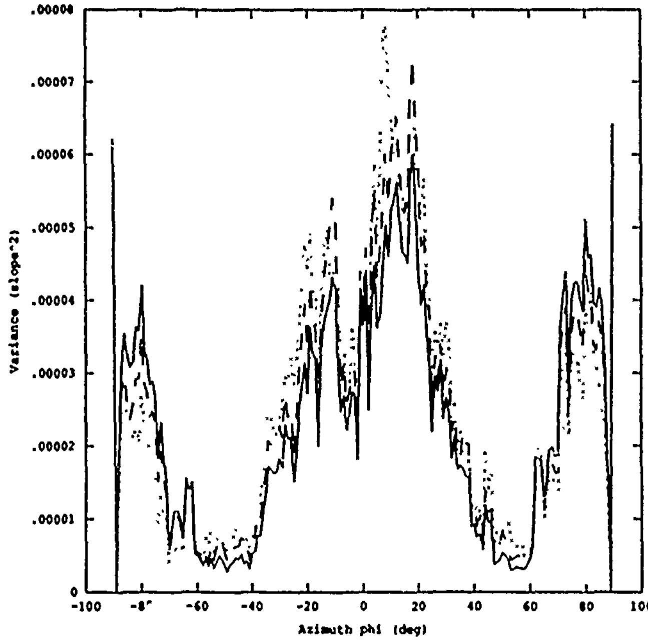

CASE 55

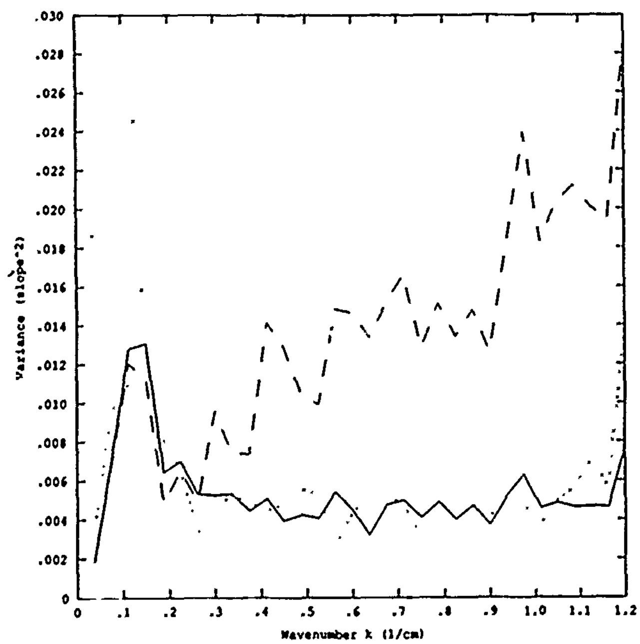

CASE 55

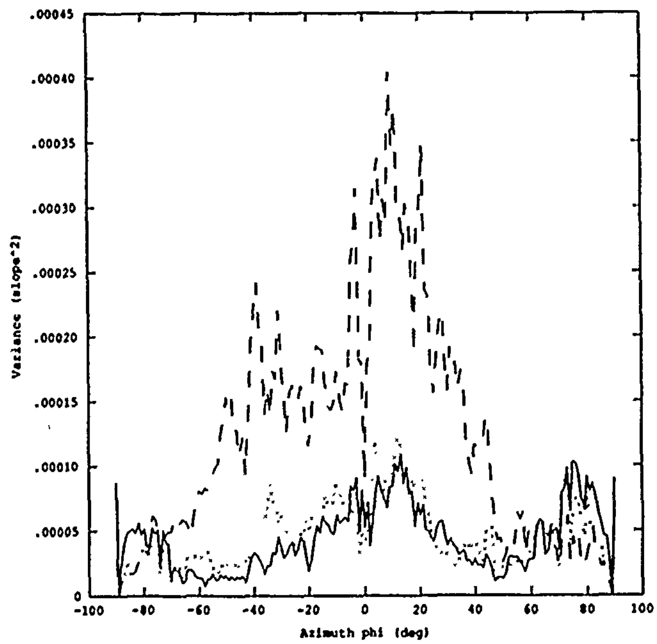

CASE 31

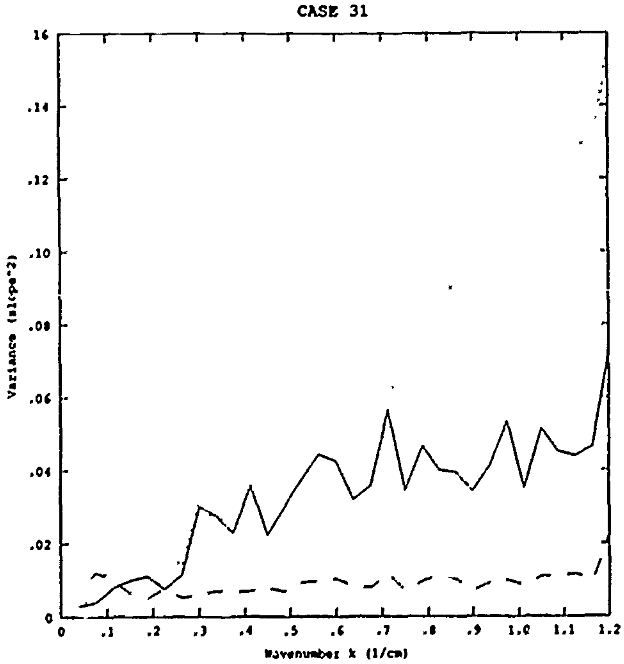

CASE 31

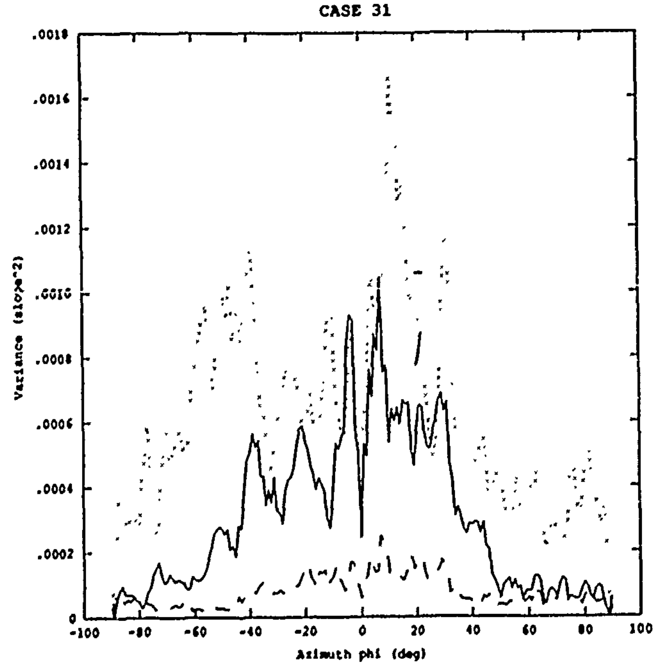

CASE 13

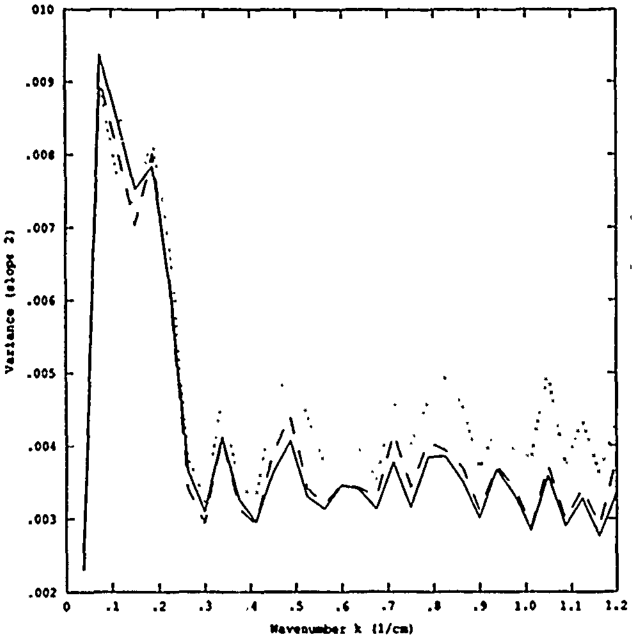

CASE 13

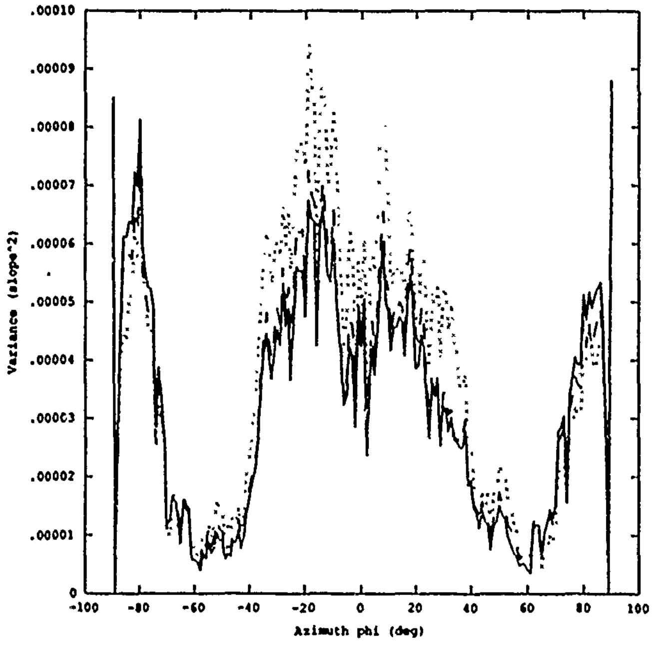

CASE 61

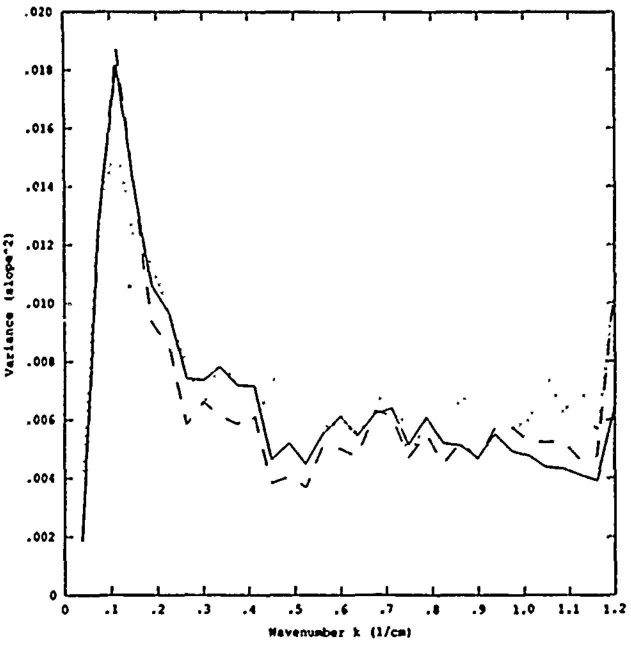

CASE 61

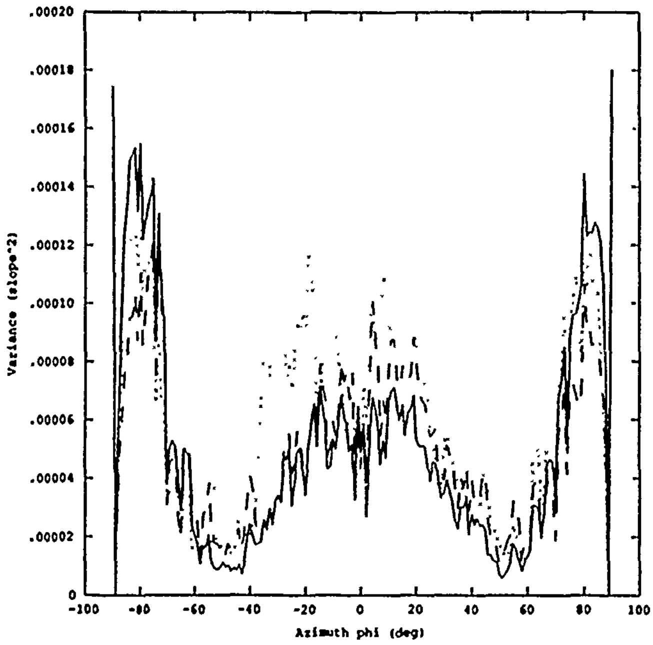

CASE 37

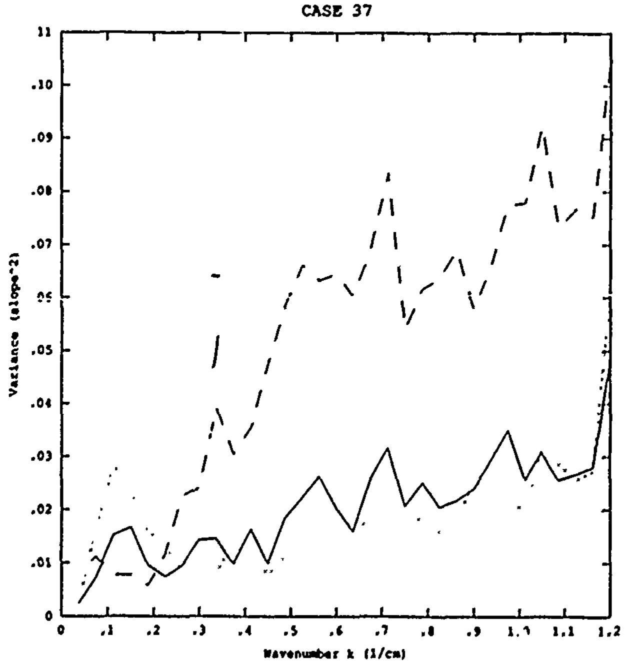

CASE 37

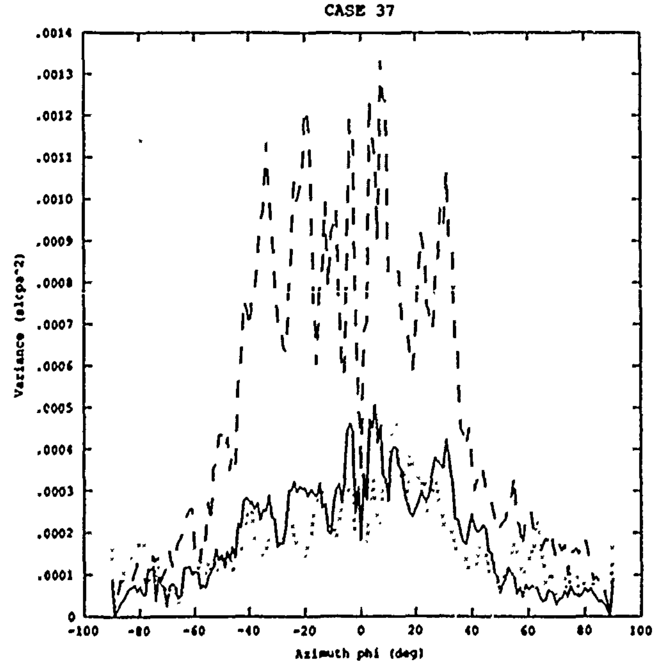

CASE 19

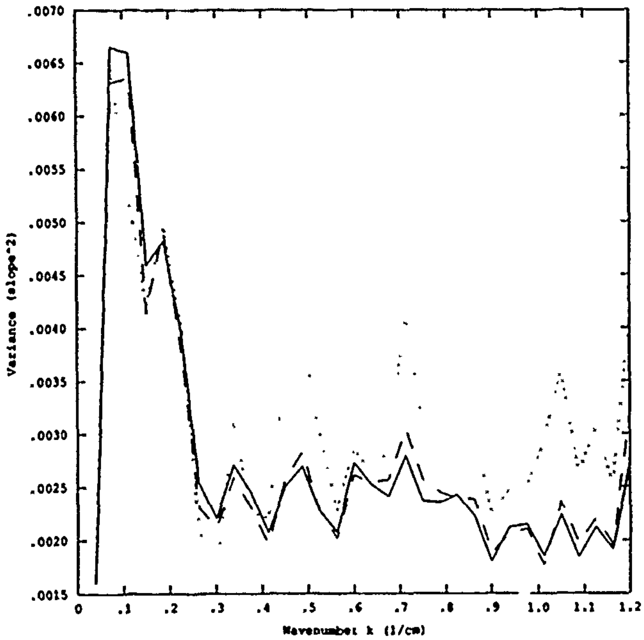

CASE 19

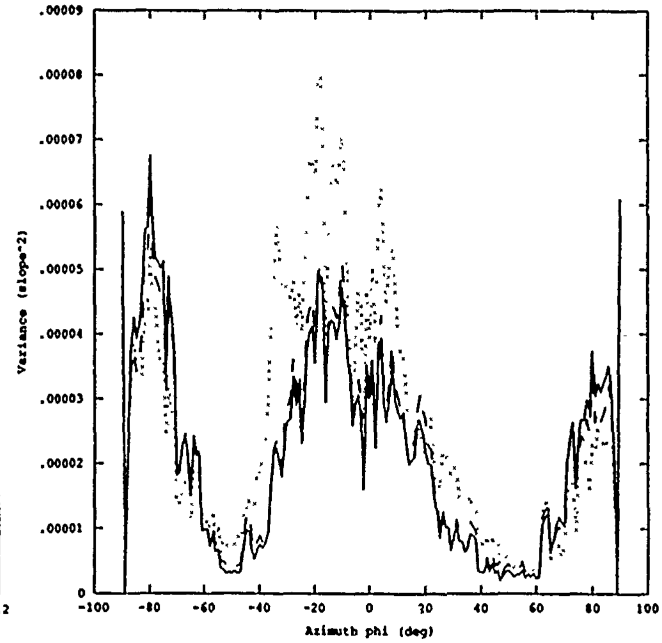

CASE 67

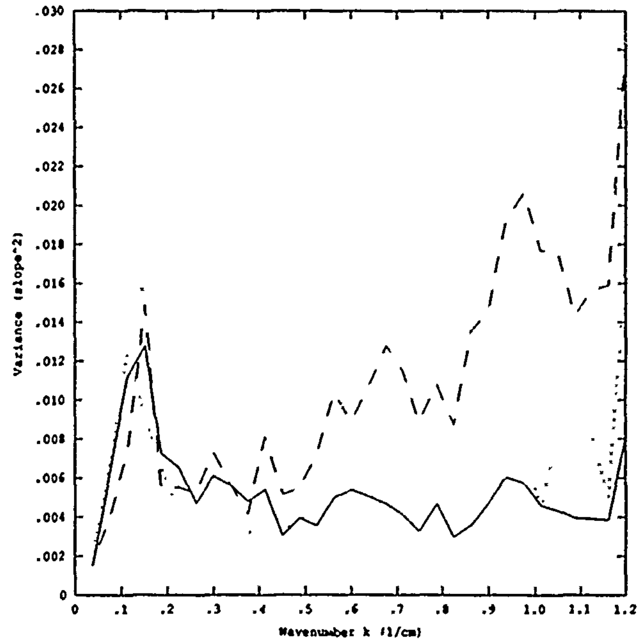

CASE 67

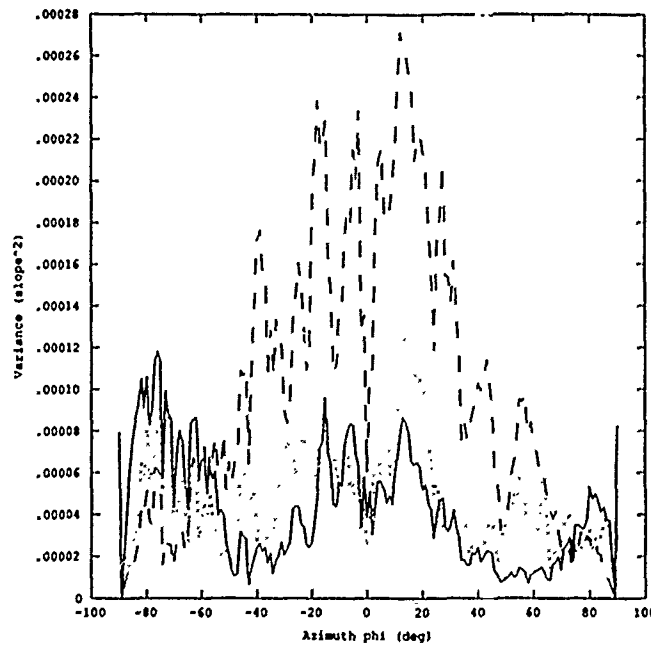

CASE 43

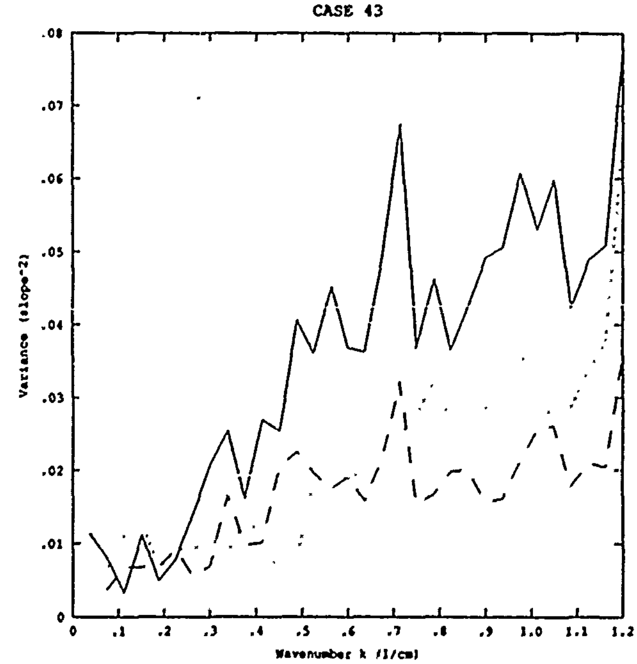

CASE 43

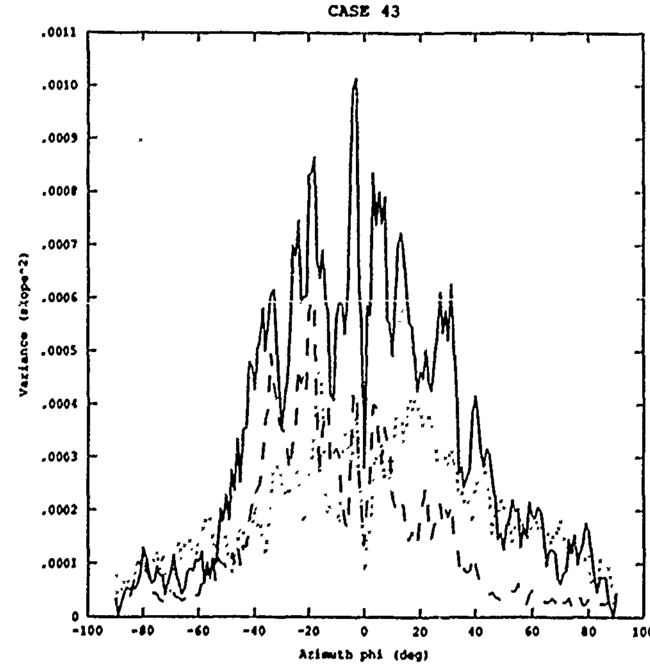

CASE 02

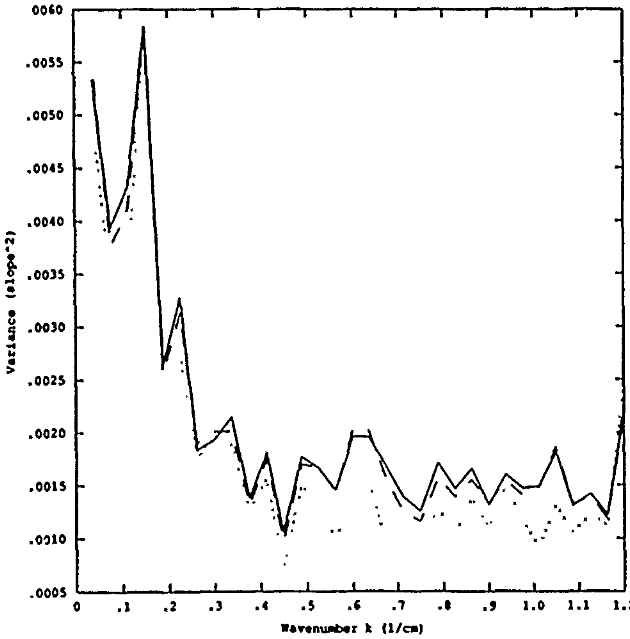

CASE 02

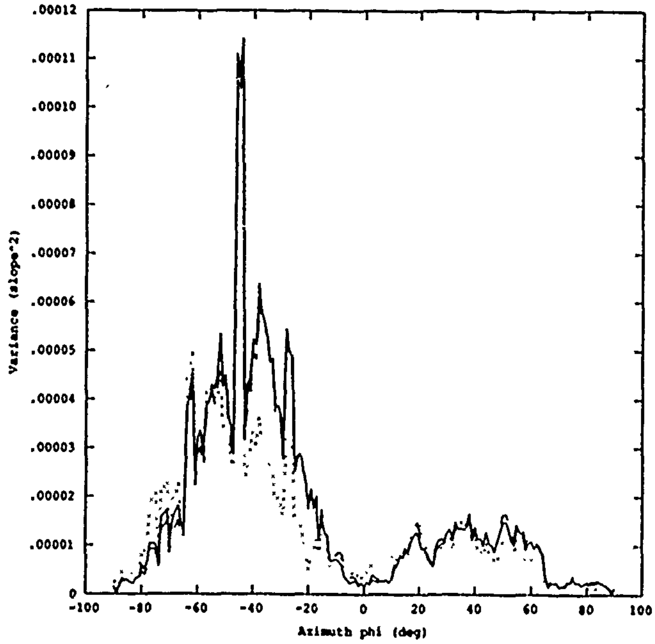

CASE 50

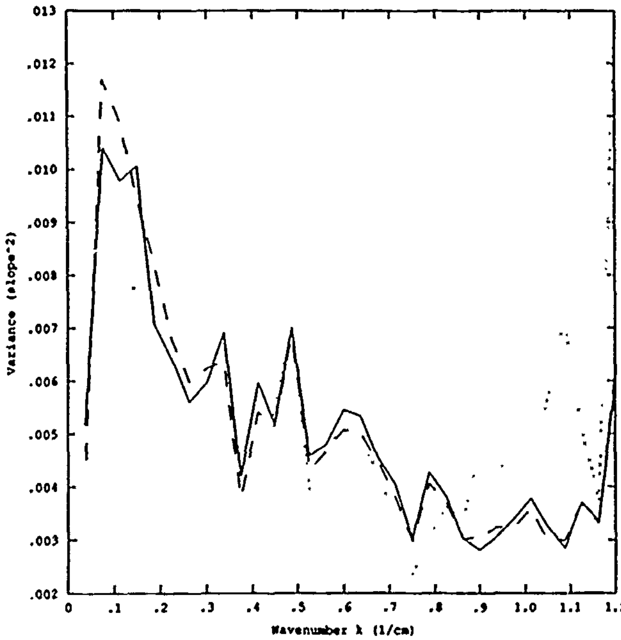

CASE 50

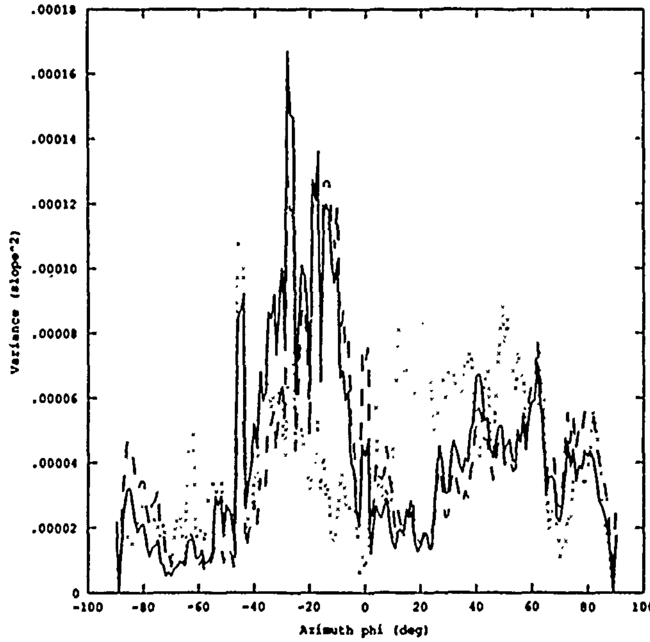

CASE 26

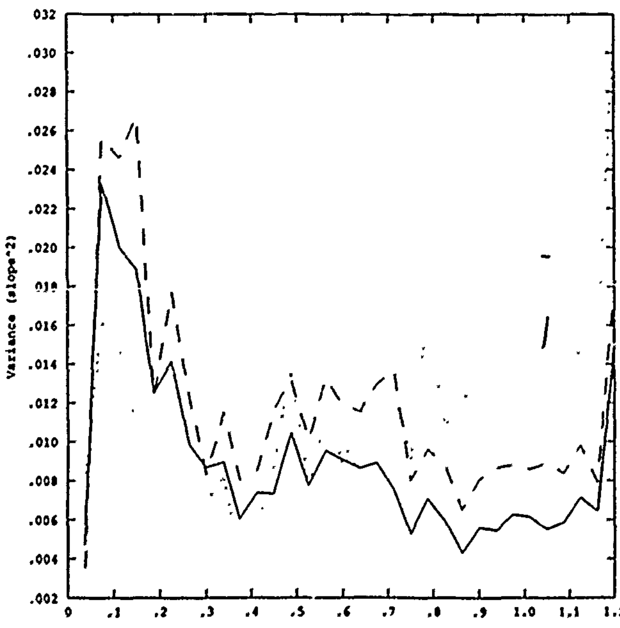

CASE 26

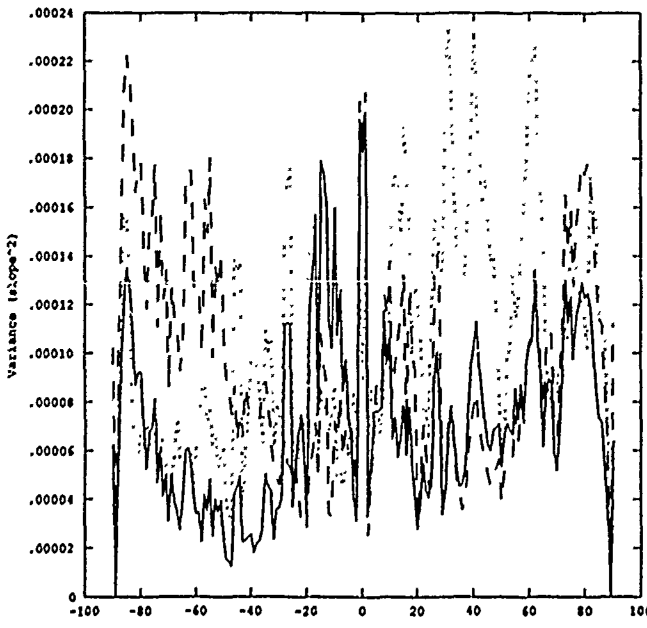

CASE 08

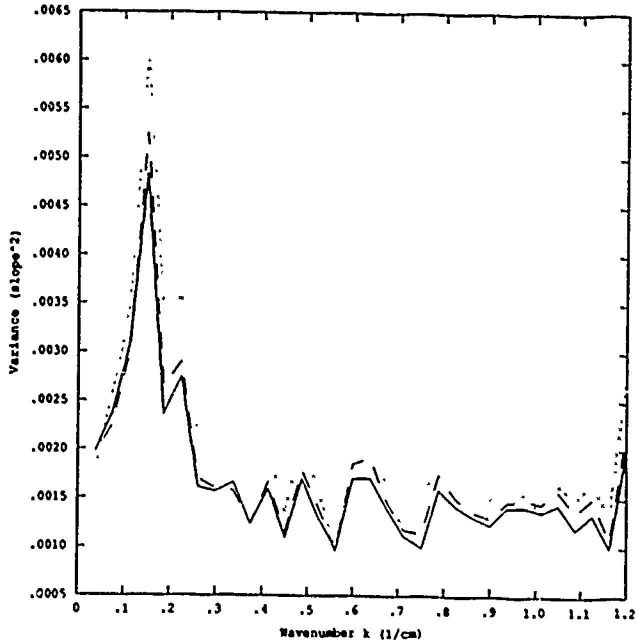

CASE 08

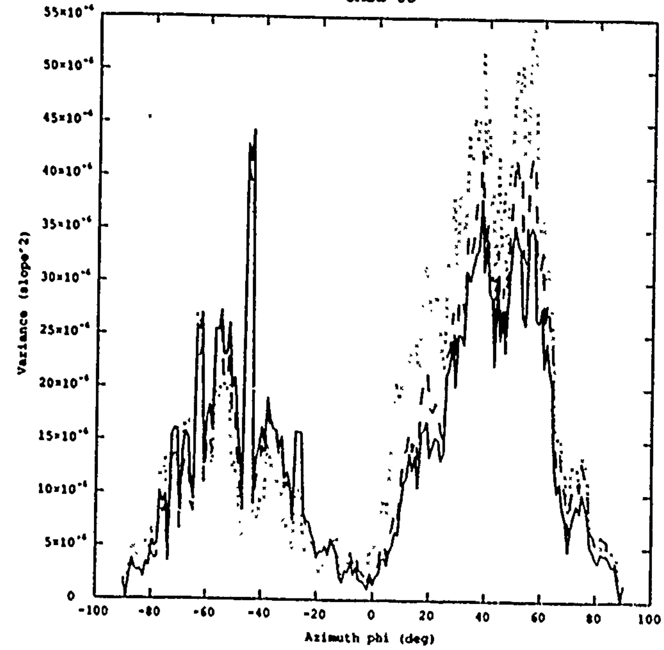

CASE 56

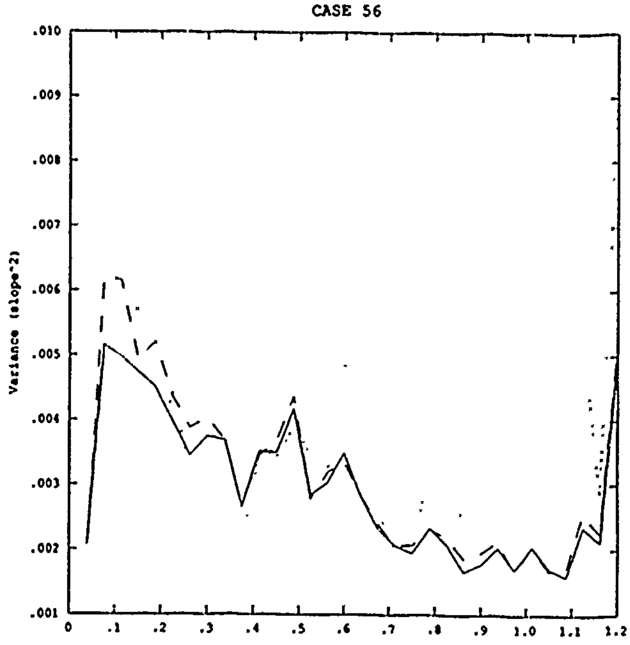

CASE 56

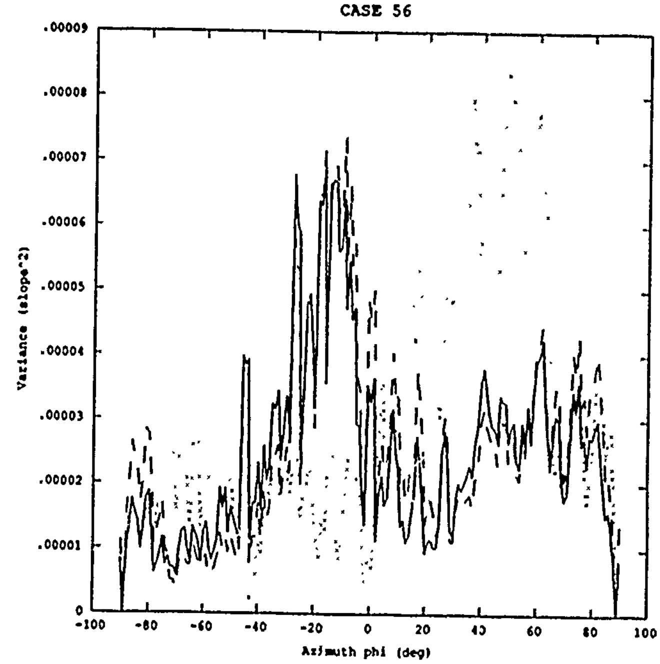

CASE 32

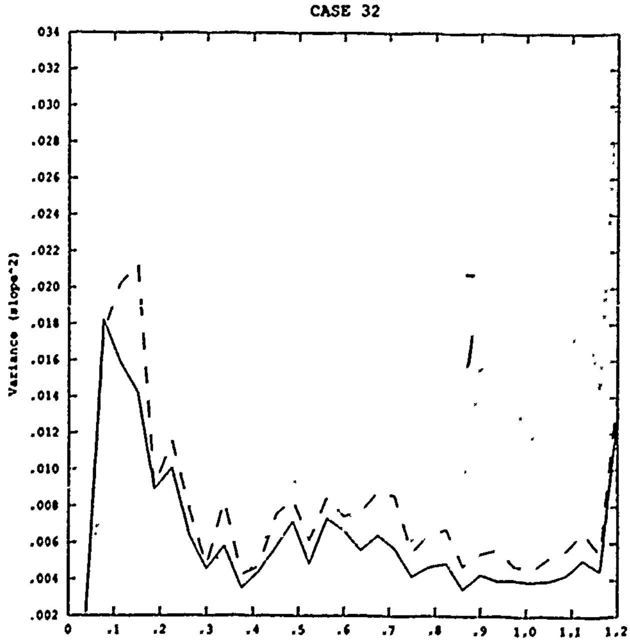

CASE 32

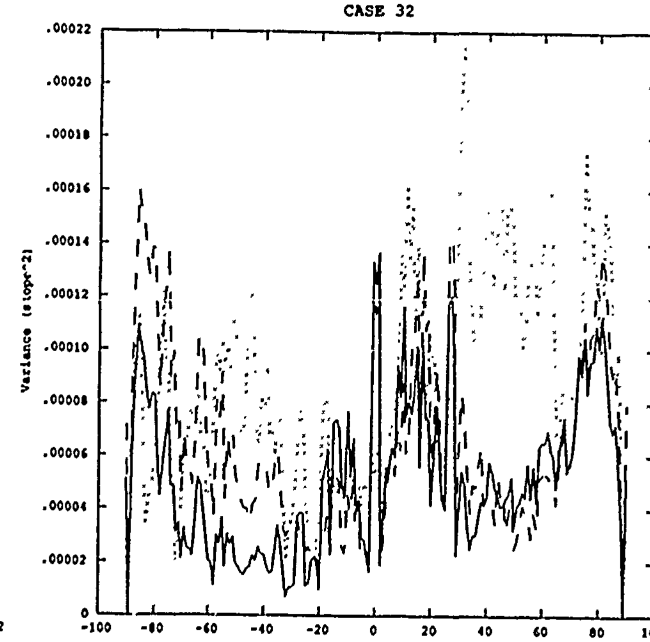

CASE 14

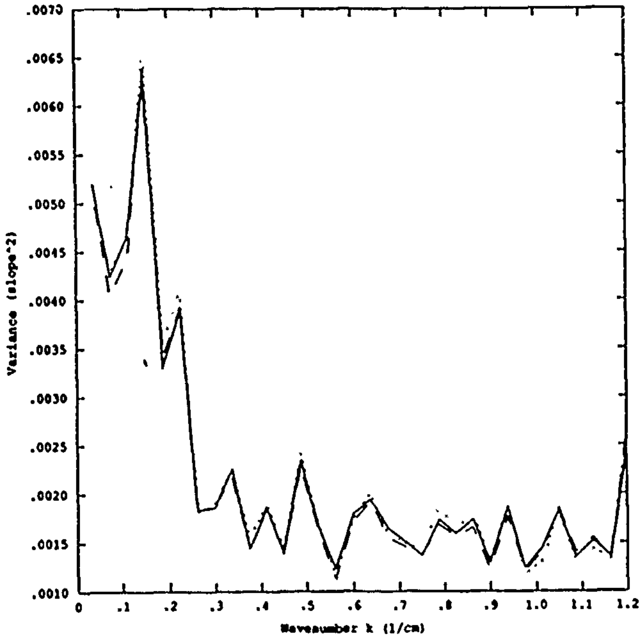

CASE 14

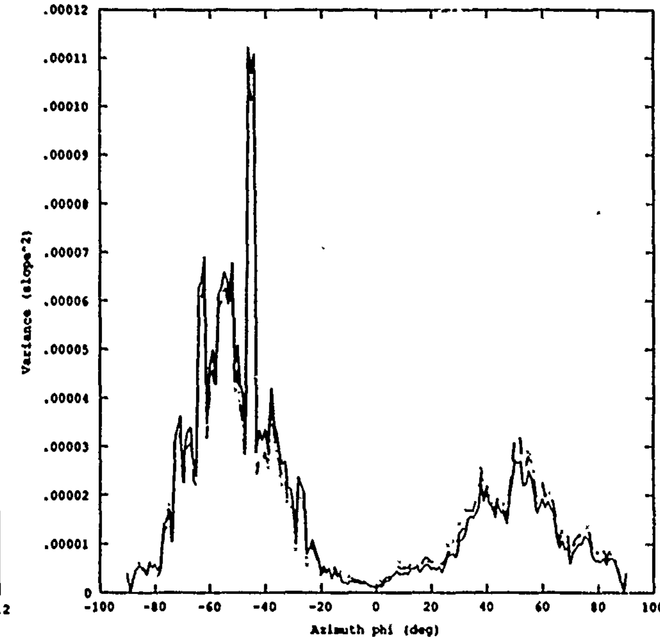

CASE 62

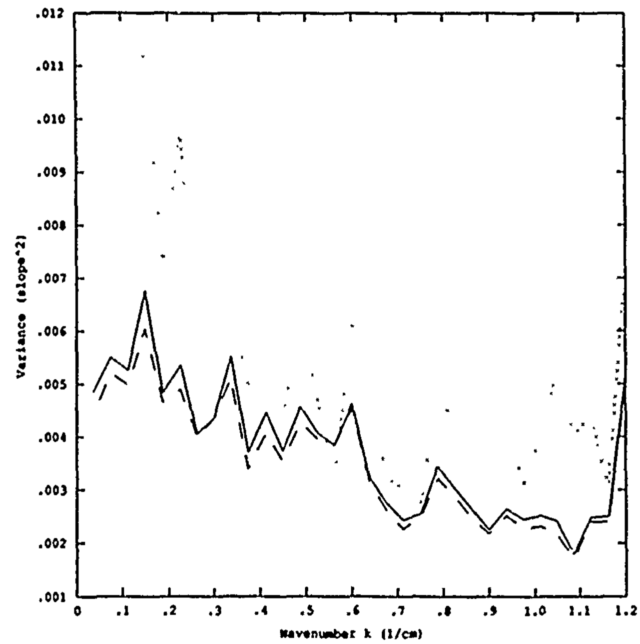

CASE 62

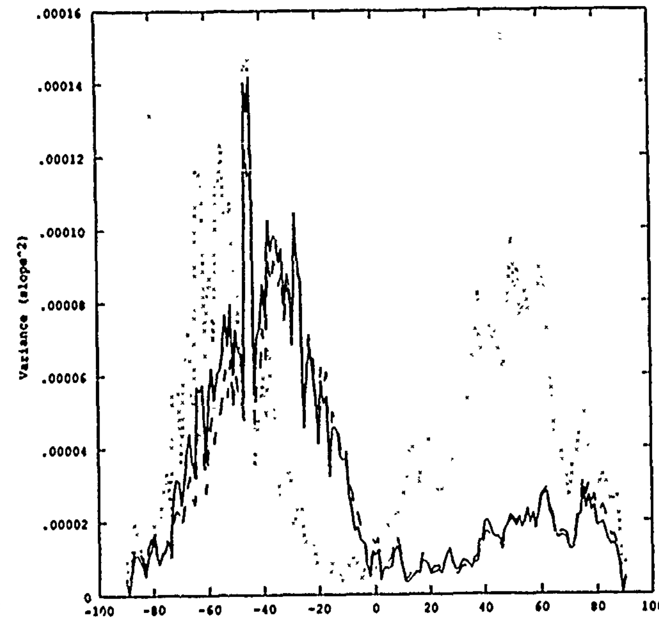

CASE 38

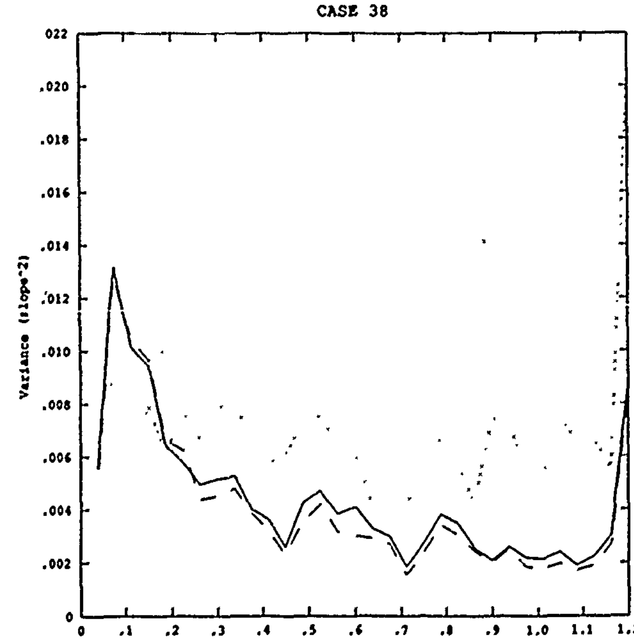

CASE 38

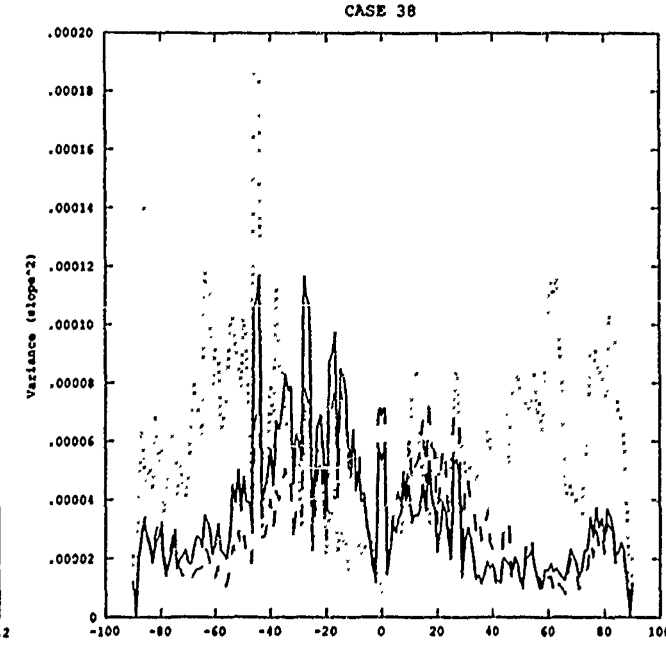

CASE 20

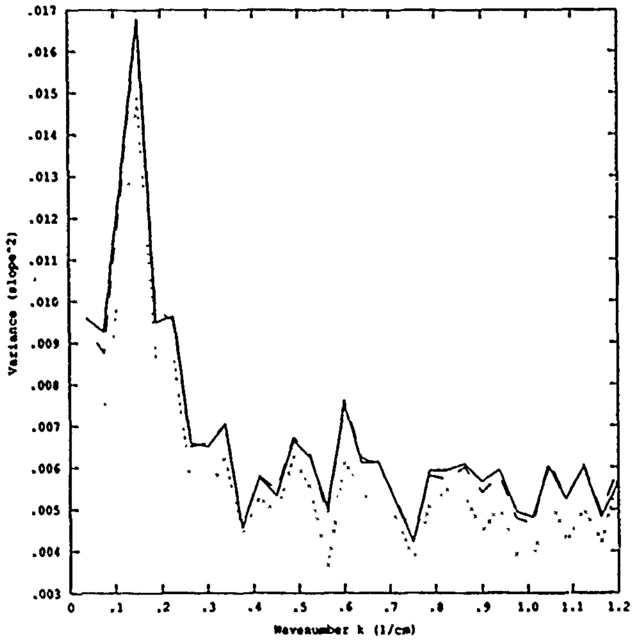

CASE 20

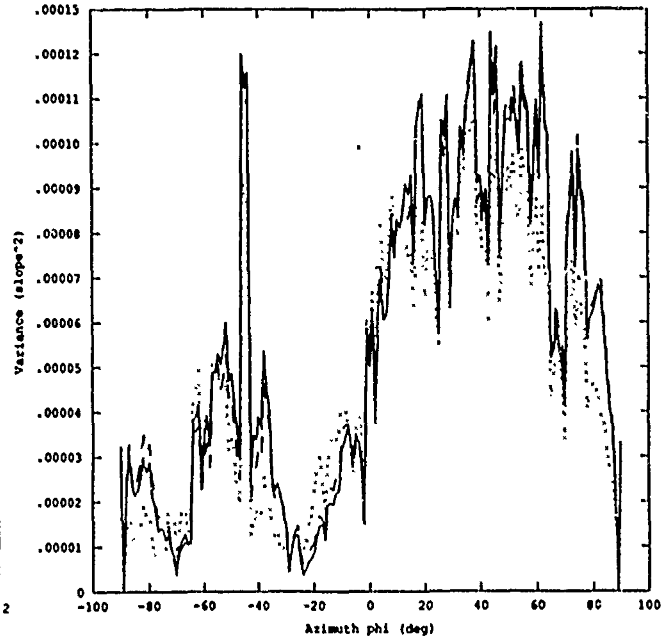

CASE 68

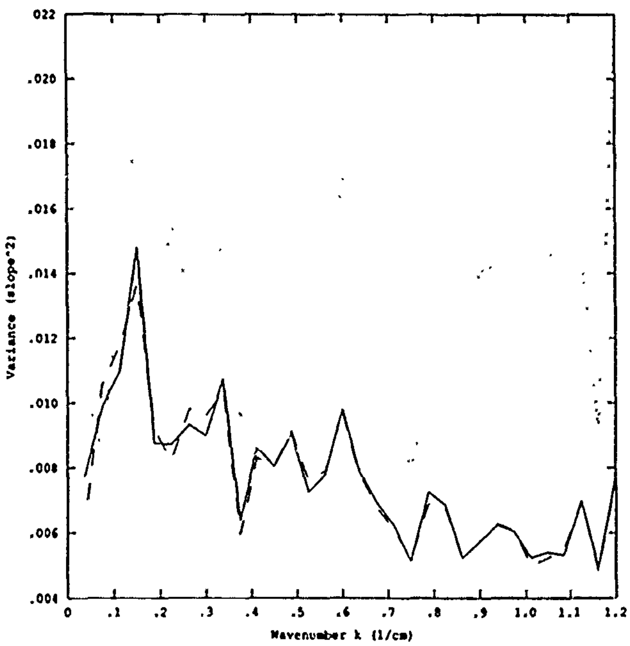

CASE 68

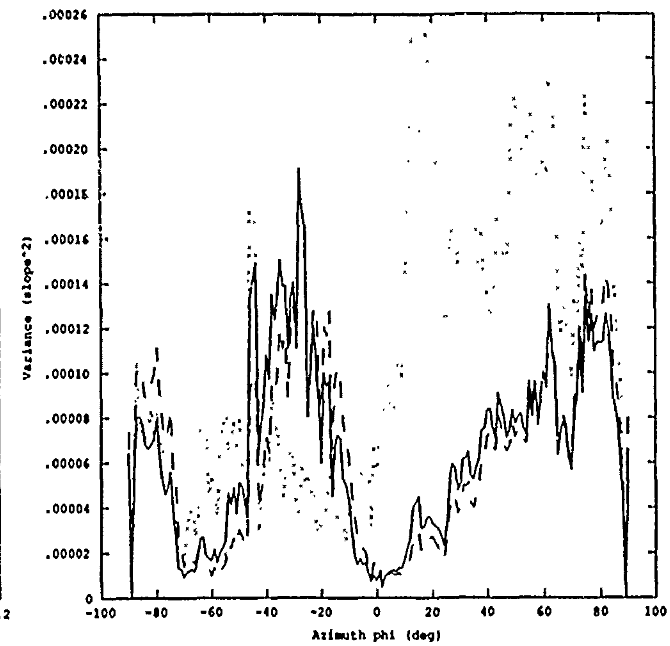

CASE 44

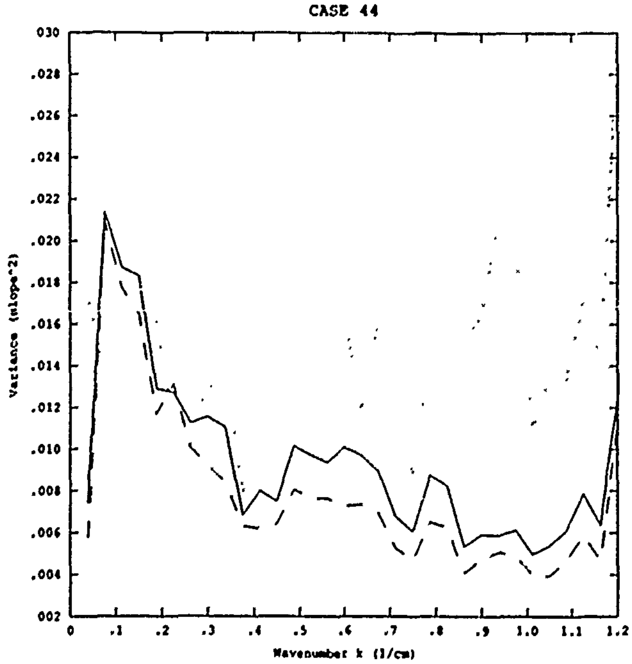

CASE 44

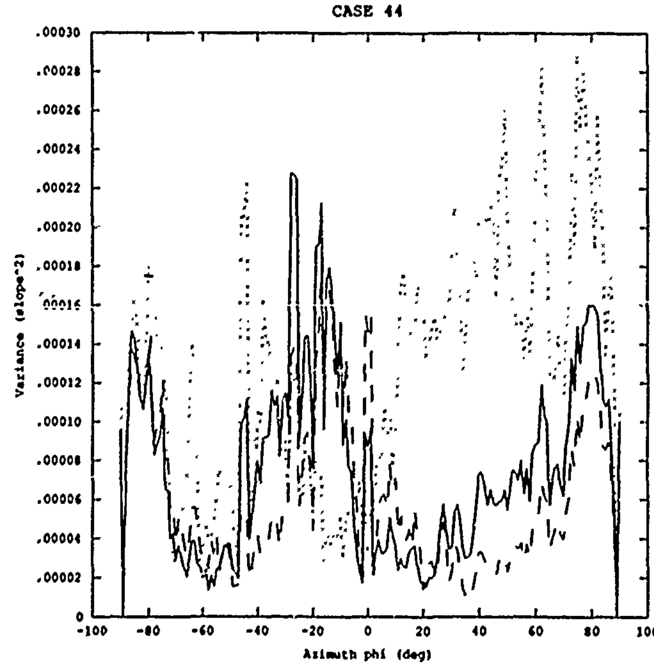

CASE 03

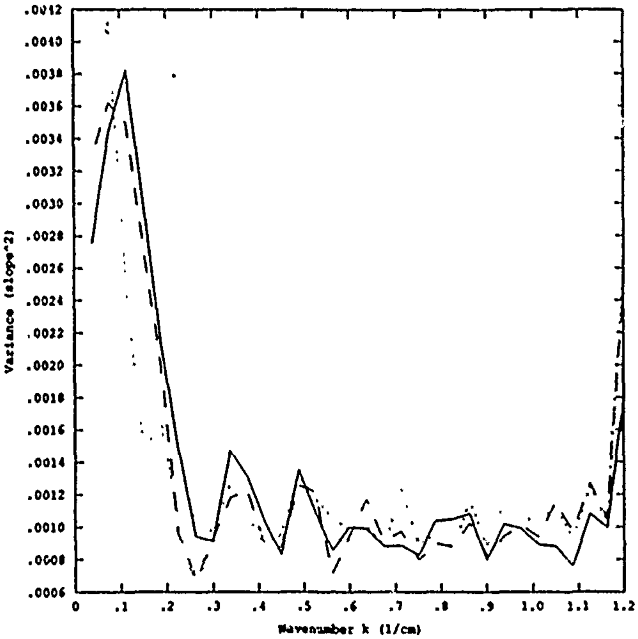

CASE 03

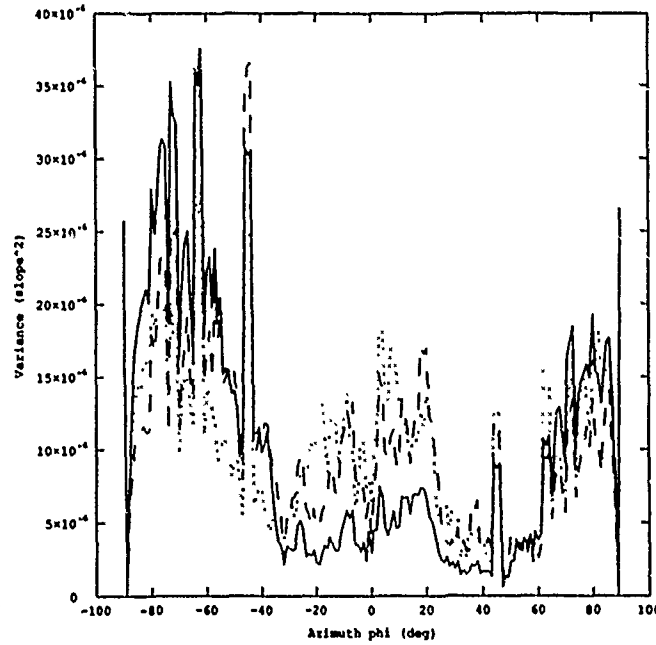

CASE 51

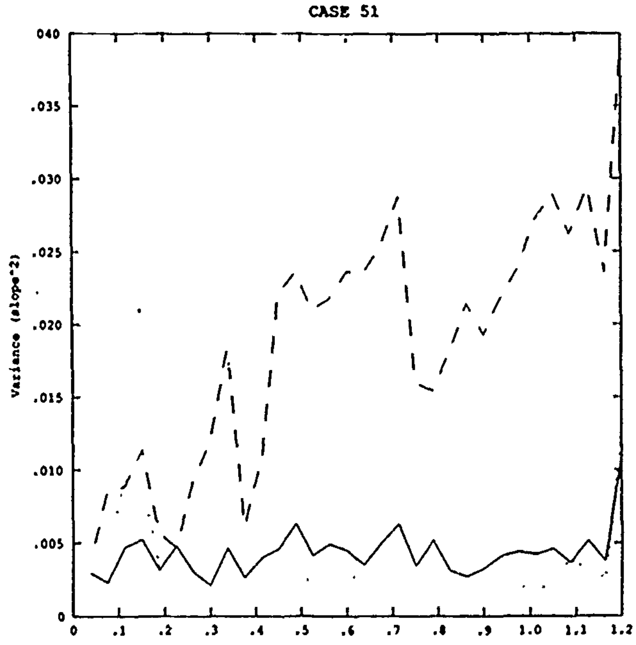

CASE 51

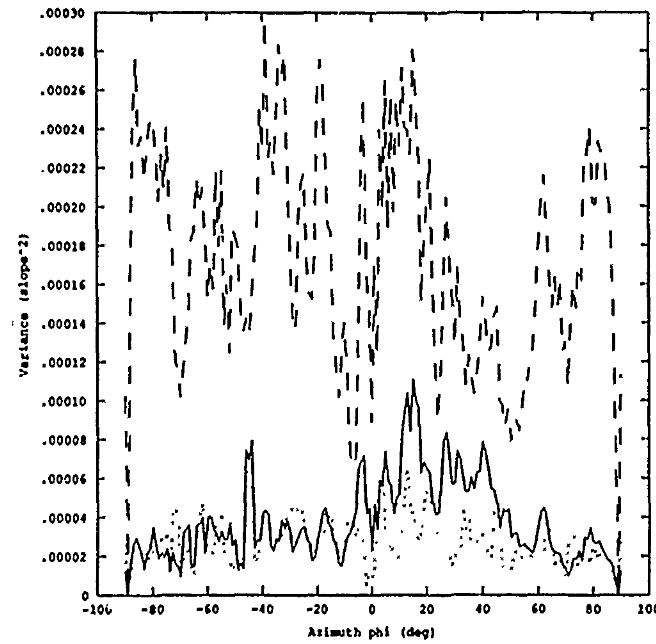

CASE 27

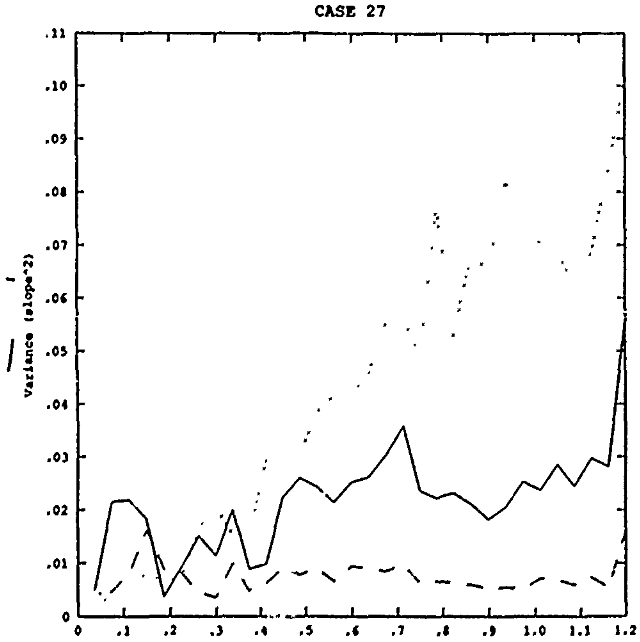

CASE 27

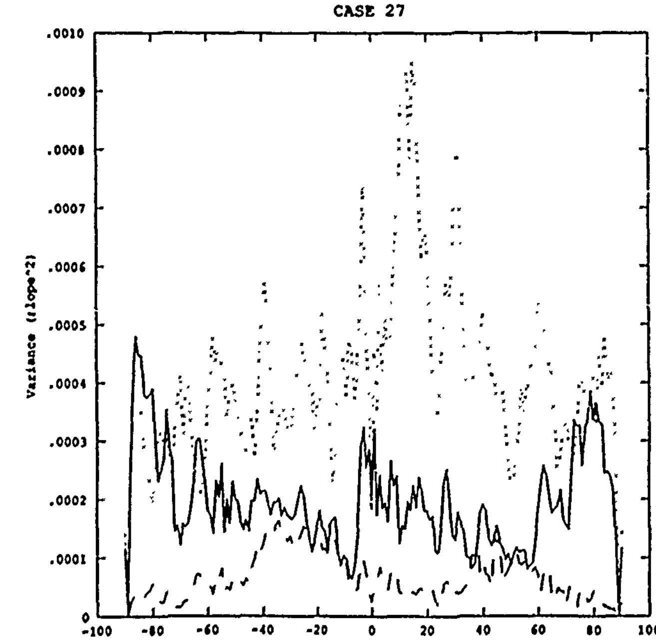

CASE 09

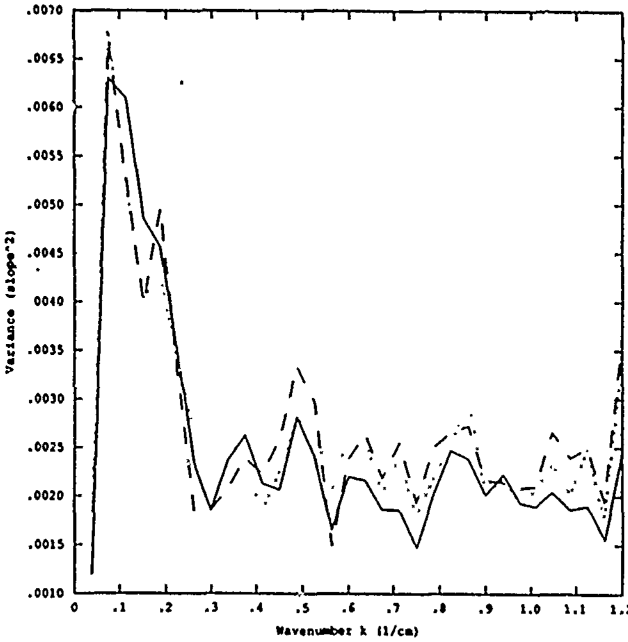

CASE 09

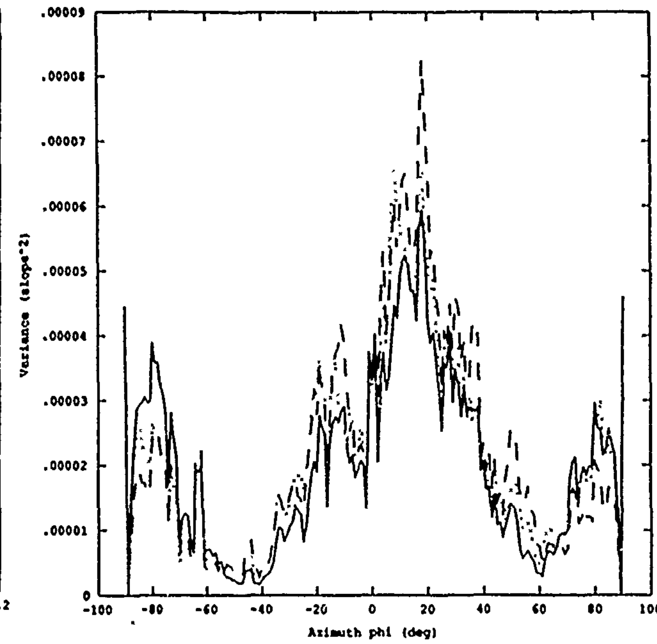

CASE 57

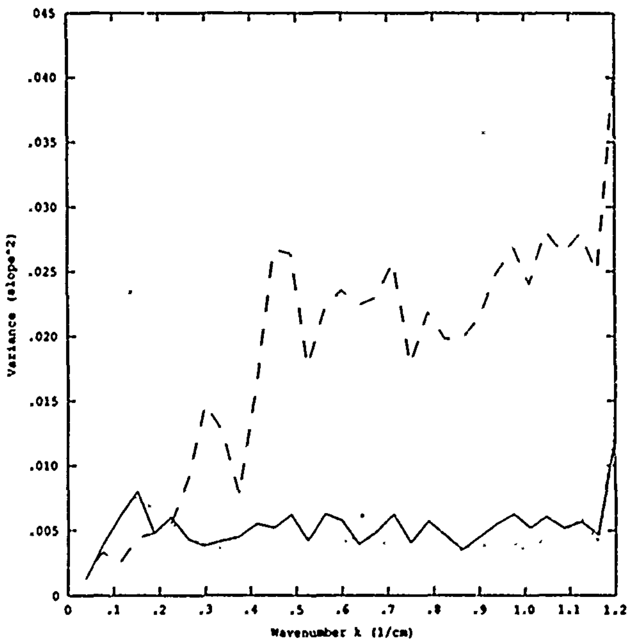

CASE 57

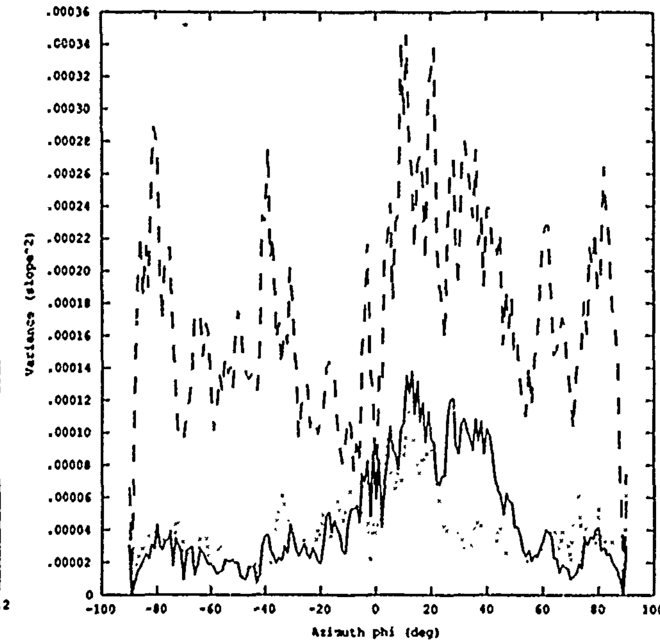

CASE 33

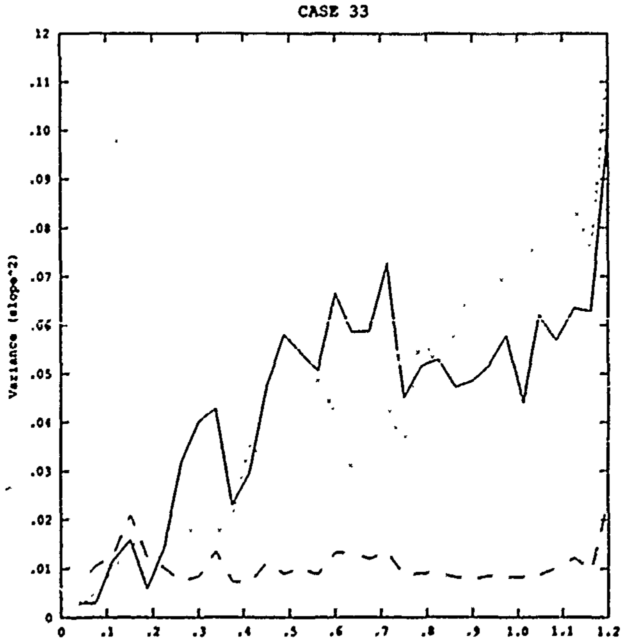

CASE 33

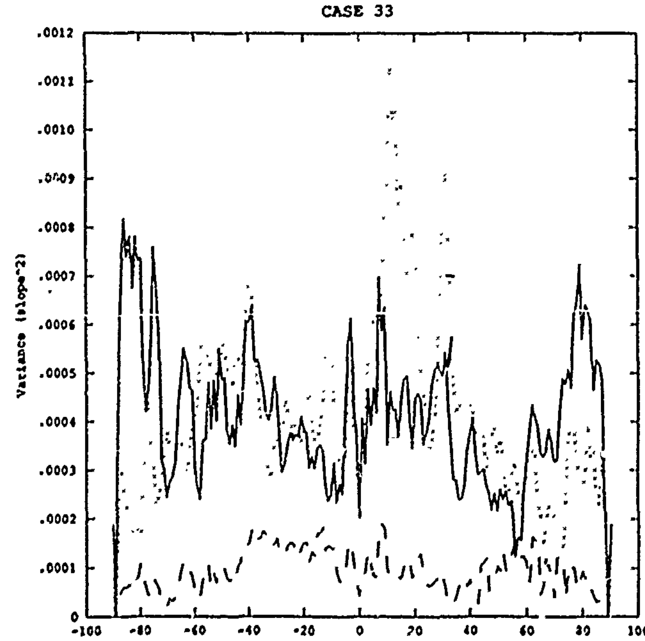

CASE 15

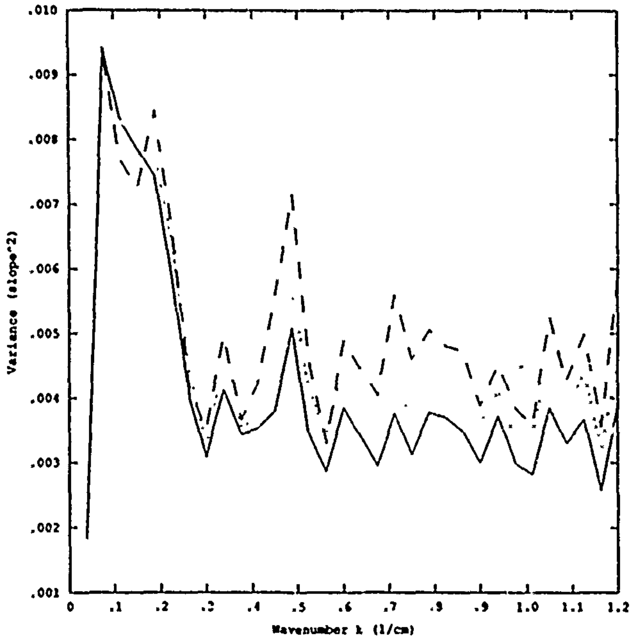

CASE 15

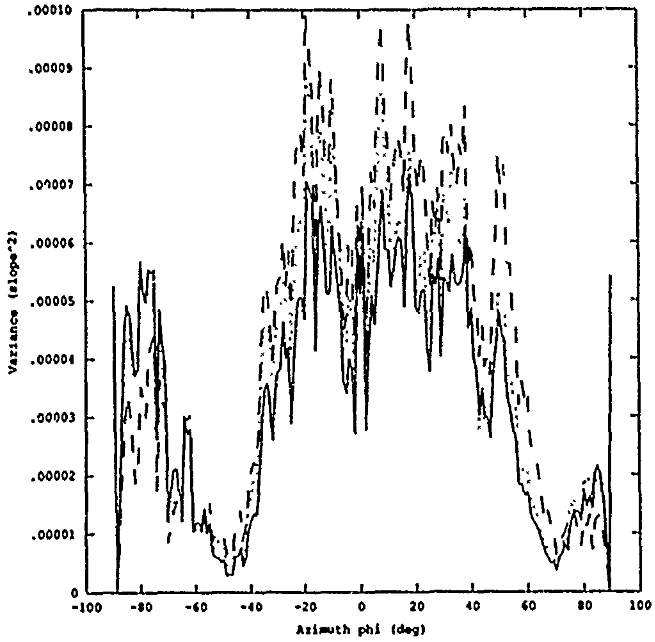

CASE 63

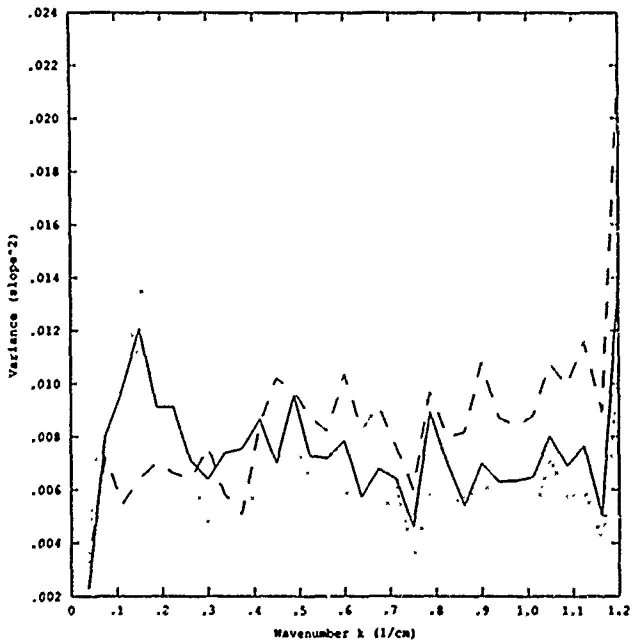

CASE 63

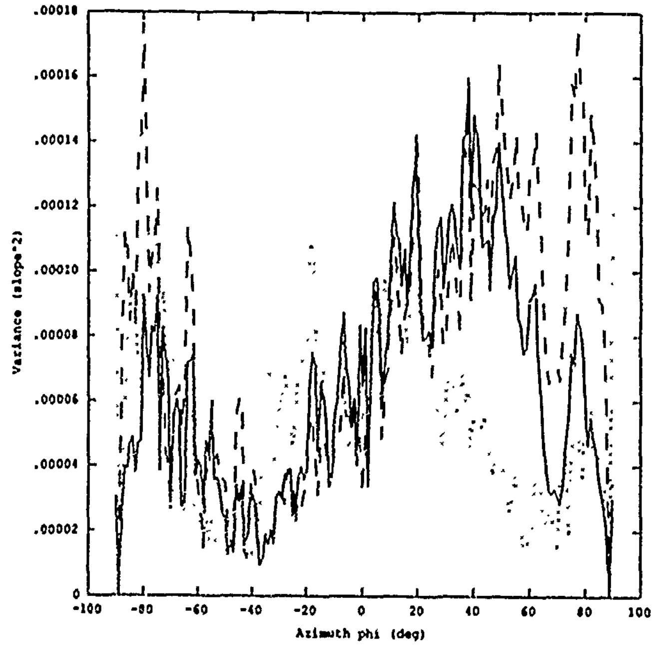

CASE 39

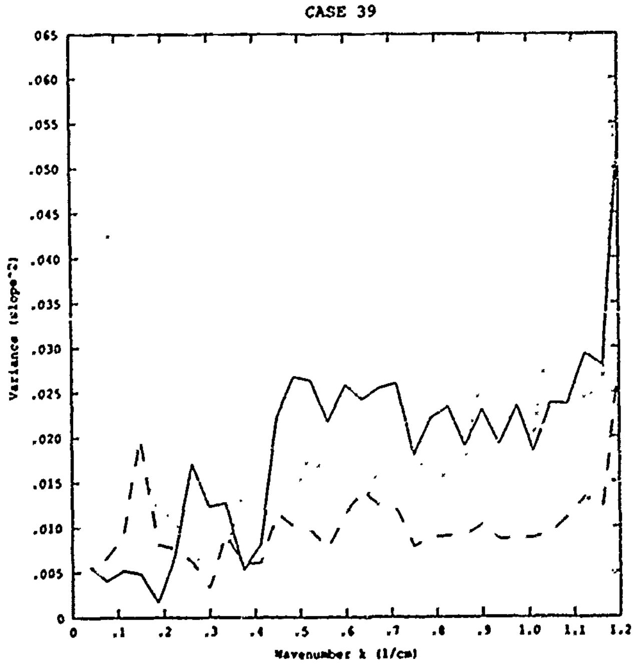

CASE 39

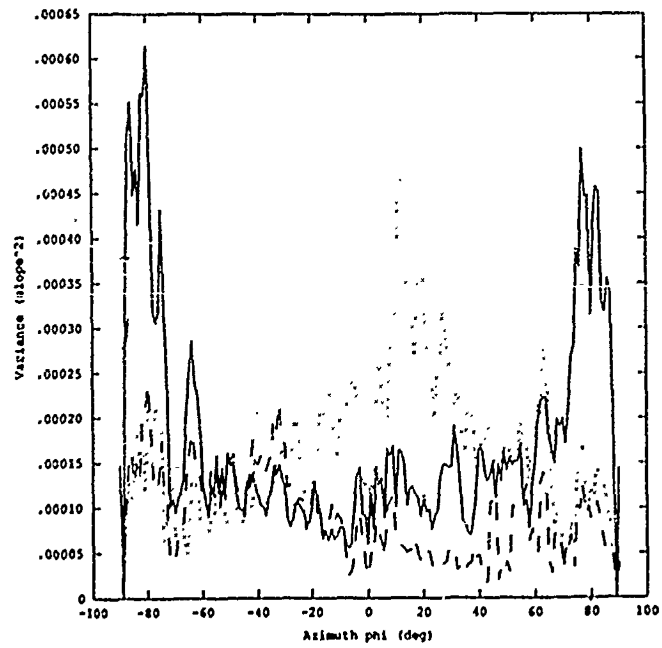

CASE 21

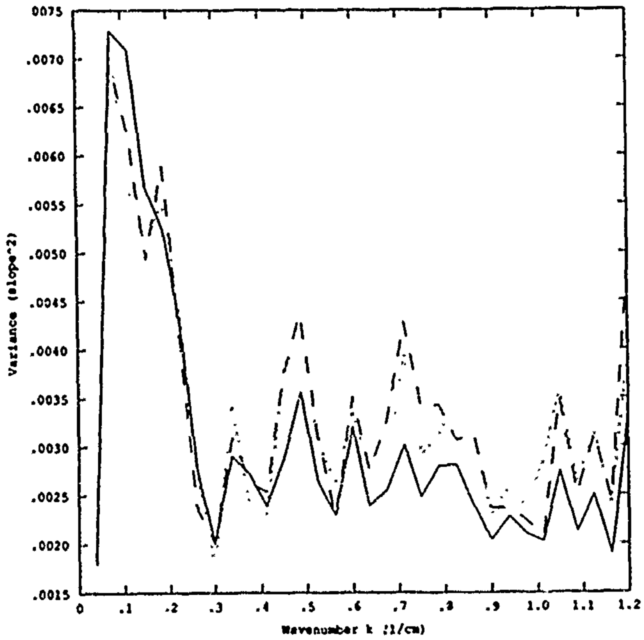

CASE 21

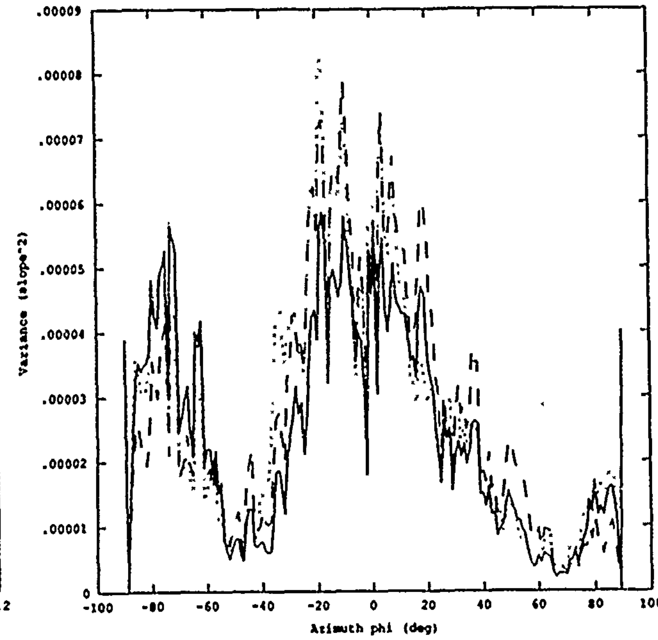

CASE 69

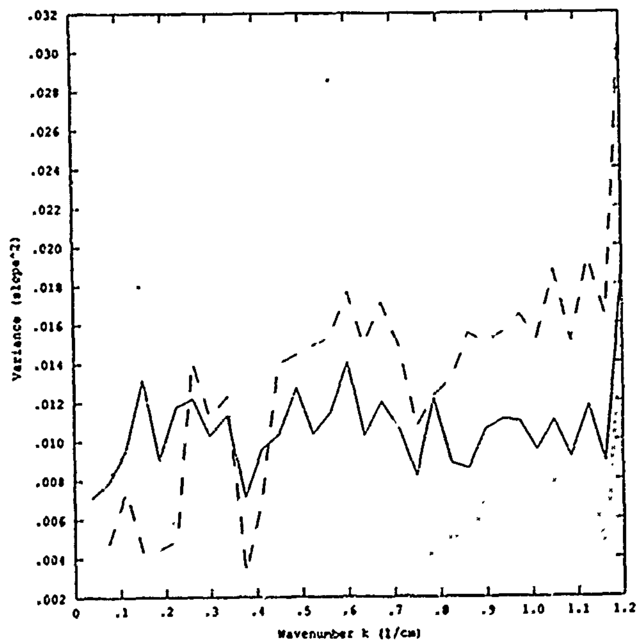

CASE 69

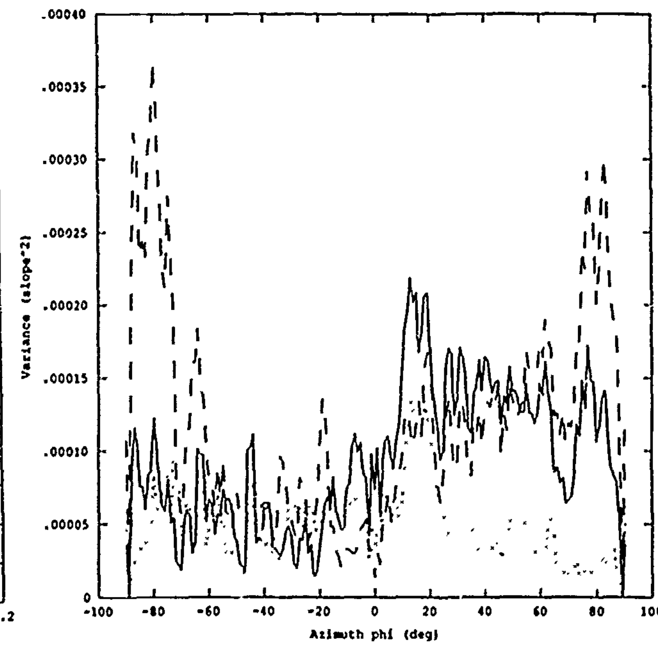

CASE 45

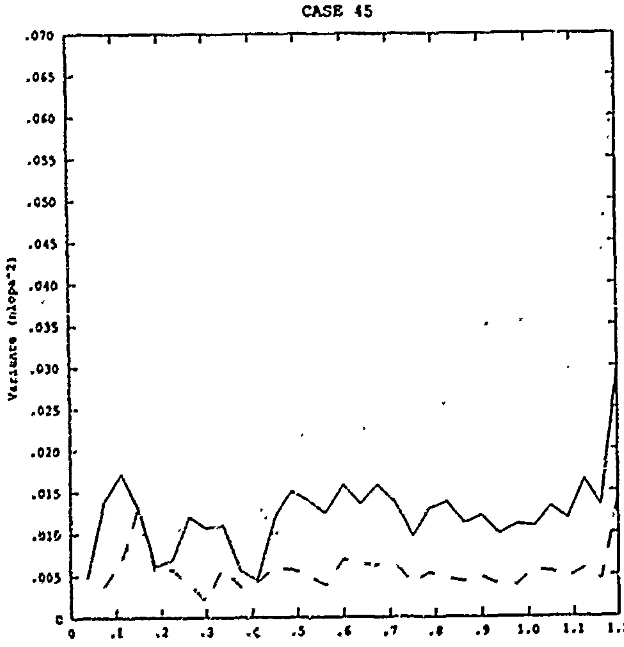

CASE 45

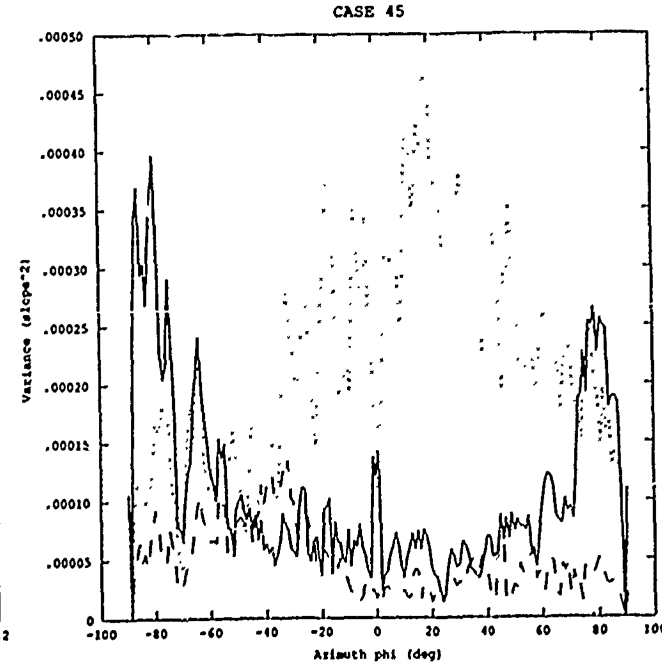

CASE 04

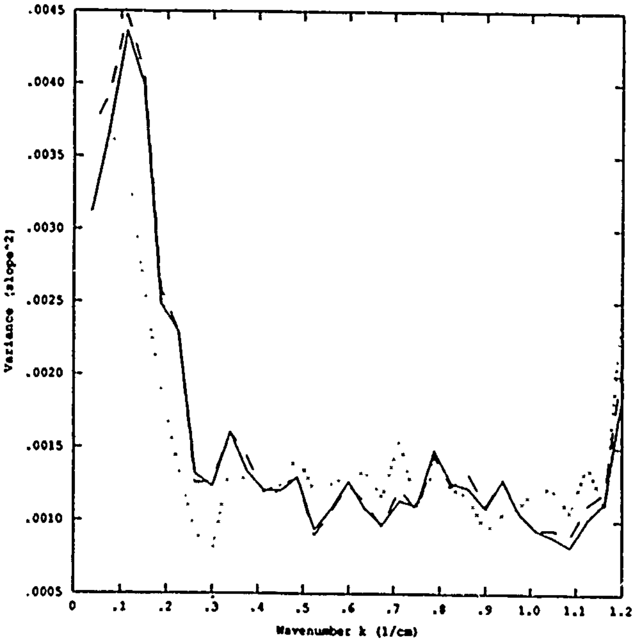

CASE 04

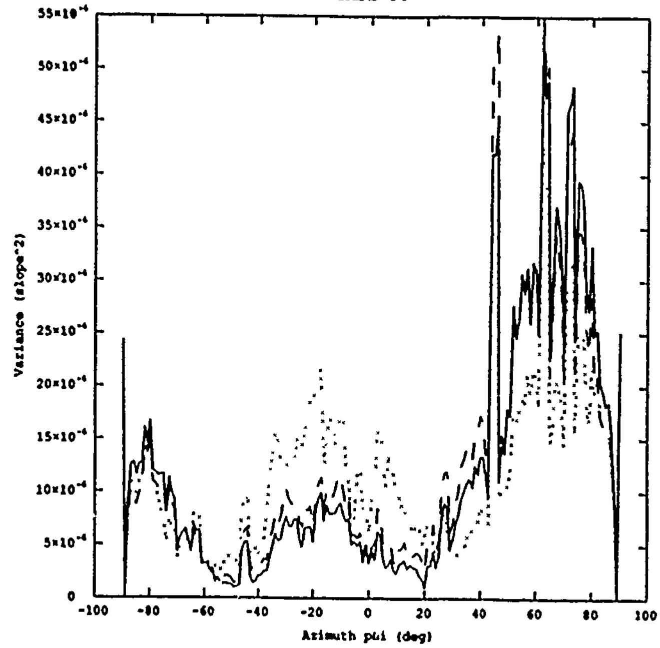

CASE 52

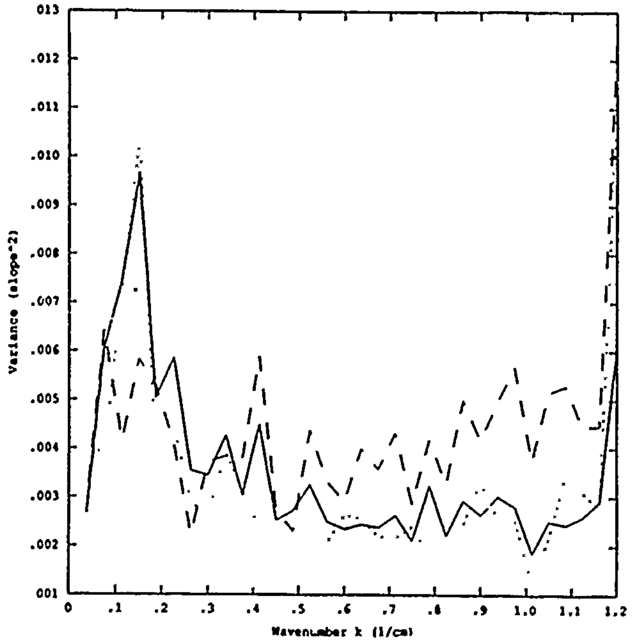

CASE 52

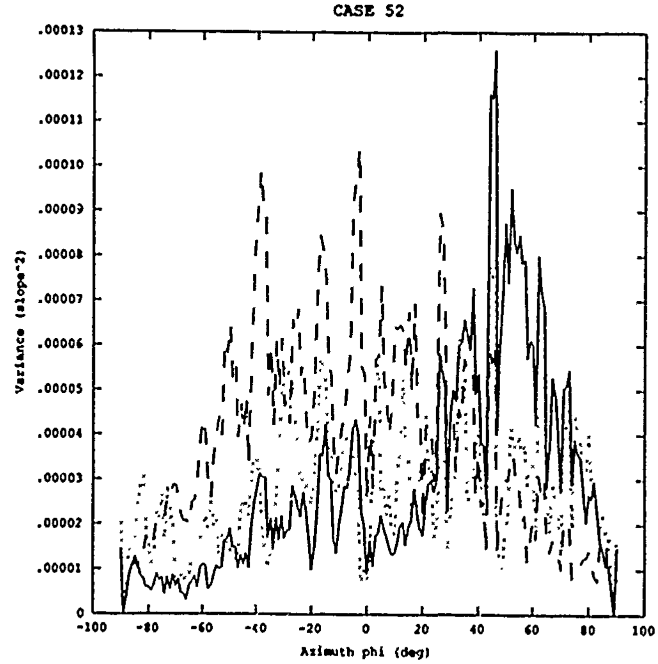

CASE 28

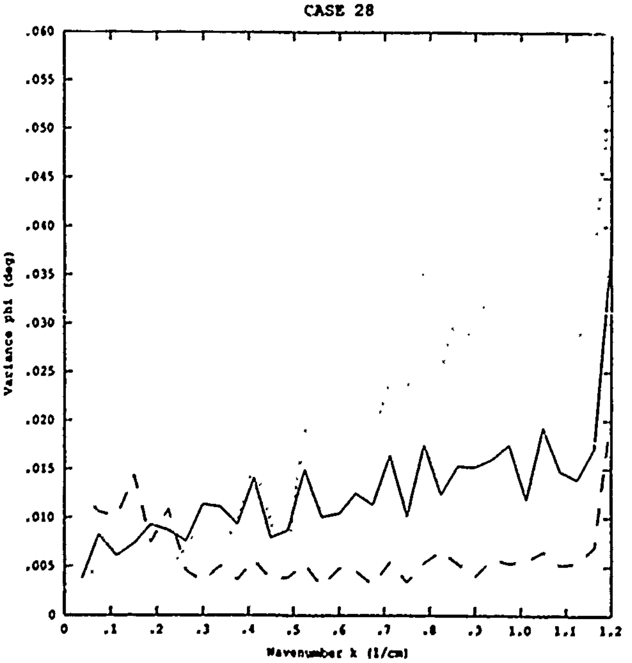

CASE 28

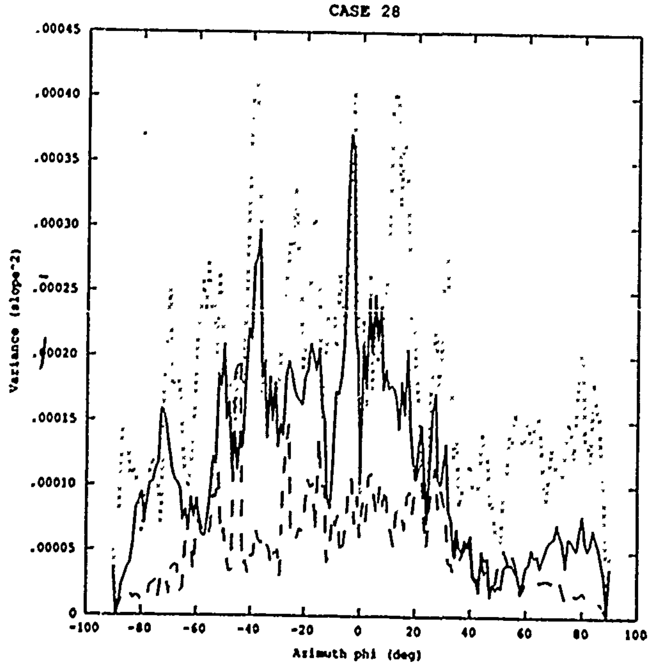

CASE 10

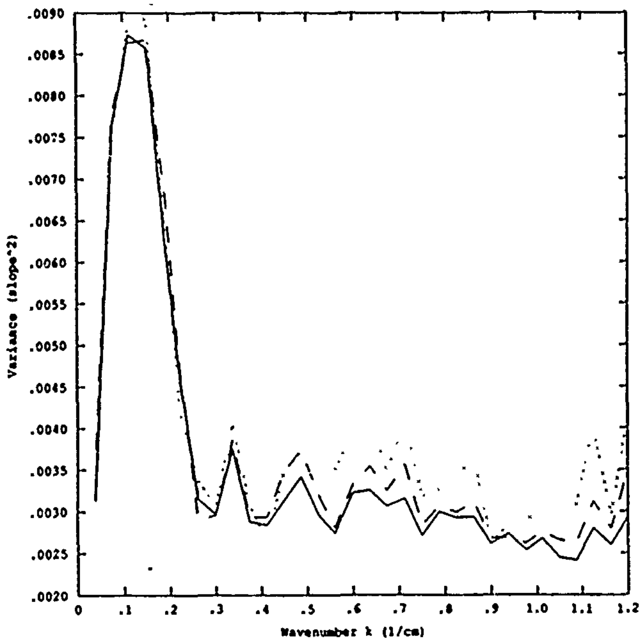

CASE 10

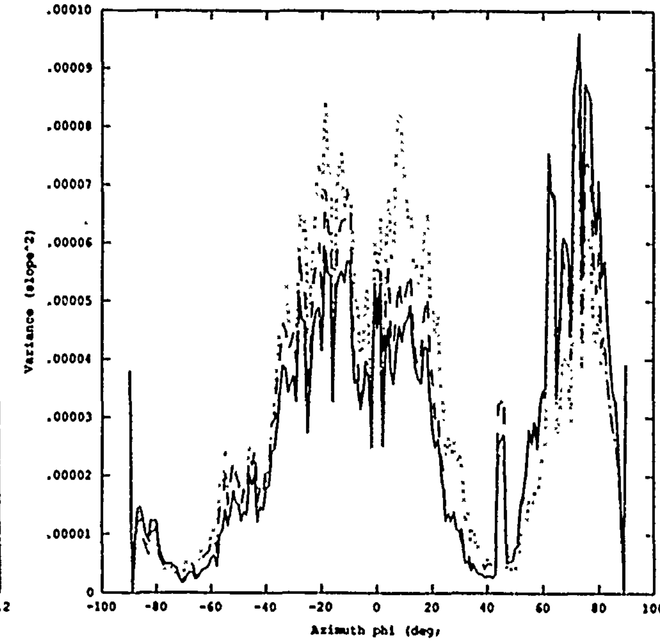

CASE 58

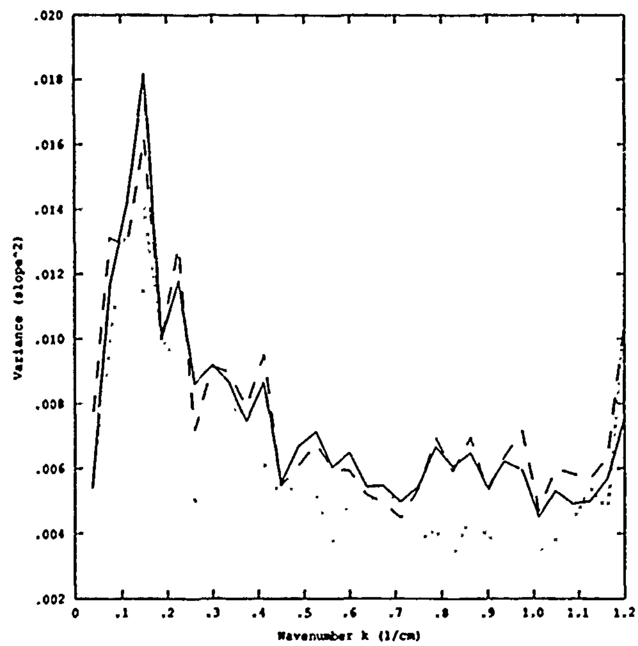

CASE 58

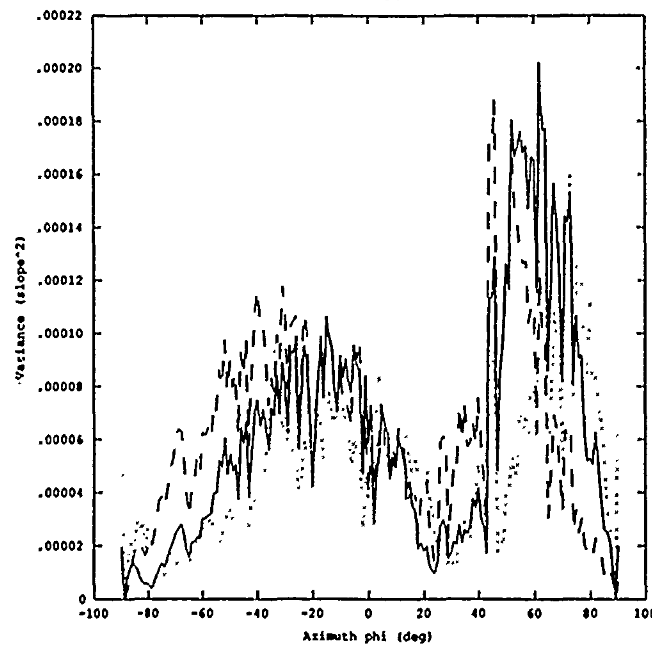

CASE 34

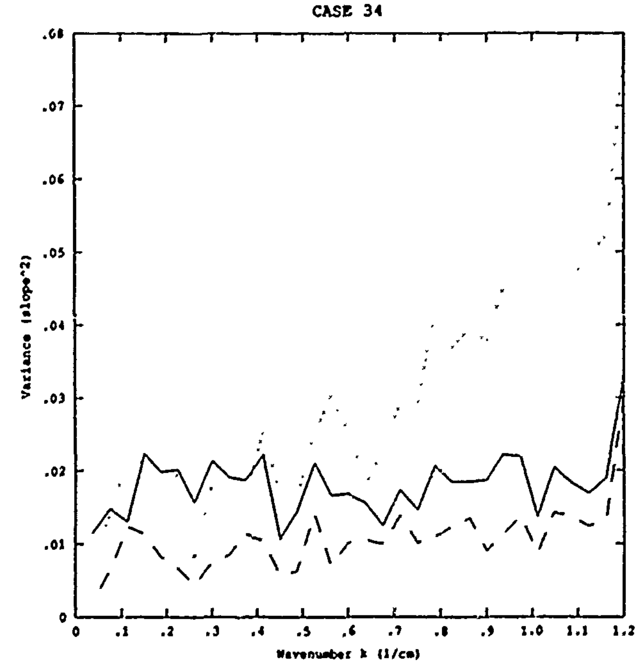

CASE 34

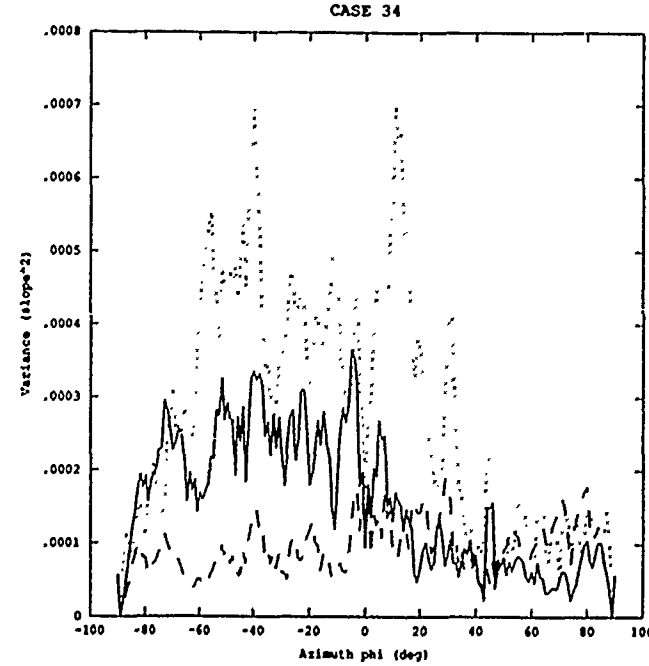

CASE 16

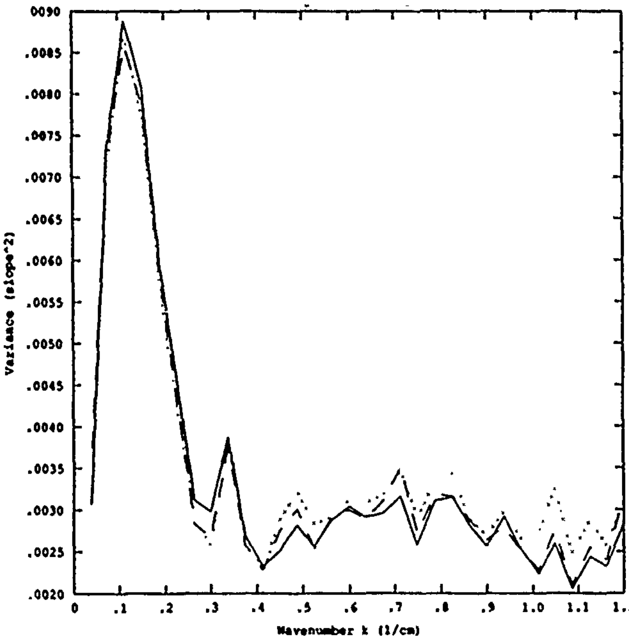

CASE 16

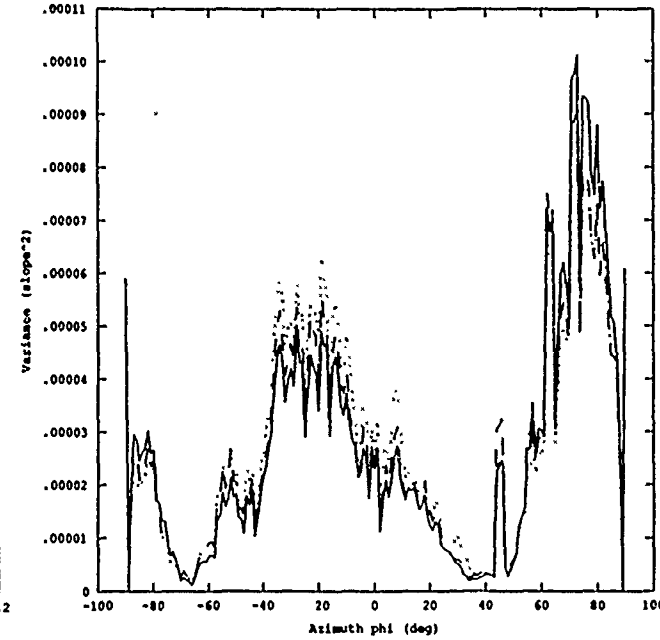

CASE 64

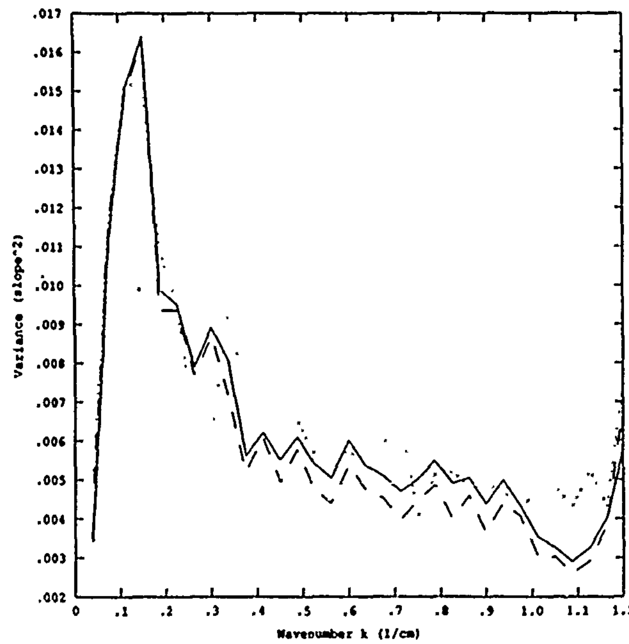

CASE 64

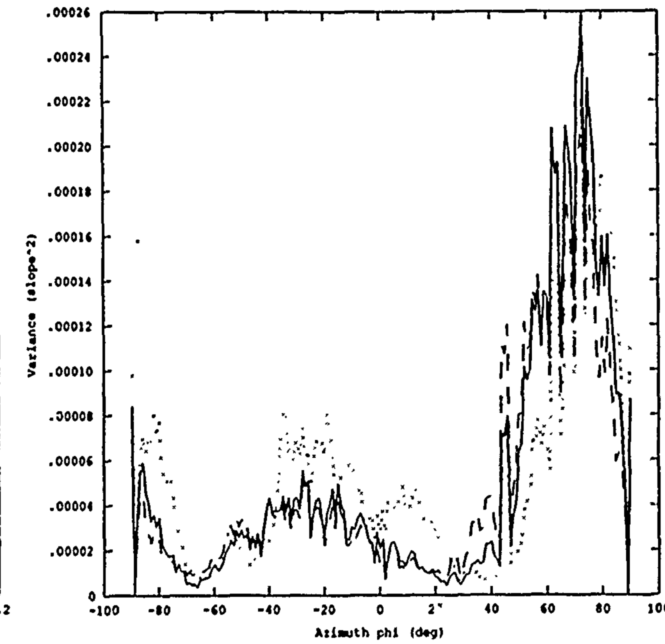

CASE 40

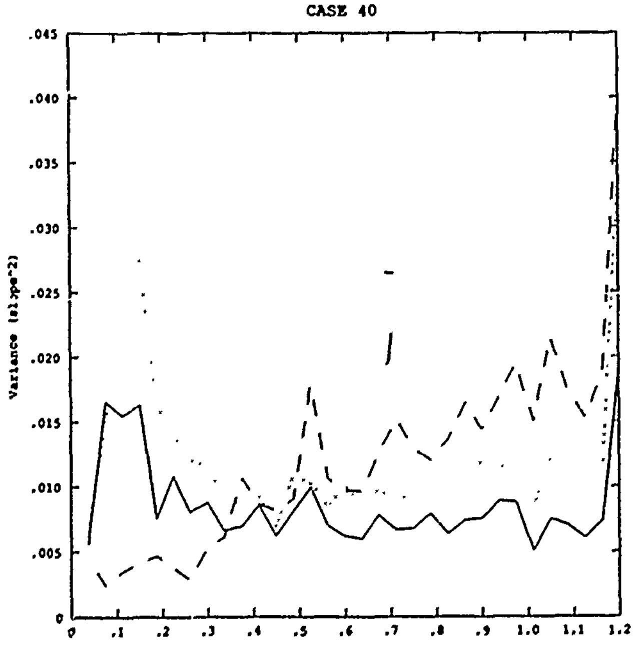

CASE 40

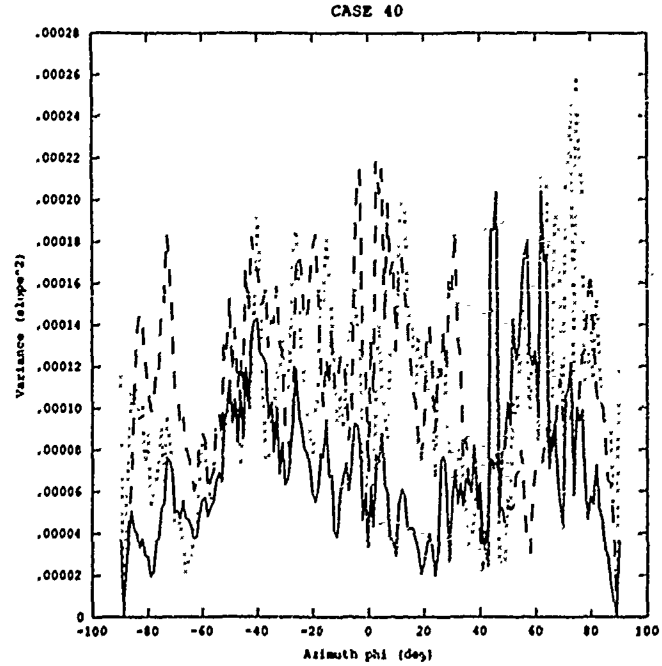

CASE 22

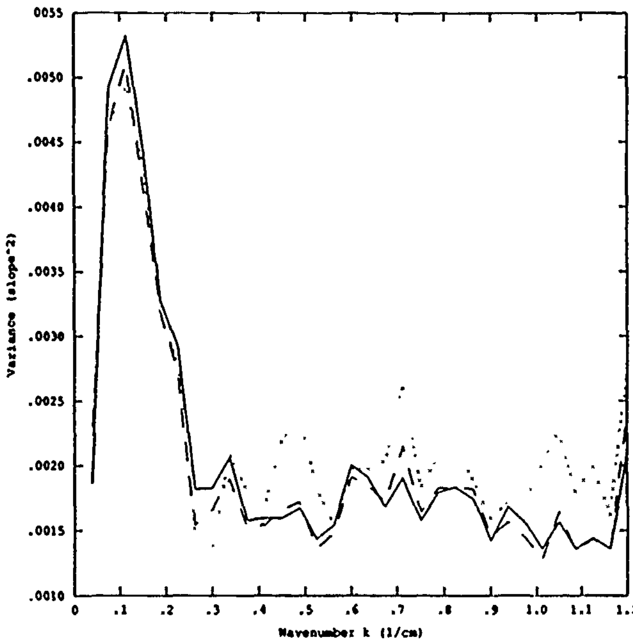

CASE 22

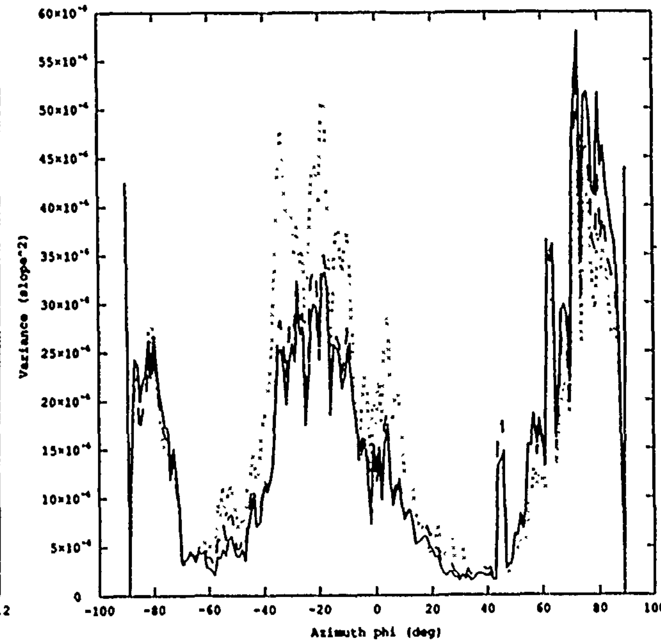

CASE 70

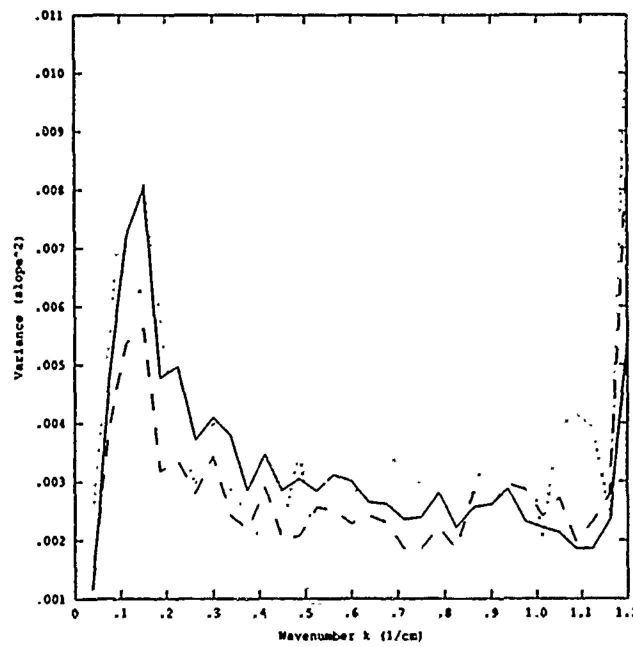

CASE 70

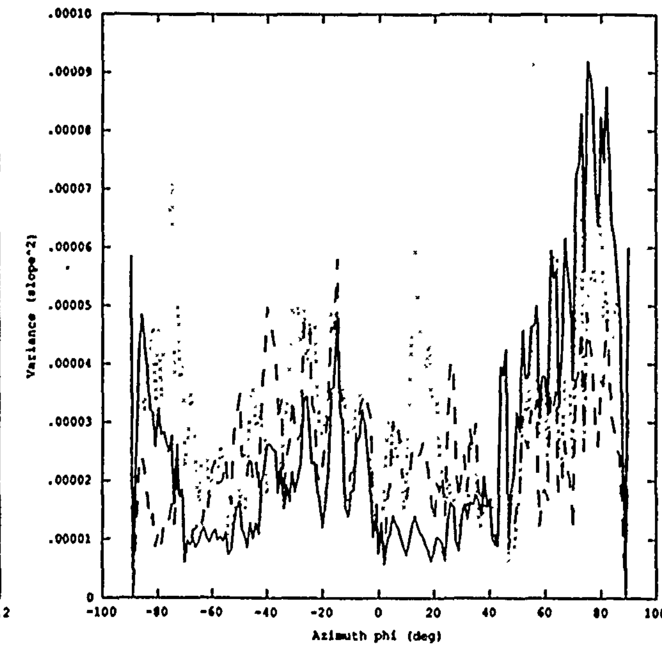

CASE 46

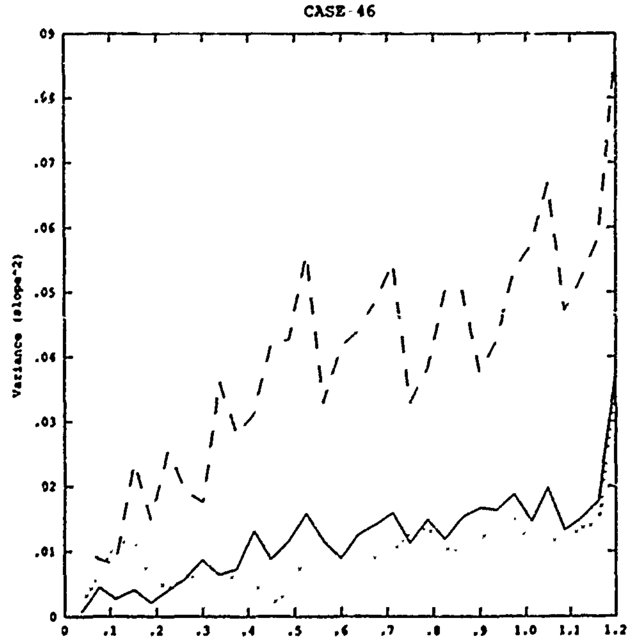

CASE 46

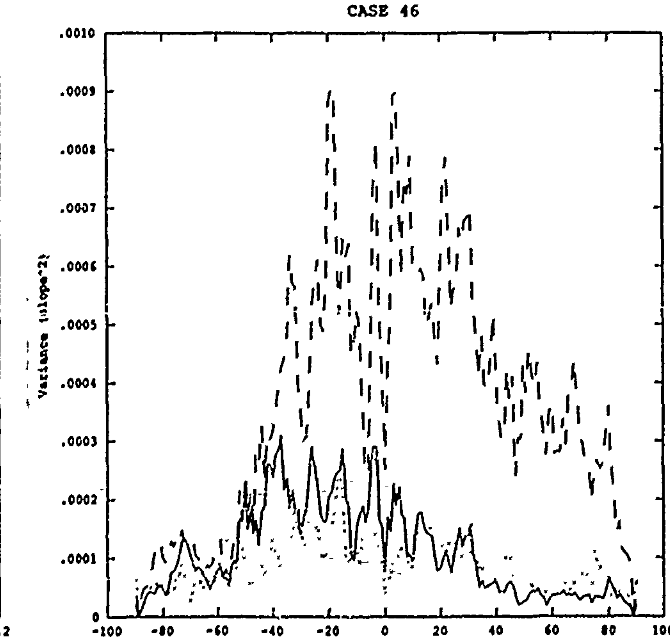

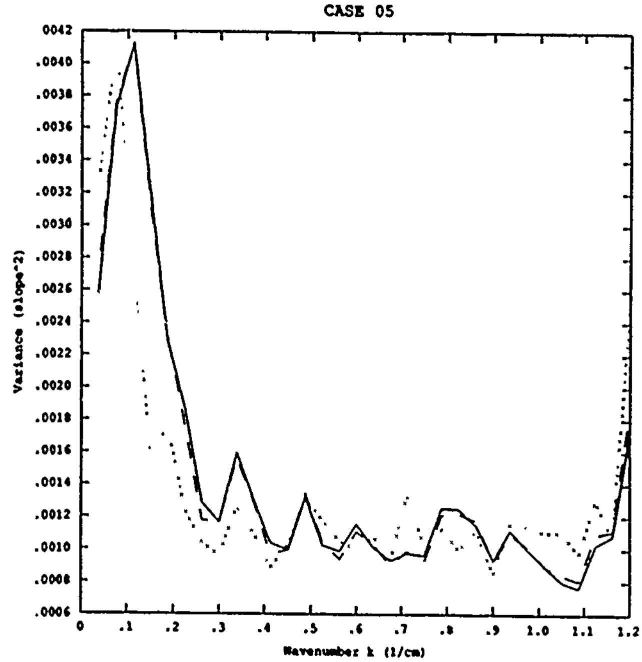
CASE 05
Variance (slope^2)
Wavenumber k (1/cm)

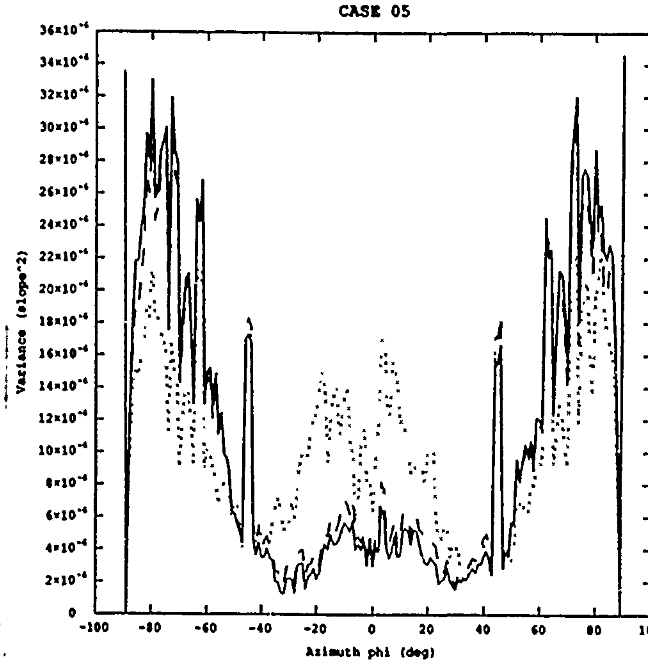
CASE 05
Variance (slope^2)
Azimuth phi (deg)

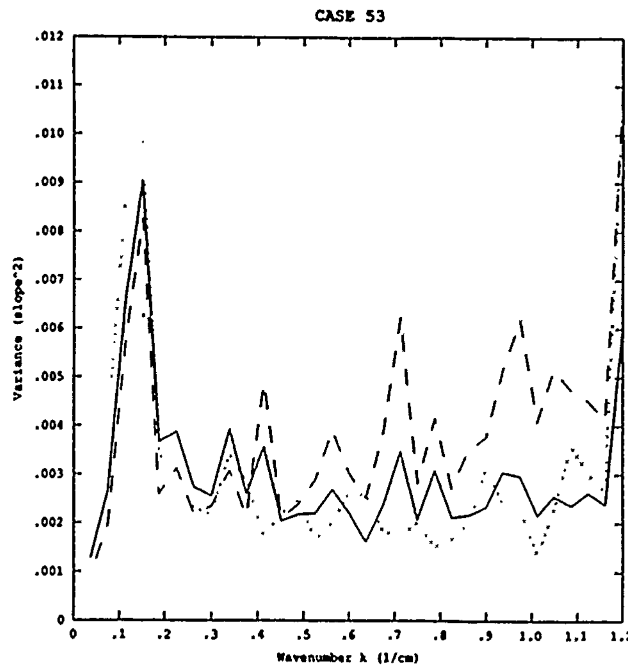
CASE 53
Variance (slope^2)
Wavenumber k (1/cm)

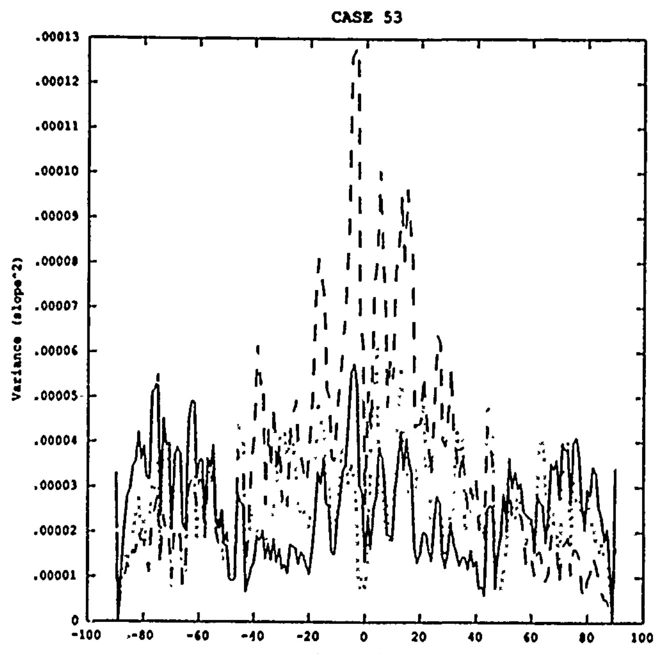
CASE 53
Variance (slope^2)
Azimuth phi (deg)

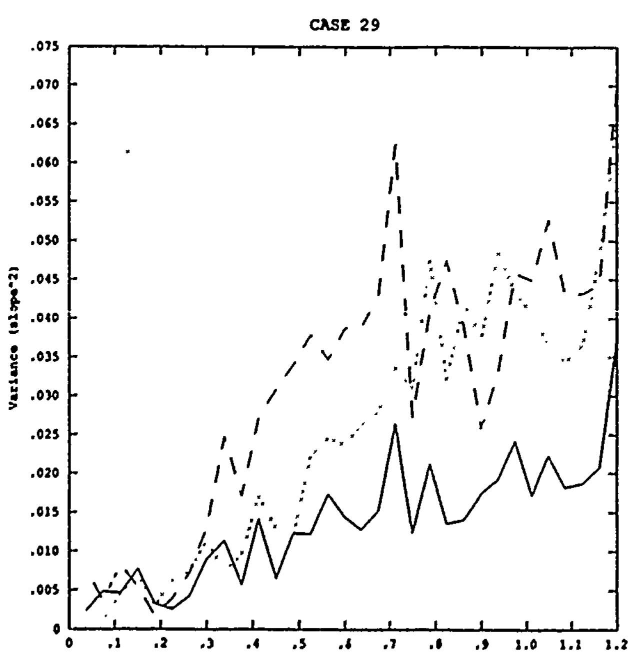
CASE 29
Variance (slope^2)
Wavenumber k (1/cm)

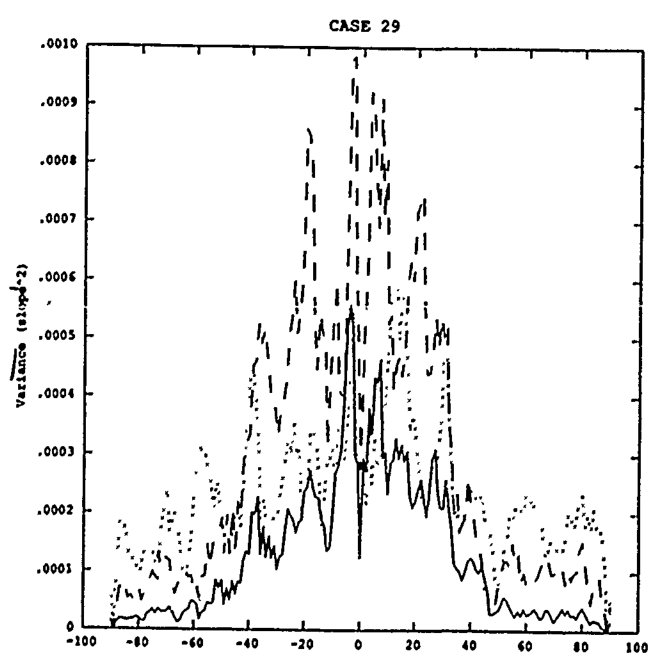
CASE 29
Variance (slope^2)
Azimuth phi (deg)

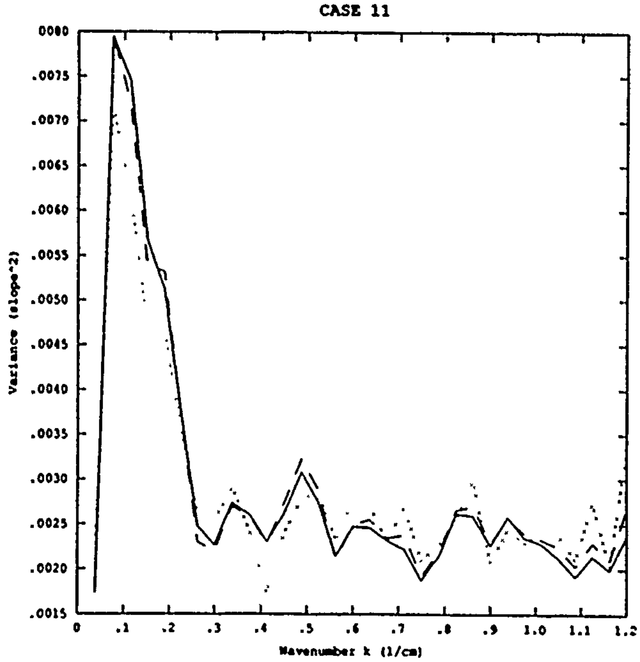
CASE 11
Variance (slope^2)
Wavenumber k (1/cm)

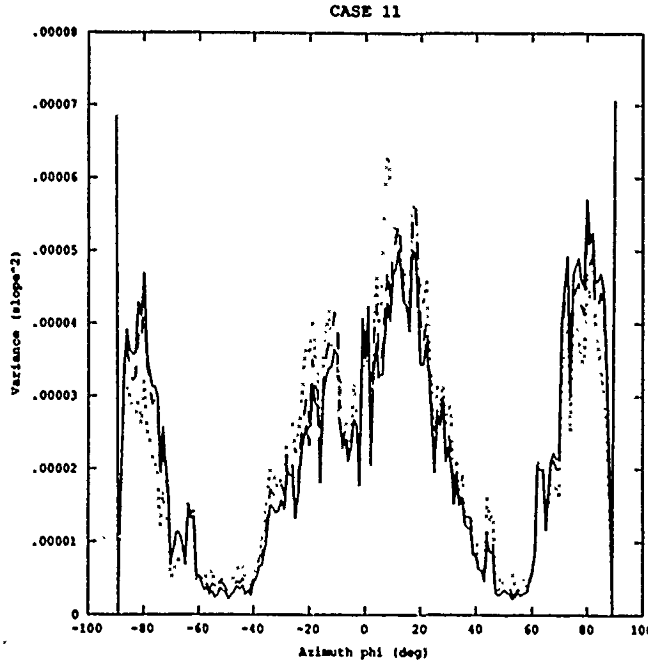
CASE 11
Variance (slope^2)
Azimuth phi (deg)

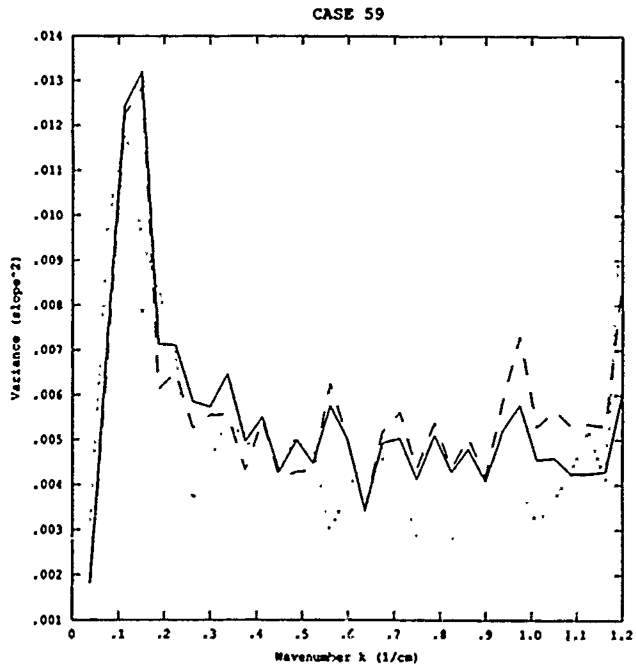
CASE 59
Variance (slope^2)
Wavenumber k (1/cm)

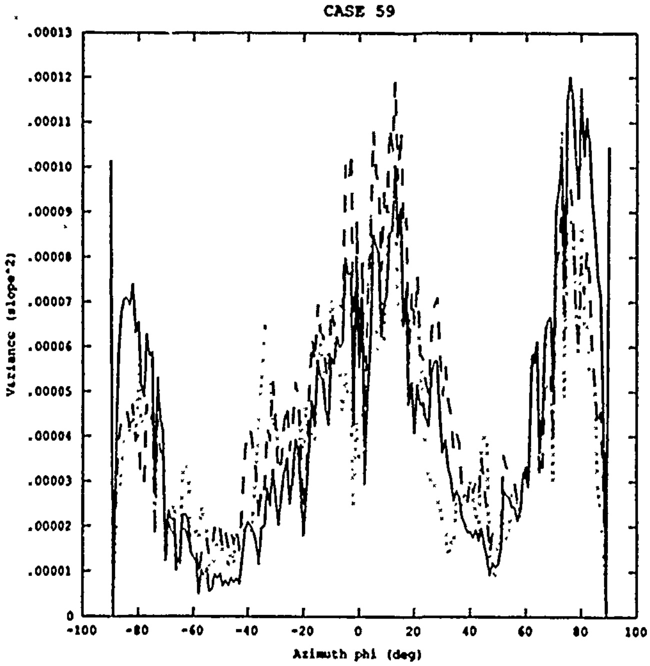
CASE 59
Variance (slope^2)
Azimuth phi (deg)

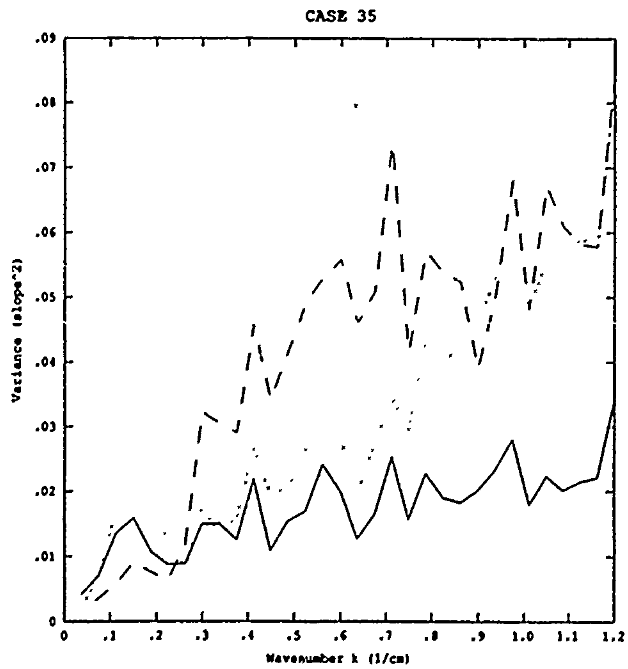
CASE 35
Variance (slope^2)
Wavenumber k (1/cm)

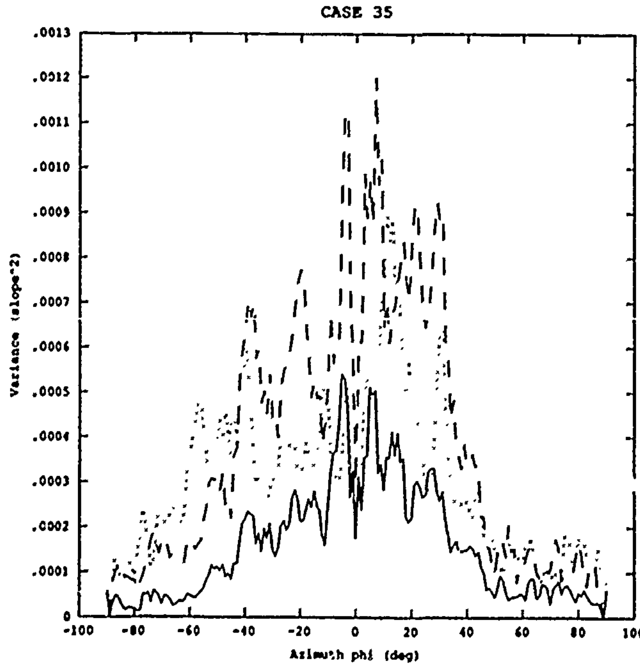
CASE 35
Variance (slope^2)
Azimuth phi (deg)

CASE 17

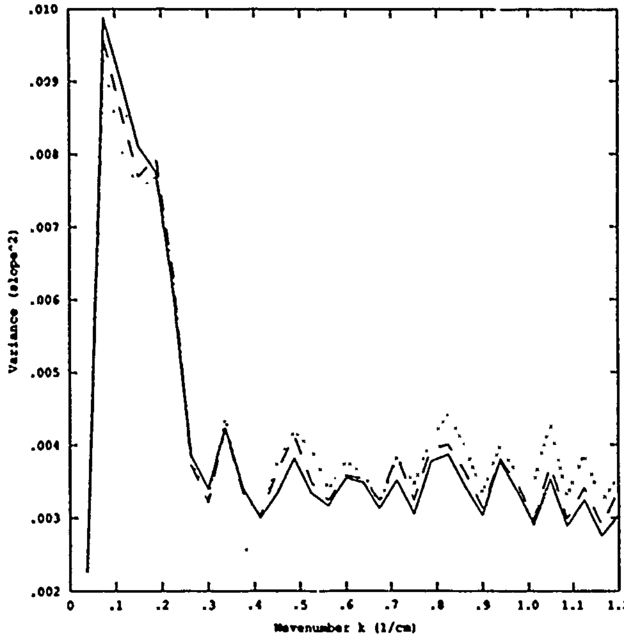

CASE 17

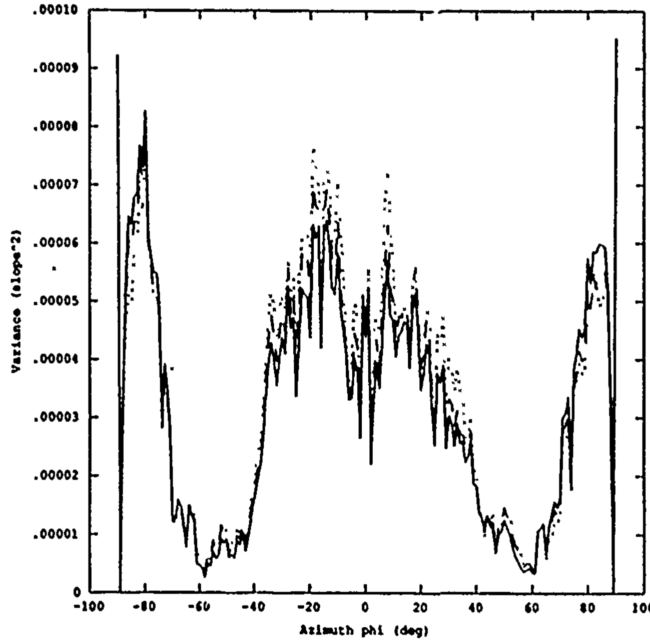

CASE 65

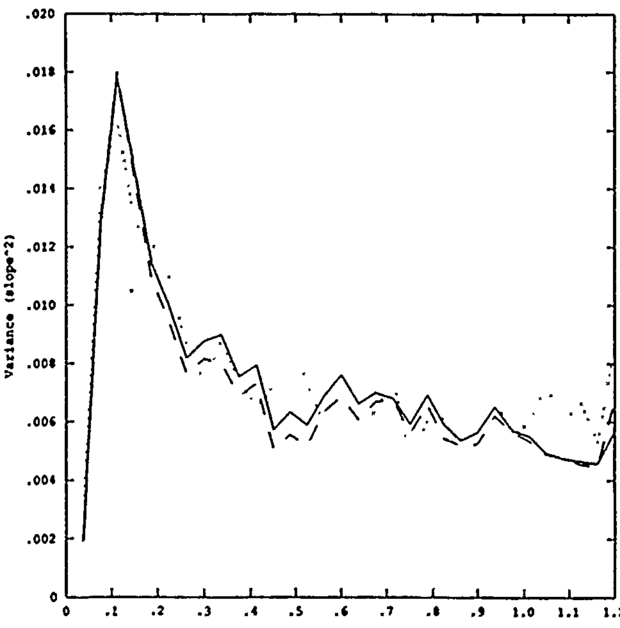

CASE 65

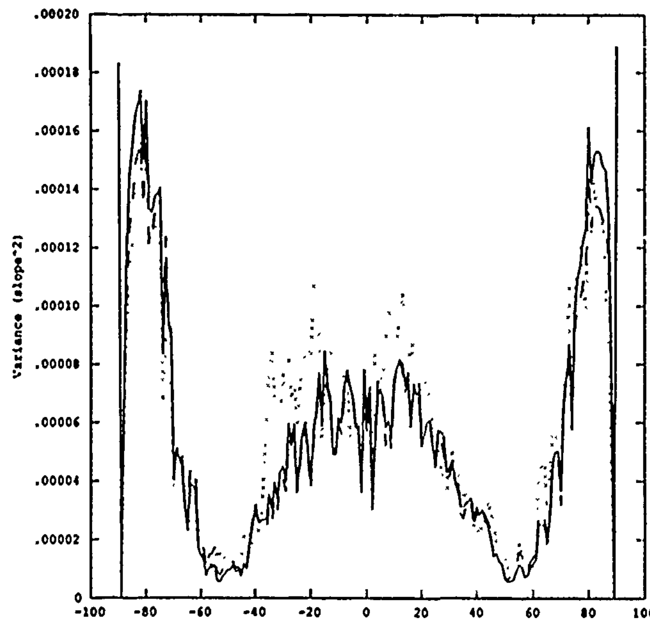

CASE 41

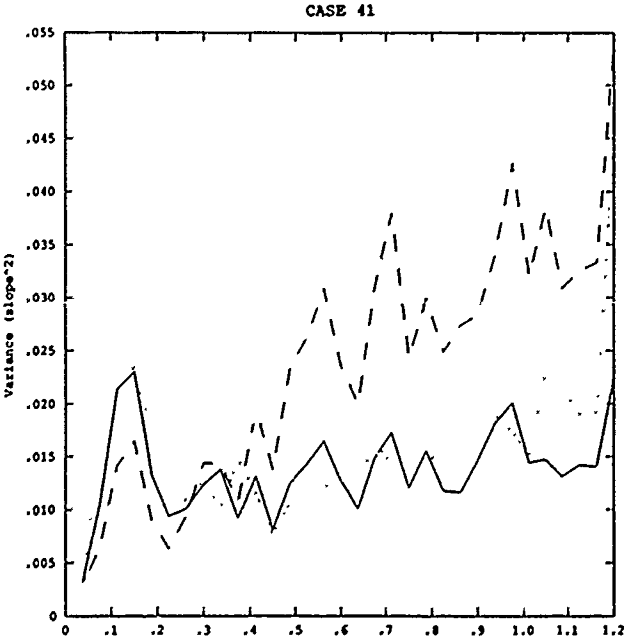

CASE 41

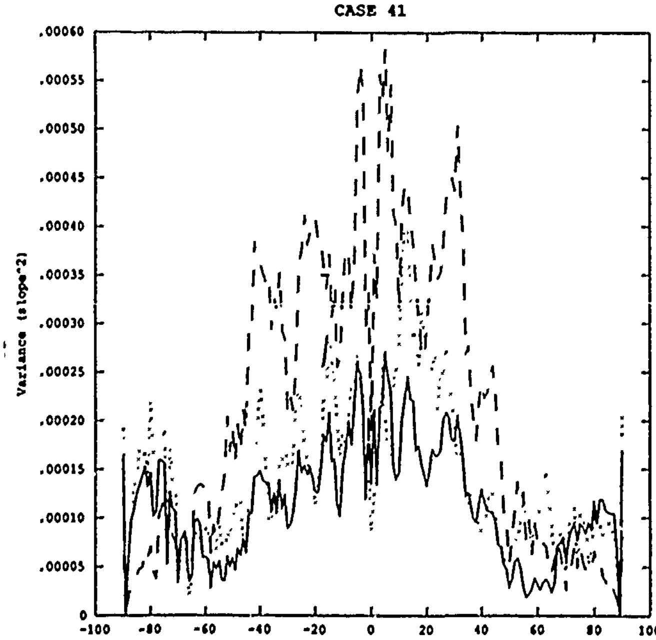

CASE 23

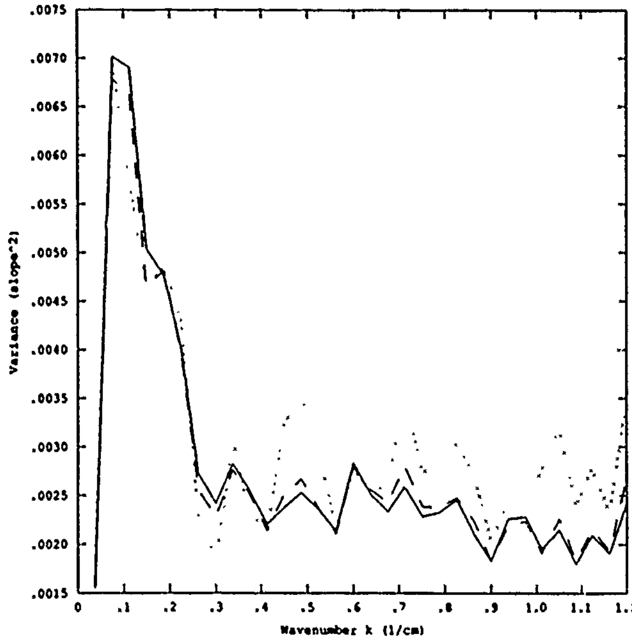

CASE 23

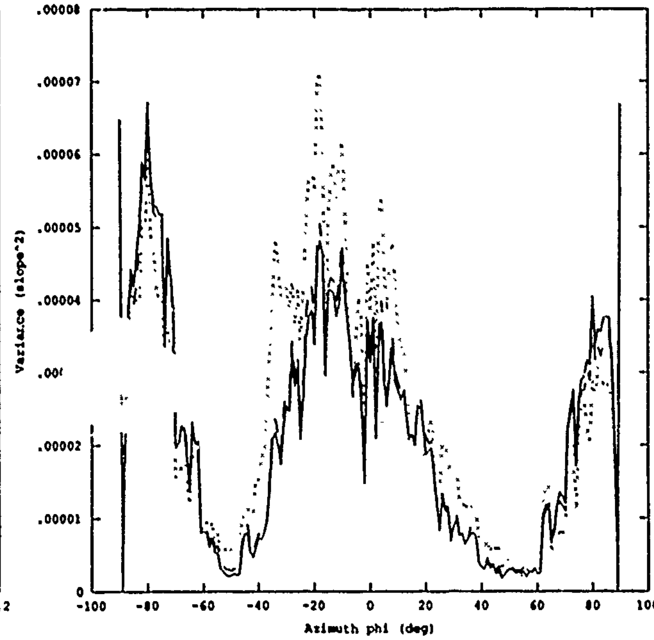

CASE 71

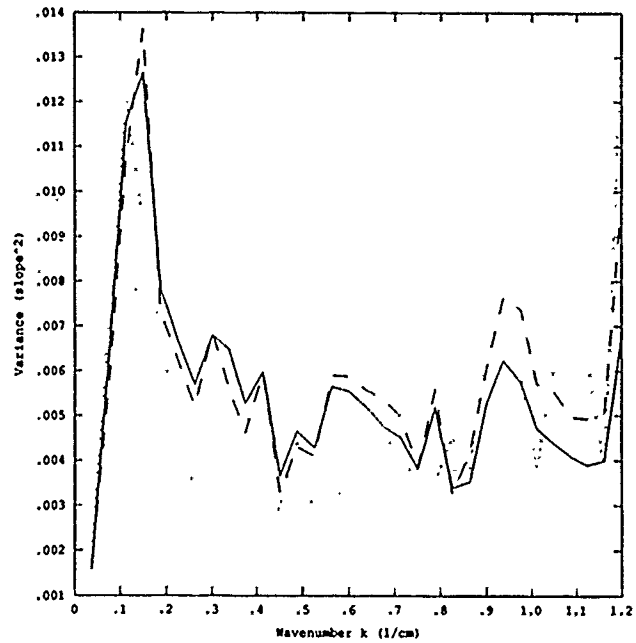

CASE 71

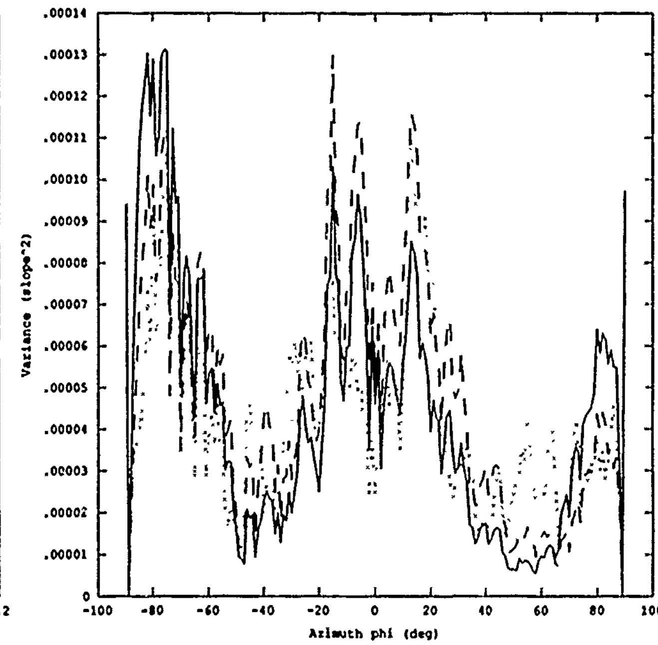

CASE 47

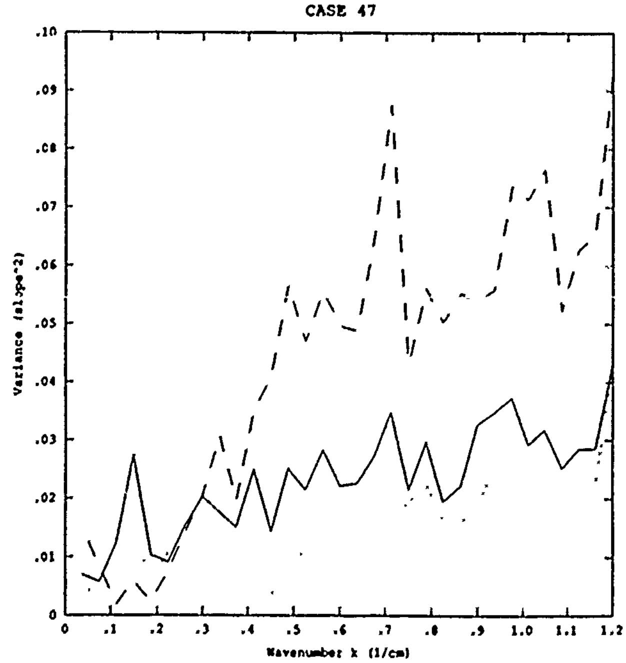

CASE 47

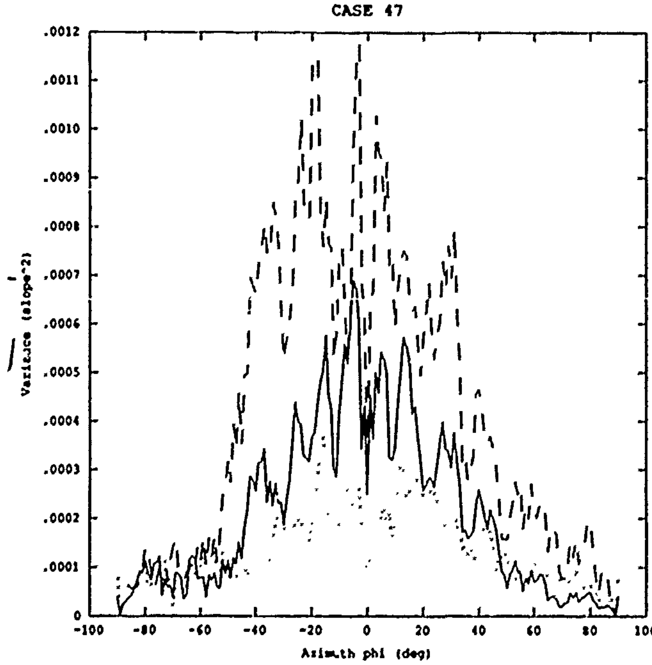

CASE 06

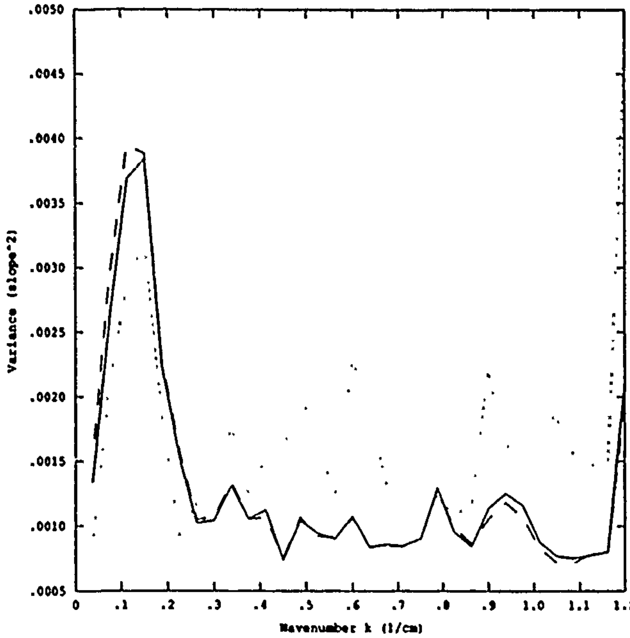

CASE 06

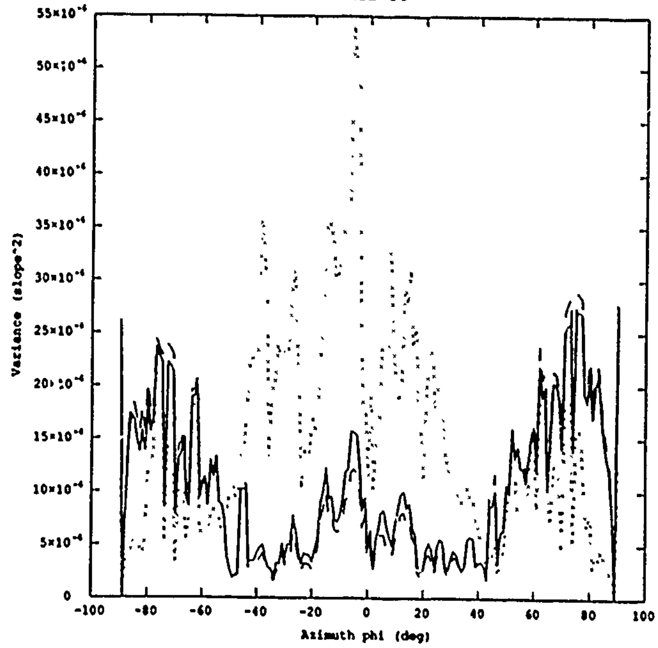

CASE 54

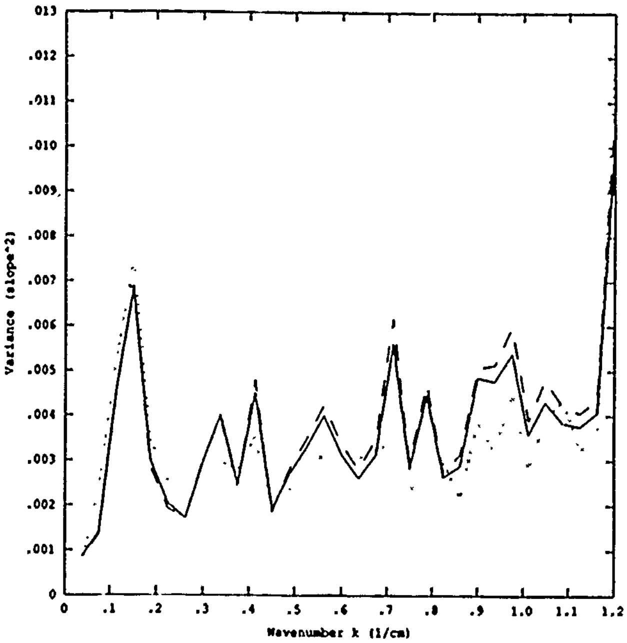

CASE 54

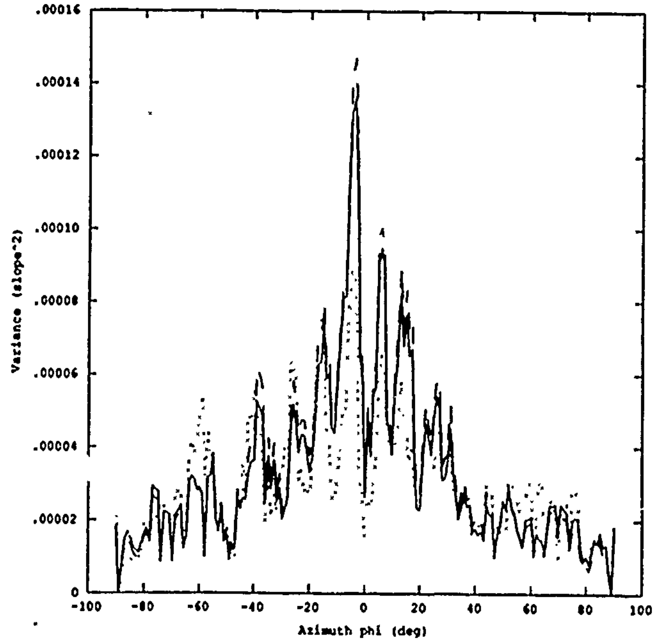

CASE 30

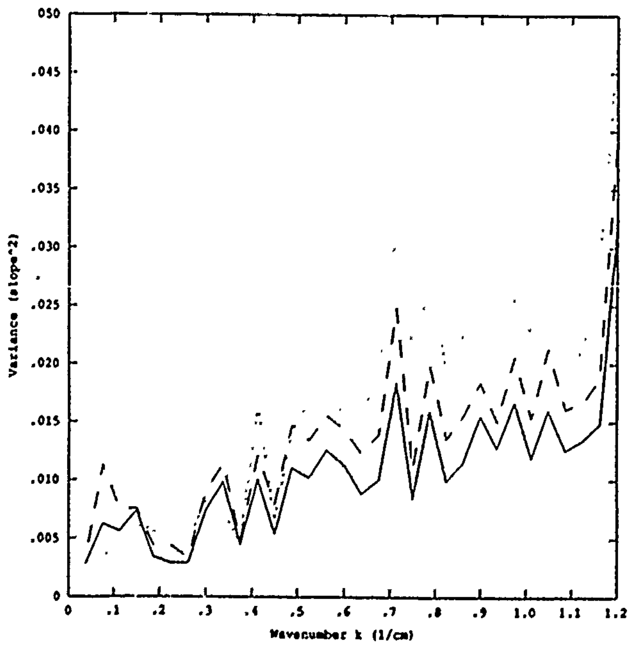

CASE 30

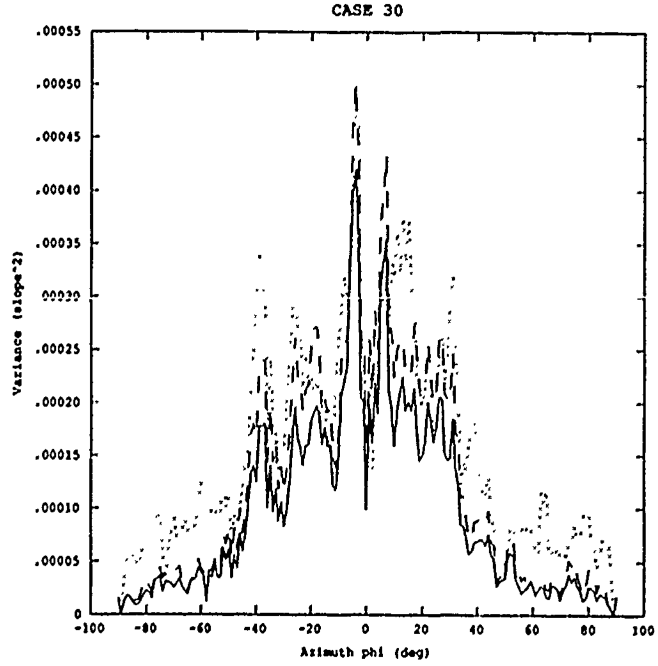

CASE 12

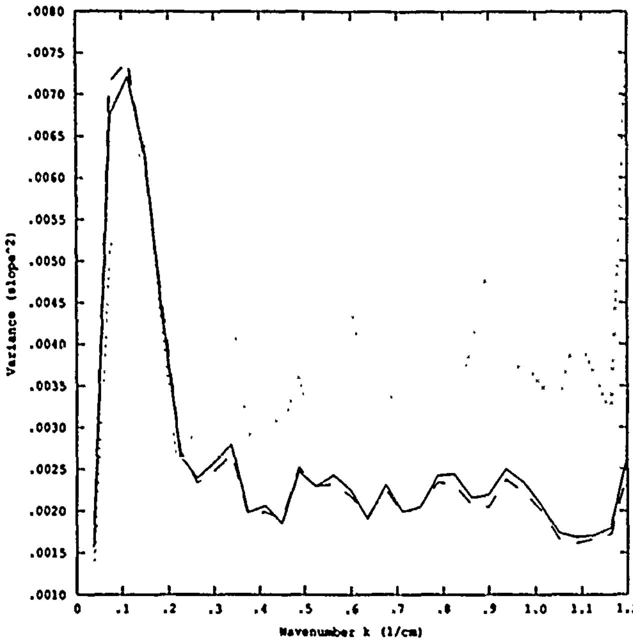

CASE 12

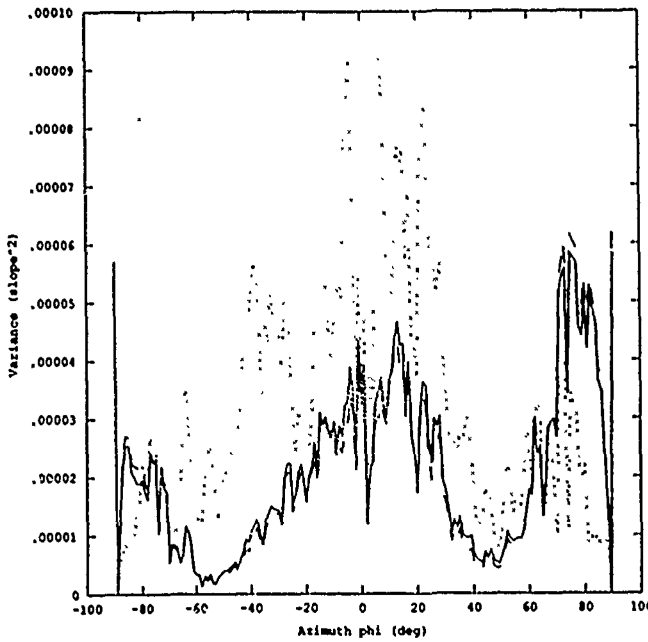

CASE 60

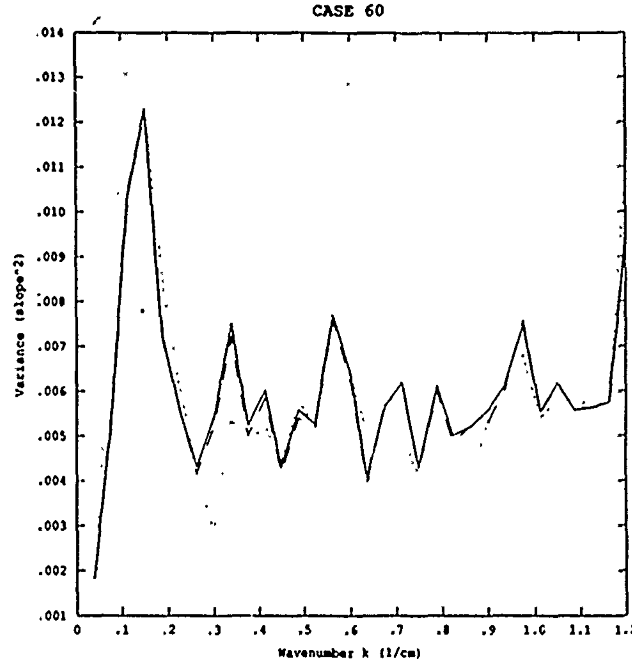

CASE 60

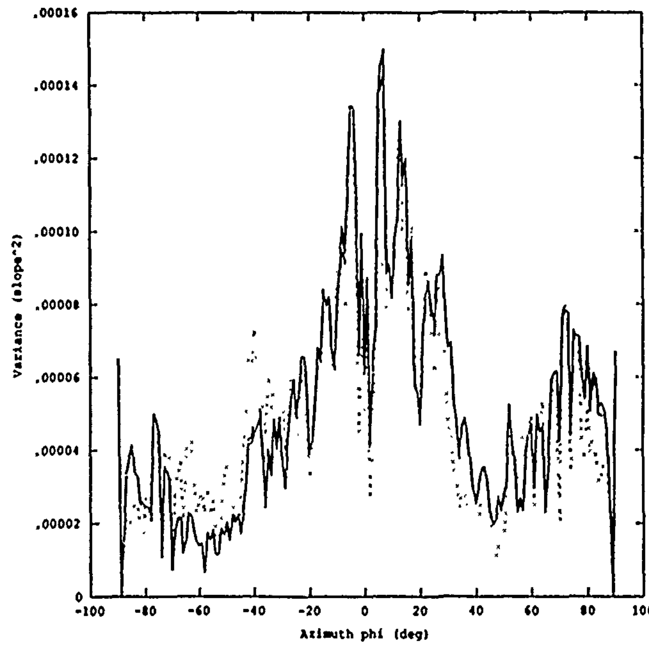

CASE 36

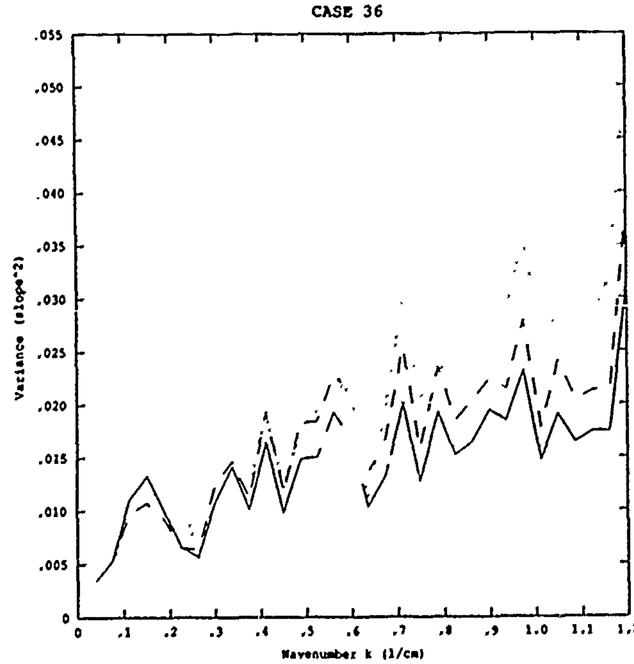

CASE 36

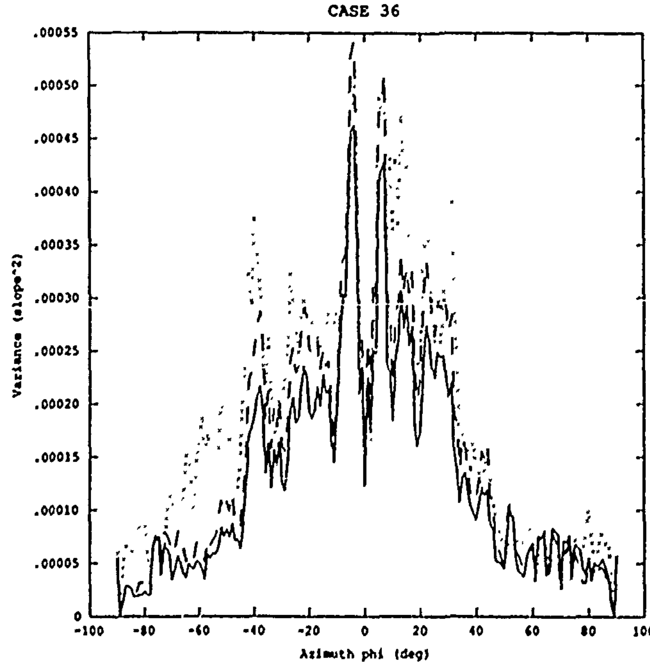

CASE 18

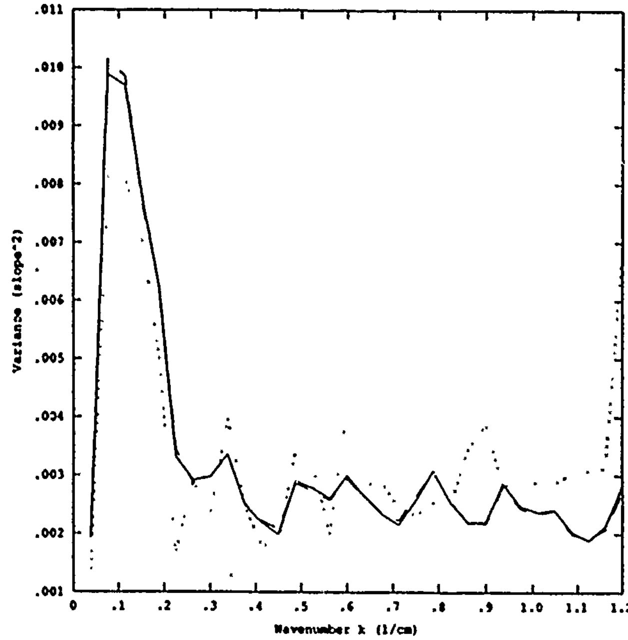

CASE 18

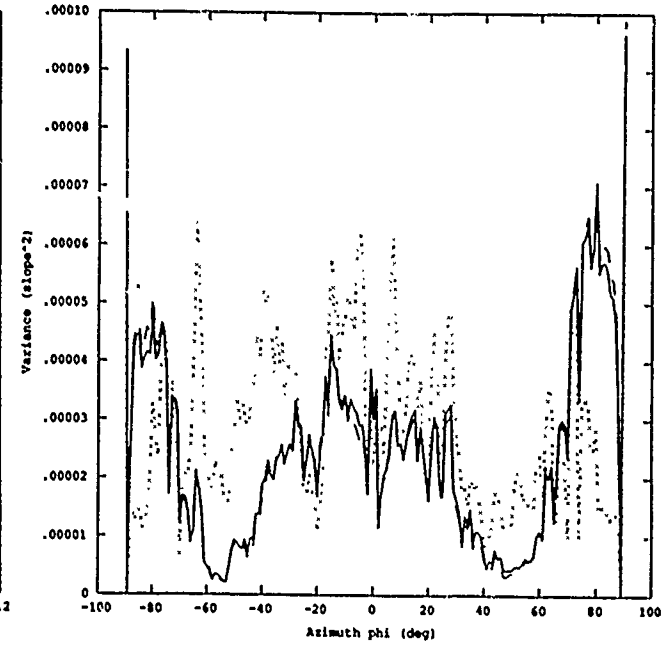

CASE 66

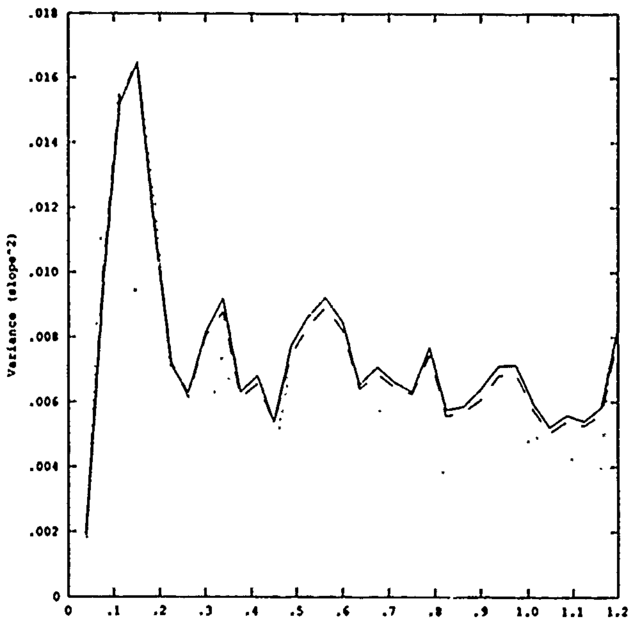

CASE 66

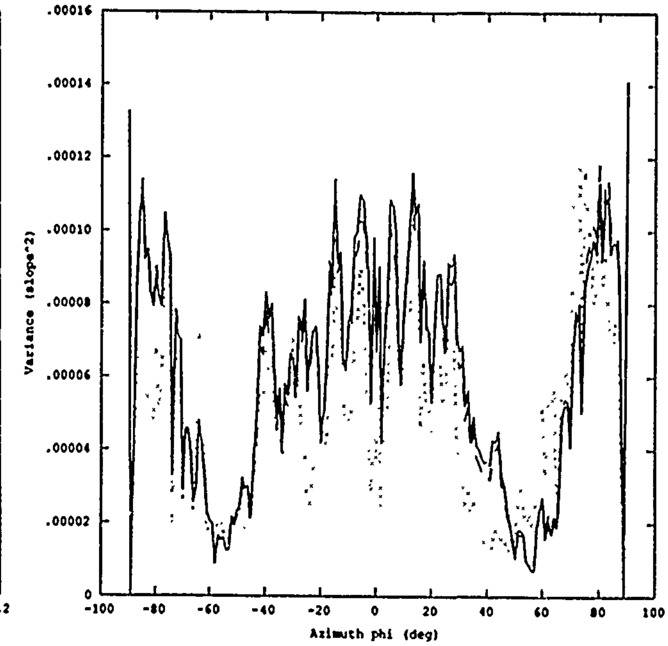

CASE 42

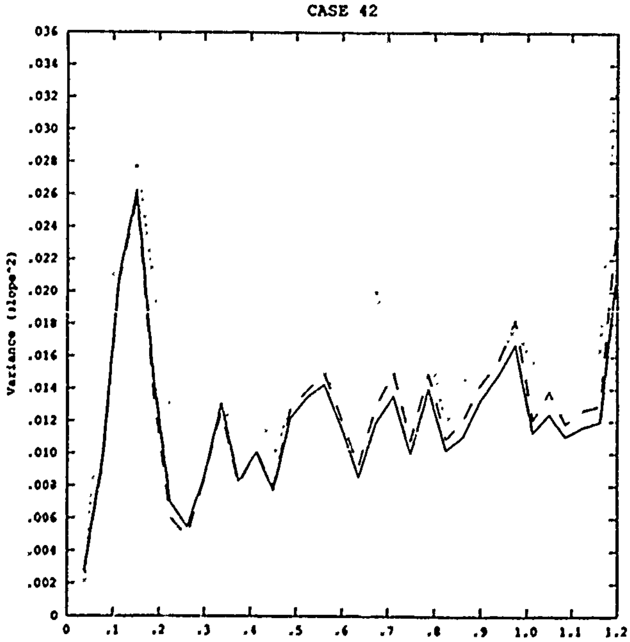

CASE 42

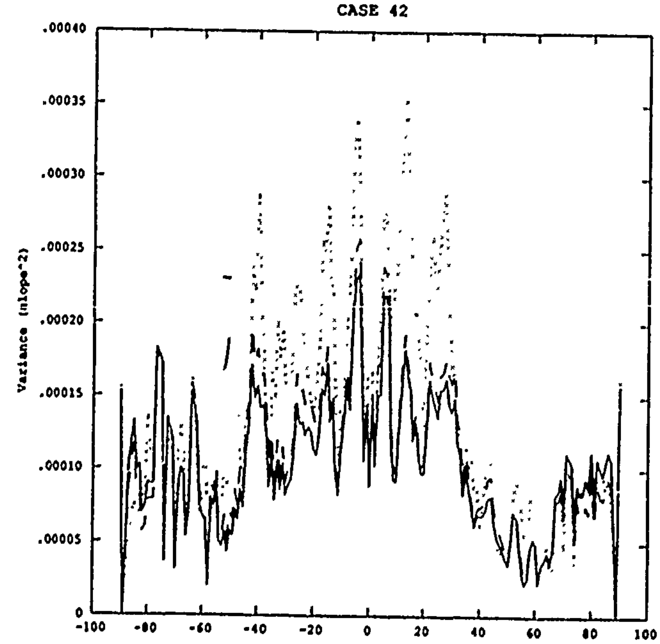

CASE 24

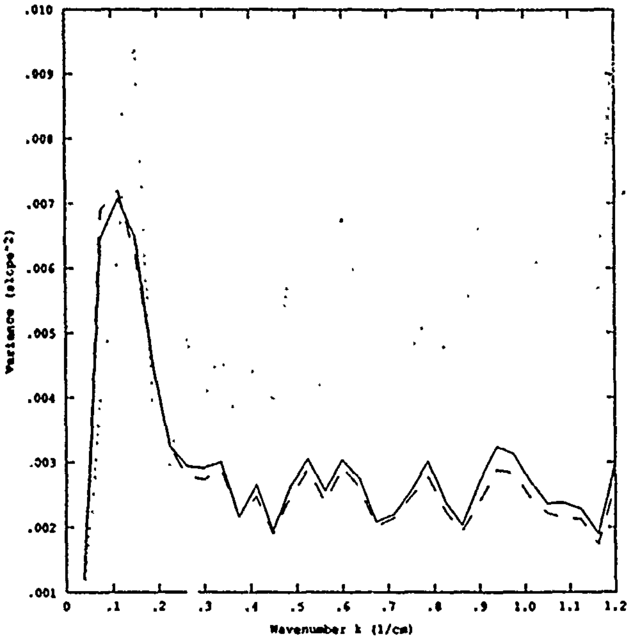

CASE 24

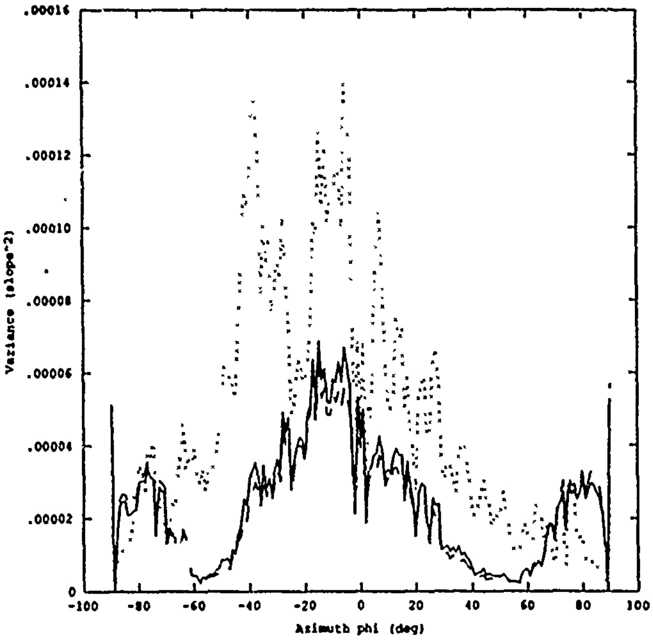

CASE 72

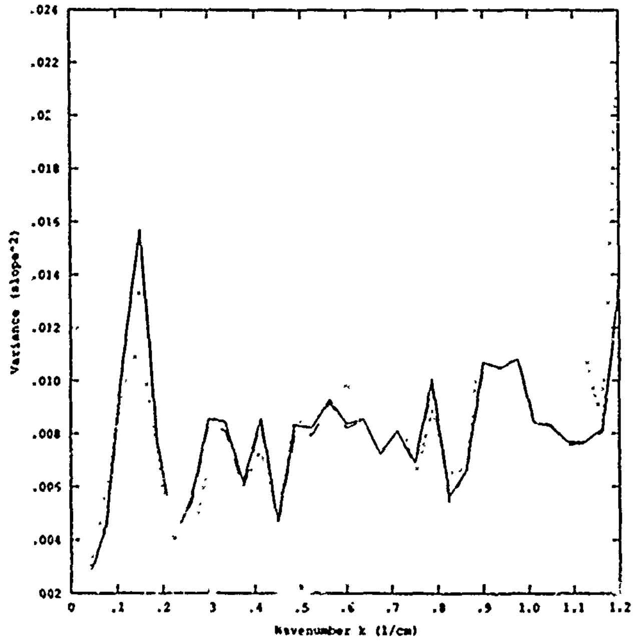

CASE 72

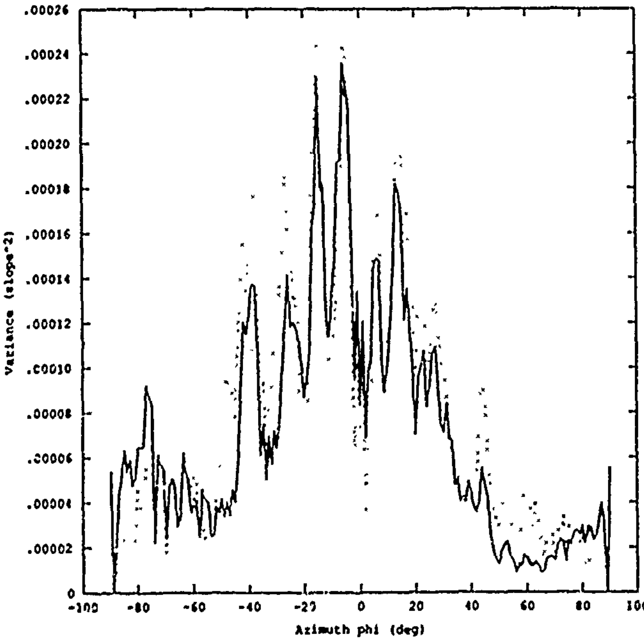

CASE 48

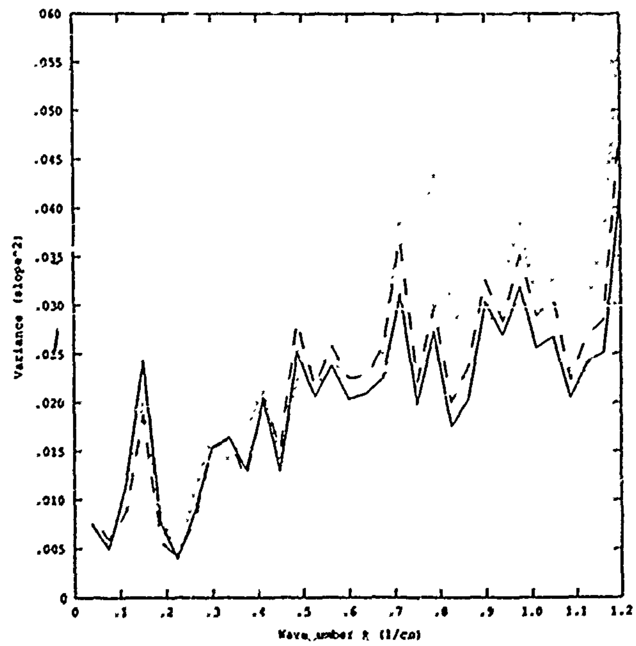

CASE 48

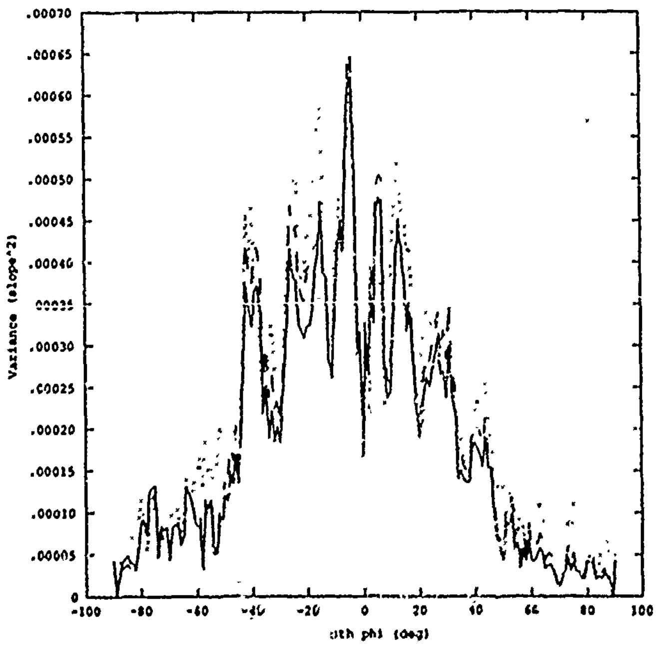

APPENDIX II - D_0 Results

The one-dimensional graphic results for the 72 combinations of solar position, dominant wind azimuth, and wind friction velocity are presented in Appendix II.

The D_1 results for each test case are organized in the following format:

PARAMETERS - The format for the input file PARM.DAT is defined in Appendix III.

MAGNITUDE ARRAY SCALING FACTORS - For each of the five radiance conditions, the parameters are defined:

XX(0,0) = Mean Radiance
High = Peak Radiance for $k > 0$
Factor = Geometric Scaling Factor between Peak Radiance and Peak Slope Magnitude

INTEGRATED VARIANCE FROM POWER SPECTRA - The variance is calculated from S0, the input slope spectrum, and for each of the five normalized radiance spectra.

A,C,S - Along-Wind, Cross-Wind, & Summed Variance
X,Y,S - Cross-Field, Along-Field, & Summed Variance

INTEGRATED SQUARED DEVIATION FROM DIF SPECTRA - The variance is calculated from the error (difference) spectra between S0, the input slope spectrum, and each of the five normalized radiance spectra.

A,C,S - Along-Wind, Cross-Wind, & Summed Variance
X,Y,S - Cross-Field, Along-Field, & Summed Variance

```
CASE01.DAT

PARAMETERS
 1.200000      3.7500001E-02   64.00000        56789.00
 12.00000      0.0000000E+00   0.0000000E+00   64.00000
 53.20000      0.0000000E+00   0.0000000E+00   100.0000
 1.337000      1.0200000E-09   99999.00        99999.00

MAGNITUDE ARRAY SCALING FACTORS
H1(0,0),HIGH,FACTOR  0.9790596     2.3192486E-02   15.81483
L1(0,0),HIGH,FACTOR  0.9915301     2.2538850E-02   16.27346
H0(0,0),HIGH,FACTOR   1.164383     2.0704437E-02   17.71529
L0(0,0),HIGH,FACTOR   1.362177     1.7567595E-02   20.87850
H3(0,0),HIGH,FACTOR  0.8974584     2.7659817E-02   13.26058

INTEGRATED VARIANCE FROM POWER SPECTRA
VAR S0 A,C,S  1.0605898E-02  6.3896347E-03  1.6995503E-02
VAR H1 A,C,S  1.0746604E-02  2.9954782E-03  1.3742088E-02
VAR L1 A,C,S  1.0789542E-02  3.0410783E-03  1.3830639E-02
VAR H0 A,C,S  1.0751334E-02  3.0255651E-03  1.3776912E-02
VAR L0 A,C,S  1.0901214E-02  3.1742381E-03  1.4075472E-02
VAR H3 A,C,S  1.2805673E-02  4.0093493E-03  1.6815042E-02

VAR S0 X,Y,S  1.0605898E-02  6.3896347E-03  1.6995503E-02
VAR H1 X,Y,S  1.0746604E-02  2.9954782E-03  1.3742088E-02
VAR L1 X,Y,S  1.0789542E-02  3.0410783E-03  1.3830639E-02
VAR H0 X,Y,S  1.0751334E-02  3.0255651E-03  1.3776912E-02
VAR L0 X,Y,S  1.0901214E-02  3.1742381E-03  1.4075472E-02
VAR H3 X,Y,S  1.2805673E-02  4.0093493E-03  1.6815042E-02

INTEGRATED SQUARED DEVIATION FROM DIF SPECTRA
DIF H1 A,C,S  4.6939135E-04  1.2719949E-03  1.7413879E-03
DIF L1 A,C,S  5.0940947E-04  1.2355722E-03  1.7449805E-03
DIF H0 A,C,S  4.9187889E-04  1.2448757E-03  1.7367585E-03
DIF L0 A,C,S  5.8747106E-04  1.1499249E-03  1.7373970E-03
DIF H3 A,C,S  8.0629782E-04  9.0592814E-04  1.7122239E-03

DIF H1 X,Y,S  4.6939135E-04  1.2719949E-03  1.7413879E-03
DIF L1 X,Y,S  5.0940947E-04  1.2355722E-03  1.7449805E-03
DIF H0 X,Y,S  4.9187889E-04  1.2448757E-03  1.7367585E-03
DIF L0 X,Y,S  5.8747106E-04  1.1499249E-03  1.7373970E-03
DIF H3 X,Y,S  8.0629782E-04  9.0592814E-04  1.7122239E-03
```

```
CASE02.DAT

PARAMETERS
 1.200000      3.7500001E-02   64.00000        56789.00
 12.00000      0.0000000E+00   0.0000000E+00   64.00000
 53.20000       45.00000       53.20000        9.885000
 1.337000      1.0200000E-09   99999.00        99999.00

MAGNITUDE ARRAY SCALING FACTORS
H1(0,0),HIGH,FACTOR  0.6247715     1.7953391E-02   20.45263
L1(0,0),HIGH,FACTOR  0.6627284     2.0325290E-02   18.04575
H0(0,0),HIGH,FACTOR  0.7304618     1.6718665E-02   21.93866
L0(0,0),HIGH,FACTOR  0.8741091     1.7895289E-02   20.49618
H3(0,0),HIGH,FACTOR  0.5828262     2.0970508E-02   17.49052

INTEGRATED VARIANCE FROM POWER SPECTRA
VAR S0 A,C,S  1.0605898E-02  6.3896347E-03  1.6995503E-02
VAR H1 A,C,S  9.7574415E-03  5.5585625E-03  1.5316016E-02
VAR L1 A,C,S  9.9829156E-03  5.0895498E-03  1.5072467E-02
VAR H0 A,C,S  9.6167121E-03  5.9525045E-03  1.5569220E-02
VAR L0 A,C,S  9.7021358E-03  5.6932503E-03  1.5395389E-02
VAR H3 A,C,S  1.0342992E-02  5.0727455E-03  1.5415745E-02

VAR S0 X,Y,S  1.0605898E-02  6.3896347E-03  1.6995503E-02
VAR H1 X,Y,S  9.7574415E-03  5.5585625E-03  1.5316016E-02
VAR L1 X,Y,S  9.9829156E-03  5.0895498E-03  1.5072467E-02
VAR H0 X,Y,S  9.6167121E-03  5.9525045E-03  1.5569220E-02
VAR L0 X,Y,S  9.7021358E-03  5.6932503E-03  1.5395389E-02
VAR H3 X,Y,S  1.0342992E-02  5.0727455E-03  1.5415745E-02

INTEGRATED SQUARED DEVIATION FROM DIF SPECTRA
DIF H1 A,C,S  1.3336245E-03  1.1877267E-03  2.5213528E-03
DIF L1 A,C,S  1.1597133E-03  1.1613404E-03  2.3210510E-03
DIF H0 A,C,S  1.4386721E-03  1.1840228E-03  2.6226970E-03
DIF L0 A,C,S  1.3273243E-03  1.1429832E-03  2.4703071E-03
DIF H3 A,C,S  1.0577217E-03  1.0952185E-03  2.1529442E-03

DIF H1 X,Y,S  1.3336245E-03  1.1877267E-03  2.5213528E-03
DIF L1 X,Y,S  1.1597133E-03  1.1613404E-03  2.3210510E-03
DIF H0 X,Y,S  1.4386721E-03  1.1840228E-03  2.6226970E-03
DIF L0 X,Y,S  1.3273243E-03  1.1429832E-03  2.4703071E-03
DIF H3 X,Y,S  1.0577217E-03  1.0952185E-03  2.1529442E-03
```

```
CASE03.DAT

PARAMETERS
 1.200000      3.7500001E-02   64.00000        56789.00
 12.00000      0.9000000E+00  0.0000000E+00    64.00000
 53.20000       90.00000       53.20000        9.885000
 1.337000      1.0200200E-09   99999.00        99999.00

MAGNITUDE ARRAY SCALING FACTORS
H1(0,0),HIGH,FACTOR  0.2317155      6.7422264E-03   54.40118
L1(0,0),HIGH,FACTOR  0.2561573      8.5639572E-03   42.82893
H0(0,0),HIGH,FACTOR  0.3374059      5.3447583E-03   68.62520
L0(0,0),HIGH,FACTOR  0.4675380      5.7723238E-03   63.54202
H3(0,0),HIGH,FACTOR  0.2079985      7.9102358E-03   46.36842

INTEGRATED VARIANCE FROM POWER SPECTRA
VAR S0 A,C,S  1.0605898E-02  6.3896347E-03  1.6995503E-02
VAR H1 A,C,S  1.0727595E-02  3.2093485E-03  1.3936925E-02
VAR L1 A,C,S  1.0926355E-02  3.2327457E-03  1.4159084E-02
VAR H0 A,C,S  1.0735123E-02  3.3982147E-03  1.4133333E-02
VAR L0 A,C,S  1.1239403E-02  3.6712477E-03  1.4910653E-02
VAR H3 A,C,S  1.2236980E-02  3.8402595E-03  1.6077235E-02

VAR S0 X,Y,S  1.0605898E-02  6.3896347E-03  1.6995503E-02
VAR H1 X,Y,S  1.0727595E-02  3.2093485E-03  1.3936925E-02
VAR L1 X,Y,S  1.0926355E-02  3.2327457E-03  1.4159084E-02
VAR H0 X,Y,S  1.0735123E-02  3.3982147E-03  1.4133333E-02
VAR L0 X,Y,S  1.1239403E-02  3.6712477E-03  1.4910653E-02
VAR H3 X,Y,S  1.2236980E-02  3.8402595E-03  1.6077235E-02

INTEGRATED SQUARED DEVIATION FROM DIF SPECTRA
DIF H1 A,C,S  4.5836368E-04  1.1700068E-03  1.6283707E-03
DIF L1 A,C,S  5.0758856E-04  1.1616988E-03  1.6692928E-03
DIF H0 A,C,S  5.1006034E-04  1.0776187E-03  1.5876786E-03
DIF L0 A,C,S  6.5042387E-04  9.7214105E-04  1.6225645E-03
DIF H3 A,C,S  6.6028541E-04  9.5055834E-04  1.6108444E-03

DIF H1 X,Y,S  4.5836368E-04  1.1700068E-03  1.6283707E-03
DIF L1 X,Y,S  5.0758856E-04  1.1616988E-03  1.6692928E-03
DIF H0 X,Y,S  5.1006034E-04  1.0776187E-03  1.5876786E-03
DIF L0 X,Y,S  6.5042387E-04  9.7214105E-04  1.6225645E-03
DIF H3 X,Y,S  6.6028541E-04  9.5055834E-04  1.6108444E-03
```

```
CASE04.DAT

PARAMETERS
 1.200000      3.7500001E-02   64.00000        56789.00
 12.00000     0.0000000E+00  0.0000000E+00     64.00000
 53.20000       135.0000       53.20000        9.885000
 1.337000      1.0200000E-09   99999.00        99999.00

MAGNITUDE ARRAY SCALING FACTORS
H1(0,0),HIGH,FACTOR  0.3407934      1.0251253E-02   35.77954
L1(0,0),HIGH,FACTOR  0.3561679      1.1652863E-02   31.47597
H0(0,0),HIGH,FACTOR  0.4464837      8.9234347E-03   41.10358
L0(0,0),HIGH,FACTOR  0.5675486      8.9315670E-03   41.06615
H3(0,0),HIGH,FACTOR  0.3154342      1.1862160E-02   30.92060

INTEGRATED VARIANCE FROM POWER SPECTRA
VAR S0 A,C,S  1.0605898E-02  6.3896347E-03  1.6995503E-02
VAR H1 A,C,S  1.1046638E-02  3.3429095E-03  1.4389525E-02
VAR L1 A,C,S  1.1044948E-02  3.2545689E-03  1.4299520E-02
VAR H0 A,C,S  1.0922277E-02  3.4321698E-03  1.4354474E-02
VAR L0 A,C,S  1.0991593E-02  3.4492635E-03  1.4440854E-02
VAR H3 A,C,S  1.2359813E-02  3.9367173E-03  1.6296523E-02

VAR S0 X,Y,S  1.0605898E-02  6.3896347E-03  1.6995503E-02
VAR H1 X,Y,S  1.1046638E-02  3.3429095E-03  1.4389525E-02
VAR L1 X,Y,S  1.1044948E-02  3.2545689E-03  1.4299520E-02
VAR H0 X,Y,S  1.0922277E-02  3.4321698E-03  1.4354474E-02
VAR L0 X,Y,S  1.0991593E-02  3.4492635E-03  1.4440854E-02
VAR H3 X,Y,S  1.2359813E-02  3.9367173E-03  1.6296523E-02

INTEGRATED SQUARED DEVIATION FROM DIF SPECTRA
DIF H1 A,C,S  5.8908731E-04  1.3127775E-03  1.9018683E-03
DIF L1 A,C,S  5.7132472E-04  1.3075595E-03  1.8788876E-03
DIF H0 A,C,S  6.5141282E-04  1.3073839E-03  1.9587954E-03
DIF L0 A,C,S  6.9430331E-04  1.2740920E-03  1.9683971E-03
DIF H3 A,C,S  7.7554921E-04  1.0569545E-03  1.8325037E-03

DIF H1 X,Y,S  5.8908731E-04  1.3127775E-03  1.9018683E-03
DIF L1 X,Y,S  5.7132472E-04  1.3075595E-03  1.8788876E-03
DIF H0 X,Y,S  6.5141282E-04  1.3073839E-03  1.9587954E-03
DIF L0 X,Y,S  6.9430331E-04  1.2740920E-03  1.9683971E-03
DIF H3 X,Y,S  7.7554921E-04  1.0569545E-03  1.8325037E-03
```

```
CASE05.DAT

PARAMETERS
 1.200000      3.7500001E-02   64.00000        56789.00
 12.00000      0.0000000E+00   0.0000000E+00   64.00000
 53.20000      180.0000        53.20000        9.885000
 1.337000      1.0200000E-09   99999.00        99999.00

MAGNITUDE ARRAY SCALING FACTORS
H1(0,0),HIGH,FACTOR  0.4624957      1.3453402E-02  27.26337
L1(0,0),HIGH,FACTOR  0.4737886      1.4737497E-02  24.88788
H0(0,0),HIGH,FACTOR  0.5681861      1.2054356E-02  30.42760
L0(0,0),HIGH,FACTOR  0.6851693      1.1939812E-02  30.71951
H3(0,0),HIGH,FACTOR  0.4325745      1.5354494E-02  23.88780

INTEGRATED VARIANCE FROM POWER SPECTRA
VAR S0 A,C,S  1.0605898E-02  6.3896347E-03  1.6995503E-02
VAR H1 A,C,S  1.0751848E-02  2.9393421E-03  1.3691191E-02
VAR L1 A,C,S  1.0789744E-02  2.9548015E-03  1.3744595E-02
VAR H0 A,C,S  1.0723243E-02  2.9455707E-03  1.3668792E-02
VAR L0 A,C,S  1.0756804E-02  2.9788320E-03  1.3735641E-02
VAR H3 A,C,S  1.2178957E-02  3.6580893E-03  1.5837045E-02

VAR S0 X,Y,S  1.0605898E-02  6.3896347E-03  1.6995503E-02
VAR H1 X,Y,S  1.0751848E-02  2.9393421E-03  1.3691191E-02
VAR L1 X,Y,S  1.0789744E-02  2.9548015E-03  1.3744595E-02
VAR H0 X,Y,S  1.0723243E-02  2.9455707E-03  1.3668792E-02
VAR L0 X,Y,S  1.0756804E-02  2.9788320E-03  1.3735641E-02
VAR H3 X,Y,S  1.2178957E-02  3.6580893E-03  1.5837045E-02

INTEGRATED SQUARED DEVIATION FROM DIF SPECTRA
DIF H1 A,C,S  4.0562998E-04  1.3370063E-03  1.7426378E-03
DIF L1 A,C,S  4.2029686E-04  1.3280771E-03  1.7483742E-03
DIF H0 A,C,S  4.1612997E-04  1.3227591E-03  1.7388887E-03
DIF L0 A,C,S  4.4801459E-04  1.2933519E-03  1.7413681E-03
DIF H3 A,C,S  6.4408034E-04  1.0170188E-03  1.6610981E-03

DIF H1 X,Y,S  4.0562998E-04  1.3370063E-03  1.7426378E-03
DIF L1 X,Y,S  4.2029686E-04  1.3280771E-03  1.7483742E-03
DIF H0 X,Y,S  4.1612997E-04  1.3227591E-03  1.7388887E-03
DIF L0 X,Y,S  4.4801459E-04  1.2933519E-03  1.7413681E-03
DIF H3 X,Y,S  6.4408034E-04  1.0170188E-03  1.6610981E-03
```

```
CASE06.DAT

PARAMETERS
 1.200000      3.7500001E-02   64.00000        56789.00
 12.00000      0.0000000E+00   0.0000000E+00   64.00000
 53.20000      0.0000000E+00   53.20000        9.885000
 1.337000      1.0200000E-09   99999.00        99999.00

MAGNITUDE ARRAY SCALING FACTORS
H1(0,0),HIGH,FACTOR  1.708915      3.6639281E-02  10.01071
L1(0,0),HIGH,FACTOR  1.772432      4.1131079E-02  8.917469
H0(0,0),HIGH,FACTOR  1.814606      3.5244357E-02  10.40692
L0(0,0),HIGH,FACTOR  1.983813      3.8338579E-02  9.566998
H3(0,0),HIGH,FACTOR  1.946132      4.1970782E-02  8.739058

INTEGRATED VARIANCE FROM POWER SPECTRA
VAR S0 A,C,S  1.0605898E-02  6.3896347E-03  1.6995503E-02
VAR H1 A,C,S  1.1827840E-02  3.5197868E-03  1.5347640E-02
VAR L1 A,C,S  1.1429348E-02  3.3040436E-03  1.4733412E-02
VAR H0 A,C,S  1.1892175E-02  3.5655941E-03  1.5457775E-02
VAR L0 A,C,S  1.1492250E-02  3.3585266E-03  1.4850751E-02
VAR H3 A,C,S  1.5504099E-02  6.0993349E-03  2.1603426E-02

VAR S0 X,Y,S  1.0605898E-02  6.3896347E-03  1.6995503E-02
VAR H1 X,Y,S  1.1827840E-02  3.5197868E-03  1.5347640E-02
VAR L1 X,Y,S  1.1429348E-02  3.3040436E-03  1.4733412E-02
VAR H0 X,Y,S  1.1892175E-02  3.5655941E-03  1.5457775E-02
VAR L0 X,Y,S  1.1492250E-02  3.3585266E-03  1.4850751E-02
VAR H3 X,Y,S  1.5504099E-02  6.0993349E-03  2.1603426E-02

INTEGRATED SQUARED DEVIATION FROM DIF SPECTRA
DIF H1 A,C,S  5.0188095E-04  1.0615377E-03  1.5634208E-03
DIF L1 A,C,S  4.3811518E-04  1.1561334E-03  1.5942472E-03
DIF H0 A,C,S  5.1579624E-04  1.0423700E-03  1.5581655E-03
DIF L0 A,C,S  4.5269734E-04  1.1274212E-03  1.5801196E-03
DIF H3 A,C,S  1.2891217E-03  7.9059153E-04  2.0797129E-03

DIF H1 X,Y,S  5.0188095E-04  1.0615377E-03  1.5634208E-03
DIF L1 X,Y,S  4.3811518E-04  1.1561334E-03  1.5942472E-03
DIF H0 X,Y,S  5.1579624E-04  1.0423700E-03  1.5581655E-03
DIF L0 X,Y,S  4.5269734E-04  1.1274212E-03  1.5801196E-03
DIF H3 X,Y,S  1.2891217E-03  7.9059153E-04  2.0797129E-03
```

CASE07.DAT

PARAMETERS

1.200000	3.7500001E-02	64.00000	56789.00
12.00000	0.0000000E+00	45.00000	64.00000
53.20000	0.0000000E+00	0.0000000E+00	100.0000
1.337000	1.0200000E-09	99999.00	99999.00

MAGNITUDE ARRAY SCALING FACTORS

H1(0,0),HIGH,FACTOR	0.9663691	2.1553256E-02	20.18031
L1(0,0),HIGH,FACTOR	0.9759609	2.1140706E-02	20.57411
H0(0,0),HIGH,FACTOR	1.151857	1.9404136E-02	22.41539
L0(0,0),HIGH,FACTOR	1.346936	1.6846012E-02	25.81924
H3(0,0),HIGH,FACTOR	0.8803946	2.3213871E-02	18.73670

INTEGRATED VARIANCE FROM POWER SPECTRA

VAR S0 A,C,S	1.0649075E-02	6.3449983E-03	1.6994014E-02
VAR H1 A,C,S	1.3324276E-02	8.3941165E-03	2.1718401E-02
VAR L1 A,C,S	1.3449105E-02	8.5145570E-03	2.1963645E-02
VAR H0 A,C,S	1.3450821E-02	8.5107880E-03	2.1961607E-02
VAR L0 A,C,S	1.3848226E-02	8.8802287E-03	2.2728480E-02
VAR H3 A,C.S	1.4138573E-02	9.1494014E-03	2.3287963E-02
VAR S0 X,Y,S	8.4970202E-03	8.4970109E-03	1.6994014E-02
VAR H1 X,Y,S	1.5874185E-02	5.9442070E-03	2.1718401E-02
VAR L1 X,Y,S	1.6028296E-02	5.9353625E-03	2.1963645E-02
VAR H0 X,Y,S	1.6026707E-02	5.9349309E-03	2.1961607E-02
VAR L0 X,Y,S	1.6508242E-02	6.2202271E-03	2.2728480E-02
VAR H3 X,Y,S	1.6673123E-02	6.6148997E-03	2.3287963E-02

INTEGRATED SQUARED DEVIATION FROM DIF SPECTRA

DIF H1 A,C,S	1.929803[illegible]-03	1.6361465E-03	3.5659471E-03
DIF L1 A,C,S	1.9493713E-03	1.6535096E-03	3.6028787E-03
DIF H0 A,C,S	1.9482735E-03	1.6531112E-03	3.6013813E-03
DIF L0 A,C,S	2.0178822E-03	1.7137438E-03	3.7316259E-03
DIF H3 A,C,S	2.0287863E-03	1.6956879E-03	3.7244821E-03
DIF H1 X,Y,S	1.8270897E-03	1.7388582E-03	3.5659471E-03
DIF L1 X,Y,S	1.9004126E-03	1.7024733E-03	3.6028787E-03
DIF H0 X,Y,S	1.8916040E-03	1.7097787E-03	3.6013813E-03
DIF L0 X,Y,S	2.1048384E-03	1.6267927E-03	3.7316259E-03
DIF H3 X,Y,S	2.2309734E-03	1.4935071E-03	3.7244021E-03

CASE08.DAT

PARAMETERS

1.200000	3.7500001E-02	64.00000	56789.00
12.00000	0.0000000E+00	45.00000	64.00000
53.20000	45.00000	53.20000	9.885000
1.337000	1.0200000E-09	99999.00	99999.00

MAGNITUDE ARRAY SCALING FACTORS

H1(0,0),HIGH,FACTOR	0.6324890	2.0326763E-02	21.39796
L1(0,0),HIGH,FACTOR	0.6656371	2.2054087E-02	19.72203
H0(0,0),HIGH,FACTOR	0.7382769	1.9370455E-02	22.45437
L0(0,0),HIGH,FACTOR	0.8772127	2.0141609E-02	21.59467
H3(0,0),HIGH,FACTOR	0.5811127	2.0660121E-02	21.05270

INTEGRATED VARIANCE FROM POWER SPECTRA

VAR S0 A,C,S	1.0649075E-02	6.3449983E-03	1.6994014E-02
VAR H1 A,C,S	1.6529508E-02	4.8296824E-03	2.1359220E-02
VAR L1 A,C,S	1.7114336E-02	5.1686037E-03	2.2282979E-02
VAR H0 A,C,S	1.6552282E-02	4.8371125E-03	2.1389436E-02
VAR L0 A,C,S	1.7181354E-02	5.1389989E-03	2.2320338E-02
VAR H3 A,C,S	1.8383536E-02	5.6448882E-03	2.4028407E-02
VAR S0 X,Y,S	8.4970202E-03	8.4970109E-03	1.6994014E-02
VAR H1 X,Y,S	1.1015816E-02	1.0343401E-02	2.1359220E-02
VAR L1 X,Y,S	1.2076405E-02	1.0206542E-02	2.2282979E-02
VAR H0 X,Y,S	1.0657494E-02	1.0731947E-02	2.1389436E-02
VAR L0 X,Y,S	1.1424644E-02	1.0895728E-02	2.2320338E-02
VAR H3 X,Y,S	1.2826443E-02	1.1201976E-02	2.4028407E-02

INTEGRATED SQUARED DEVIATION FROM DIF SPECTRA

DIF H1 A,C,S	1.0922957E-03	9.2131220E-04	2.0136090E-03
DIF L1 A,C,S	1.2529632E-03	9.0072595E-04	2.1536872E-03
DIF H0 A,C,S	1.0962893E-03	9.1051857E-04	2.0068064E-03
DIF L0 A,C,S	1.2454551E-03	8.7652548E-04	2.1219780E-03
DIF H3 A,C,S	1.6121409E-03	8.7410398E-04	2.4862445E-03
DIF H1 X,Y,S	9.7821641E-04	1.0353923E-03	2.0136090E-03
DIF L1 X,Y,S	1.0751315E-03	1.0785615E-03	2.1536872E-03
DIF H0 X,Y,S	9.7513461E-04	1.0316728E-03	2.0068064E-03
DIF L0 X,Y,S	1.0433807E-03	1.0785997E-03	2.1219780E-03
DIF H3 X,Y,S	1.2638383E-03	1.2224050E-03	2.4862445E-03

```
CASE09.DAT

PARAMETERS
 1.200000      3.7500001E-02   64.00000       56789.00
 12.00000      0.0000000E+00   45.00000       64.00000
 53.20000       90.00000       53.20000       9.885000
 1.337000      1.0200000E-09   99999.00       99999.00

MAGNITUDE ARRAY SCALING FACTORS
H1(0,0),HIGH,FACTOR  0.2319100      6.2539992E-03   69.54771
L1(0,0),HIGH,FACTOR  0.2524389      8.0012875E-03   54.36016
H0(0,0),HIGH,FACTOR  0.3376979      5.0363950E-03   86.36163
L0(0,0),HIGH,FACTOR  0.4640146      5.5711875E-03   78.07156
H3(0,0),HIGH,FACTOR  0.2052276      6.7613232E-03   64.32932

INTEGRATED VARIANCE FROM POWER SPECTRA
VAR S0 A,C,S  1.0649075E-02  6.3449983E-03  1.6994014E-02
VAR H1 A,C,S  1.4888551E-02  7.7039208E-03  2.2592455E-02
VAR L1 A,C,S  1.4498282E-02  7.7737719E-03  2.2272006E-02
VAR H0 A,C,S  1.5721593E-02  7.9157315E-03  2.3637330E-02
VAR L0 A,C,S  1.6027095E-02  8.3681438E-03  2.4395257E-02
VAR H3 A,C,S  1.5098419E-02  8.1891306E-03  2.3287576E-02

VAR S0 X,Y,S  8.4970202E-03  8.4970109E-03  1.6994014E-02
VAR H1 X,Y,S  1.5786350E-02  6.8061128E-03  2.2592455E-02
VAR L1 X,Y,S  1.5682261E-02  6.5897778E-03  2.2272006E-02
VAR H0 X,Y,S  1.6190013E-02  7.4472865E-03  2.3637330E-02
VAR L0 X,Y,S  1.6636403E-02  7.7588325E-03  2.4395257E-02
VAR H3 X,Y,S  1.6161703E-02  7.1258480E-03  2.3287576E-02

INTEGRATED SQUARED DEVIATION FROM DIF SPECTRA
DIF H1 A,C,S  1.7148135E-03  1.3221649E-03  3.0369780E-03
DIF L1 A,C,S  1.7441006E-03  1.3935184E-03  3.1376174E-03
DIF H0 A,C,S  1.7701995E-03  1.2635458E-03  3.0337465E-03
DIF L0 A,C,S  1.9154331E-03  1.3619228E-03  3.2773588E-03
DIF H3 A,C,S  1.8527806E-03  1.3862705E-03  3.2390505E-03

DIF H1 X,Y,S  1.6691079E-03  1.3678706E-03  3.0369780E-03
DIF L1 X,Y,S  1.7095691E-03  1.4280492E-03  3.1376174E-03
DIF H0 X,Y,S  1.7987142E-03  1.2350267E-03  3.0337465E-03
DIF L0 X,Y,S  2.0597964E-03  1.2175600E-03  3.2773588E-03
DIF H3 X,Y,S  1.9105881E-03  1.3284634E-03  3.2390505E-03
```

```
CASE10.DAT

PARAMETERS
 1.200000      3.7500001E-02   64.00000       56789.00
 12.00000      0.0000000E+00   45.00000       64.00000
 53.20000       135.0000       53.20000       9.885000
 1.337000      1.0200000E-09   99999.00       99999.00

MAGNITUDE ARRAY SCALING FACTORS
H1(0,0),HIGH,FACTOR  0.3377088      8.9936415E-03   48.36209
L1(0,0),HIGH,FACTOR  0.3503164      1.0155986E-02   42.82709
H0(0,0),HIGH,FACTOR  0.4434966      7.8516882E-03   55.39590
L0(0,0),HIGH,FACTOR  0.5618922      7.8747338E-03   55.23378
H3(0,0),HIGH,FACTOR  0.3095516      9.0892045E-03   47.85361

INTEGRATED VARIANCE FROM POWER SPECTRA
VAR S0 A,C,S  1.0649075E-02  6.3449983E-03  1.6994014E-02
VAR H1 A,C,S  1.0802118E-02  1.0990591E-02  2.1792740E-02
VAR L1 A,C,S  1.1332154E-02  1.0765111E-02  2.2097223E-02
VAR H0 A,C,S  1.0536979E-02  1.1439664E-02  2.1976665E-02
VAR L0 A,C,S  1.0976007E-02  1.1610906E-02  2.2586942E-02
VAR H3 A,C,S  1.2645886E-02  1.2265611E-02  2.4911504E-02

VAR S0 X,Y,S  8.4970202E-03  8.4970109E-03  1.6994014E-02
VAR H1 X,Y,S  1.5989481E-02  5.8032386E-03  2.1792740E-02
VAR L1 X,Y,S  1.6304400E-02  5.7928297E-03  2.2097223E-02
VAR H0 X,Y,S  1.5980538E-02  5.9960959E-03  2.1976665E-02
VAR L0 X,Y,S  1.6436875E-02  6.1500389E-03  2.2586942E-02
VAR H3 X,Y,S  1.8066773E-02  6.8447292E-03  2.4911504E-02

INTEGRATED SQUARED DEVIATION FROM DIF SPECTRA
DIF H1 A,C,S  2.3250512E-03  1.9767422E-03  4.3017948E-03
DIF L1 A,C,S  2.2950359E-03  1.9904911E-03  4.2855288E-03
DIF H0 A,C,S  2.3572170E-03  2.0493325E-03  4.4065528E-03
DIF L0 A,C,S  2.3499208E-03  2.1487060E-03  4.4986228E-03
DIF H3 A,C,S  2.4080733E-03  2.3920981E-03  4.8001758E-03

DIF H1 X,Y,S  2.2595557E-03  2.0422379E-03  4.3017948E-03
DIF L1 X,Y,S  2.2985798E-03  1.9869469E-03  4.2855288E-03
DIF H0 X,Y,S  2.3649042E-03  2.0416472E-03  4.4065528E-03
DIF L0 X,Y,S  2.5325539E-03  1.9660755E-03  4.4986228E-03
DIF H3 X,Y,S  2.9898977E-03  1.8102751E-03  4.8001758E-03
```

```
CASE11.DAT

PARAMETERS
 1.200000     3.7500001E-02   64.00000     56789.00
 12.00000     0.0000000E+00   45.60000     64.00000
 53.20000      180.0000       53.20000     9.885000
 1.337000     1.0200000E-09   99999.00     99999.00

MAGNITUDE ARRAY SCALING FACTORS
H1(0,0),HIGH,FACTOR  0.4582272     1.2372605E-02   35.15438
L1(0,0),HIGH,FACTOR  0.4674055     1.3490552E-02   32.24118
H0(0,0),HIGH,FACTOR  0.5640151     1.1152427E-02   39.00060
L0(0,0),HIGH,FACTOR  0.6789812     1.1051445E-02   39.35696
H3(0,0),HIGH,FACTOR  0.4248831     1.2980908E-02   33.50700

INTEGRATED VARIANCE FROM POWER SPECTRA
VAR S0 A C,S  1.0649075E-02  6.3449983E-03  1.6994014E-02
VAR H1 A,C,S  1.2863121E-02  8.0941636E-03  2.0957269E-02
VAR L1 A,C,S  1.2858900E-02  8.1248945E-03  2.0983795E-02
VAR H0 A,C,S  1.2942028E-02  8.1621390E-03  2.1104205E-02
VAR L0 A,C,S  1.3042567E-02  8.2899174E-03  2.1332467E-02
VAR H3 A,C,S  1.3312777E-02  8.5486965E-03  2.1861432E-02

VAR S0 X,Y,S  8.4970202E-03  8.4970109E-03  1.6994014E-02
VAR H1 X,Y,S  1.5411285E-02  5.5460143E-03  2.0957269E-02
VAR L1 X,Y,S  1.5419249E-02  5.5645546E-03  2.0983795E-02
VAR H0 X,Y,S  1.5504861E-02  5.5993125E-03  2.1104205E-02
VAR L0 X,Y,S  1.5639862E-02  5.6926101E-03  2.1332467E-02
VAR H3 X,Y,S  1.5814118E-02  6.0473396E-03  2.1861432E-02

INTEGRATED SQUARED DEVIATION FROM DIF SPECTRA
DIF H1 A,C,S  1.8988448E-03  1.6038719E-03  3.5027161E-03
DIF L1 A,C,S  1.8962764E-03  1.6058472E-03  3.5021203E-03
DIF H0 A,C,S  1.9056031E-03  1.6125349E-03  3.5181376E-03
DIF L0 A,C,S  1.9159885E-03  1.6289004E-03  3.5448852E-03
DIF H3 A,C,S  1.9071788E-03  1.5870153E-03  3.4941877E-03

DIF H1 X,Y,S  1.6434977E-03  1.8592236E-03  3.5027161E-03
DIF L1 X,Y,S  1.6644619E-03  1.8376623E-03  3.5021203E-03
DIF H0 X,Y,S  1.6801300E-03  1.8380057E-03  3.5181376E-03
DIF L0 X,Y,S  1.7551382E-03  1.7897506E-03  3.5448852E-03
DIF H3 X,Y,S  1.8891388E-03  1.6050531E-03  3.4941877E-03
```

```
CASE12.DAT

PARAMETERS
 1.200000     3.7500001E-02   64.00000     56789.00
 12.00000     0.0000000E+00   45.00000     64.00000
 53.20000     0.0000000E+00   53.20000     9.885000
 1.337000     1.0200000E-09   99999.00     99999.00

MAGNITUDE ARRAY SCALING FACTORS
H1(0,0),HIGH,FACTOR  1.718274     3.5939805E-02   12.10222
L1(0,0),HIGH,FACTOR  1.773931     4.0016800E-02   10.86922
H0(0,0),HIGH,FACTOR  1.824061     3.4724467E-02   12.52579
L0(0,0),HIGH,FACTOR  1.985507     3.7582196E-02   11.57333
H3(0,0),HIGH,FACTOR  1.950853     4.0151652E-02   10.83271

INTEGRATED VARIANCE FROM POWER SPECTRA
VAR S0 A,C,S  1.0649075E-02  6.3449983E-03  1.6994014E-02
VAR H1 A,C,S  1.2168342E-02  8.3105192E-03  2.0478847E-02
VAR L1 A,C,S  1.1857730E-02  8.0703888E-03  1.9928142E-02
VAR H0 A,C,S  1.2192477E-02  8.3539002E-03  2.0546351E-02
VAR L0 A,C,S  1.1861366E-02  8.1202509E-03  1.9981597E-02
VAR H3 A,C,S  1.5325218E-02  1.1803962E-02  2.7129119E-02

VAR S0 X,Y,S  8.4970202E-03  8.4970109E-03  1.6994014E-02
VAR H1 X,Y,S  1.4924021E-02  5.5548423E-03  2.0478847E-02
VAR L1 X,Y,S  1.4612147E-02  5.3159734E-03  1.9928142E-02
VAR H0 X,Y,S  1.4952708E-02  5.5936882E-03  2.0546351E-02
VAR L0 X,Y,S  1.4625248E-02  5.3563616E-03  1.9981597E-02
VAR H3 X,Y,S  1.7882787E-02  9.2463465E-03  2.7129119E-02

INTEGRATED SQUARED DEVIATION FROM DIF SPECTRA
DIF H1 A,C,S  1.7985214E-03  1.4201046E-03  3.2186310E-03
DIF L1 A,C,S  1.7905866E-03  1.4097518E-03  3.2003412E-03
DIF H0 A,C,S  1.7946775E-03  1.4191521E-03  3.2138280E-03
DIF L0 A,C,S  1.7818530E-03  1.4030912E-03  3.1849453E-03
DIF H3 A,C,S  2.2695151E-03  2.2316792E-03  4.5011961E-03

DIF H1 X,Y,S  1.5494113E-03  1.6692173E-03  3.2186310E-03
DIF L1 X,Y,S  1.4421387E-03  1.7582020E-03  3.2003412E-03
DIF H0 X,Y,S  1.5630024E-03  1.6508265E-03  3.2138280E-03
DIF L0 X,Y,S  1.4529217E-03  1.7320238E-03  3.1849453E-03
DIF H3 X,Y,S  2.8791185E-03  1.6220743E-03  4.5011961E-03
```

```
CASE13.DAT

PARAMETERS
 1.200000     3.7500001E-02   64.00000        56789.00
 12.00000     0.0000000E+00   90.00000        64.00000
 53.20000     5.0000000E+00   0.0000000E+00   100.0000
 1.337000     1.0200000E-09   99999.00        99999.00

MAGNITUDE ARRAY SCALING FACTORS
H1(0,0),HIGH,FACTOR  0.9463229    1.6765064E-02   21.87794
L1(0,0),HIGH,FACTOR  0.9533488    1.6673984E-02   21.99745
H0(0,0),HIGH,FACTOR   1.131999    1.5293626E-02   23.98287
L0(0,0),HIGH,FACTOR   1.324701    1.3732953E-02   26.70839
H3(0,0),HIGH,FACTOR  0.8640521    1.5217487E-02   24.10287

INTEGRATED VARIANCE FROM POWER SPECTRA
VAR S0 A,C,S  1.0605882E-02  6.3896296E-03  1.6995508E-02
VAR H1 A,C,S  7.5966557E-03  1.4392884E-02  2.1989554E-02
VAR L1 A,C,S  7.6304922E-03  1.4429243E-02  2.2059659E-02
VAR H0 A,C,S  7.6619764E-03  1.4460417E-02  2.2122402E-02
VAR L0 A,C,S  7.8185434E-03  1.4639320E-02  2.2457868E-02
VAR H3 A,C,S  8.6988593E-03  1.6235027E-02  2.4933942E-02

VAR S0 X,Y,S  6.3896300E-03  1.0605882E-02  1.6995508E-02
VAR H1 X,Y,S  1.4392884E-02  7.5966562E-03  2.1989554E-02
VAR L1 X,Y,S  1.4429243E-02  7.6304922E-03  2.2059659E-02
VAR H0 X,Y,S  1.4460417E-02  7.6619759E-03  2.2122402E-02
VAR L0 X,Y,S  1.4639320E-02  7.8185434E-03  2.2457868E-02
VAR H3 X,Y,S  1.6235027E-02  8.6988593E-03  2.4933942E-02

INTEGRATED SQUARED DEVIATION FROM DIF SPECTRA
DIF H1 A,C,S  2.3762535E-03  2.4902024E-03  4.8664468E-03
DIF L1 A,C,S  2.3534810E-03  2.5223093E-03  4.8757833E-03
DIF H0 A,C,S  2.3462176E-03  2.5339902E-03  4.8802085E-03
DIF L0 A,C,S  2.2808637E-03  2.6498614E-03  4.9307286E-03
DIF H3 A,C,S  2.2550195E-03  3.3153067E-03  5.5703185E-03

DIF H1 X,Y,S  2.4902024E-03  2.3762533E-03  4.8664468E-03
DIF L1 X,Y,S  2.5223091E-03  2.3534810E-03  4.8757833E-03
DIF H0 X,Y,S  2.5339902E-03  2.3462176E-03  4.8802085E-03
DIF L0 X,Y,S  2.6498614E-03  2.2808637E-03  4.9307286E-03
DIF H3 X,Y,S  3.3153067E-03  2.2550193E-03  5.5703185E-03
```

```
CASE14.DAT

PARAMETERS
 1.200003     3.7500001E-02   64.00000   56789.00
 12.00000     0.0000000E+00   90.00000   64.00000
 53.20000      45.00000       53.20000   9.885000
 1.337000     1.0200000E-09   99999.00   99999.00

MAGNITUDE ARRAY SCALING FACTORS
H1(0,0),HIGH,FACTOR  0.6396829    1.8694542E-02   19.61990
L1(0,0),HIGH,FACTOR  0.6658432    1.9711750E-02   18.60744
H0(0,0),HIGH,FACTOR  0.7455862    1.8148819E-02   20.20986
L0(0,0),HIGH,FACTOR  0.8776498    1.8620141E-02   19.69830
H3(0,0),HIGH,FACTOR  0.5800271    1.8138792E-02   20.22103

INTEGRATED VARIANCE FROM POWER SPECTRA
VAR S0 A,C,S  1.0605882E-02  6.3896296E-03  1.6995508E-02
VAR H1 A,C,S  1.0143002E-02  6.4229933E-03  1.6565975E-02
VAR L1 A,C,S  1.0176001E-02  7.3185232E-03  1.7494487E-02
VAR H0 A,C,S  1.0382374E-02  6.1070151E-03  1.6489422E-02
VAR L0 A,C,S  1.0589804E-02  6.6799670E-03  1.7269770E-02
VAR H3 A,C,S  1.0408917E-02  6.8047494E-03  1.7213659E-02

VAR S0 X,Y,S  6.3896300E-03  1.0605882E-02  1.6995508E-02
VAR H1 X,Y,S  6.4229928E-03  1.0143002E-02  1.6565975E-02
VAR L1 X,Y,S  7.3185228E-03  1.0176001E-02  1.7494487E-02
VAR H0 X,Y,S  6.1070146E-03  1.0382374E-02  1.6489422E-02
VAR L0 X,Y,S  6.6799666E-03  1.0589804E-02  1.7269770E-02
VAR H3 X,Y,S  6.8047494E-03  1.0408917E-02  1.7213659E-02

INTEGRATED SQUARED DEVIATION FROM DIF SPECTRA
DIF H1 A,C,S  1.5590638E-03  1.1088561E-03  2.6679211E-03
DIF L1 A,C,S  1.6509299E-03  1.1370622E-03  2.7879935E-03
DIF H0 A,C,S  1.4826785E-03  1.0981616E-03  2.5808420E-03
DIF L0 A,C,S  1.5342711E-03  1.0966852E-03  2.6309541E-03
DIF H3 A,C,S  1.5645114E-03  1.1225190E-03  2.7070274E-03

DIF H1 X,Y,S  1.1088562E-03  1.5590638E-03  2.6679211E-03
DIF L1 X,Y,S  1.1370622E-03  1.6509298E-03  2.7879935E-03
DIF H0 X,Y,S  1.0981616E-03  1.4826785E-03  2.5808420E-03
DIF L0 X,Y,S  1.0966852E-03  1.5342711E-03  2.6309541E-03
DIF H3 X,Y,S  1.1225190E-03  1.5845113E-03  2.7070274E-03
```

CASE15.DAT

PARAMETERS

1.200000	3.7500001E-02	64.00000	56789.00
12.00000	0.0000000E+00	90.00000	64.00000
53.20000	90.00000	53.20000	9.885000
1.337000	1.0200000E-09	99999.00	99999.00

MAGNITUDE ARRAY SCALING FACTORS

H1(0,0),HIGH,FACTOR	0.2311470	4.4725928E-03	82.00726
L1(0,0),HIGH,FACTOR	0.2469401	5.5664536E-03	65.89206
H0(0,0),HIGH,FACTOR	0.3370503	3.6561021E-03	100.3214
L0(0,0),HIGH,FACTOR	0.4587466	3.9185770E-03	93.60161
H3(0,0),HIGH,FACTOR	0.2029305	4.2490112E-03	86.32246

INTEGRATED VARIANCE FROM POWER SPECTRA

VAR S0 A,C,S	1.0605882E-02	6.3896296E-03	1.6995508E-02
VAR H1 A,C,S	9.8175965E-03	1.5708292E-02	2.5525887E-02
VAR L1 A,C,S	9.6632391E-03	1.6127219E-02	2.5790431E-02
VAR H0 A,C,S	1.0924796E-02	1.6218759E-02	2.7143553E-02
VAR L0 A,C,S	1.1877696E-02	1.7747005E-02	2.9624652E-02
VAR H3 A,C,S	1.0272576E-02	1.6703218E-02	2.6975773E-02
VAR S0 X,Y,S	6.3896300E-03	1.0605882E-02	1.6995508E-02
VAR H1 X,Y,S	1.5708290E-02	9.8175965E-03	2.5525887E-02
VAR L1 X,Y,S	1.6127219E-02	9.6632401E-03	2.5790431E-02
VAR H0 X,Y,S	1.6218759E-02	1.0924796E-02	2.7143553E-02
VAR L0 X,Y,S	1.7747005E-02	1.1877696E-02	2.9624652E-02
VAR H3 X,Y,S	1.6703220E-02	1.0272576E-02	2.6975773E-02

INTEGRATED SQUARED DEVIATION FROM DIF SPECTRA

DIF H1 A,C,S	1.9768833E-03	2.9677858E-03	4.9446728E-03
DIF L1 A,C,S	2.0517830E-03	3.2000248E-03	5.2518067E-03
DIF H0 A,C,S	1.9108414E-03	3.2089821E-03	5.1198294E-03
DIF L0 A,C,S	2.9260366E-03	3.9828131E-03	6.9088389E-03
DIF H3 A,C,S	2.0578685E-03	3.4445030E-03	5.5023688E-03
DIF H1 X,Y,S	2.9677858E-03	1.9768833E-03	4.9446728E-03
DIF L1 X,Y,S	3.2000246E-03	2.0517830E-03	5.2518067E-03
DIF H0 X,Y,S	3.2089821E-03	1.9108413E-03	5.1198294E-03
DIF L0 X,Y,S	3.9828126E-03	2.9260366E-03	6.9088388E-03
DIF H3 X,Y,S	3.4445033E-03	2.0578605E-03	5.5023688E-03

CASE16.DAT

PARAMETERS

1.200000	3.7500001E-02	64.00000	56789.00
12.30000	9.0000000E+00	90.00000	64.00000
53.20000	135.0000	53.20000	9.885000
1.337000	1.0200000E-09	99999.00	99999.00

MAGNITUDE ARRAY SCALING FACTORS

H1(0,0),HIGH,FACTOR	0.3325742	8.1447642E-03	45.03324
L1(0,0),HIGH,FACTOR	0.3420186	8.9132441E-03	41.15057
H0(0,0),HIGH,FACTOR	0.4384775	7.3251775E-03	59.07184
L0(0,0),HIGH,FACTOR	0.5538252	7.2750715E-03	50.41670
H3(0,0),HIGH,FACTOR	0.3043880	7.5686998E-03	40.46078

INTEGRATED VARIANCE FROM POWER SPECTRA

VAR S0 A,C,S	1.0605882E-02	6.3896296E-03	1.6995508E-02
VAR H1 A,C,S	7.0397388E-03	1.1372326E-02	1.8412022E-02
VAR L1 A,C,S	7.0699155E-03	1.1882270E-02	1.8952180E-02
VAR H0 A,C,S	7.1953754E-03	1.1132345E-02	1.8327711E-02
VAR L0 A,C,S	7.3809694E-03	1.1553068E-02	1.8934054E-02
VAR H3 A,C,S	7.7165491E-03	1.2276269E-02	1.9992812E-02
VAR S0 X,Y,S	6.3896300E-03	1.0605882E-02	1.6995508E-02
VAR H1 X,Y,S	1.1372326E-02	7.0397384E-03	1.8412022E-02
VAR L1 X,Y,S	1.1882271E-02	7.0699155E-03	1.8952180E-02
VAR H0 X,Y,S	1.1132345E-02	7.1953754E-03	1.8327711E-02
VAR L0 X,Y,S	1.1553068E-02	7.3809694E-03	1.8934054E-02
VAR H3 X,Y,S	1.2276269E-02	7.7165491E-03	1.9992812E-02

INTEGRATED SQUARED DEVIATION FROM DIF SPECTRA

DIF H1 A,C,S	2.4637198E-03	1.6541410E-03	4.1178591E-03
DIF L1 A,C,S	2.4331054E-03	1.7902745E-03	4.2233830E-03
DIF H0 A,C,S	2.4204561E-03	1.6428413E-03	4.0632961E-03
DIF L0 A,C,S	2.3338886E-03	1.7986184E-03	4.1325102E-03
DIF H3 A,C,S	2.2736026E-03	1.9768979E-03	4.2504999E-03
DIF H1 X,Y,S	1.6541409E-03	2.4637198E-03	4.1178591E-03
DIF L1 X,Y,S	1.7902745E-03	2.4331054E-03	4.2233830E-03
DIF H0 X,Y,S	1.6428411E-03	2.4204561E-03	4.0632961E-03
DIF L0 X,Y,S	1.7986182E-03	2.3338886E-03	4.1325102E-03
DIF H3 X,Y,S	1.9768979E-03	2.2736026E-03	4.2504999E-03

CASE17.DAT

PARAMETERS

1.200000	3.7500001E-02	64.00000	56789.00
12.00000	0.0000000E+00	98.00000	64.00000
53.20000	180.0000	53.20000	9.885000
1.337000	1.0200000E-09	99999.00	99999.00

MAGNITUDE ARRAY SCALING FACTORS

H1(0,0),HIGH,FACTOR	0.4501194	9.2856940E-03	39.50002
L1(0,0),HIGH,FACTOR	0.4567570	9.9748746E-03	36.77090
H0(0,0),HIGH,FACTOR	0.5560228	8.4662307E-03	43.32331
L0(0,0),HIGH,FACTOR	0.6685636	8.3367899E-03	45.99596
H3(0,0),HIGH,FACTOR	0.4175930	8.6326599E-03	42.48808

INTEGRATED VARIANCE FROM POWER SPECTRA

VAR S0 A,C,S	1.0605882E-02	6.3896296E-03	1.6995508E-02
VAR H1 A,C,S	7.4455538E-03	1.4351269E-02	2.1796813E-02
VAR L1 A,C,S	7.5716837E-03	1.4558070E-02	2.2129759E-02
VAR H0 A,C,S	7.4706986E-03	1.4363201E-02	2.1833959E-02
VAR L0 A,C,S	7.6731676E-03	1.4659278E-02	2.2332411E-02
VAR H3 A,C,S	7.9204850E-03	1.5083080E-02	2.3003578E-02
VAR S0 X,Y,S	6.3896300E-03	1.0605882E-02	1.6995508E-02
VAR H1 X,Y,S	1.4351269E-02	7.4455538E-03	2.1796813E-02
VAR L1 X,Y,S	1.4558070E-02	7.5716833E-03	2.2129759E-02
VAR H0 X,Y,S	1.4363202E-02	7.4706981E-03	2.1833859E-02
VAR L0 X,Y,S	1.4659270E-02	7.6731676E-03	2.2332441E-02
VAR H3 X,Y,S	1.5083080E-02	7.9204850E-03	2.3003578E-02

INTEGRATED SQUARED DEVIATION FROM DIF SPECTRA

DIF H1 A,C,S	2.4873014E-03	2.4226152E-03	4.9093203E-03
DIF L1 A,C,S	2.4541889E-03	2.5192907E-03	4.9734833E-03
DIF H0 A,C,S	2.4669615E-03	2.4392316E-03	4.9061924E-03
DIF L0 A,C,S	2.4045447E-03	2.5900770E-03	4.9946225E-03
DIF H3 A,C,S	2.3677231E-03	2.7789089E-03	5.1466175E-03
DIF H1 X,Y,S	2.4226152E-03	2.4873011E-03	4.9093203E-03
DIF L1 X,Y,S	2.5192907E-03	2.4541882E-03	4.9734833E-03
DIF H0 X,Y,S	2.4392316E-03	2.4669615E-03	4.9061924E-03
DIF L0 X,Y,S	2.5900770E-03	2.4045450E-03	4.9946229E-03
DIF H3 X,Y,S	2.7789092E-03	2.3677221E-03	5.1466175E-03

CASE18.DAT

PARAMETERS

1.200000	3.7500001E-02	64.00000	56789.00
12.00000	0.0000000E+00	98.00000	64.00000
53.20000	0.0000000E+00	53.20000	9.885000
1.337000	1.0250000E-09	99999.00	99999.00

MAGNITUDE ARRAY SCALING FACTORS

H1(0,0),HIGH,FACTOR	1.719939	2.8818058E-02	12.72762
L1(0,0),HIGH,FACTOR	1.765594	3.1830506E-02	11.53176
H0(0,0),HIGH,FACTOR	1.825842	2.7977532E-02	13.10999
L0(0,0),HIGH,FACTOR	1.977491	3.0124452E-02	12.17566
H3(0,0),HIGH,FACTOR	1.950317	3.2681592E-02	11.22382

INTEGRATED VARIANCE FROM POWER SPECTRA

VAR S0 A,C,S	1.0605882E-02	6.3896296E-03	1.6995508E-02
VAR H1 A,C,S	6.6653597E-03	1.2079223E-02	1.8744573E-02
VAR L1 A,C,S	6.5159919E-03	1.2038279E-02	1.8554291E-02
VAR H0 A,C,S	6.6777952E-03	1.2042022E-02	1.8719839E-02
VAR L0 A,C,S	6.5173767E-03	1.1955025E-02	1.8472390E-02
VAR H3 A,C,S	1.0325875E-02	1.2856302E-02	2.3182228E-02
VAR S0 X,Y,S	6.3896300E-03	1.0605882E-02	1.6995508E-02
VAR H1 X,Y,S	1.2079223E-02	6.6653597E-03	1.8744573E-02
VAR L1 X,Y,S	1.2038279E-02	6.5159923E-03	1.8554291E-02
VAR H0 X,Y,S	1.2042022E-02	6.6777952E-03	1.8719839E-02
VAR L0 X,Y,S	1.1955025E-02	6.5173762E-03	1.8472390E-02
VAR H3 X,Y,S	1.2856302E-02	1.0325875E-02	2.3182228E-02

INTEGRATED SQUARED DEVIATION FROM DIF SPECTRA

DIF H1 A,C,S	2.3363722E-03	1.5902841E-03	3.9266543E-03
DIF L1 A,C,S	2.4134463E-03	1.5732005E-03	3.9866548E-03
DIF H0 A,C,S	2.3173015E-03	1.5806175E-03	3.8979221E-03
DIF L0 A,C,S	2.3860694E-03	1.5498431E-03	3.9359359E-03
DIF H3 A,C,S	1.9596560E-03	2.1567922E-03	4.1164388E-03
DIF H1 X,Y,S	1.5902841E-03	2.3363722E-03	3.9266543E-03
DIF L1 X,Y,S	1.5732005E-03	2.4134463E-03	3.9866548E-03
DIF H0 X,Y,S	1.5806175E-03	2.3173017E-03	3.8979221E-03
DIF L0 X,Y,S	1.5498430E-03	2.3860994E-03	3.9359359E-03
DIF H3 X,Y,S	2.1567822E-03	1.9596568E-03	4.1164388E-03

CASE19.DAT

PARAMETERS

1.200000	3.7500001E-02	64.00000	56789.00
12.00000	0.0000000E+00	135.0000	64.00000
53.20000	0.0000000E+00	0.0000000E+00	100.0000
1.337000	1.0200000E-09	99999.00	99999.00

MAGNITUDE ARRAY SCALING FACTORS

H1(0,0),HIGH,FACTOR	0.9648941	2.2538722E-02	19.29796
L1(0,0),HIGH,FACTOR	0.9742209	2.2283187E-02	19.51926
H0(0,0),HIGH,FACTOR	1.150338	2.0418724E-02	21.30160
L0(0,0),HIGH,FACTOR	1.345093	1.8045209E-02	24.10343
H3(0,0),HIGH,FACTOR	0.8012733	2.3601868E-02	18.36643

INTEGRATED VARIANCE FROM POWER SPECTRA

VAR S0 A,C,S	1.0649079E-02	6.3450006E-03	1.6994022E-02
VAR H1 A,C,S	1.2474400E-02	7.6932698E-03	2.0167669E-02
VAR L1 A,C,S	1.2479660E-02	7.6789404E-03	2.0158570E-02
VAR H0 A,C,S	1.2479561E-02	7.7030440E-03	2.0182589E-02
VAR L0 A,C,S	1.2548639E-02	7.7522821E-03	2.0300908E-02
VAR H3 A,C,S	1.4522227E-02	8.8069327E-03	2.3329204E-02

VAR S0 X,Y,S	8.4970063E-03	8.4970193E-03	1.6994022E-02
VAR H1 X,Y,S	1.4785443E-02	5.3822407E-03	2.0167669E-02
VAR L1 X,Y,S	1.4756318E-02	5.4022390E-03	2.0158570E-02
VAR H0 X,Y,S	1.4776551E-02	5.4060584E-03	2.0182589E-02
VAR L0 X,Y,S	1.4800604E-02	5.5003101E-03	2.0300908E-02
VAR H3 X,Y,S	1.6795227E-02	6.5339315E-03	2.3329204E-02

INTEGRATED SQUARED DEVIATION FROM DIF SPECTRA

DIF H1 A,C,S	1.8731877E-03	1.4374180E-03	3.3106050E-03
DIF L1 A,C,S	1.8732058E-03	1.4293230E-03	3.3025315E-03
DIF H0 A,C,S	1.8729613E-03	1.4318327E-03	3.3047905E-03
DIF L0 A,C,S	1.8812079E-03	1.4233622E-03	3.3045667E-03
DIF H3 A,C,S	2.2386448E-03	1.5873470E-03	3.8259998E-03

DIF H1 X,Y,S	1.5446621E-03	1.7659459E-03	3.3106050E-03
DIF L1 X,Y,S	1.5611843E-03	1.7413460E-03	3.3025315E-03
DIF H0 X,Y,S	1.5606490E-03	1.7441447E-03	3.3047905E-03
DIF L0 X,Y,S	1.6254581E-03	1.6791188E-03	3.3045667E-03
DIF H3 X,Y,S	2.2777887E-03	1.5482103E-03	3.8259998E-03

CASE20.DAT

PARAMETERS

1.200000	3.7500001E-02	64.00000	56789.00
12.00000	0.0000000E+00	135.0000	64.00000
53.20000	45.00000	53.20000	9.885000
1.337000	1.0200000E-09	99999.00	99999.00

MAGNITUDE ARRAY SCALING FACTORS

H1(0,0),HIGH,FACTOR	0.6355228	1.3683862E-02	31.78572
L1(0,0),HIGH,FACTOR	0.6677608	1.6001366E-02	27.18214
H0(0,0),HIGH,FACTOR	0.7412856	1.2737983E-02	34.14602
L0(0,0),HIGH,FACTOR	0.8792865	1.3757907E-02	31.61465
H3(0,0),HIGH,FACTOR	0.5824110	1.4671355E-02	29.64630

INTEGRATED VARIANCE FROM POWER SPECTRA

VAR S0 A,C,S	1.0649079E-02	6.3450006E-03	1.6994022E-02
VAR H1 A,C,S	1.2057226E-02	2.1421649E-02	3.3478897E-02
VAR L1 A,C,S	1.1195125E-02	1.8774049E-02	2.9969225E-02
VAR H0 A,C,S	1.2661862E-02	2.2619950E-02	3.5281815E-02
VAR L0 A,C,S	1.2477761E-02	2.1447405E-02	3.3925273E-02
VAR H3 A,C,S	1.2326711E-02	1.9706136E-02	3.2032907E-02

VAR S0 X,Y,S	8.4970063E-03	8.4970193E-03	1.6994022E-02
VAR H1 X,Y,S	1.7619681E-02	1.5859196E-02	3.3478897E-02
VAR L1 X,Y,S	1.6960656E-02	1.3008592E-02	2.9969225E-02
VAR H0 X,Y,S	1.7647941E-02	1.7633874E-02	3.5281815E-02
VAR L0 X,Y,S	1.7689530E-02	1.6235739E-02	3.3925273E-02
VAR H3 X,Y,S	1.7909454E-02	1.4123423E-02	3.2032907E-02

INTEGRATED SQUARED DEVIATION FROM DIF SPECTRA

DIF H1 A,C,S	2.8754934E-03	5.2791261E-03	8.1546092E-03
DIF L1 A,C,S	2.6323230E-03	4.1007013E-03	6.7330245E-03
DIF H0 A,C,S	3.0046252E-03	5.8535952E-03	8.8582272E-03
DIF L0 A,C,S	2.8276551E-03	5.2893898E-03	8.1170527E-03
DIF H3 A,C,S	2.4958027E-03	4.5361225E-03	7.0319348E-03

DIF H1 X,Y,S	4.2035501E-03	3.9510690E-03	8.1546092E-03
DIF L1 X,Y,S	3.6945355E-03	3.0384976E-03	6.7330245E-03
DIF H0 X,Y,S	4.3325434E-03	4.5256848E-03	8.8582272E-03
DIF L0 X,Y,S	4.1513611E-03	3.9656814E-03	8.1170527E-03
DIF H3 X,Y,S	3.8882589E-03	3.1436733E-03	7.0319348E-03

```
CASE21.DAT

PARAMETERS
 1.200000     3.7500001E-02  64.00000      56789.00
 12.60000     0.0000000E+00  135.0000      64.00000
 53.20000      90.00000      53.20000      9.885000
 1.337000     1.0200000E-09  99999.00      99999.00

MAGNITUDE ARRAY SCALING FACTORS
H1(0,0),HIGH,FACTOR  0.2329347      5.8767921E-03   74.01170
L1(0,0),HIGH,FACTOR  0.2533004      7.5043021E-03   57.96027
H0(0,0),HIGH,FACTOR  0.3386976      4.7378102E-03   91.80431
L0(0,0),HIGH,FACTOR  0.4648261      5.2006384E-03   83.63423
H3(0,0),HIGH,FACTOR  0.2058222      6.3799699E-03   68.17452

INTEGRATED VARIANCE FROM POWER SPECTRA
VAR S0 A,C,S  1.0649079E-02  6.3450006E-03  1.6994022E-02
VAR H1 A,C,S  1.2446433E-02  1.0162100E-02  2.2608571E-02
VAR L1 A,C,S  1.2796094E-02  9.8636970E-03  2.2659810E-02
VAR H0 A,C,S  1.2450058E-02  1.0752472E-02  2.3202548E-02
VAR L0 A,C,S  1.3418423E-02  1.1121014E-02  2.4539439E-02
VAR H3 A,C,S  1.4061336E-02  1.0235731E-02  2.4297021E-02

VAR S0 X,Y,S  8.4970063E-03  8.4970193E-03  1.6994022E-02
VAR H1 X,Y,S  1.6339354E-02  6.2691723E-03  2.2608571E-02
VAR L1 X,Y,S  1.6457189E-02  6.2026032E-03  2.2659810E-02
VAR H0 X,Y,S  1.6464541E-02  6.7379852E-03  2.3202548E-02
VAR L0 X,Y,S  1.7317683E-02  7.2217565E-03  2.4539439E-02
VAR H3 X,Y,S  1.7455615E-02  6.8414137E-03  2.4297021E-02

INTEGRATED SQUARED DEVIATION FROM DIF SPECTRA
DIF H1 A,C,S  2.0265912E-03  1.6520832E-03  3.6786739E-03
DIF L1 A,C,S  2.1226627E-03  1.6601700E-03  3.7828344E-03
DIF H0 A,C,S  1.9984301E-03  1.7092113E-03  3.7076403E-03
DIF L0 A,C,S  2.1955555E-03  1.8705010E-03  4.0660524E-03
DIF H3 A,C,S  2.2591690E-03  1.7671263E-03  4.0262924E-03

DIF H1 X,Y,S  2.1440969E-03  1.5345698E-03  3.6786739E-03
DIF L1 X,Y,S  2.2122643E-03  1.5705709E-03  3.7828344E-03
DIF H0 X,Y,S  2.2691835E-03  1.4384583E-03  3.7076403E-03
DIF L0 X,Y,S  2.6596657E-03  1.4063838E-03  4.0660524E-03
DIF H3 X,Y,S  2.5249876E-03  1.5013057E-03  4.0262924E-03
```

```
CASE22.DAT

PARAMETERS
 1.200000     3.7500001E-02  64.00000      56789.00
 12.00000     0.0000000E+00  135.0000      64.00000
 53.20000      135.0000      53.20000      9.885000
 1.337000     1.0200000E-09  99999.00      99999.00

MAGNITUDE ARRAY SCALING FACTORS
H1(0,0),HIGH,FACTOR  0.3381905      1.1072428E-02   39.28239
L1(0,0),HIGH,FACTOR  0.3508317      1.2275639E-02   35.43208
H0(0,0),HIGH,FACTOR  0.4439534      9.8857451E-03   43.99784
L0(0,0),HIGH,FACTOR  0.5623575      9.9033313E-03   43.91970
H3(0,0),HIGH,FACTOR  0.3103007      1.1537363E-02   37.69938

INTEGRATED VARIANCE FROM POWER SPECTRA
VAR S0 A,C,S  1.0649079E-02  6.3450006E-03  1.6994022E-02
VAR H1 A,C,S  1.3081426E-02  5.3527490E-03  1.8434161E-02
VAR L1 A,C,S  1.3048702E-02  5.6150239E-03  1.8663706E-02
VAR H0 A,C,S  1.3149981E-02  5.1518916E-03  1.8301897E-02
VAR L0 A,C,S  1.3204739E-02  5.3008976E-03  1.8505668E-02
VAR H3 A,C,S  1.4240128E-02  6.0125897E-03  2.0252723E-02

VAR S0 X,Y,S  8.4970063E-03  8.4970193E-03  1.6994022E-02
VAR H1 X,Y,S  1.2601698E-02  5.8324579E-03  1.8434161E-02
VAR L1 X,Y,S  1.2922759E-02  5.7409564E-03  1.8663706E-02
VAR H0 X,Y,S  1.2330793E-02  5.9710727E-03  1.8301897E-02
VAR L0 X,Y,S  1.2504511E-02  6.0011218E-03  1.8505668E-02
VAR H3 X,Y,S  1.3805350E-02  6.4473688E-03  2.0252723E-02

INTEGRATED SQUARED DEVIATION FROM DIF SPECTRA
DIF H1 A,C,S  1.2266146E-03  1.2517134E-03  2.4783262E-03
DIF L1 A,C,S  1.3284029E-03  1.2567517E-03  2.5851582E-03
DIF H0 A,C,S  1.1627851E-03  1.2346046E-03  2.3973873E-03
DIF L0 A,C,S  1.2279828E-03  1.2081020E-03  2.4360823E-03
DIF H3 A,C,S  1.5181506E-03  1.1926471E-03  2.7107988E-03

DIF H1 X,Y,S  9.3429571E-04  1.5440327E-03  2.4783262E-03
DIF L1 X,Y,S  1.0195884E-03  1.5655711E-03  2.5851582E-03
DIF H0 X,Y,S  9.0629433E-04  1.4910952E-03  2.3973873E-03
DIF L0 X,Y,S  9.8367140E-04  1.4524100E-03  2.4360823E-03
DIF H3 X,Y,S  1.2933828E-03  1.4174134E-03  2.7107988E-03
```

```
CASE23.DAT

PARAMETERS
 1.200000     3.7500001E-02   64.00000     56789.00
 12.00000     0.0000000E+00   135.0000     64.00000
 53.20000     180.0000        53.20000     9.885000
 1.337000     1.0200000E-09   99999.00     99999.00

MAGNITUDE ARRAY SCALING FACTORS
H1(0,0),HIGH,FACTOR  0.4576920     1.2644354E-02   34.39886
L1(0,0),HIGH,FACTOR  0.4668326     1.3780513E-02   31.56279
H0(0,0),HIGH,FACTOR  0.5634549     1.1457671E-02   37.96159
L0(0,0),HIGH,FACTOR  0.6783584     1.1407901E-02   38.12721
H3(0,0),HIGH,FACTOR  0.4254104     1.3032638E-02   33.37401

INTEGRATED VARIANCE FROM POWER SPECTRA
VAR S0 A,C,S  1.0649079E-02  6.3450006E-03  1.6994022E-02
VAR H1 A,C,S  1.2577793E-02  7.7209668E-03  2.0298755E-02
VAR L1 A,C,S  1.2657330E-02  7.7422662E-03  2.0399585E-02
VAR H0 A,C,S  1.2543903E-02  7.7075084E-03  2.0251391E-02
VAR L0 A,C,S  1.2630225E-02  7.7414624E-03  2.0371718E-02
VAR H3 A,C,S  1.4049080E-02  8.4563708E-03  2.2505350E-02

VAR S0 X,Y,S  8.4970063E-03  8.4970193E-03  1.6994022E-02
VAR H1 X,Y,S  1.4935043E-02  5.3637377E-03  2.0298755E-02
VAR L1 X,Y,S  1.4994601E-02  5.4050204E-03  2.0399585E-02
VAR H0 X,Y,S  1.4890510E-02  5.3608851E-03  2.0251391E-02
VAR L0 X,Y,S  1.4948195E-02  5.4234979E-03  2.0371718E-02
VAR H3 X,Y,S  1.6330823E-02  6.1745332E-03  2.2505350E-02

INTEGRATED SQUARED DEVIATION FROM DIF SPECTRA
DIF H1 A,C,S  1.3788996E-03  1.4762604E-03  3.3551580E-03
DIF L1 A,C,S  1.8932822E-03  1.4735786E-03  3.3668624E-03
DIF H0 A,C,S  1.3746982E-03  1.4673908E-03  3.3420858E-03
DIF L0 A,C,S  1.3925290E-03  1.4586583E-03  3.3511850E-03
DIF H3 A,C,S  2.1329643E-03  1.5583459E-03  3.6913105E-03

DIF H1 X,Y,S  1.5232764E-03  1.8318817E-03  3.3551580E-03
DIF L1 X,Y,S  1.5574906E-03  1.8093709E-03  3.3668624E-03
DIF H0 X,Y,S  1.5223671E-03  1.8197218E-03  3.3420858E-03
DIF L0 X,Y,S  1.5740301E-03  1.7771572E-03  3.3511850E-03
DIF H3 X,Y,S  2.0438512E-03  1.6474589E-03  3.6913105E-03
```

```
CASE24.DAT

PARAMETERS
 1.200000     3.7500001E-02   64.00000     56789.00
 12.00000     0.0000000E+00   135.0000     64.00000
 53.20000     0.0000000E+00   53.20000     9.885000
 1.337000     1.0200000E-09   99999.00     99999.00

MAGNITUDE ARRAY SCALING FACTORS
H1(0,0),HIGH,FACTOR  1.718323     3.3154391E-02   13.11897
L1(0,0),HIGH,FACTOR  1.773826     3.7351359E-02   11.64486
H0(0,0),HIGH,FACTOR  1.824086     3.1971715E-02   13.60426
L0(0,0),HIGH,FACTOR  1.985352     3.4982521E-02   12.43339
H3(0,0),HIGH,FACTOR  1.949976     3.5597853E-02   12.21847

INTEGRATED VARIANCE FROM POWER SPECTRA
VAR S0 A,C,S  1.0649079E-02  6.3450006E-03  1.6994022E-02
VAR H1 A,C,S  1.5164242E-02  8.9362729E-03  2.4100466E-02
VAR L1 A,C,S  1.4530931E-02  8.4992275E-03  2.3030173E-02
VAR H0 A,C,S  1.5278570E-02  8.9961477E-03  2.4274705E-02
VAR L0 A,C,S  1.4670216E-02  8.5604219E-03  2.3230599E-02
VAR H3 A,C,S  2.2099258E-02  1.3050897E-02  3.5150152E-02

VAR S0 X,Y,S  8.4970063E-03  8.4970193E-03  1.6994022E-02
VAR H1 X,Y,S  1.7226977E-02  6.8735303E-03  2.4100466E-02
VAR L1 X,Y,S  1.6579771E-02  6.4503993E-03  2.3030173E-02
VAR H0 X,Y,S  1.7318444E-02  6.9562807E-03  2.4274705E-02
VAR L0 X,Y,S  1.6677121E-02  6.5535214E-03  2.3230599E-02
VAR H3 X,Y,S  2.2277975E-02  1.2872167E-02  3.5150152E-02

INTEGRATED SQUARED DEVIATION FROM DIF SPECTRA
DIF H1 A,C,S  2.0341277E-03  1.5854259E-03  3.6195528E-03
DIF L1 A,C,S  1.9333727E-03  1.5347890E-03  3.4681619E-03
DIF H0 A,C,S  2.0487618E-03  1.5878789E-03  3.6366410E-03
DIF L0 A,C,S  1.9412483E-03  1.5298044E-03  3.4710560E-03
DIF H3 A,C,S  3.8419475E-03  2.4770389E-03  6.3189911E-03

DIF H1 X,Y,S  2.1349054E-03  1.4846519E-03  3.6195528E-03
DIF L1 X,Y,S  1.9075609E-03  1.5606011E-03  3.4681619E-03
DIF H0 X,Y,S  2.1678414E-03  1.4687984E-03  3.6366410E-03
DIF L0 X,Y,S  1.9396804E-03  1.5313755E-03  3.4710560E-03
DIF H3 X,Y,S  4.2822739E-03  2.0367103E-03  6.3189911E-03
```

CASE25.DAT

```
PARAMETERS
 1.200000      3.7500001E-02   64.00000      56789.00
 60.00000      0.0000000E+00   0.0000000E+00   64.00000
 53.20000      0.0000000E+00   0.0000000E+00   100.0000
 1.337000      1.0200000E-09   99999.00      99999.00

MAGNITUDE ARRAY SCALING FACTORS
H1(0,0),HIGH,FACTOR  0.9273533      5.8624996E-03   94.74679
L1(0,0),HIGH,FACTOR  0.9720474      5.6511504E-03   98.29025
H0(0,0),HIGH,FACTOR   1.108595      6.7353207E-03   82.46868
L0(0,0),HIGH,FACTOR   1.334532      1.2614572E-02   44.03265
H3(0,0),HIGH,FACTOR  0.9492382      1.9311747E-02   28.76244

INTEGRATED VARIANCE FROM POWER SPECTRA
VAR S0 A,C,S  3.9197806E-02  2.3548655E-02  6.2746458E-02
VAR H1 A,C,S  9.7741470E-02  4.5564171E-02  0.1433059
VAR L1 A,C,S  9.0582393E-02  4.0327933E-02  0.1309104
VAR H0 A,C,S  9.3708426E-02  4.0718209E-02  0.1344265
VAR L0 A,C,S  5.2038904E-02  1.7553739E-02  6.9592565E-02
VAR H3 A,C,S  0.1370472      9.4082139E-02  0.2311293

VAR S0 X,Y,S  3.9197806E-02  2.3548655E-02  6.2746458E-02
VAR H1 X,Y,S  9.7741470E-02  4.5564171E-02  0.1433059
VAR L1 X,Y,S  9.0582393E-02  4.0327933E-02  0.1309104
VAR H0 X,Y,S  9.3708426E-02  4.0718209E-02  0.1344265
VAR L0 X,Y,S  5.2938904E-02  1.7553739E-02  6.9592565E-02
VAR H3 X,Y,S  0.1370472      9.4082139E-02  0.2311293

INTEGRATED SQUARED DEVIATION FROM DIF SPECTRA
DIF H1 A,C,S  2.5031963E-02  7.6490906E-03  3.2681040E-02
DIF L1 A,C,S  1.9655135E-02  5.7003810E-03  2.5365550E-02
DIF H0 A,C,S  2.0931663E-02  5.8132303E-03  2.6744921E-02
DIF L0 A,C,S  4.1576964E-03  2.6929409E-03  6.8506435E-03
DIF H3 A,C,S  4.3148708E-02  3.2640681E-02  7.5789206E-02

DIF H1 X,Y,S  2.5031963E-02  7.6490996E-03  3.2681040E-02
DIF L1 X,Y,S  1.9655135E-02  5.7003810E-03  2.5365550E-02
DIF H0 X,Y,S  2.0931663E-02  5.8132303E-03  2.6744921E-02
DIF L0 X,Y,S  4.1576964E-03  2.6929409E-03  6.8506435E-03
DIF H3 X,Y,S  4.3148798E-02  3.2640681E-02  7.5789206E-02
```

CASE26.DAT

```
PARAMETERS
 1.200000      3.7500001E-02   64.00000      56789.00
 60.00000      0.0000000E+00   0.0000000E+00   64.00000
 53.20000       45.00000       53.20000      9.885000
 1.337000      1.0200000E-09   99999.00      99999.00

MAGNITUDE ARRAY SCALING FACTORS
H1(0,0),HIGH,FACTOR  0.5894849      1.4269713E-02   38.92531
L1(0,0),HIGH,FACTOR  0.6465675      1.4882816E-02   37.32177
H0(0,0),HIGH,FACTOR  0.6944247      1.3427813E-02   41.36586
L0(0,0),HIGH,FACTOR  0.6564470      1.3203467E-02   42.06872
H3(0,0),HIGH,FACTOR  0.6071439      2.4026804E-02   23.11806

INTEGRATED VARIANCE FROM POWER SPECTRA
VAR S0 A,C,S  3.9197806E-02  2.3548655E-02  6.2746458E-02
VAR H1 A,C,S  3.3124074E-02  4.0562354E-02  7.3686332E-02
VAR L1 A,C,S  3.2562204E-02  4.0115342E-02  7.2677612E-02
VAR H0 A,C,S  3.6189917E-02  4.5407683E-02  8.1597589E-02
VAR L0 A,C,S  4.0980197E-02  5.0730448E-02  9.1710791E-02
VAR H3 A,C,S  4.8804887E-02  4.1850913E-02  9.0655819E-02

VAR S0 X,Y,S  3.9197806E-02  2.3548655E-02  6.2746458E-02
VAR H1 X,Y,S  3.3124074E-02  4.0562354E-02  7.3686332E-02
VAR L1 X,Y,S  3.2562204E-02  4.0115342E-02  7.2677612E-02
VAR H0 X,Y,S  3.6189917E-02  4.5407683E-02  8.1597589E-02
VAR L0 X,Y,S  4.0980197E-02  5.0730448E-02  9.1710791E-02
VAR H3 X,Y,S  4.8804887E-02  4.1850913E-02  9.0655819E-02

INTEGRATED SQUARED DEVIATION FROM DIF SPECTRA
DIF H1 A,C,S  5.9182160E-03  4.9372646E-03  1.0855496E-02
DIF L1 A,C,S  5.9207538E-03  4.8246882E-03  1.0745448E-02
DIF H0 A,C,S  5.9944531E-03  6.1575142E-03  1.2151985E-02
DIF L0 A,C,S  6.2110359E-03  7.9053584E-03  1.4116383E-02
DIF H3 A,C,S  7.4260924E-03  6.8695792E-03  1.4295688E-02

DIF H1 X,Y,S  5.9182160E-03  4.9372646E-03  1.0855498E-02
DIF L1 X,Y,S  5.9207538E-03  4.8246882E-03  1.0745448E-02
DIF H0 X,Y,S  5.9944531E-03  6.1575142E-03  1.2151985E-02
DIF L0 X,Y,S  6.2110359E-03  7.9053584E-03  1.4116383E-02
DIF H3 X,Y,S  7.4260924E-03  6.8695792E-03  1.4295688E-02
```

```
CASE27.DAT

PARAMETERS
 1.200000        3.7500001E-02   64.00000        56789.00
 60.00000        0.0000000E+00   0.0000000E+00   64.00000
 53.20000         90.00000       53.20000        9.885000
 1.337000        1.0200000E-09   99999.00        99999.00

MAGNITUDE ARRAY SCALING FACTORS
H1(0,0),HIGH,FACTOR  0.2468761       2.5686375E-03   216.2442
L1(0,0),HIGH,FACTOR  0.2882640       2.9682522E-03   187.1313
H0(0,0),HIGH,FACTOR  0.3518159       3.3398822E-03   166.3092
L0(0,0),HIGH,FACTOR  0.4981435       5.5835275E-03   99.48066
H3(0,0),HIGH,FACTOR  0.2282159       5.8940407E-03   94.23976

INTEGRATED VARIANCE FROM POWER SPECTRA
VAR S0 A,C,S  3.9197806E-02  2.3548655E-02  6.2746458E-02
VAR H1 A,C,S  6.5042593E-02  6.1779581E-02  0.1268222
VAR L1 A,C,S  5.4490086E-02  5.6783099E-02  0.1112735
VAR H0 A,C,S  6.6251434E-02  4.3985810E-02  0.1102372
VAR L0 A,C,S  5.2103356E-02  2.5900764E-02  7.8004196E-02
VAR H3 A,C,S  0.1126230      7.6469347E-02  0.1890924

VAR S0 X,Y,S  3.9197806E-02  2.3548655E-02  6.2746458E-02
VAR H1 X,Y,S  6.5042593E-02  6.1779581E-02  0.1268222
VAR L1 X,Y,S  5.4490086E-02  5.6783099E-02  0.1112735
VAR H0 X,Y,S  6.6251434E-02  4.3985810E-02  0.1102372
VAR L0 X,Y,S  5.2103356E-02  2.5900764E-02  7.8004196E-02
VAR H3 X,Y,S  0.1126230      7.6469347E-02  0.1890924

INTEGRATED SQUARED DEVIATION FROM DIF SPECTRA
DIF H1 A,C,S  1.1847564E-02  1.4425768E-02  2.6273319E-02
DIF L1 A,C,S  9.3972906E-03  1.2195912E-02  2.1593204E-02
DIF H0 A,C,S  9.6537685E-03  7.7358340E-03  1.7389590E-02
DIF L0 A,C,S  5.1601045E-03  3.7955195E-03  8.9556267E-03
DIF H3 A,C,S  2.9326528E-02  2.2957630E-02  5.2284252E-02

DIF H1 X,Y,S  1.1847564E-02  1.4425768E-02  2.6273319E-02
DIF L1 X,Y,S  9.3972906E-03  1.2195912E-02  2.1593204E-02
DIF H0 X,Y,S  9.6537685E-03  7.7358340E-03  1.7389590E-02
DIF L0 X,Y,S  5.1601045E-03  3.7955195E-03  8.9556267E-03
DIF H3 X,Y,S  2.9326528E-02  2.2957630E-02  5.2284252E-02
```

```
CASE28.DAT

PARAMETERS
 1.200000        3.7500001E-02   64.00000        56789.00
 60.00000        0.0000000E+00   0.0000000E+00   64.00000
 53.20000         135.0000       53.20000        9.885000
 1.337000        1.0200000E-09   99999.00        99999.00

MAGNITUDE ARRAY SCALING FACTORS
H1(0,0),HIGH,FACTOR  0.3120794       3.5045424E-03   158.4952
L1(0,0),HIGH,FACTOR  0.3429015       3.1275579E-03   177.5996
H0(0,0),HIGH,FACTOR  0.4170192       3.0371838E-03   182.8842
L0(0,0),HIGH,FACTOR  0.5527810       5.0889873E-03   109.1480
H3(0,0),HIGH,FACTOR  0.3234790       1.0991149E-02   50.95362

INTEGRATED VARIANCE FROM POWER SPECTRA
VAR S0 A,C,S  3.9197806E-02  2.3548655E-02  6.2746459E-02
VAR H1 A,C,S  6.4175986E-02  4.0676013E-02  0.1048520
VAR L1 A,C,S  7.1016520E-02  4.5425445E-02  0.1164419
VAR H0 A,C,S  7.5869337E-02  5.2499790E-02  0.1283690
VAR L0 A,C,S  4.2559907E-02  2.2385295E-02  6.4945213E-02
VAR H3 A,C,S  7.6284960E-02  4.7607768E-02  0.1238929

VAR S0 X,Y,S  3.9197806E-02  2.3548655E-02  6.2746458E-02
VAR H1 X,Y,S  6.4175986E-02  4.0676013E-02  0.1048520
VAR L1 X,Y,S  7.1016520E-02  4.5425445E-02  0.1164419
VAR H0 X,Y,S  7.5869337E-02  5.2499790E-02  0.1283690
VAR L0 X,Y,S  4.2559907E-02  2.2385295E-02  6.4945213E-02
VAR H3 X,Y,S  7.6284960E-02  4.7607768E-02  0.1238929

INTEGRATED SQUARED DEVIATION FROM DIF SPECTRA
DIF H1 A,C,S  9.8184776E-03  5.4872185E-03  1.5305679E-02
DIF L1 A,C,S  1.2118548E-02  6.9576045E-03  1.9076185E-02
DIF H0 A,C,S  1.4724582E-02  9.1596805E-03  2.3884283E-02
DIF L0 A,C,S  5.0698435E-03  2.7301686E-03  7.8000198E-03
DIF H3 A,C,S  1.3772319E-02  9.5384624E-03  2.3310764E-02

DIF H1 X,Y,S  9.8184776E-03  5.4872185E-03  1.5305679E-02
DIF L1 X,Y,S  1.2118548E-02  6.9576045E-03  1.9076185E-02
DIF H0 X,Y,S  1.4724582E-02  9.1596805E-03  2.3884283E-02
DIF L0 X,Y,S  5.0698435E-03  2.7301686E-03  7.8000198E-03
DIF H3 X,Y,S  1.3772319E-02  9.5384624E-03  2.3310764E-02
```

CASE29.DAT

PARAMETERS

1.200000	3.7500001E-02	64.00000	56789.
60.00000	0.0000000E+00	0.0000000E+00	64.
53.20000	180.0000	53.20000	9.8
1.337000	1.0200000E-09	99999.00	999

MAGNITUDE ARRAY SCALING FACTORS

H1(0,0),HIGH,FACTOR	0.4029414	4.5045316E-03	125.3098
L1(0,0),HIGH,FACTOR	0.4291545	4.0044119E-03	138.7103
H0(0,0),HIGH,FACTOR	0.5078812	3.6818879E-03	150.8609
L0(0,0),HIGH,FACTOR	0.6390342	3.4096909E-03	162.9042
H3(0,0),HIGH,FACTOR	0.4364834	1.3238719E-02	41.95670

INTEGRATED VARIANCE FROM POWER SPECTRA

VAR S0 A,C,S	3.9197806E-02	2.3548655E-02	6.2746458E-02
VAR H1 A,C,S	7.5474553E-02	3.0962927E-02	0.1064375
VAR L1 A,C,S	8.3650619E-02	3.5928752E-02	0.1195794
VAR H0 A,C,S	8.7784559E-02	4.0736794E-02	0.1285213
VAR L0 A,C,S	0.1072620	5.0374527E-02	0.1576364
VAR H3 A,C,S	8.9100286E-02	5.2696194E-02	0.1417964
VAR S0 X,Y,S	3.9197806E-02	2.3548655E-02	6.2746458E-02
VAR H1 X,Y,S	7.5474553E-02	3.0962927E-02	0.1064375
VAR L1 X,Y,S	8.3650619E-02	3.5928752E-02	0.1195794
VAR H0 X,Y,S	8.7784559E-02	4.0736794E-02	0.1285213
VAR L0 X,Y,S	0.1072620	5.0374527E-02	0.1576364
VAR H3 X,Y,S	8.9100286E-02	5.2696194E-02	0.1417964

INTEGRATED SQUARED DEVIATION FROM DIF SPECTRA

DIF H1 A,C,S	1.3058504E-02	3.5532389E-03	1.6611731E-02
DIF L1 A,C,S	1.6280742E-02	4.7883056E-03	2.1069014E-02
DIF H0 A,C,S	2.0605642E-02	6.2149307E-03	2.6820576E-02
DIF L0 A,C,S	2.8159866E-02	9.2800101E-03	3.7439838E-02
DIF H3 A,C,S	1.8331535E-02	1.1802287E-02	3.0133776E-02
DIF H1 X,Y,S	1.3058504E-02	3.5532389E-03	1.6611731E-02
DIF L1 X,Y,S	1.6280742E-02	4.7883056E-03	2.1069014E-02
DIF H0 X,Y,S	2.0605642E-02	6.2149307E-03	2.6820576E-02
DIF L0 X,Y,S	2.8159866E-02	9.2800101E-03	3.7439838E-02
DIF H3 X,Y,S	1.8331535E-02	1.1802287E-02	3.0133776E-02

CASE30.DAT

PARAMETERS

1.200000	3.7500001E-02	64.00000	56789.00
60.00000	0.0000000E+00	0.0000000E+00	64.00000
53.20000	0.0000000E+00	53.20000	9.885000
1.337000	1.0200000E-09	99999.00	99999.00

MAGNITUDE ARRAY SCALING FACTORS

H1(0,0),HIGH,FACTOR	1.159265	1.7324189E-02	32.06228
L1(0,0),HIGH,FACTOR	1.238066	1.8274236E-02	30.39541
H0(0,0),HIGH,FACTOR	1.264205	1.6175989E-02	34.33812
L0(0,0),HIGH,FACTOR	1.447946	1.6027214E-02	34.65686
H3(0,0),HIGH,FACTOR	1.528120	4.5147933E-02	12.30296

INTEGRATED VARIANCE FROM POWER SPECTRA

VAR S0 A,C,S	3.9197806E-02	2.3548655E-02	6.2746458E-02
VAR H1 A,C,S	6.5950297E-02	2.8206835E-02	9.4157174E-02
VAR L1 A,C,S	6.5326504E-02	2.7649645E-02	9.2976190E-02
VAR H0 A,C,S	6.8586290E-02	3.0690106E-02	9.9276260E-02
VAR L0 A,C,S	7.0767589E-02	3.2647740E-02	0.1034153
VAR H3 A,C,S	7.6551653E-02	3.9498415E-02	0.1160499
VAR S0 X,Y,S	3.9197806E-02	2.3548655E-02	6.2746458E-02
VAR H1 X,Y,S	6.5950297E-02	2.8206835E-02	9.4157174E-02
VAR L1 X,Y,S	6.5326504E-02	2.7649645E-02	9.2976190E-02
VAR H0 X,Y,S	6.8586290E-02	3.0690106E-02	9.9276260E-02
VAR L0 X,Y,S	7.0767589E-02	3.2647740E-02	0.1034153
VAR H3 X,Y,S	7.6551653E-02	3.9498415E-02	0.1160499

INTEGRATED SQUARED DEVIATION FROM DIF SPECTRA

DIF H1 A,C,S	9.7940862E-03	3.0024901E-03	1.2796566E-02
DIF L1 A,C,S	9.3775941E-03	2.9089910E-03	1.2286601E-02
DIF H0 A,C,S	1.1351245E-02	3.4467203E-03	1.4797980E-02
DIF L0 A,C,S	1.2535381E-02	3.8518833E-03	1.6387267E-02
DIF H3 A,C,S	1.3710412E-02	6.1443602E-03	1.9854786E-02
DIF H1 X,Y,S	9.7940862E-03	3.0024901E-03	1.2796566E-02
DIF L1 X,Y,S	9.3775941E-03	2.9089910E-03	1.2286601E-02
DIF H0 X,Y,S	1.1351245E-02	3.4467203E-03	1.4797980E-02
DIF L0 X,Y,S	1.2535381E-02	3.8518833E-03	1.6387267E-02
DIF H3 X,Y,S	1.3710412E-02	6.1443602E-03	1.9854786E-02

CASE31.DAT

PARAMETERS

1.200000	3.7500001E-02	64.00000	56789.00
60.00000	0.0000000E+00	45.00000	64.00000
53.20000	0.0000000E+00	0.0000000E+00	100.0000
1.337000	1.0200000E-09	99999.00	99999.00

MAGNITUDE ARRAY SCALING FACTORS

H1(0,0),HIGH,FACTOR	0.9621119	6.0443743E-03	100.2137
L1(0,0),HIGH,FACTOR	0.9965774	4.7523417E-03	127.4590
H0(0,0),HIGH,FACTOR	1.143609	5.8417576E-03	103.6895
L0(0,0),HIGH,FACTOR	1.359572	1.0445863E-02	57.98745
H3(0,0),HIGH,FACTOR	0.9714906	2.0316185E-02	29.81509

INTEGRATED VARIANCE FROM POWER SPECTRA

VAR S0 A,C,S	3.9235316E-02	2.3511158E-02	6.2746525E-02
VAR H1 A,C,S	8.5413337E-02	6.9903858E-02	0.1553171
VAR L1 A,C,S	0.1040368	8.2555898E-02	0.1865927
VAR H0 A,C,S	9.6223243E-02	7.4296872E-02	0.1705142
VAR L0 A,C,S	4.4956453E-02	2.9915985E-02	7.4872285E-02
VAR H3 A,C,S	0.1223952	0.1082555	0.2306513
VAR S0 X,Y,S	3.1373270E-02	3.1373236E-02	6.2746525E-02
VAR H1 X,Y,S	9.9381961E-02	5.5935159E-02	0.1553171
VAR L1 X,Y,S	0.1167732	6.9819696E-02	0.1865927
VAR H0 X,Y,S	0.1080948	6.2419403E-02	0.1705142
VAR L0 X,Y,S	5.0221730E-02	2.4659579E-02	7.4872285E-02
VAR H3 X,Y,S	0.1341004	9.6550584E-02	0.2306513

INTEGRATED SQUARED DEVIATION FROM DIF SPECTRA

DIF H1 A,C,S	1.9824209E-02	1.9650375E-02	3.9474554E-02
DIF L1 A,C,S	2.7437326E-02	2.6592355E-02	5.4029696E-02
DIF H0 A,C,S	2.3558598E-02	2.2382353E-02	4.5940958E-02
DIF L0 A,C,S	5.8570397E-03	5.0078938E-03	1.0864952E-02
DIF H3 A,C,S	3.5794158E-02	4.1642286E-02	7.7436522E-02
DIF H1 X,Y,S	2.9248286E-02	1.0226246E-02	3.9474554E-02
DIF L1 X,Y,S	3.9052676E-02	1.4977101E-02	5.4029696E-02
DIF H0 X,Y,S	3.4126863E-02	1.1814054E-02	4.5940958E-02
DIF L0 X,Y,S	6.6316333E-03	4.2333077E-03	1.0864952E-02
DIF H3 X,Y,S	4.7165561E-02	3.0270882E-02	7.7436522E-02

CASE32.DAT

PARAMETERS

1.200000	3.7500001E-02	64.00000	56789.00
60.00000	0.0000000E+00	45.00000	64.00000
53.20000	45.00000	53.20000	9.885000
1.337000	1.0200000E-09	99999.00	99999.00

MAGNITUDE ARRAY SCALING FACTORS

H1(0,0),HIGH,FACTOR	0.6255851	1.6330251E-02	37.09244
L1(0,0),HIGH,FACTOR	0.6809896	1.7139293E-02	35.34153
H0(0,0),HIGH,FACTOR	0.7306808	1.5334897E-02	39.50003
L0(0,0),HIGH,FACTOR	0.8911809	1.5767585E-02	38.41609
H3(0,0),HIGH,FACTOR	0.6380583	2.7766220E-02	21.81532

INTEGRATED VARIANCE FROM POWER SPECTRA

VAR S0 A,C,S	3.9235316E-02	2.3511158E-02	6.2746525E-02
VAR H1 A,C,S	4.6890285E-02	2.7928263E-02	7.4818403E-02
VAR L1 A,C,S	4.6768826E-02	2.6484529E-02	7.3253438E-02
VAR H0 A,C,S	4.7472551E-02	3.3868797E-02	8.1341363E-02
VAR L0 A,C,S	4.4735041E-02	3.5925560E-02	8.0660492E-02
VAR H3 A,C,S	6.3173421E-02	3.3194270E-02	9.6367553E-02
VAR S0 X,Y,S	3.1373270E-02	3.1373236E-02	6.2746525E-02
VAR H1 X,Y,S	2.6738722E-02	4.8079710E-02	7.4818403E-02
VAR L1 X,Y,S	2.6290711E-02	4.6954710E-02	7.3253438E-02
VAR H0 X,Y,S	2.8803688E-02	5.2537631E-02	8.1341363E-02
VAR L0 X,Y,S	2.8778536E-02	5.1882058E-02	8.0660492E-02
VAR H3 X,Y,S	4.4412062E-02	5.1955476E-02	9.6367553E-02

INTEGRATED SQUARED DEVIATION FROM DIF SPECTRA

DIF H1 A,C,S	4.4948384E-03	3.2808841E-03	7.7757179E-03
DIF L1 A,C,S	4.3185819E-03	3.1237775E-03	7.4423687E-03
DIF H0 A,C,S	5.1085963E-03	4.2404160E-03	9.3490062E-03
DIF L0 A,C,S	5.0026742E-03	4.5636697E-03	9.5663415E-03
DIF H3 A,C,S	6.7753885E-03	4.8398757E-03	1.1615276E-02
DIF H1 X,Y,S	4.0122750E-03	3.7634587E-03	7.7757179E-03
DIF L1 X,Y,S	3.9631501E-03	3.4792100E-03	7.4423687E-03
DIF H0 X,Y,S	4.2480240E-03	5.1009869E-03	9.3490062E-03
DIF L0 X,Y,S	4.3309461E-03	5.2353991E-03	9.5663415E-03
DIF H3 X,Y,S	5.4955482E-03	6.1197085E-03	1.1615276E-02

CASE33.DAT

PARAMETERS

1.200000	3.7500001E-02	64.00000	56789.00
60.00000	0.0000000E+00	45.00000	64.00000
53.20000	90.00000	53.20000	9.885000
1.337000	1.0200000E-09	99999.00	99999.00

MAGNITUDE ARRAY SCALING FACTORS

H1(0,0),HIGH,FACTOR	0.2598848	2.1182687E-03	285.9547
L1(0,0),HIGH,FACTOR	0.2974848	2.4818366E-03	244.0648
H0(0,0),HIGH,FACTOR	0.3649804	3.0709964E-03	197.2418
L0(0,0),HIGH,FACTOR	0.5076761	4.5816670E-03	132.2071
H3(0,0),HIGH,FACTOR	0.2389007	6.4186505E-03	94.37014

INTEGRATED VARIANCE FROM POWER SPECTRA

VAR S0 A,C,S	3.9235316E-02	2.3511158E-02	6.2746525E-02
VAR H1 A,C,S	0.1050620	8.8117555E-02	0.1931807
VAR L1 A,C,S	9.1455705E-02	7.1840094E-02	0.1633037
VAR H0 A,C,S	5.4556007E-02	5.5758692E-02	0.1103246
VAR L0 A,C,S	3.8610999E-02	4.1046299E-02	7.9657316E-02
VAR H3 A,C,S	0.1070286	8.2931802E-02	0.1899605

VAR S0 X,Y,S	3.1373270E-02	3.1373236E-02	6.2746525E-02
VAR H1 X,Y,S	9.3411572E-02	9.9769108E-02	0.1931807
VAR L1 X,Y,S	7.7531569E-02	8.5771956E-02	0.1633037
VAR H0 X,Y,S	6.0201392E-02	5.0123371E-02	0.1103246
VAR L0 X,Y,S	4.8622258E-02	3.1035131E-02	7.9657316E-02
VAR H3 X,Y,S	0.1075170	8.2443513E-02	0.1899605

INTEGRATED SQUARED DEVIATION FROM DIF SPECTRA

DIF H1 A,C,S	2.5611673E-02	2.8034693E-02	5.3646434E-02
DIF L1 A,C,S	1.8818287E-02	1.9505888E-02	3.8324215E-02
DIF H0 A,C,S	8.8497894E-03	1.2113719E-02	2.0963509E-02
DIF L0 A,C,S	6.2658614E-03	6.4775315E-03	1.2743392E-02
DIF H3 A,C,S	2.5954157E-02	2.6180815E-02	5.2135006E-02

DIF H1 X,Y,S	2.5459429E-02	2.8186992E-02	5.3646434E-02
DIF L1 X,Y,S	1.7649775E-02	2.0674407E-02	3.8324215E-02
DIF H0 X,Y,S	1.1496628E-02	9.4669042E-03	2.0963509E-02
DIF L0 X,Y,S	6.9567533E-03	5.7866424E-03	1.2743392E-02
DIF H3 X,Y,S	3.0808825E-02	2.1326132E-02	5.2135006E-02

CASE34.DAT

PARAMETERS

1.200000	3.7500001E-02	64.00000	56789.00
60.00000	0.0000000E+00	45.00000	64.00000
53.20000	135.0000	53.20000	9.885000
1.337000	1.0200000E-09	99999.00	99999.00

MAGNITUDE ARRAY SCALING FACTORS

H1(0,0),HIGH,FACTOR	0.3286527	4.3000062E-03	140.8670
L1(0,0),HIGH,FACTOR	0.3555836	4.2145676E-03	143.7227
H0(0,0),HIGH,FACTOR	0.4337483	3.7998403E-03	159.4090
L0(0,0),HIGH,FACTOR	0.5657750	4.3222089E-03	140.1434
H3(0,0),HIGH,FACTOR	0.3359067	1.0231853E-02	59.20031

INTEGRATED VARIANCE FROM POWER SPECTRA

VAR S0 A,C,S	3.9235316E-02	2.3511158E-02	6.2746525E-02
VAR H1 A,C,S	4.9008753E-02	6.5288939E-02	0.1142977
VAR L1 A,C,S	4.9714219E-02	6.6834122E-02	0.1165482
VAR H0 A,C,S	6.5647051E-02	6.1864577E-02	0.1275117
VAR L0 A,C,S	6.3585125E-02	4.0110089E-02	0.1036952
VAR H3 A,C,S	6.8250097E-02	7.5453207E-02	0.1437033

VAR S0 X,Y,S	3.1373270E-02	3.1373236E-02	6.2746525E-02
VAR H1 X,Y,S	6.0197864E-02	5.4999858E-02	0.1142977
VAR L1 X,Y,S	6.3646480E-02	5.2901864E-02	0.1165482
VAR H0 X,Y,S	5.8926005E-02	6.8585746E-02	0.1275117
VAR L0 X,Y,S	4.8839383E-02	5.4855932E-02	0.1036952
VAR H3 X,Y,S	8.6116895E-02	5.7586260E-02	0.1437633

INTEGRATED SQUARED DEVIATION FROM DIF SPECTRA

DIF H1 A,C,S	7.6029864E-03	1.4095031E-02	2.1698026E-02
DIF L1 A,C,S	8.1197983E-03	1.4885928E-02	2.3005718E-02
DIF H0 A,C,S	8.6946338E-03	1.2936196E-02	2.1630863E-02
DIF L0 A,C,S	6.8893256E-03	5.8294912E-03	1.2718819E-02
DIF H3 A,C,S	1.4161595E-02	2.1726476E-02	3.5888098E-02

DIF H1 X,Y,S	1.2257195E-02	9.4408067E-03	2.1698026E-02
DIF L1 X,Y,S	1.3467896E-02	9.5378216E-03	2.3005718E-02
DIF H0 X,Y,S	1.0400996E-02	1.1229847E-02	2.1630863E-02
DIF L0 X,Y,S	6.8665138E-03	5.8522895E-03	1.2718819E-02
DIF H3 X,Y,S	2.2264501E-02	1.3623569E-02	3.5888098E-02

CASE35.DAT

PARAMETERS

1.200000	3.7500001E-02	64.00000	56789.00
60.00000	0.0000000E+00	45.00000	64.00000
53.20000	180.0000	53.20000	9.885000
1.337000	1.0200000E-09	99999.00	99999.00

MAGNITUDE ARRAY SCALING FACTORS

H1(0,0),HIGH,FACTOR	0.4223123	5.1191803E-03	118.3254
L1(0,0),HIGH,FACTOR	0.4456466	5.2172765E-03	116.1006
H0(0,0),HIGH,FACTOR	0.5274080	3.9918926E-03	151.7398
L0(0,0),HIGH,FACTOR	0.6558380	3.2330176E-03	187.3571
H3(0,0),HIGH,FACTOR	0.4511395	1.3186130E-02	45.93682

INTEGRATED VARIANCE FROM POWER SPECTRA

VAR S0 A,C,S	3.9235316E-02	2.3511158E-02	6.2746525E-02
VAR H1 A,C,S	6.1300684E-02	4.8174240E-02	0.1094749
VAR L1 A,C,S	5.7166379E-02	4.5541279E-02	0.1027076
VAR H0 A,C,S	7.4146517E-02	5.9910361E-02	0.1340576
VAR L0 A,C,S	9.8796599E-02	7.8358844E-02	0.1771557
VAR H3 A,C,S	8.5651226E-02	7.1000554E-02	0.1566519
VAR S0 X,Y,S	3.1373270E-02	3.1373236E-02	6.2746525E-02
VAR H1 X,Y,S	7.4933864E-02	3.4540925E-02	0.1094749
VAR L1 X,Y,S	7.0258707E-02	3.2448940E-02	0.1027076
VAR H0 X,Y,S	8.7915689E-02	4.6141218E-02	0.1340579
VAR L0 X,Y,S	0.1121249	6.5030515E-02	0.1771557
VAR H3 X,Y,S	9.5835447E-02	6.0816549E-02	0.1566519

INTEGRATED SQUARED DEVIATION FROM DIF SPECTRA

DIF H1 A,C,S	1.0894313E-02	1.0116485E-02	2.1010809E-02
DIF L1 A,C,S	9.8538697E-03	9.1157882E-03	1.8969649E-02
DIF H0 A,C,S	1.5493823E-02	1.5077713E-02	3.0571524E-02
DIF L0 A,C,S	2.5187775E-02	2.4549024E-02	4.9736746E-02
DIF H3 A,C,S	1.7953616E-02	2.0665651E-02	3.8619310E-02
DIF H1 X,Y,S	1.5581101E-02	5.4297205E-03	2.1010809E-02
DIF L1 X,Y,S	1.3694853E-02	5.2748160E-03	1.8969649E-02
DIF H0 X,Y,S	2.3082923E-02	7.4886112E-03	3.0571524E-02
DIF L0 X,Y,S	3.6516260E-02	1.3220568E-02	4.9736746E-02
DIF H3 X,Y,S	2.4870556E-02	1.3748758E-02	3.8619310E-02

CASE36.DAT

PARAMETERS

1.200000	3.7500001E-02	64.00000	56789.00
60.00000	0.0000000E+00	45.00000	64.00000
53.20000	0.0000000E+00	53.20000	9.885000
1.337000	1.0200000E-09	99999.00	99999.00

MAGNITUDE ARRAY SCALING FACTORS

H1(0,0),HIGH,FACTOR	1.210453	1.8328948E-02	33.04766
L1(0,0),HIGH,FACTOR	1.288554	1.9428257E-02	31.17773
H0(0,0),HIGH,FACTOR	1.315548	1.7045917E-02	35.53513
L0(0,0),HIGH,FACTOR	1.498745	1.6871074E-02	35.90340
H3(0,0),HIGH,FACTOR	1.579957	4.4608247E-02	13.57886

INTEGRATED VARIANCE FROM POWER SPECTRA

VAR S0 A,C,S	3.9235316E-02	2.3511158E-02	6.2746525E-02
VAR H1 A,C,S	5.6786552E-02	4.4092510E-02	0.1008789
VAR L1 A,C,S	5.5940866E-02	4.3501206E-02	9.9442236E-02
VAR H0 A,C,S	5.9770368E-02	4.6842393E-02	0.1066128
VAR L0 A,C,S	6.1936982E-02	4.8961360E-02	0.1108983
VAR H3 A,C,S	6.7592032E-02	5.4695588E-02	0.1222876
VAR S0 X,Y,S	3.1373270E-02	3.1373236E-02	6.2746525E-02
VAR H1 X,Y,S	6.7204595E-02	3.3674352E-02	0.1008789
VAR L1 X,Y,S	6.6567779E-02	3.2874260E-02	9.9442236E-02
VAR H0 X,Y,S	6.9962718E-02	3.6649898E-02	0.1066128
VAR L0 X,Y,S	7.2044820E-02	3.8853548E-02	0.1108983
VAR H3 X,Y,S	7.7590324E-02	4.4697247E-02	0.1222876

INTEGRATED SQUARED DEVIATION FROM DIF SPECTRA

DIF H1 A,C,S	8.9125957E-03	8.5863099E-03	1.7498905E-02
DIF L1 A,C,S	8.6913276E-03	8.3428733E-03	1.7034223E-02
DIF H0 A,C,S	9.6998829E-03	9.5601389E-03	1.9260047E-02
DIF L0 A,C,S	1.0287875E-02	1.0302716E-02	2.0590642E-02
DIF H3 A,C,S	1.1378060E-02	1.2651021E-02	2.4029057E-02
DIF H1 X,Y,S	1.2516121E-02	4.9827583E-03	1.7498905E-02
DIF L1 X,Y,S	1.2093929E-02	4.9402853E-03	1.7034223E-02
DIF H0 X,Y,S	1.3980604E-02	5.2794069E-03	1.9260047E-02
DIF L0 X,Y,S	1.4995794E-02	5.5947881E-03	2.0590642E-02
DIF H3 X,Y,S	1.6545562E-02	7.4835196E-03	2.4029057E-02

CASE37.DAT

PARAMETERS

1.200000	3.7500001E-02	64.00000	56789.00
60.00000	0.0000000E+00	90.00000	64.00000
53.20000	0.0000000E+00	0.0000000E+00	100.0000
1.337000	1.0200000E-09	99999.00	99999.00

MAGNITUDE ARRAY SCALING FACTORS

H1(0,0),HIGH,FACTOR	1.014915	6.9529316E-03	79.88760
L1(0,0),HIGH,FACTOR	1.040330	5.3715473E-03	103.4065
H0(0,0),HIGH,FACTOR	1.195437	5.5982117E-03	99.21972
L0(0,0),HIGH,FACTOR	1.403373	4.6612527E-03	119.1639
H3(0,0),HIGH,FACTOR	0.9827309	2.6173647E-02	21.22184

INTEGRATED VARIANCE FROM POWER SPECTRA

VAR S0 A,C,S	3.9197750E-02	2.3548668E-02	6.2746502E-02
VAR H1 A,C,S	4.5189317E-02	6.5274857E-02	0.1104640
VAR L1 A,C,S	5.6384034E-02	7.8228109E-02	0.1346122
VAR H0 A,C,S	5.9818812E-02	8.3116300E-02	0.1429352
VAR L0 A,C,S	7.8886442E-02	0.1138920	0.1927782
VAR H3 A,C,S	4.2269852E-02	5.7646729E-02	9.9916525E-02

VAR S0 X,Y,S	2.3548666E-02	3.9197750E-02	6.2746502E-02
VAR H1 X,Y,S	6.5274857E-02	4.5189321E-02	0.1104640
VAR L1 X,Y,S	7.8228109E-02	5.6384038E-02	0.1346122
VAR H0 X,Y,S	8.3116300E-02	5.9818808E-02	0.1429352
VAR L0 X,Y,S	0.1138920	7.8886442E-02	0.1927782
VAR H3 X,Y,S	5.7646729E-02	4.2269852E-02	9.9916525E-02

INTEGRATED SQUARED DEVIATION FROM DIF SPECTRA

DIF H1 A,C,S	7.3338477E-03	1.7199839E-02	2.4533655E-02
DIF L1 A,C,S	9.9001387E-03	2.4624147E-02	3.4524292E-02
DIF H0 A,C,S	1.0930142E-02	2.8055647E-02	3.8985766E-02
DIF L0 A,C,S	1.7047880E-02	4.5483440E-02	6.2531278E-02
DIF H3 A,C,S	8.8947844E-03	1.3472479E-02	2.2367224E-02

DIF H1 X,Y,S	1.7199839E-02	7.3338482E-03	2.4533655E-02
DIF L1 X,Y,S	2.4624147E-02	9.9001387E-03	3.4524292E-02
DIF H0 X,Y,S	2.8055646E-02	1.0930141E-02	3.8985766E-02
DIF L0 X,Y,S	4.5483444E-02	1.7047880E-02	6.2531278E-02
DIF H3 X,Y,S	1.3472479E-02	8.8947844E-03	2.2367224E-02

CASE38.DAT

PARAMETERS

1.200000	3.7500001E-02	64.00000	56789.00
60.00000	0.0000000E+00	90.00000	64.00000
53.20000	45.00000	53.20000	9.885000
1.337000	1.0200000E-09	99999.00	99999.00

MAGNITUDE ARRAY SCALING FACTORS

H1(0,0),HIGH,FACTOR	0.7042264	2.1802938E-02	25.47606
L1(0,0),HIGH,FACTOR	0.7599957	2.2388529E-02	24.80971
H0(0,0),HIGH,FACTOR	0.8093932	2.1810012E-02	25.46780
L0(0,0),HIGH,FACTOR	0.9703294	2.2402743E-02	24.79397
H3(0,0),HIGH,FACTOR	0.6778143	2.9767817E-02	18.65951

INTEGRATED VARIANCE FROM POWER SPECTRA

VAR S0 A,C,S	3.9197750E-02	2.3548668E-02	6.2746502E-02
VAR H1 A,C,S	3.9737388E-02	1.4534242E-02	5.4271653E-02
VAR L1 A,C,S	4.0062048E-02	1.4783937E-02	5.4845951E-02
VAR H0 A,C,S	3.9397921E-02	1.4033841E-02	5.3431772E-02
VAR L0 A,C,S	3.9414089E-02	1.3807974E-02	5.3222116E-02
VAR H3 A,C,S	4.5634720E-02	2.5410837E-02	7.1045533E-02

VAR S0 X,Y,S	2.3548666E-02	3.9197750E-02	6.2746502E-02
VAR H1 X,Y,S	1.4534242E-02	3.9737388E-02	5.4271653E-02
VAR L1 X,Y,S	1.4783936E-02	4.0062048E-02	5.4845951E-02
VAR H0 X,Y,S	1.4033840E-02	3.9397918E-02	5.3431772E-02
VAR L0 X,Y,S	1.3807974E-02	3.9414089E-02	5.3222116E-02
VAR H3 X,Y,S	2.5410837E-02	4.5634720E-02	7.1045533E-02

INTEGRATED SQUARED DEVIATION FROM DIF SPECTRA

DIF H1 A,C,S	1.9872761E-03	3.3024775E-03	5.2897511E-03
DIF L1 A,C,S	2.1339254E-03	3.3698229E-03	5.5037448E-03
DIF H0 A,C,S	1.7421396E-03	3.2262821E-03	4.9684262E-03
DIF L0 A,C,S	1.6638706E-03	3.2466054E-03	4.9104756E-03
DIF H3 A,C,S	4.7156513E-03	3.5617796E-03	8.2774376E-03

DIF H1 X,Y,S	3.3024775E-03	1.9872761E-03	5.2897511E-03
DIF L1 X,Y,S	3.3698229E-03	2.1339254E-03	5.5037448E-03
DIF H0 X,Y,S	3.2262821E-03	1.7421397E-03	4.9684262E-03
DIF L0 X,Y,S	3.2466056E-03	1.6638706E-03	4.9104756E-03
DIF H3 X,Y,S	3.5617799E-03	4.7156513E-03	8.2774376E-03

```
CASE39.DAT

PARAMETERS
 1.200000      3.7500001E-02  64.00000     56789.00
 60.00000      0.0000000E+00  90.00000     64.00000
 53.20000       90.00000      53.20000     9.885000
 1.337000      1.0200000E-09  99999.00     99999.00

MAGNITUDE ARRAY SCALING FACTORS
H1(0,0),HIGH,FACTOR  0.2902646      3.0600512E-03   181.5175
L1(0,0),HIGH,FACTOR  0.3280184      3.5222711E-03   157.6974
H0(0,0),HIGH,FACTOR  0.3954314      3.5907016E-03   154.6920
L0(0,0),HIGH,FACTOR  0.5383521      4.4783089E-03   124.0296
H3(0,0),HIGH,FACTOR  0.2501593      7.3835081E-03   75.22887

INTEGRATED VARIANCE FROM POWER SPECTRA
VAR S0 A,C,S  3.9197750E-02  2.3548668E-02  6.2746502E-02
VAR H1 A,C,S  8.4206164E-02  4.5169353E-02  0.1293756
VAR L1 A,C,S  7.3721804E-02  3.8913805E-02  0.1126357
VAR H0 A,C,S  6.3736111E-02  3.9179180E-02  0.1029153
VAR L0 A,C,S  5.1156182E-02  3.6305457E-02  8.7461598E-02
VAR H3 A,C,S  5.2767605E-02  5.6367524E-02  0.1091351

VAR S0 X,Y,S  2.3548666E-02  3.9197750E-02  6.2746502E-02
VAR H1 X,Y,S  4.5169353E-02  8.4206171E-02  0.1293756
VAR L1 X,Y,S  3.3913805E-02  7.3721804E-02  0.1126357
VAR H0 X,Y,S  3.9179180E-02  6.3736111E-02  0.1029153
VAR L0 X,Y,S  3.6305457E-02  5.1156182E-02  8.7461598E-02
VAR H3 X,Y,S  5.6367524E-02  5.2767605E-02  0.1091351

INTEGRATED SQUARED DEVIATION FROM DIF SPECTRA
DIF H1 A,C,S  1.5071589E-02  7.6907724E-03  2.2762371E-02
DIF L1 A,C,S  1.1251027E-02  5.5608908E-03  1.6811926E-02
DIF H0 A,C,S  9.1129271E-03  6.1779823E-03  1.5290914E-02
DIF L0 A,C,S  6.6813300E-03  5.3744032E-03  1.2055730E-02
DIF H3 A,C,S  9.2101041E-03  1.2306225E-02  2.1516293E-02

DIF H1 X,Y,S  7.6907724E-03  1.5071589E-02  2.2762371E-02
DIF L1 X,Y,S  5.5608908E-03  1.1251027E-02  1.6811926E-02
DIF H0 X,Y,S  6.1779823E-03  9.1129271E-03  1.5290914E-02
DIF L0 X,Y,S  5.3744032E-03  6.6813300E-03  1.2055730E-02
DIF H3 X,Y,S  1.2306225E-02  9.2101041E-03  2.1516293E-02
```

```
CASE40.DAT

PARAMETERS
 1.200000      3.7500001E-02  64.00000     56789.00
 60.00000      0.0000000E+00  90.00000     64.00000
 53.20000       135.0000      53.20000     9.885000
 1.337000      1.0200000E-09  99999.00     99999.00

MAGNITUDE ARRAY SCALING FACTORS
H1(0,0),HIGH,FACTOR  0.3517864      5.3096423E-03   104.6121
L1(0,0),HIGH,FACTOR  0.3779574      5.3783702E-03   103.2753
H0(0,0),HIGH,FACTOR  0.4569533      4.3628574E-03   127.3140
L0(0,0),HIGH,FACTOR  0.5882912      3.6361918E-03   152.7568
H3(0,0),HIGH,FACTOR  0.3433594      1.3040362E-02   42.59491

INTEGRATED VARIANCE FROM POWER SPECTRA
VAR S0 A,C,S  3.9197750E-02  2.3548668E-02  6.2746502E-02
VAR H1 A,C,S  3.7705429E-02  3.2959737E-02  7.0665054E-02
VAR L1 A,C,S  3.6275730E-02  3.5060722E-02  7.1336471E-02
VAR H0 A,C,S  4.8155911E-02  3.4730144E-02  8.2886174E-02
VAR L0 A,C,S  6.1713938E-02  4.3987826E-02  0.1057019
VAR H3 A,C,S  3.2063100E-02  4.0605191E-02  7.2668247E-02

VAR S0 X,Y,S  2.3548666E-02  3.9197750E-02  6.2746502E-02
VAR H1 X,Y,S  3.2959737E-02  3.7705429E-02  7.0665054E-02
VAR L1 X,Y,S  3.5060722E-02  3.6275730E-02  7.1336471E-02
VAR H0 X,Y,S  3.4730148E-02  4.8155908E-02  8.2886174E-02
VAR L0 X,Y,S  4.3987826E-02  6.1713934E-02  0.1057019
VAR H3 X,Y,S  4.0605191E-02  3.2063100E-02  7.2668247E-02

INTEGRATED SQUARED DEVIATION FROM DIF SPECTRA
DIF H1 A,C,S  5.2545122E-03  5.0617922E-03  1.0316323E-02
DIF L1 A,C,S  5.8025699E-03  5.4794350E-03  1.1282013E-02
DIF H0 A,C,S  4.3040086E-03  5.1088110E-03  9.4128232E-03
DIF L0 A,C,S  6.3969051E-03  7.9746293E-03  1.4371535E-02
DIF H3 A,C,S  7.5465995E-03  7.0341467E-03  1.4580738E-02

DIF H1 X,Y,S  5.0617922E-03  5.2545122E-03  1.0316323E-02
DIF L1 X,Y,S  5.4794350E-03  5.8025699E-03  1.1282013E-02
DIF H0 X,Y,S  5.1088110E-03  4.3040086E-03  9.4128232E-03
DIF L0 X,Y,S  7.9746293E-03  6.3969051E-03  1.4371535E-02
DIF H3 X,Y,S  7.0341467E-03  7.5465995E-03  1.4580738E-02
```

```
CASE41.DAT

PARAMETERS
 1.200000       3.7500001E-02   64.00000     56789.00
 60.00000       0.0000000E+00   90.00000     64.00000
 53.20000        180.0000       53.20000     9.885000
 1.337000       1.0200000E-09   99999.00     99999.00

MAGNITUDE ARRAY SCALING FACTORS
H1(0,0),HIGH,FACTOR  0.4508024      5.7330262E-03   96.88653
L1(0,0),HIGH,FACTOR  0.4721721      5.9106438E-03   93.97504
H0(0,0),HIGH,FACTOR  0.5559694      4.5804321E-03   121.2665
L0(0,0),HIGH,FACTOR  0.6825058      3.6556330E-03   151.9444
H3(0,0),HIGH,FACTOR  0.4597161      1.4531134E-02   38.22503

INTEGRATED VARIANCE FROM POWER SPECTRA
VAR S0 A,C,S  3.9197750E-02  2.3548668E-02  6.2746502E-02
VAR H1 A,C,S  3.0908570E-02  5.1483624E-02  8.2392305E-02
VAR L1 A,C,S  3.0995654E-02  5.2157864E-02  8.3153382E-02
VAR H0 A,C,S  3.6297858E-02  5.6583390E-02  9.2881508E-02
VAR L0 A,C,S  4.7812212E-02  7.0089296E-02  0.1179016
VAR H3 A,C,S  3.6605757E-02  5.4495901E-02  9.1101691E-02

VAR S0 X,Y,S  2.3548666E-02  3.9197750E-02  6.2746502E-02
VAR H1 X,Y,S  5.1483624E-02  3.0908572E-02  8.2392365E-02
VAR L1 X,Y,S  5.2157864E-02  3.0995654E-02  8.3153382E-02
VAR H0 X,Y,S  5.6583390E-02  3.6297858E-02  9.2881508E-02
VAR L0 X,Y,S  7.0089296E-02  4.7812212E-02  0.1179016
VAR H3 X,Y,S  5.4495901E-02  3.6605757E-02  9.1101691E-02

INTEGRATED SQUARED DEVIATION FROM DIF SPECTRA
DIF H1 A,C,S  6.8817963E-03  9.6851252E-03  1.6566923E-02
DIF L1 A,C,S  6.9883033E-03  9.7055528E-03  1.6693849E-02
DIF H0 A,C,S  6.7129722E-03  1.2850733E-02  1.9563708E-02
DIF L0 A,C,S  8.2504489E-03  2.0348720E-02  2.8599132E-02
DIF H3 A,C,S  8.2379738E-03  1.1345840E-02  1.9583818E-02

DIF H1 X,Y,S  9.6851252E-03  6.8817954E-03  1.6566923E-02
DIF L1 X,Y,S  9.7055528E-03  6.9883023E-03  1.6693849E-02
DIF H0 X,Y,S  1.2850733E-02  6.7129717E-03  1.9563708E-02
DIF L0 X,Y,S  2.0348720E-02  8.2504479E-03  2.8599132E-02
DIF H3 X,Y,S  1.1345840E-02  8.2379738E-03  1.9583818E-02
```

```
CASE42.DAT

PARAMETERS
 1.200000       3.7500001E-02   64.00000     56789.00
 60.00000       0.0000000E+00   90.00000     64.00000
 53.20000       0.0000000E+00   53.20000     9.885000
 1.337000       1.0200000E-09   99999.00     99999.00

MAGNITUDE ARRAY SCALING FACTORS
H1(0,0),HIGH,FACTOR   1.279023      1.9490402E-02   28.49880
L1(0,0),HIGH,FACTOR   1.356384      2.0852182E-02   26.63764
H0(0,0),HIGH,FACTOR   1.384190      1.8343739E-02   36.28025
L0(0,0),HIGH,FACTOR   1.566718      1.8549705E-02   29.94403
H3(0,0),HIGH,FACTOR   1.614009      4.2860251E-02   12.95963

INTEGRATED VARIANCE FROM POWER SPECTRA
VAR S0 A,C,S  3.9197750E-02  2.3548668E-02  6.2746502E-02
VAR H1 A,C,S  3.0496554E-02  4.5965850E-02  7.6462589E-02
VAR L1 A,C,S  2.9871946E-02  4.5693219E-02  7.5565264E-02
VAR H0 A,C,S  3.1964581E-02  4.6871118E-02  7.8835532E-02
VAR L0 A,C,S  3.2619074E-02  4.7265410E-02  7.9884544E-02
VAR H3 A,C,S  3.6881376E-02  5.5162832E-02  9.2044286E-02

VAR S0 X,Y,S  2.3548666E-02  3.9197750E-02  6.2746502E-02
VAR H1 X,Y,S  4.5965850E-02  3.0496556E-02  7.6462589E-02
VAR L1 X,Y,S  4.5693219E-02  2.9871946E-02  7.5565264E-02
VAR H0 X,Y,S  4.6871118E-02  3.1964581E-02  7.8835532E-02
VAR L0 X,Y,S  4.7265410E-02  3.2619074E-02  7.9884544E-02
VAR H3 X,Y,S  5.5162836E-02  3.6881376E-02  9.2044286E-02

INTEGRATED SQUARED DEVIATION FROM DIF SPECTRA
DIF H1 A,C,S  6.7044087E-03  7.9095867E-03  1.4613987E-02
DIF L1 A,C,S  6.7819082E-03  7.6160985E-03  1.4397994E-02
DIF H0 A,C,S  6.5908544E-03  8.4724575E-03  1.5063323E-02
DIF L0 A,C,S  6.5660910E-03  8.6222952E-03  1.5188391E-02
DIF H3 A,C,S  7.4604466E-03  1.1387363E-02  1.8847823E-02

DIF H1 X,Y,S  7.9095867E-03  6.7044087E-03  1.4613987E-02
DIF L1 X,Y,S  7.6160980E-03  6.7819082E-03  1.4397994E-02
DIF H0 X,Y,S  8.4724575E-03  6.5908544E-03  1.5063323E-02
DIF L0 X,Y,S  8.6222962E-03  6.5660910E-03  1.5188391E-02
DIF H3 X,Y,S  1.1387364E-02  7.4604466E-03  1.8847823E-02
```

```
CASE43.DAT

PARAMETERS
 1.200000       3.7500001E-02  64.00000       56789.00
 60.00000       0.0000000E+00  135.0000       64.00000
 53.20000       0.0000000E+00  0.0000000E+00  100.0000
 1.337000       1.0200000E-09  99999.00       99999.00

MAGNITUDE ARRAY SCALING FACTORS
H1(0,0),HIGH,FACTOR  0.9644604    6.0477504E-03   100.1577
L1(0,0),HIGH,FACTOR  0.9977144    4.7524720E-03   127.4555
H0(0,0),HIGH,FACTOR   1.145888    5.6085116E-03   108.0017
L0(0,0),HIGH,FACTOR   1.360579    8.6066881E-03   70.37886
H3(0,0),HIGH,FACTOR  0.9634795    2.7588138E-02   21.95614

INTEGRATED VARIANCE FROM POWER SPECTRA
VAR S0 A,C,S  3.9235324E-02  2.3511153E-02  6.2746540E-02
VAR H1 A,C,S  8.0069893E-02  7.2346963E-02  0.1604165
VAR L1 A,C,S  0.1120533      8.4735818E-02  0.1967889
VAR H0 A,C,S  0.1105317      8.1798628E-02  0.1923299
VAR L0 A,C,S  6.9909692E-02  4.2309232E-02  0.1122187
VAR H3 A,C,S  6.6336840E-02  5.6128416E-02  0.1224654

VAR S0 X,Y,S  3.1373221E-02  3.1373285E-02  6.2746540E-02
VAR H1 X,Y,S  0.1023749      5.8041781E-02  0.1604165
VAR L1 X,Y,S  0.1232555      7.3533140E-02  0.1967889
VAR H0 X,Y,S  0.1214180      7.0912361E-02  0.1923299
VAR L0 X,Y,S  7.4581482E-02  3.7637267E-02  0.1122187
VAR H3 X,Y,S  7.2583653E-02  4.9881533E-02  0.1224654

INTEGRATED SQUARED DEVIATION FROM DIF SPECTRA
DIF H1 A,C,S  2.2059284E-02  2.0775730E-02  4.2834956E-02
DIF L1 A,C,S  3.2275952E-02  2.7250173E-02  5.9526172E-02
DIF H0 A,C,S  3.1003602E-02  2.5558639E-02  5.6562312E-02
DIF L0 A,C,S  1.1974258E-02  7.7757440E-03  1.9749997E-02
DIF H3 A,C,S  1.1858423E-02  1.3477480E-02  2.5335893E-02

DIF H1 X,Y,S  3.1540934E-02  1.1294050E-02  4.2834956E-02
DIF L1 X,Y,S  4.2875111E-02  1.6651921E-02  5.9526172E-02
DIF H0 X,Y,S  4.1397352E-02  1.5164952E-02  5.6562312E-02
DIF L0 X,Y,S  1.4646686E-02  5.1033353E-03  1.9749997E-02
DIF H3 X,Y,S  1.5911007E-02  9.4248001E-03  2.5335893E-02
```

```
CASE44.DAT

PARAMETERS
 1.200000       3.7500001E-02  64.00000       56789.00
 60.00000       0.0000000E+00  135.0000       64.00000
 53.20000       45.00000       53.20000       9.885000
 1.337000       1.0200000E-09  99999.00       99999.00

MAGNITUDE ARRAY SCALING FACTORS
H1(0,0),HIGH,FACTOR  0.6563633    1.8849863E-02   32.13440
L1(0,0),HIGH,FACTOR  0.7138804    1.9422451E-02   31.18705
H0(0,0),HIGH,FACTOR  0.7614262    1.8928031E-02   32.00169
L0(0,0),HIGH,FACTOR  0.9240062    1.9945603E-02   30.36905
H3(0,0),HIGH,FACTOR  0.6476634    2.5048418E-02   24.18232

INTEGRATED VARIANCE FROM POWER SPECTRA
VAR S0 A,C,S  3.9235324E-02  2.3511153E-02  6.2746540E-02
VAR H1 A,C,S  3.6602188E-02  3.7485007E-02  7.4087106E-02
VAR L1 A,C,S  3.6088303E-02  3.7912898E-02  7.4001223E-02
VAR H0 A,C,S  3.9446849E-02  3.4404475E-02  7.3851191E-02
VAR L0 A,C,S  4.0594045E-02  3.1082107E-02  7.1676321E-02
VAR H3 A,C,S  4.2731281E-02  5.4614730E-02  9.7345948E-02

VAR S0 X,Y,S  3.1373221E-02  3.1373285E-02  6.2746540E-02
VAR H1 X,Y,S  2.4054796E-02  5.0032262E-02  7.4087106E-02
VAR L1 X,Y,S  2.3907822E-02  5.0093438E-02  7.4001223E-02
VAR H0 X,Y,S  2.3373080E-02  5.0478106E-02  7.3851191E-02
VAR L0 X,Y,S  2.2340050E-02  4.9336202E-02  7.1676321E-02
VAR H3 X,Y,S  4.1691132E-02  5.5654798E-02  9.7345948E-02

INTEGRATED SQUARED DEVIATION FROM DIF SPECTRA
DIF H1 A,C,S  6.1894190E-03  5.1224078E-03  1.1311817E-02
DIF L1 A,C,S  6.3616587E-03  5.1924003E-03  1.1554053E-02
DIF H0 A,C,S  5.6243655E-03  4.6520531E-03  1.0276408E-02
DIF L0 A,C,S  5.2545643E-03  4.1934829E-03  9.4480189E-03
DIF H3 A,C,S  7.1875346E-03  1.0211359E-02  1.7398888E-02

DIF H1 X,Y,S  5.4937704E-03  5.8180601E-03  1.1311817E-02
DIF L1 X,Y,S  5.6165154E-03  5.9375442E-03  1.1554053E-02
DIF H0 X,Y,S  5.0275442E-03  5.2488730E-03  1.0276408E-02
DIF L0 X,Y,S  4.9030189E-03  4.5450293E-03  9.4480189E-03
DIF H3 X,Y,S  7.5716404E-03  9.8272702E-03  1.7398888E-02
```

CASE45.DAT

PARAMETERS

1.200000	3.7500001E-02	64.00000	56789.00
60.00000	0.0000000E+00	135.0000	64.00000
53.20000	90.00000	53.20000	9.885000
1.337000	1.0200000E-09	99999.00	99999.00

MAGNITUDE ARRAY SCALING FACTORS

H1(0,0),HIGH,FACTOR	0.2764732	4.3352535E-03	139.7217
L1(0,0),HIGH,FACTOR	0.3181050	4.8266877E-03	125.4958
H0(0,0),HIGH,FACTOR	0.3815361	5.2463133E-03	115.4580
L0(0,0),HIGH,FACTOR	0.5282308	7.1965405E-03	84.16946
H3(0,0),HIGH,FACTOR	0.2408674	7.3930700E-03	81.93199

INTEGRATED VARIANCE FROM POWER SPECTRA

VAR S0 A,C,S	3.9235324E-02	2.3511153E-02	6.2746540E-02
VAR H1 A,C,S	5.7363257E-02	3.9168634E-02	9.6531920E-02
VAR L1 A,C,S	5.5166058E-02	3.6478665E-02	9.1644727E-02
VAR H0 A,C,S	5.9837051E-02	2.7602131E-02	8.7439194E-02
VAR L0 A,C,S	5.5034626E-02	2.0541701E-02	7.5576253E-02
VAR H3 A,C,S	6.7575462E-02	6.4217843E-02	0.1317935

VAR S0 X,Y,S	3.1373221E-02	3.1373285E-02	6.2746540E-02
VAR H1 X,Y,S	3.4720883E-02	6.1811004E-02	9.6531920E-02
VAR L1 X,Y,S	3.1966712E-02	5.9678055E-02	9.1644727E-02
VAR H0 X,Y,S	3.7687242E-02	4.9752016E-02	8.7439194E-02
VAR L0 X,Y,S	3.7388057E-02	3.8188241E-02	7.5576253E-02
VAR H3 X,Y,S	7.3791683E-02	5.8001865E-02	0.1317935

INTEGRATED SQUARED DEVIATION FROM DIF SPECTRA

DIF H1 A,C,S	7.9855518E-03	6.7463843E-03	1.4731930E-02
DIF L1 A,C,S	7.6957452E-03	6.1803544E-03	1.3876104E-02
DIF H0 A,C,S	5.8496566E-03	3.3727728E-03	9.2224190E-03
DIF L0 A,C,S	3.9558657E-03	2.5750396E-03	6.5309075E-03
DIF H3 A,C,S	1.1965857E-02	1.5883598E-02	2.7849454E-02

DIF H1 X,Y,S	5.0826883E-03	9.6492562E-03	1.4731930E-02
DIF L1 X,Y,S	5.0724349E-03	8.8036563E-03	1.3876104E-02
DIF H0 X,Y,S	3.7678042E-03	5.4546194E-03	9.2224190E-03
DIF L0 X,Y,S	3.0800046E-03	3.4509012E-03	6.5309075E-03
DIF H3 X,Y,S	1.6341446E-02	1.1508023E-02	2.7849454E-02

CASE46.DAT

PARAMETERS

1.200000	3.7500001E-02	64.00000	56789.00
60.00000	0.0000000E+00	135.0000	64.00000
53.20000	135.0000	53.20000	9.885000
1.337000	1.0200000E-09	99999.00	99999.00

MAGNITUDE ARRAY SCALING FACTORS

H1(0,0),HIGH,FACTOR	0.3305837	3.8802845E-03	156.1043
L1(0,0),HIGH,FACTOR	0.3599336	3.8902366E-03	155.7049
H0(0,0),HIGH,FACTOR	0.4356466	2.7262312E-03	222.1855
L0(0,0),HIGH,FACTOR	0.5700595	2.8539905E-03	212.2393
H3(0,0),HIGH,FACTOR	0.3332355	1.4245982E-02	42.51928

INTEGRATED VARIANCE FROM POWER SPECTRA

VAR S0 A,C,S	3.9235324E-02	2.3511153E-02	6.2746540E-02
VAR H1 A,C,S	6.9990657E-02	3.7103798E-02	0.1070945
VAR L1 A,C,S	6.3975126E-02	3.5636675E-02	9.9611856E-02
VAR H0 A,C,S	9.9026673E-02	7.4242972E-02	0.1732691
VAR L0 A,C,S	8.7486044E-02	8.6918227E-02	0.1744042
VAR H3 A,C,S	5.2485634E-02	3.3552527E-02	8.6038247E-02

VAR S0 X,Y,S	3.1373221E-02	3.1373285E-02	6.2746540E-02
VAR H1 X,Y,S	6.0217552E-02	4.6876889E-02	0.1070945
VAR L1 X,Y,S	5.6941785E-02	4.2670138E-02	9.9611856E-02
VAR H0 X,Y,S	9.3571775E-02	7.9697780E-02	0.1732691
VAR L0 X,Y,S	0.1031918	7.1212366E-02	0.1744042
VAR H3 X,Y,S	5.1000999E-02	3.5029218E-02	8.6038247E-02

INTEGRATED SQUARED DEVIATION FROM DIF SPECTRA

DIF H1 A,C,S	9.0039792E-03	5.2763522E-03	1.4280319E-02
DIF L1 A,C,S	7.6870406E-03	5.1715402E-03	1.2858582E-02
DIF H0 A,C,S	2.2270523E-02	1.9917550E-02	4.2188037E-02
DIF L0 A,C,S	2.0860326E-02	2.6451640E-02	4.7311906E-02
DIF H3 A,C,S	6.2509892E-03	5.4180198E-03	1.1669027E-02

DIF H1 X,Y,S	9.4788177E-03	4.8015020E-03	1.4280319E-02
DIF L1 X,Y,S	8.5954545E-03	4.2631291E-03	1.2858582E-02
DIF H0 X,Y,S	2.5858266E-02	1.6329806E-02	4.2188037E-02
DIF L0 X,Y,S	3.1387404E-02	1.5924517E-02	4.7311906E-02
DIF H3 X,Y,S	6.8672239E-03	4.8018075E-03	1.1669027E-02

```
CASE47.DAT

PARAMETERS
 1.200000       3.7500001E-02  64.00000       56789.00
 60.00000       0.0000000E+00  135.0000       64.00000
 53.20000       180.0000       53.20000       9.885000
 1.337000       1.0200000E-09  99999.00       99999.00

MAGNITUDE ARRAY SCALING FACTORS
H1(0,0),HIGH,FACTOR  0.4237172      4.7737663E-03  126.8870
L1(0,0),HIGH,FACTOR  0.4469672      4.9122730E-03  123.3093
H0(0,0),HIGH,FACTOR  0.5287802      3.8294455E-03  158.1767
L0(0,0),HIGH,FACTOR  0.6570932      3.2215109E-03  188.0264
H3(0,0),HIGH,FACTOR  0.4478621      1.6117226E-02  37.58270

INTEGRATED VARIANCE FROM POWER SPECTRA
VAR S0 A,C,S  3.9235324E-02  2.3511153E-02  6.2746540E-02
VAR H1 A,C,S  6.9921263E-02  5.7302698E-02  0.1272242
VAR L1 A,C,S  6.4745925E-02  5.3303406E-02  0.1180492
VAR H0 A,C,S  8.1152737E-02  6.6467784E-02  0.1476208
VAR L0 A,C,S  0.1029618      7.9722963E-02  0.1826849
VAR H3 A,C,S  5.6721538E-02  4.5701038E-02  0.1024226

VAR S0 X,Y,S  3.1373221E-02  3.1373285E-02  6.2746540E-02
VAR H1 X,Y,S  8.7471075E-02  3.9753027E-02  0.1272242
VAR L1 X,Y,S  8.1157431E-02  3.6891993E-02  0.1180492
VAR H0 X,Y,S  9.7056963E-02  5.0563402E-02  0.1476208
VAR L0 X,Y,S  0.1156321      6.7053065E-02  0.1826849
VAR H3 X,Y,S  6.3618645E-02  3.8803838E-02  0.1024226

INTEGRATED SQUARED DEVIATION FROM DIF SPECTRA
DIF H1 A,C,S  1.4375106E-02  1.3534699E-02  2.7909793E-02
DIF L1 A,C,S  1.2663497E-02  1.1846534E-02  2.4510011E-02
DIF H0 A,C,S  1.9292403E-02  1.7999300E-02  3.7291750E-02
DIF L0 A,C,S  2.8421668E-02  2.4890551E-02  5.3312205E-02
DIF H3 A,C,S  8.7638423E-03  8.9753373E-03  1.7739195E-02

DIF H1 X,Y,S  2.1028444E-02  6.8813562E-03  2.7909793E-02
DIF L1 X,Y,S  1.8100303E-02  6.4097038E-03  2.4510011E-02
DIF H0 X,Y,S  2.8014641E-02  9.2771063E-03  3.7291750E-02
DIF L0 X,Y,S  3.9009310E-02  1.4302905E-02  5.3312205E-02
DIF H3 X,Y,S  1.1329573E-02  6.4096157E-03  1.7739195E-02
```

```
CASE48.DAT

PARAMETERS
 1.200000       3.7500001E-02  64.00000       56789.00
 60.00000       0.0000000E+00  135.0000       64.00000
 53.20000       0.0000000E+00  53.20000       9.885000
 1.337000       1.0200000E-09  99999.00       99999.00

MAGNITUDE ARRAY SCALING FACTORS
H1(0,0),HIGH,FACTOR  1.214504       1.6711012E-02  36.24729
L1(0,0),HIGH,FACTOR  1.292861       1.7679026E-02  34.26257
H0(0,0),HIGH,FACTOR  1.319567       1.5800202E-02  38.33678
L0(0,0),HIGH,FACTOR  1.502987       1.5856480E-02  38.20072
H3(0,0),HIGH,FACTOR  1.572605       4.2102780E-02  14.38691

INTEGRATED VARIANCE FROM POWER SPECTRA
VAR S0 A,C,S  3.9235324E-02  2.3511153E-02  6.2746540E-02
VAR H1 A,C,S  6.8277337E-02  5.1525868E-02  0.1198034
VAR L1 A,C,S  6.7759126E-02  5.1029056E-02  0.1187883
VAR H0 A,C,S  6.9843724E-02  5.2936088E-02  0.1227797
VAR L0 A,C,S  7.0925824E-02  5.3776244E-02  0.1246961
VAR H3 A,C,S  7.9254314E-02  5.7385482E-02  0.1366400

VAR S0 X,Y,S  3.1373221E-02  3.1373285E-02  6.2746540E-02
VAR H1 X,Y,S  7.9927526E-02  3.9875992E-02  0.1198034
VAR L1 X,Y,S  7.9617567E-02  3.9170608E-02  0.1187883
VAR H0 X,Y,S  8.0749080E-02  4.2030390E-02  0.1227797
VAR L0 X,Y,S  8.1227645E-02  4.3468498E-02  0.1246961
VAR H3 X,Y,S  8.6769752E-02  4.9870152E-02  0.1366400

INTEGRATED SQUARED DEVIATION FROM DIF SPECTRA
DIF H1 A,C,S  1.3345358E-02  1.1015781E-02  2.4361162E-02
DIF L1 A,C,S  1.3064545E-02  1.0758821E-02  2.3823369E-02
DIF H0 A,C,S  1.4004637E-02  1.1593582E-02  2.5598235E-02
DIF L0 A,C,S  1.4382414E-02  1.1879852E-02  2.6262311E-02
DIF H3 A,C,S  1.5857097E-02  1.3181894E-02  2.9038986E-02

DIF H1 X,Y,S  1.7828109E-02  6.5330341E-03  2.4361162E-02
DIF L1 X,Y,S  1.7386850E-02  6.4364988E-03  2.3823369E-02
DIF H0 X,Y,S  1.8760119E-02  6.8381280E-03  2.5598235E-02
DIF L0 X,Y,S  1.9193318E-02  7.0689484E-03  2.6262311E-02
DIF H3 X,Y,S  2.0342248E-02  8.6967219E-03  2.9038986E-02
```

CASE49.DAT

PARAMETERS

1.200000	3.7500001E-02	64.00000	56789.00
36.00000	0.0000000E+00	0.0000000E+00	64.00000
53.20000	0.0000000E+00	0.0000000E+00	100.0000
1.337000	1.0200000E-09	99999.00	99999.00

MAGNITUDE ARRAY SCALING FACTORS

H1(0,0),HIGH,FACTOR	0.9919936	1.0226829E-02	42.07218
L1(0,0),HIGH,FACTOR	1.021375	8.0383560E-03	53.52649
H0(0,0),HIGH,FACTOR	1.175502	7.2049345E-03	59.71810
L0(0,0),HIGH,FACTOR	1.388392	3.7794111E-03	113.8445
H3(0,0),HIGH,FACTOR	0.9690911	3.2236971E-02	13.34694

INTEGRATED VARIANCE FROM POWER SPECTRA

VAR S0 A,C,S	2.2875596E-02	1.3741832E-02	3.6617365E-02
VAR H1 A,C,S	2.7738005E-02	9.8730875E-03	3.7611037E-02
VAR L1 A,C,S	3.0132117E-02	1.2109077E-02	4.2241268E-02
VAR H0 A,C,S	3.7174772E-02	1.5638402E-02	5.2813258E-02
VAR L0 A,C,S	8.1552714E-02	4.4856183E-02	0.1264088
VAR H3 A,C,S	2.6457880E-02	1.2447290E-02	3.8905188E-02
VAR S0 X,Y,S	2.2875596E-02	1.3741832E-02	3.6617365E-02
VAR H1 X,Y,S	2.7738005E-02	9.8730875E-03	3.7611037E-02
VAR L1 X,Y,S	3.0132117E-02	1.2109077E-02	4.2241268E-02
VAR H0 X,Y,S	3.7174772E-02	1.5638402E-02	5.2813258E-02
VAR L0 X,Y,S	8.1552714E-02	4.4856183E-02	0.1264088
VAR H3 X,Y,S	2.6457880E-02	1.2447290E-02	3.8905188E-02

INTEGRATED SQUARED DEVIATION FROM DIF SPECTRA

DIF H1 A,C,S	2.3373240E-03	1.6385566E-03	3.9758803E-03
DIF L1 A,C,S	3.2513610E-03	1.6287901E-03	4.8801620E-03
DIF H0 A,C,S	5.2680989E-03	1.8442333E-03	7.1123256E-03
DIF L0 A,C,S	2.7525896E-02	1.2715291E-02	4.0241159E-02
DIF H3 A,C,S	2.5818059E-03	2.0210675E-03	4.6028825E-03
DIF H1 X,Y,S	2.3373240E-03	1.6385566E-03	3.9758803E-03
DIF L1 X,Y,S	3.2513610E-03	1.6287901E-03	4.8801620E-03
DIF H0 X,Y,S	5.2680989E-03	1.8442333E-03	7.1123256E-03
DIF L0 X,Y,S	2.7525896E-02	1.2715291E-02	4.0241159E-02
DIF H3 X,Y,S	2.5818059E-03	2.0210675E-03	4.6028825E-03

CASE50.DAT

PARAMETERS

1.200000	3.7500001E-02	64.00000	56789.00
36.00000	0.0000000E+00	0.0000000E+00	64.00000
53.20000	45.00000	53.20000	9.885000
1.337000	1.0200000E-09	99999.06	99999.00

MAGNITUDE ARRAY SCALING FACTORS

H1(0,0),HIGH,FACTOR	0.6278706	1.4331153E-02	30.02306
L1(0,0),HIGH,FACTOR	0.6820835	1.5297975E-02	28.12562
H0(0,0),HIGH,FACTOR	0.7332069	1.3579370E-02	31.68520
L0(0,0),HIGH,FACTOR	0.8927562	1.3699757E-02	31.40676
H3(0,0),HIGH,FACTOR	0.6164612	2.1685239E-02	19.84138

INTEGRATED VARIANCE FROM POWER SPECTRA

VAR S0 A,C,S	2.2875596E-02	1.3741832E-02	3.6617365E-02
VAR H1 A,C,S	1.8799685E-02	1.9026782E-02	3.7826449E-02
VAR L1 A,C,S	1.9061428E-02	1.8133456E-02	3.7194934E-02
VAR H0 A,C,S	1.8034173E-02	2.0408677E-02	3.8442764E-02
VAR L0 A,C,S	1.7672008E-02	2.0990072E-02	3.8661990E-02
VAR H3 A,C,S	2.7328525E-02	1.8052770E-02	4.5381259E-02
VAR S0 X,Y,S	2.2875596E-02	1.3741832E-02	3.6617365E-02
VAR H1 X,Y,S	1.8799685E-02	1.9026782E-02	3.7826449E-02
VAR L1 X,Y,S	1.9061428E-02	1.8133456E-02	3.7194934E-02
VAR H0 X,Y,S	1.8034173E-02	2.0408677E-02	3.8442764E-02
VAR L0 X,Y,S	1.7672008E-02	2.0990072E-02	3.8661990E-02
VAR H3 X,Y,S	2.7328525E-02	1.8052770E-02	4.5381259E-02

INTEGRATED SQUARED DEVIATION FROM DIF SPECTRA

DIF H1 A,C,S	3.7715081E-03	2.4070079E-03	6.1785025E-03
DIF L1 A,C,S	3.7621958E-03	2.3792775E-03	6.1414777E-03
DIF H0 A,C,S	3.7118474E-03	2.4410449E-03	6.1528822E-03
DIF L0 A,C,S	3.6843063E-03	2.4822147E-03	6.1665196E-03
DIF H3 A,C,S	3.1653997E-03	2.5569673E-03	5.7223723E-03
DIF H1 X,Y,S	3.7715081E-03	2.4070079E-03	6.1785025E-03
DIF L1 X,Y,S	3.7621958E-03	2.3792775E-03	6.1414777E-03
DIF H0 X,Y,S	3.7118474E-03	2.4410449E-03	6.1528822E-03
DIF L0 X,Y,S	3.6843063E-03	2.4822147E-03	6.1665196E-03
DIF H3 X,Y,S	3.1653997E-03	2.5569673E-03	5.7223723E-03

```
CASE51.DAT

PARAMETERS
 1.200000     3.7500001E-02   64.00000        56789.00
 36.00000     0.0000000E+00   0.0000000E+00   64.00000
 53.20000     70.00000        53.20000        9.885000
 1.337000     1.0200000E-09   99999.00        99999.00

MAGNITUDE ARRAY SCALING FACTORS
H1(0,0),HIGH,FACTOR  0.2458206     3.0857385E-03   139.4366
L1(0,0),HIGH,FACTOR  0.2828577     4.0900074E-03   105.1991
H0(0,0),HIGH,FACTOR  0.3511569     1.8517275E-03   232.3587
L0(0,0),HIGH,FACTOR  0.4935304     1.8395105E-03   233.9919
H3(0,0),HIGH,FACTOR  0.2264158     9.3421191E-03   46.05647

INTEGRATED VARIANCE FROM POWER SPECTRA
VAR S0 A,C,S  2.2875596E-02  1.3741832E-02  3.6617365E-02
VAR H1 A,C,S  3.0781027E-02  1.6182270E-02  4.6963383E-02
VAR L1 A,C,S  2.6155148E-02  1.2529409E-02  3.8684562E-02
VAR H0 A,C,S  4.4117637E-02  3.4438588E-02  7.8556113E-02
VAR L0 A,C,S  4.8099041E-02  4.2181652E-02  9.0280809E-02
VAR H3 A,C,S  2.4318743E-02  1.1072905E-02  3.5391659E-02

VAR S0 X,Y,S  2.2875596E-02  1.3741632E-02  3.6617365E-02
VAR H1 X,Y,S  3.0781027E-02  1.6182270E-02  4.6963383E-02
VAR L1 X,Y,S  2.6155148E-02  1.2529409E-02  3.8684562E-02
VAR H0 X,Y,S  4.4117637E-02  3.4438588E-02  7.8556113E-02
VAR L0 X,Y,S  4.8099041E-02  4.2181652E-02  9.0280809E-02
VAR H3 X,Y,S  2.4318743E-02  1.1072905E-02  3.5391659E-02

INTEGRATED SQUARED DEVIATION FROM DIF SPECTRA
DIF H1 A,C,S  3.1030346E-03  2.0351906E-03  5.1382259E-03
DIF L1 A,C,S  2.1644537E-03  1.7119033E-03  3.8763594E-03
DIF H0 A,C,S  8.4576504E-03  7.8005660E-03  1.6258202E-02
DIF L0 A,C,S  1.1178816E-02  1.1307973E-02  2.2486756E-02
DIF H3 A,C,S  2.0141555E-03  1.8592430E-03  3.8734048E-03

DIF H1 X,Y,S  3.1030346E-03  2.0351906E-03  5.1382259E-03
DIF L1 X,Y,S  2.1644537E-03  1.7119033E-03  3.8763594E-03
DIF H0 X,Y,S  8.4576504E-03  7.8005660E-03  1.6258202E-02
DIF L0 X,Y,S  1.1178816E-02  1.1307973E-02  2.2486756E-02
DIF H3 X,Y,S  2.0141555E-03  1.8592430E-03  3.8734048E-03
```

```
CASE52.DAT

PARAMETERS
 1.200000     3.7500001E-02   64.00000        56789.00
 36.00000     0.0000000E+00   0.0000000E+00   64.00000
 53.20000     135.0000        53.20000        9.885000
 1.337000     1.0200000E-09   99999.00        99999.00

MAGNITUDE ARRAY SCALING FACTORS
H1(0,0),HIGH,FACTOR  0.3375495     6.3457675E-03   67.80346
L1(0,0),HIGH,FACTOR  0.3627760     6.9849845E-03   61.59856
H0(0,0),HIGH,FACTOR  0.4428858     4.8048701E-03   89.54769
L0(0,0),HIGH,FACTOR  0.5734487     3.9112358E-03   110.0074
H3(0,0),HIGH,FACTOR  0.3334148     1.3973022E-02   30.79255

INTEGRATED VARIANCE FROM POWER SPECTRA
VAR S0 A,C,S  2.2875596E-02  1.3741832E-02  3.6617365E-02
VAR H1 A,C,S  2.3228347E-02  9.6502230E-03  3.2878507E-02
VAR L1 A,C,S  2.2690920E-02  8.6279567E-03  3.1318933E-02
VAR H0 A,C,S  2.4731116E-02  1.2923197E-02  3.7654337E-02
VAR L0 A,C,S  2.7655602E-02  1.6622925E-02  4.4278629E-02
VAR H3 A,C,S  2.4959991E-02  1.1069224E-02  3.6029186E-02

VAR S0 X,Y,S  2.2875596E-02  1.3741832E-02  3.6617365E-02
VAR H1 X,Y,S  2.3228347E-02  9.6502230E-03  3.2878507E-02
VAR L1 X,Y,S  2.2690920E-02  8.6279567E-03  3.1318933E-02
VAR H0 X,Y,S  2.4731116E-02  1.2923197E-02  3.7654337E-02
VAR L0 X,Y,S  2.7655602E-02  1.6622925E-02  4.4278629E-02
VAR H3 X,Y,S  2.4959991E-02  1.1069224E-02  3.6029186E-02

INTEGRATED SQUARED DEVIATION FROM DIF SPECTRA
DIF H1 A,C,S  2.1472559E-03  2.1110419E-03  4.2582983E-03
DIF L1 A,C,S  1.8792632E-03  2.2672898E-03  4.1465531E-03
DIF H0 A,C,S  2.7653703E-03  1.7531270E-03  4.5184931E-03
DIF L0 A,C,S  3.4181611E-03  1.8812172E-03  5.2993726E-03
DIF H3 A,C,S  2.0962798E-03  1.9215163E-03  4.0177998E-03

DIF H1 X,Y,S  2.1472559E-03  2.1110419E-03  4.2582983E-03
DIF L1 X,Y,S  1.8792632E-03  2.2672898E-03  4.1465531E-03
DIF H0 X,Y,S  2.7653703E-03  1.7531270E-03  4.5184931E-03
DIF L0 X,Y,S  3.4181611E-03  1.8812172E-03  5.2993726E-03
DIF H3 X,Y,S  2.0962798E-03  1.9215163E-03  4.0177998E-03
```

CASE53.DAT

PARAMETERS

1.200000	3.7500001E-02	64.00000	56789.00
36.00000	0.0000000E+00	0.0000000E+00	64.00000
53.20000	180.0000	53.20000	9.885000
1.337000	1.0200000E-09	99999.00	99999.00

MAGNITUDE ARRAY SCALING FACTORS

H1(0,0),HIGH,FACTOR	0.4488286	8.1063444E-03	53.07756
L1(0,0),HIGH,FACTOR	0.4687488	8.8254223E-03	48.75291
H0(0,0),HIGH,FACTOR	0.5541650	6.3570538E-03	67.68300
L0(0,0),HIGH,FACTOR	0.6794215	5.3272257E-03	80.76718
H3(0,0),HIGH,FACTOR	0.4541388	1.8322222E-02	23.48323

INTEGRATED VARIANCE FROM POWER SPECTRA

VAR S0 A,C,S	2.2875596E-02	1.3741832E-02	3.6617365E-02
VAR H1 A,C,S	2.5626143E-02	7.9436274E-03	3.3569779E-02
VAR L1 A,C,S	2.4475290E-02	7.4370434E-03	3.1912349E-02
VAR H0 A,C,S	2.8331993E-02	9.6641919E-03	3.7996173E-02
VAR L0 A,C,S	3.0994585E-02	1.1691522E-02	4.2686116E-02
VAR H3 A,C,S	2.4376977E-02	1.0333366E-02	3.4710389E-02

VAR S0 X,Y,S	2.2875596E-02	1.3741832E-02	3.6617365E-02
VAR H1 X,Y,S	2.5626143E-02	7.9436274E-03	3.3569779E-02
VAR L1 X,Y,S	2.4475290E-02	7.4370434E-03	3.1912349E-02
VAR H0 X,Y,S	2.8331993E-02	9.6641919E-03	3.7996173E-02
VAR L0 X,Y,S	3.0994585E-02	1.1691522E-02	4.2686116E-02
VAR H3 X,Y,S	2.4376977E-02	1.0333366E-02	3.4710389E-02

INTEGRATED SQUARED DEVIATION FROM DIF SPECTRA

DIF H1 A,C,S	1.5849394E-03	2.0581731E-03	3.6431155E-03
DIF L1 A,C,S	1.3911274E-03	2.2197051E-03	3.6108340E-03
DIF H0 A,C,S	2.3139163E-03	1.6631188E-03	3.9770352E-03
DIF L0 A,C,S	3.1956227E-03	1.5316515E-03	4.7272728E-03
DIF H3 A,C,S	1.9061875E-03	1.8810238E-03	3.7872111E-03

DIF H1 X,Y,S	1.5849394E-03	2.0581731E-03	3.6431155E-03
DIF L1 X,Y,S	1.3911274E-03	2.2197051E-03	3.6108340E-03
DIF H0 X,Y,S	2.3139163E-03	1.6631188E-03	3.9770352E-03
DIF L0 X,Y,S	3.1956227E-03	1.5316515E-03	4.7272728E-03
DIF H3 X,Y,S	1.9061875E-03	1.8810238E-03	3.7872111E-03

CASE54.DAT

PARAMETERS

1.200000	3.7500001E-02	64.00000	56789.00
36.00000	0.0000000E+00	0.0000000E+00	64.00000
53.20000	0.0000000E+00	53.20000	9.885000
1.337000	1.0200000E-09	99999.00	99999.00

MAGNITUDE ARRAY SCALING FACTORS

H1(0,0),HIGH,FACTOR	1.419238	2.3482593E-02	18.32272
L1(0,0),HIGH,FACTOR	1.500022	2.6038328E-02	16.52429
H0(0,0),HIGH,FACTOR	1.524574	2.1785045E-02	19.75048
L0(0,0),HIGH,FACTOR	1.710694	2.2621470E-02	19.02021
H3(0,0),HIGH,FACTOR	1.747829	4.9159650E-02	8.752402

INTEGRATED VARIANCE FROM POWER SPECTRA

VAR S0 A,C,S	2.2875596E-02	1.3741832E-02	3.6617365E-02
VAR H1 A,C,S	3.1561270E-02	1.1317615E-02	4.2878933E-02
VAR L1 A,C,S	2.9607065E-02	1.0278562E-02	3.9885592E-02
VAR H0 A,C,S	3.3254158E-02	1.2308263E-02	4.5562420E-02
VAR L0 A,C,S	3.2318294E-02	1.1925312E-02	4.4243604E-02
VAR H3 A,C,S	2.9667296E-02	1.2695429E-02	4.2362742E-02

VAR S0 X,Y,S	2.2875596E-02	1.3741832E-02	3.6617365E-02
VAR H1 X,Y,S	3.1561270E-02	1.1317615E-02	4.2878933E-02
VAR L1 X,Y,S	2.9607065E-02	1.0278562E-02	3.9885592E-02
VAR H0 X,Y,S	3.3254158E-02	1.2308263E-02	4.5562420E-02
VAR L0 X,Y,S	3.2318294E-02	1.1925312E-02	4.4243604E-02
VAR H3 X,Y,S	2.9667296E-02	1.2695429E-02	4.2362742E-02

INTEGRATED SQUARED DEVIATION FROM DIF SPECTRA

DIF H1 A,C,S	2.9267534E-03	1.5024336E-03	4.4291830E-03
DIF L1 A,C,S	2.4162212E-03	1.5926182E-03	4.0088422E-03
DIF H0 A,C,S	3.4228093E-03	1.4710914E-03	4.8939008E-03
DIF L0 A,C,S	3.1809881E-03	1.4761277E-03	4.6571158E-03
DIF H3 A,C,S	2.4560019E-03	1.6565275E-03	4.1125366E-03

DIF H1 X,Y,S	2.9267534E-03	1.5024336E-03	4.4291830E-03
DIF L1 X,Y,S	2.4162212E-03	1.5926182E-03	4.0088422E-03
DIF H0 X,Y,S	3.4228093E-03	1.4710914E-03	4.8939008E-03
DIF L0 X,Y,S	3.1809881E-03	1.4761277E-03	4.6571158E-03
DIF H3 X,Y,S	2.4560019E-03	1.6565275E-03	4.1125366E-03

CASE55.DAT

PARAMETERS

1.200000	3.7500001E-02	64.00000	56789.00
36.00000	0.0000000E+00	45.00000	64.00000
53.20000	0.0000000E+00	0.0000000E+00	100.0000
1.337000	1.0200000E-09	99999.00	99999.00

MAGNITUDE ARRAY SCALING FACTORS

H1(0,0),HIGH,FACTOR	1.008094	1.1980299E-02	39.16583
L1(0,0),HIGH,FACTOR	1.030069	1.0568053E-02	44.39970
H0(0,0),HIGH,FACTOR	1.191794	9.4451793E-03	49.67807
L0(0,0),HIGH,FACTOR	1.397467	5.6332685E-03	83.29415
H3(0,0),HIGH,FACTOR	0.9544371	3.0098449E-02	15.58945

INTEGRATED VARIANCE FROM POWER SPECTRA

VAR S0 A,C,S	2.2896349E-02	1.3720996E-02	3.6617398E-02
VAR H1 A,C,S	2.4932394E-02	1.7510744E-02	4.2443044E-02
VAR L1 A,C,S	2.5128221E-02	1.8134061E-02	4.3262216E-02
VAR H0 A,C,S	2.7334739E-02	2.0235274E-02	4.7569972E-02
VAR L0 A,C,S	4.0377144E-02	3.3534754E-02	7.3911898E-02
VAR H3 A,C,S	2.5035074E-02	1.9095292E-02	4.4130281E-02

VAR S0 X,Y,S	1.8308684E-02	1.8308697E-02	3.6617398E-02
VAR H1 X,Y,S	3.0177280E-02	1.2265820E-02	4.2443044E-02
VAR L1 X,Y,S	3.0366221E-02	1.2896063E-02	4.3262210E-02
VAR H0 X,Y,S	3.2971404E-02	1.4598572E-02	4.7569972E-02
VAR L0 X,Y,S	4.7635749E-02	2.6276167E-02	7.3911898E-02
VAR H3 X,Y,S	2.9658346E-02	1.4472049E-02	4.4130281E-02

INTEGRATED SQUARED DEVIATION FROM DIF SPECTRA

DIF H1 A,C,S	3.5822173E-03	2.8839428E-03	6.4661605E-03
DIF L1 A,C,S	3.6251219E-03	2.9847021E-03	6.6098273E-03
DIF H0 A,C,S	3.9830925E-03	3.3533848E-03	7.3364791E-03
DIF L0 A,C,S	8.1229135E-03	8.1356466E-03	1.6258573E-02
DIF H3 A,C,S	3.5124288E-03	3.1106551E-03	6.6230926E-03

DIF H1 X,Y,S	3.2788040E-03	3.1873505E-03	6.4661605E-03
DIF L1 X,Y,S	3.5215805E-03	3.0882482E-03	6.6098273E-03
DIF H0 X,Y,S	4.4697383E-03	2.8667392E-03	7.3364791E-03
DIF L0 X,Y,S	1.1507508E-02	4.7510648E-03	1.6258573E-02
DIF H3 X,Y,S	3.6349965E-03	2.9880942E-03	6.6230926E-03

CASE56.DAT

PARAMETERS

1.200000	3.7500001E-02	64.00000	56789.00
36.00000	0.0000000E+00	45.00000	64.00000
53.20000	45.00000	53.20000	9.885000
1.337000	1.0200000E-09	99999.00	99999.00

MAGNITUDE ARRAY SCALING FACTORS

H1(0,0),HIGH,FACTOR	0.6563759	1.7659539E-02	26.51925
L1(0,0),HIGH,FACTOR	0.7079940	1.8786263E-02	24.97667
H0(0,0),HIGH,FACTOR	0.7618241	1.6845772E-02	27.85377
L0(0,0),HIGH,FACTOR	0.9188905	1.7156072E-02	27.34999
H3(0,0),HIGH,FACTOR	0.6278647	2.4300184E-02	19.30925

INTEGRATED VARIANCE FROM POWER SPECTRA

VAR S0 A,C,S	2.2896349E-02	1.3720996E-02	3.6617398E-02
VAR H1 A,C,S	2.8118761E-02	1.0399437E-02	3.8518135E-02
VAR L1 A,C,S	2.8805107E-02	9.9771740E-03	3.8782269E-02
VAR H0 A,C,S	2.7468899E-02	1.1230610E-02	3.8699538E-02
VAR L0 A,C,S	2.7453218E-02	1.1389715E-02	3.8842916E-02
VAR H3 A,C,S	3.5684031E-02	1.3672792E-02	4.9356788E-02

VAR S0 X,Y,S	1.8308684E-02	1.8308697E-02	3.6617398E-02
VAR H1 X,Y,S	1.5327693E-02	2.3190463E-02	3.8518135E-02
VAR L1 X,Y,S	1.6160009E-02	2.2622341E-02	3.8782269E-02
VAR H0 X,Y,S	1.4515343E-02	2.4184128E-02	3.8699538E-02
VAR L0 X,Y,S	1.4402239E-02	2.4440669E-02	3.8842916E-02
VAR H3 X,Y,S	2.5007652E-02	2.4349179E-02	4.9356788E-02

INTEGRATED SQUARED DEVIATION FROM DIF SPECTRA

DIF H1 A,C,S	1.7093248E-03	1.8555638E-03	3.5648835E-03
DIF L1 A,C,S	1.6036234E-03	1.8691845E-03	3.4728101E-03
DIF H0 A,C,S	1.8889653E-03	1.8505873E-03	3.7395498E-03
DIF L0 A,C,S	1.9113834E-03	1.8646686E-03	3.7760541E-03
DIF H3 A,C,S	2.6861895E-03	1.5002813E-03	4.1864752E-03

DIF H1 X,Y,S	2.1444261E-03	1.4204594E-03	3.5648835E-03
DIF L1 X,Y,S	2.0302630E-03	1.4425463E-03	3.4728101E-03
DIF H0 X,Y,S	2.2675071E-03	1.4720454E-03	3.7395498E-03
DIF L0 X,Y,S	2.2735209E-03	1.5025303E-03	3.7760541E-03
DIF H3 X,Y,S	2.1332924E-03	2.0531795E-03	4.1864752E-03

CASE57.DAT

PARAMETERS

1.200000	3.7500001E-02	64.00000	56789.00
36.00000	0.0000000E+00	45.00000	64.00000
53.20000	90.00000	53.20000	9.885000
1.337000	1.0200000E-09	99999.00	99999.00

MAGNITUDE ARRAY SCALING FACTORS

H1(0,0),HIGH,FACTOR	0.2549144	3.4278177E-03	136.8854
L1(0,0),HIGH,FACTOR	0.2887039	4.5686848E-03	102.7031
H0(0,0),HIGH,FACTOR	0.3603626	2.2072336E-03	212.5821
L0(0,0),HIGH,FACTOR	0.4996004	1.9842812E-03	236.4677
H3(0,0),HIGH,FACTOR	0.2284821	8.4968824E-03	55.22241

INTEGRATED VARIANCE FROM POWER SPECTRA

VAR S0 A,C,S	2.2896349E-02	1.3720996E-02	3.6617398E-02
VAR H1 A,C,S	3.6698870E-02	1.9468962E-02	5.6166839E-02
VAR L1 A,C,S	3.2737046E-02	1.6645659E-02	4.9382728E-02
VAR H0 A,C,S	4.7983419E-02	2.9956756E-02	7.7940151E-02
VAR L0 A,C,S	5.8311008E-02	4.0132724E-02	9.8443732E-02
VAR H3 A,C,S	2.7338983E-02	1.7793855E-02	4.5132779E-02

VAR S0 X,Y,S	1.8308684E-02	1.8308697E-02	3.6617398E-02
VAR H1 X,Y,S	3.4431513E-02	2.1735352E-02	5.6166839E-02
VAR L1 X,Y,S	3.1539153E-02	1.7843559E-02	4.9382728E-02
VAR H0 X,Y,S	4.1754038E-02	3.6186155E-02	7.7940151E-02
VAR L0 X,Y,S	4.9719337E-02	4.8724398E-02	9.8443732E-02
VAR H3 X,Y,S	2.9504415E-02	1.5620386E-02	4.5132779E-02

INTEGRATED SQUARED DEVIATION FROM DIF SPECTRA

DIF H1 A,C,S	3.8963892E-03	2.3817348E-03	6.2781228E-03
DIF L1 A,C,S	3.0018897E-03	2.0358376E-03	5.0377259E-03
DIF H0 A,C,S	7.8096129E-03	5.5826241E-03	1.3392263E-02
DIF L0 A,C,S	1.2221515E-02	1.0074758E-02	2.2296293E-02
DIF H3 A,C,S	3.0416066E-03	2.6003495E-03	5.6419498E-03

DIF H1 X,Y,S	4.0843063E-03	2.1938167E-03	6.2781228E-03
DIF L1 X,Y,S	3.0821103E-03	1.9556158E-03	5.0377259E-03
DIF H0 X,Y,S	7.5161392E-03	5.8761141E-03	1.3392263E-02
DIF L0 X,Y,S	1.1392376E-02	1.0903901E-02	2.2296293E-02
DIF H3 X,Y,S	3.0972620E-03	2.5446874E-03	5.6419498E-03

CASE58.DAT

PARAMETERS

1.200000	3.7500001E-02	64.00000	56789.00
36.00000	0.0000000E+00	45.00000	64.00000
53.20000	135.0000	53.20000	9.885000
1.337000	1.0200000E-09	99999.00	99999.00

MAGNITUDE ARRAY SCALING FACTORS

H1(0,0),HIGH,FACTOR	0.3476106	6.2083569E-03	75.57850
L1(0,0),HIGH,FACTOR	0.3701479	7.1112234E-03	65.98278
H0(0,0),HIGH,FACTOR	0.4530588	4.9651847E-03	94.50169
L0(0,0),HIGH,FACTOR	0.5810444	4.5945328E-03	102.1254
H3(0,0),HIGH,FACTOR	0.3334030	1.2695652E-02	36.95898

INTEGRATED VARIANCE FROM POWER SPECTRA

VAR S0 A,C,S	2.2896349E-02	1.3720996E-02	3.6617398E-02
VAR H1 A,C,S	1.7999362E-02	2.5078749E-02	4.3078121E-02
VAR L1 A,C,S	1.7567474E-02	2.2536753E-02	4.0104225E-02
VAR H0 A,C,S	1.8551167E-02	2.8147370E-02	4.6698507E-02
VAR L0 A,C,S	1.8644666E-02	2.7983220E-02	4.6627920E-02
VAR H3 A,C,S	1.9257130E-02	2.0256875E-02	3.9513953E-02

VAR S0 X,Y,S	1.8308684E-02	1.8308697E-02	3.6617398E-02
VAR H1 X,Y,S	2.8838331E-02	1.4239796E-02	4.3078121E-02
VAR L1 X,Y,S	2.7885417E-02	1.2218775E-02	4.0104225E-02
VAR H0 X,Y,S	2.8707240E-02	1.7991293E-02	4.6698507E-02
VAR L0 X,Y,S	2.7689883E-02	1.8937964E-02	4.6627920E-02
VAR H3 X,Y,S	2.7208552E-02	1.2305440E-02	3.9513953E-02

INTEGRATED SQUARED DEVIATION FROM DIF SPECTRA

DIF H1 A,C,S	5.1305937E-03	3.7436830E-03	8.8742916E-03
DIF L1 A,C,S	5.1346584E-03	3.2720994E-03	8.4067639E-03
DIF H0 A,C,S	4.8755691E-03	4.4456189E-03	9.3211951E-03
DIF L0 A,C,S	4.6952148E-03	4.4083185E-03	9.1035375E-03
DIF H3 A,C,S	4.1905348E-03	3.1246215E-03	7.3151584E-03

DIF H1 X,Y,S	4.5550647E-03	4.3192171E-03	8.8742916E-03
DIF L1 X,Y,S	3.9339233E-03	4.4728327E-03	8.4067639E-03
DIF H0 X,Y,S	5.1726452E-03	4.1485331E-03	9.3211951E-03
DIF L0 X,Y,S	5.0805467E-03	4.0229829E-03	9.1035375E-03
DIF H3 X,Y,S	3.4958592E-03	3.8192885E-03	7.3151584E-03

```
CASE59.DAT

PARAMETERS
 1.200000      3.7500001E-02   64.00000      56789.00
 36.00000      0.0000000E+00   45.00000      64.00000
 53.20000       180.0000       53.20000      9.885000
 1.337000      1.0200000E-09   99999.00      99999.00

MAGNITUDE ARRAY SCALING FACTORS
H1(0,0),HIGH,FACTOR  0.4606828      8.3272867E-03   56.34708
L1(0,0),HIGH,FACTOR  0.4787847      9.1470275E-03   51.29736
H0(0,0),HIGH,FACTOR  0.5661303      6.8956339E-03   68.04571
L0(0,0),HIGH,FACTOR  0.6896812      6.2586530E-03   74.97113
H3(0,0),HIGH,FACTOR  0.4534822      1.6790370E-02   27.94568

INTEGRATED VARIANCE FROM POWER SPECTRA
VAR S0 A,C,S  2.2896349E-02  1.3720996E-02  3.6617398E-02
VAR H1 A,C,S  2.4670066E-02  1.6607841E-02  4.1277926E-02
VAR L1 A,C,S  2.3779966E-02  1.6045403E-02  3.9825354E-02
VAP H0 A,C,S  2.5489671E-02  1.7684536E-02  4.3174207E-02
VAR L0 A,C,S  2.5517885E-02  1.8420994E-02  4.3938830E-02
VAR H3 A,C,S  2.3509864E-02  1.7276773E-02  4.0786620E-02

VAR S0 X,Y,S  1.8308684E-02  1.8308697E-02  3.6617398E-02
VAR H1 X,Y,S  3.0020539E-02  1.1257360E-02  4.1277926E-02
VAR L1 X,Y,S  2.9093733E-02  1.0731663E-02  3.9825354E-02
VAR H0 X,Y,S  3.0985456E-02  1.2188720E-02  4.3174207E-02
VAR L0 X,Y,S  3.1174179E-02  1.2764687E-02  4.3938830E-02
VAR H3 X,Y,S  2.8085470E-02  1.2701144E-02  4.0786620E-02

INTEGRATED SQUARED DEVIATION FROM DIF SPECTRA
DIF H1 A,C,S  3.7012997E-03  2.9205685E-03  6.6218679E-03
DIF L1 A,C,S  3.6467665E-03  2.8734591E-03  6.5202275E-03
DIF H0 A,C,S  3.7645109E-03  2.9906456E-03  6.7551611E-03
DIF L0 A,C,S  3.7919371E-03  3.0525867E-03  6.8445322E-03
DIF H3 A,C,S  3.2746440E-03  2.7746828E-03  6.0493373E-03

DIF H1 X,Y,S  2.9996426E-03  3.6222239E-03  6.6218679E-03
DIF L1 X,Y,S  2.7162652E-03  3.8039566E-03  6.5202275E-03
DIF H0 X,Y,S  3.4732311E-03  3.2819160E-03  6.7551611E-03
DIF L0 X,Y,S  3.7213906E-03  3.1231402E-03  6.8445322E-03
DIF H3 X,Y,S  2.9117456E-03  3.1375880E-03  6.0493373E-03
```

```
CASE60.DAT

PARAMETERS
 1.200000      3.7500001E-02   64.00000      56789.00
 36.00000      0.0000000E+00   45.00000      64.00000
 53.20000      0.0000000E+00   53.20000      9.885000
 1.337000      1.0200000E-09   99999.00      99999.00

MAGNITUDE ARRAY SCALING FACTORS
H1(0,0),HIGH,FACTOR  1.458013    2.4327507E-02   19.28756
L1(0,0),HIGH,FACTOR  1.535191    2.6925165E-02   17.42676
H0(0,0),HIGH,FACTOR  1.563462    2.2942539E-02   20.45189
L0(0,0),HIGH,FACTOR  1.746088    2.4143755E-02   19.43435
H3(0,0),HIGH,FACTOR  1.766542    4.5680322E-02   10.27178

INTEGRATED VARIANCE FROM POWER SPECTRA
VAR S0 A,C,S  2.2896349E-02  1.3720996E-02  3.6617398E-02
VAR H1 A,C,S  2.7537160E-02  1.9721597E-02  4.7258761E-02
VAR L1 A,C,S  2.6192579E-02  1.8681724E-02  4.4874277E-02
VAR H0 A,C,S  2.8228475E-02  2.0407911E-02  4.8636351E-02
VAR L0 A,C,S  2.7191071E-02  1.9745568E-02  4.6936586E-02
VAR H3 A,C,S  2.7756875E-02  2.0940965E-02  4.8697911E-02

VAR S0 X,Y,S  1.8308684E-02  1.8308697E-02  3.6617398E-02
VAR H1 X,Y,S  3.3276126E-02  1.3982646E-02  4.7258761E-02
VAR L1 X,Y,S  3.1895254E-02  1.2979092E-02  4.4874277E-02
VAR H0 X,Y,S  3.4005884E-02  1.4630489E-02  4.8636351E-02
VAR L0 X,Y,S  3.2948788E-02  1.3987760E-02  4.6936586E-02
VAR H3 X,Y,S  3.2711338E-02  1.5986526E-02  4.8697911E-02

INTEGRATED SQUARED DEVIATION FROM DIF SPECTRA
DIF H1 A,C,S  3.9982609E-03  3.2676957E-03  7.2659547E-03
DIF L1 A,C,S  3.8213280E-03  3.0754611E-03  6.8967873E-03
DIF H0 A,C,S  4.1017081E-03  3.3975362E-03  7.4992469E-03
DIF L0 A,C,S  3.9393264E-03  3.2440135E-03  7.1833385E-03
DIF H3 A,C,S  3.6100477E-03  3.3992219E-03  7.0092641E-03

DIF H1 X,Y,S  4.3482827E-03  2.9176674E-03  7.2659547E-03
DIF L1 X,Y,S  3.8179136E-03  3.0788768E-03  6.8967873E-03
DIF H0 X,Y,S  4.6653212E-03  2.8339245E-03  7.4992469E-03
DIF L0 X,Y,S  4.2864555E-03  2.8968912E-03  7.1833385E-03
DIF H3 X,Y,S  4.0759719E-03  2.9332922E-03  7.0092641E-03
```

```
CASE61.DAT

PARAMETERS
 1.200000      3.7500001E-02  64.00000       56789.00
 36.00000      0.0000000E+00  90.00000       64.00000
 53.20000      0.0000000E+00  0.0000000E+00  100.0000
 1.337000      1.0200000E-09  99999.00       99999.00

MAGNITUDE ARRAY SCALING FACTORS
H1(0,0),HIGH,FACTOR   1.033041    1.3824837E-02  31.12261
L1(0,0),HIGH,FACTOR   1.049619    1.3159366E-02  32.69648
H0(0,0),HIGH,FACTOR   1.217480    1.1826080E-02  36.38272
L0(0,0),HIGH,FACTOR   1.416898    9.1755698E-03  46.89246
H3(0,0),HIGH,FACTOR   0.9452816   2.5605777E-02  16.80343

INTEGRATED VARIANCE FROM POWER SPECTRA
VAR S0 A,C,S  2.2875609E-02  1.3741827E-02  3.6617476E-02
VAR H1 A,C,S  1.3198626E-02  2.3858380E-02  3.7056923E-02
VAR L1 A,C,S  1.2982123E-02  2.3298597E-02  3.6280677E-02
VAR H0 A,C,S  1.3624724E-02  2.3938602E-02  3.7563376E-02
VAR L0 A,C,S  1.4547333E-02  2.3945739E-02  3.8493045E-02
VAR H3 A,C,S  1.5130291E-02  2.6785214E-02  4.1915528E-02

VAR S0 X,Y,S  1.3741827E-02  2.2875609E-02  3.6617476E-02
VAR H1 X,Y,S  2.3858380E-02  1.3198625E-02  3.7056923E-02
VAR L1 X,Y,S  2.3298597E-02  1.2982123E-02  3.6280677E-02
VAR H0 X,Y,S  2.3938602E-02  1.3624723E-02  3.7563376E-02
VAR L0 X,Y,S  2.3945739E-02  1.4547331E-02  3.8493045E-02
VAR H3 X,Y,S  2.6785214E-02  1.5130291E-02  4.1915528E-02

INTEGRATED SQUARED DEVIATION FROM DIF SPECTRA
DIF H1 A,C,S  5.0728116E-03  2.9058096E-03  7.9786275E-03
DIF L1 A,C,S  5.0615873E-03  2.8238709E-03  7.8854589E-03
DIF H0 A,C,S  4.7870367E-03  3.0402613E-03  7.8273062E-03
DIF L0 A,C,S  4.3403627E-03  3.3905031E-03  7.7308728E-03
DIF H3 A,C,S  4.8044138E-03  4.2536971E-03  9.0581011E-03

DIF H1 X,Y,S  2.9058098E-03  5.0728116E-03  7.9786275E-03
DIF L1 X,Y,S  2.8238709E-03  5.0615873E-03  7.8854589E-03
DIF H0 X,Y,S  3.0402613E-03  4.7870371E-03  7.8273062E-03
DIF L0 X,Y,S  3.3905031E-03  4.3403627E-03  7.7308728E-03
DIF H3 X,Y,S  4.2536971E-03  4.8044133E-03  9.0581011E-03
```

```
CASE62.DAT

PARAMETERS
 1.200000      3.7500001E-02  64.00000       56789.00
 36.00000      0.0000000E+00  90.00000       64.00000
 53.20000      45.00000       53.20000       9.885000
 1.337000      1.0200000E-09  99997.00       99999.00

MAGNITUDE ARRAY SCALING FACTORS
H1(0,0),HIGH,FACTOR  0.7099528    2.0508908E-02  20.97942
L1(0,0),HIGH,FACTOR  0.7583873    2.1795165E-02  19.74131
H0(0,0),HIGH,FACTOR  0.8153951    1.9791866E-02  21.73949
L0(0,0),HIGH,FACTOR  0.9692719    2.0358250E-02  21.13466
H3(0,0),HIGH,FACTOR  0.6416683    2.2322357E-02  19.27507

INTEGRATED VARIANCE FROM POWER SPECTRA
VAR S0 A,C,S  2.2875609E-02  1.3741827E-02  3.6617476E-02
VAR H1 A,C,S  2.2701500E-02  9.6876770E-03  3.2389171E-02
VAR L1 A,C,S  2.1776592E-02  1.0203403E-02  3.1979974E-02
VAR H0 A,C,S  2.3815500E-02  9.3544573E-03  3.3169899E-02
VAR L0 A,C,S  2.3758864E-02  9.4157998E-03  3.3174634E-02
VAR H3 A,C,S  2.6344150E-02  1.7774219E-02  4.4118419E-02

VAR S0 X,Y,S  1.3741827E-02  2.2875609E-02  3.6617476E-02
VAR H1 X,Y,S  9.6876770E-03  2.2701502E-02  3.2389171E-02
VAR L1 X,Y,S  1.0203403E-02  2.1776592E-02  3.1979974E-02
VAR H0 X,Y,S  9.3544573E-03  2.3815500E-02  3.3169899E-02
VAR L0 X,Y,S  9.4157998E-03  2.3758866E-02  3.3174634E-02
VAR H3 X,Y,S  1.7774219E-02  2.6344150E-02  4.4118419E-02

INTEGRATED SQUARED DEVIATION FROM DIF SPECTRA
DIF H1 A,C,S  2.1158669E-03  2.3741212E-03  4.4899923E-03
DIF L1 A,C,S  2.3972294E-03  2.3937335E-03  4.7909669E-03
DIF H0 A,C,S  1.9008132E-03  2.3122446E-03  4.2130612E-03
DIF L0 A,C,S  1.9418763E-03  2.3107405E-03  4.2526186E-03
DIF H3 A,C,S  3.6027147E-03  2.6743594E-03  6.2770671E-03

DIF H1 X,Y,S  2.3741212E-03  2.1158669E-03  4.4899923E-03
DIF L1 X,Y,S  2.3937335E-03  2.3972294E-03  4.7909669E-03
DIF H0 X,Y,S  2.3122446E-03  1.9008132E-03  4.2130612E-03
DIF L0 X,Y,S  2.3107405E-03  1.9418763E-03  4.2526186E-03
DIF H3 X,Y,S  2.6743594E-03  3.6027150E-03  6.2770671E-03
```

```
CASE63.DAT

PARAMETERS
 1.200000     3.7500001E-02   64.00000     56789.00
 36.00000     0.0000000E+00   90.00000     64.00000
 53.20000      90.00000       53.20000     9.885000
 1.337000     1.0200000E-09   99999.00     99999.00

MAGNITUDE ARRAY SCALING FACTORS
H1(0,0),HIGH,FACTOR  0.2716419      3.5562778E-03   120.9875
L1(0,0),HIGH,FACTOR  0.3030993      4.6642888E-03   92.24665
H0(0,0),HIGH,FACTOR  0.3770842      2.8510368E-03   150.9153
L0(0,0),HIGH,FACTOR  0.5139840      2.9183044E-03   147.4366
H3(0,0),HIGH,FACTOR  0.2396687      7.0414296E-03   [illegible]0478

INTEGRATED VARIANCE FROM POWER SPECTRA
VAR S0 A,C,S  2.2875609E-02  1.3741827E-02  3.6617476E-02
VAR H1 A,C,S  2.9145464E-02  2.9051362E-02  5.8196776E-02
VAR L1 A,C,S  2.3797860E-02  2.7719352E-02  5.1517271E-02
VAR H0 A,C,S  3.5384227E-02  2.6406310E-02  6.1790522E-02
VAR L0 A,C,S  3.8075518E-02  2.7065914E-02  6.51[illegible]56E-02
VAR H3 A,C,S  1.8081361E-02  2.6974086E-02  4.5[illegible]E-02

VAR S0 X,Y,S  1.3741827E-02  2.2875609E-02  3.6617476E-02
VAR H1 X,Y,S  2.9051362E-02  2.9145465E-02  5.8196776E-02
VAR L1 X,Y,S  2.7719351E-02  2.3797860E-02  5.1517271E-02
VAR H0 X,Y,S  2.6406310E-02  3.5384227E-02  6.1790522E-02
VAR L0 X,Y,S  2.7065914E-02  3.8075518E-02  6.5141656E-02
VAR H3 X,Y,S  2.6974084E-02  1.8081361E-02  4.5055442E-02

INTEGRATED SQUARED DEVIATION FROM DIF SPECTRA
DIF H1 A,C,S  4.0567243E-03  4.8957509E-03  8.9524612E-03
DIF L1 A,C,S  3.4942393E-03  4.3109371E-03  7.8051668E-03
DIF H0 A,C,S  5.2267285E-03  4.2165010E-03  9.4432374E-03
DIF L0 A,C,S  5.7947575E-03  4.4631241E-03  1.0257889E-02
DIF H3 A,C,S  3.7915939E-03  4.1055596E-03  7.8971507E-03

DIF H1 X,Y,S  4.3957509E-03  4.0567243E-03  8.9524612E-03
DIF L1 X,Y,S  4.3109371E-03  3.4942301E-03  7.8051668E-03
DIF H0 X,Y,S  4.2165010E-03  5.2267290E-03  9.4432374E-03
DIF L0 X,Y,S  4.4631241E-03  5.7947575E-03  1.0257889E-02
DIF H3 X,Y,S  4.1055596E-03  3.7915937E-03  7.8971507E-03
```

```
CASE64.DAT

PARAMETERS
 1.200000     3.7500001E-02   64.00000     56789.00
 36.00000     0.0000000E+00   90.00000     64.05000
 53.20000      135.0000       53.20000     9.885000
 1.337000     1.0200000E-09   99999.00     99999.00

MAGNITUDE ARRAY SCALING FACTORS
H1(0,0),HIGH,FACTOR  0.3608291      7.5173066E-03   57.23659
L1(0,0),HIGH,FACTOR  0.3816517      8.4450627E-03   50.94870
H0(0,0),HIGH,FACTOR  0.4662714      6.4062090E-03   67.16375
L0(0,0),HIGH,FACTOR  0.5925364      6.2236874E-03   6[illegible]13345
H3(0,0),HIGH,FACTOR  0.3324033      1.2028616E-02   35.77012

INTEGRATED VARIANCE FROM POWER SPECTRA
VAR S0 A,C,S  2.2875609E-02  1.3741827E-02  3.6617476E-02
VAR H1 A,C,S  1.4047557E-02  1.8569328E-02  3.2616902E-02
VAR L1 A,C,S  1.2893368E-02  1.8784145E-02  3.1677503E-02
VAR H0 A,C,S  1.5415759E-02  1.7836850E-02  3.3252586E-02
VAR L0 A,C,S  1.4953306E-02  1.7231157E-02  3.2184495E-02
VAR H3 A,C,S  1.3531144E-02  2.1212796E-02  3.4743920E-02

VAR S0 X,Y,S  1.3741827E-02  2.2875609E-02  3.6617476E-02
VAR H1 X,Y,S  1.8569328E-02  1.4047557E-02  3.2616902E-02
VAR L1 X,Y,S  1.8784143E-02  1.2893367E-02  3.1677503E-02
VAR H0 X,Y,S  1.7836850E-02  1.5415757E-02  3.3252586E-02
VAR L0 X,Y,S  1.7231157E-02  1.4953306E-02  3.2184485E-02
VAR H3 X,Y,S  2.1212796E-02  1.3531143E-02  3.4743920E-02

INTEGRATED SQUARED DEVIATION FROM DIF SPECTRA
DIF H1 A,C,S  5.2692886E-03  2.3126544E-03  7.5819413E-03
DIF L1 A,C,S  5.5762194E-03  2.1723052E-03  7.7485200E-03
DIF H0 A,C,S  4.8002768E-03  2.4411457E-03  7.2414191E-03
DIF L0 A,C,S  4.7918153E-03  2.3909628E-03  7.1827699E-03
DIF H3 A,C,S  5.2472735E-03  2.7843381E-03  8.0316206E-03

DIF H1 X,Y,S  2.3126542E-03  5.2692886E-03  7.5819413E-03
DIF L1 X,Y,S  2.1723052E-03  5.5762194E-03  7.7485200E-03
DIF H0 X,Y,S  2.4411457E-03  4.8002768E-03  7.2414191E-03
DIF L0 X,Y,S  2.3909628E-03  4.7918153E-03  7.1827699E-03
DIF H3 X,Y,S  2.7843381E-03  5.2472730E-03  8.0316206E-03
```

CASE65.DAT

PARAMETERS

1.200000	3.7500001E-02	64.00000	56789.00
36.00000	0.0050000E+00	90.00000	64.00000
53.20000	180.0000	53.20000	9.885000
1.337000	1.0200000E-09	99999.00	99999.00

MAGNITUDE ARRAY SCALING FACTORS

H1(0,0),HIGH,FACTOR	0.4768308	8.3096810E-03	51.77876
L1(0,0),HIGH,FACTOR	0.4930539	9.2170909E-03	46.68122
H0(0,0),HIGH,FACTOR	0.5822732	7.1988958E-03	59.76820
L0(0,0),HIGH,FACTOR	0.7039387	6.9952589E-03	61.50809
H3(0,0),HIGH,FACTOR	0.4508535	1.3799264E-02	31.18029

INTEGRATED VARIANCE FROM POWER SPECTRA

VAR S0 A,C,S	2.2875609E-02	1.3741827E-02	3.6617476E-02
VAR H1 A,C,S	1.3674027E-02	2.5906678E-02	3.9580807E-02
VAR L1 A,C,S	1.3236324E-02	2.5280034E-02	3.8516447E-02
VAR H0 A,C,S	1.3916882E-02	2.5928123E-02	3.9844967E-02
VAR L0 A,C,S	1.3597312E-02	2.5103139E-02	3.8700443E-02
VAR H3 A,C,S	1.4384513E-02	2.6577163E-02	4.0961765E-02
VAR S0 X,Y,S	1.3741827E-02	2.2875609E-02	3.6617476E-02
VAR H1 X,Y,S	2.5906682E-02	1.3674027E-02	3.9580807E-02
VAR L1 X,Y,S	2.5280034E-02	1.3236325E-02	3.8516447E-02
VAR H0 X,Y,S	2.5928123E-02	1.3916882E-02	3.9844967E-02
VAR L0 X,Y,S	2.5103139E-02	1.3597312E-02	3.8700443E-02
VAR H3 X,Y,S	2.6577165E-02	1.4384513E-02	4.0961765E-02

INTEGRATED SQUARED DEVIATION FROM DIF SPECTRA

DIF H1 A,C,S	5.4172128E-03	3.3877317E-03	8.8049350E-03
DIF L1 A,C,S	5.5912733E-03	3.1814300E-03	8.7727048E-03
DIF H0 A,C,S	5.1779719E-03	3.4682788E-03	8.6462339E-03
DIF L0 A,C,S	5.1417082E-03	3.2732945E-03	8.4150797E-03
DIF H3 A,C,S	5.2094539E-03	3.9895074E-03	9.1989497E-03
DIF H1 X,Y,S	3.3877320E-03	5.4172128E-03	8.8049350E-03
DIF L1 X,Y,S	3.1814300E-03	5.5912733E-03	8.7727048E-03
DIF H0 X,Y,S	3.4682788E-03	5.1779719E-03	8.6462339E-03
DIF L0 X,Y,S	3.2732943E-03	5.1417882E-03	8.4150797E-03
DIF H3 X,Y,S	3.9895074E-03	5.2094539E-03	9.1989497E-03

CASE66.DAT

PARAMETERS

1.200000	3.7500001E-02	64.00000	56789.00
36.00000	0.0000000E+00	90.00000	64.00000
53.20000	0.0000000E+00	53.20000	9.885000
1.337000	1.0200000E-09	99999.00	99999.00

MAGNITUDE ARRAY SCALING FACTORS

H1(0,0),HIGH,FACTOR	1.509012	2.2896502E-02	18.79173
L1(0,0),HIGH,FACTOR	1.581743	2.5594333E-02	16.81095
H0(0,0),HIGH,FACTOR	1.614454	2.1787735E-02	19.74804
L0(0,0),HIGH,FACTOR	1.792627	2.3372402E-02	18.40911
H3(0,0),HIGH,FACTOR	1.781519	4.1420560E-02	10.38772

INTEGRATED VARIANCE FROM POWER SPECTRA

VAR S0 A,C,S	2.2875609E-02	1.3741827E-02	3.6617476E-02
VAR H1 A,C,S	1.6659552E-02	2.8881593E-02	4.5541059E-02
VAR L1 A,C,S	1.5666367E-02	2.7834566E-02	4.3500870E-02
VAR H0 A,C,S	1.7069744E-02	2.9235529E-02	4.6305321E-02
VAR L0 A,C,S	1.6242608E-02	2.8276470E-02	4.4519089E-02
VAR H3 A,C,S	1.6092438E-02	2.4681238E-02	4.0773623E-02
VAR S0 X,Y,S	1.3741827E-02	2.2875609E-02	3.6617476E-02
VAR H1 X,Y,S	2.8881593E-02	1.6659552E-02	4.5541059E-02
VAR L1 X,Y,S	2.7834566E-02	1.5666367E-02	4.3500870E-02
VAR H0 X,Y,S	2.9235529E-02	1.7069744E-02	4.6345321E-02
VAR L0 X,Y,S	2.8276470E-02	1.6242608E-02	4.4519089E-02
VAR H3 X,Y,S	2.4681238E-02	1.6092438E-02	4.0773623E-02

INTEGRATED SQUARED DEVIATION FROM DIF SPECTRA

DIF H1 A,C,S	4.4486602E-03	4.5673372E-03	9.0159941E-03
DIF L1 A,C,S	4.6931454E-03	4.1230894E-03	8.8162469E-03
DIF H0 A,C,S	4.3531740E-03	4.7344123E-03	9.0875831E-03
DIF L0 A,C,S	4.5077540E-03	4.3388284E-03	8.8465670E-03
DIF H3 A,C,S	4.1983472E-03	3.3413579E-03	7.5397133E-03
DIF H1 X,Y,S	4.5673372E-03	4.4486602E-03	9.0159941E-03
DIF L1 X,Y,S	4.1230894E-03	4.6931454E-03	8.8162469E-03
DIF H0 X,Y,S	4.7344123E-03	4.3531740E-03	9.0875831E-03
DIF L0 X,Y,S	4.3388284E-03	4.5077540E-03	8.8465670E-03
DIF H3 X,Y,S	3.3413579E-03	4.1983472E-03	7.5397133E-03

```
CASE67.DAT

PARAMETERS
 1.200000      3.7500001E-02  64.00000      56789.00
 36.00000      0.0000000E+00  135.0000      64.00000
 53.20000      0.0000000E+00  0.0000000E+00 100.0000
 1.337000      1.0200000E-09  99999.00      99999.00

MAGNITUDE ARRAY SCALING FACTORS
H1(0,0),HIGH,FACTOR  1.009322      1.2579173E-02  37.30120
L1(0,0),HIGH,FACTOR  1.030421      1.1376479E-02  41.24460
H0(0,0),HIGH,FACTOR  1.192787      9.8754177E-03  47.51377
L0(0,0),HIGH,FACTOR  1.397352      6.1078724E-03  76.82189
H3(0,0),HIGH,FACTOR  0.9466130     3.0060632E-02  15.60906

INTEGRATED VARIANCE FROM POWER SPECTRA
VAR S0 A,C,S  2.2896348E-02  1.3720991E-02  3.6617409E-02
VAR H1 A,C,S  2.2270110E-02  1.6937997E-02  3.9208118E-02
VAR L1 A,C,S  2.1884004E-02  1.6655752E-02  3.8539786E-02
VAR H0 A,C,S  2.4900179E-02  1.9618915E-02  4.4519123E-02
VAR L0 A,C,S  3.5643876E-02  2.9418312E-02  6.5062165E-02
VAR H3 A,C,S  2.4837142E-02  1.8293021E-02  4.3130141E-02

VAR S0 X,Y,S  1.8308669E-02  1.8308718E-02  3.6617409E-02
VAR H1 X,Y,S  2.7991861E-02  1.1216183E-02  3.9208118E-02
VAR L1 X,Y,S  2.7212836E-02  1.1326938E-02  3.8539786E-02
VAR H0 X,Y,S  3.0953538E-02  1.3565579E-02  4.4519123E-02
VAR L0 X,Y,S  4.1992453E-02  2.3063678E-02  6.5062165E-02
VAR H3 X,Y,S  2.8492155E-02  1.4638031E-02  4.3130141E-02

INTEGRATED SQUARED DEVIATION FROM DIF SPECTRA
DIF H1 A,C,S  3.5608774E-03  2.6737752E-03  6.2346621E-03
DIF L1 A,C,S  3.4625253E-03  2.6554505E-03  6.1179660E-03
DIF H0 A,C,S  3.8525991E-03  3.1431823E-03  6.9957860E-03
DIF L0 A,C,S  6.5320176E-03  6.4665019E-03  1.2998511E-02
DIF H3 A,C,S  3.5736030E-03  3.1849579E-03  6.7585637E-03

DIF H1 X,Y,S  2.8830850E-03  3.3515764E-03  6.2346621E-03
DIF L1 X,Y,S  2.8458915E-03  3.2720929E-03  6.1179660E-03
DIF H0 X,Y,S  4.0088887E-03  2.9869003E-03  6.9957860E-03
DIF L0 X,Y,S  9.0789441E-03  3.9195726E-03  1.2998511E-02
DIF H3 X,Y,S  3.5822843E-03  3.1762756E-03  6.7585637E-03
```

```
CASE68.DAT

PARAMETERS
 1.200000      3.7500001E-02  64.00000      56789.00
 36.00000      0.0000000E+00  135.0000      64.00000
 53.20000      45.00000       53.20000      9.885000
 1.337000      1.0200000E-09  99999.00      99999.00

MAGNITUDE ARRAY SCALING FACTORS
H1(0,0),HIGH,FACTOR  0.6757497     1.5909381E-02  29.49319
L1(0,0),HIGH,FACTOR  0.7276610     1.6656209E-02  28.17077
H0(0,0),HIGH,FACTOR  0.7810686     1.5413662E-02  30.44172
L0(0,0),HIGH,FACTOR  0.9382986     1.5662502E-02  29.95807
H3(0,0),HIGH,FACTOR  0.6286256     1.7584424E-02  26.68375

INTEGRATED VARIANCE FROM POWER SPECTRA
VAR S0 A,C,S  2.2896348E-02  1.3720991E-02  3.6617409E-02
VAR H1 A,C,S  1.9237043E-02  2.8303960E-02  4.7540985E-02
VAR L1 A,C,S  1.8541198E-02  2.9075243E-02  4.7616467E-02
VAR H0 A,C,S  2.0772342E-02  2.7617762E-02  4.8390131E-02
VAR L0 A,C,S  2.1250617E-02  2.7648635E-02  4.8899274E-02
VAR H3 A,C,S  2.7202604E-02  4.1428760E-02  6.8631262E-02

VAR S0 X,Y,S  1.8308669E-02  1.8308718E-02  3.6617409E-02
VAR H1 X,Y,S  1.7395156E-02  3.0145865E-02  4.7540985E-02
VAR L1 X,Y,S  1.8382244E-02  2.9234193E-02  4.7616467E-02
VAR H0 X,Y,S  1.6419858E-02  3.1970184E-02  4.8390131E-02
VAR L0 X,Y,S  1.6219653E-02  3.2679614E-02  4.8899274E-02
VAR H3 X,Y,S  3.4012966E-02  3.4618289E-02  6.8631262E-02

INTEGRATED SQUARED DEVIATION FROM DIF SPECTRA
DIF H1 A,C,S  4.7903918E-03  4.4349264E-03  9.2252996E-03
DIF L1 A,C,S  4.9364921E-03  4.549[illegible]E-03  9.4856359E-03
DIF H0 A,C,S  4.6613873E-03  4.4057434E-03  9.0671265E-03
DIF L0 A,C,S  4.7056172E-03  4.4600686E-03  9.1656856E-03
DIF H3 A,C,S  5.4739206E-03  9.6529089E-03  1.5126840E-02

DIF H1 X,Y,S  4.1626957E-03  5.0626225E-03  9.2252996E-03
DIF L1 X,Y,S  4.3303184E-03  5.1553268E-03  9.4856359E-03
DIF H0 X,Y,S  3.9418144E-03  5.1253154E-03  9.0671265E-03
DIF L0 X,Y,S  3.9191325E-03  5.2465596E-03  9.1656856E-03
DIF H3 X,Y,S  7.3268204E-03  7.7999984E-03  1.5126840E-02
```

```
CASE69.DAT

PARAMETERS
 1.200000    3.7500001E-02   64.00000    56789.00
 36.00000    0.0000000E+00   135.0000    64.00000
 53.20000     90.00000       53.20000    9.885000
 1.337000    1.0200000E-09   99999.00    99999.00

MAGNITUDE ARRAY SCALING FACTORS
H1(0,0),HIGH,FACTOR  0.2618286    3.0775403E-03   152.4654
L1(0,0),HIGH,FACTOR  0.2969914    4.2020525E-03   111.6641
H0(0,0),HIGH,FACTOR  0.3671474    2.3882277E-03   196.4713
L0(0,0),HIGH,FACTOR  0.5076290    2.5744168E-03   182.2620
H3(0,0),HIGH,FACTOR  0.2279700    8.0634207E-03   58.19098

INTEGRATED VARIANCE FROM POWER SPECTRA
VAR S0 A,C,S  2.2896348E-02  1.3720991E-02  3.6617409E-02
VAR H1 A,C,S  2.8371876E-02  3.7324071E-02  6.5695912E-02
VAR L1 A,C,S  2.2365561E-02  2.8782798E-02  5.1148374E-02
VAR H0 A,C,S  3.6413241E-02  4.0500913E-02  7.6914117E-02
VAR L0 A,C,S  3.9827820E-02  3.6340915E-02  7.6168917E-02
VAR H3 A,C,S  2.3835992E-02  2.0562878E-02  4.4398893E-02

VAR S0 X,Y,S  1.8308669E-02  1.8308718E-02  3.6617409E-02
VAR H1 X,Y,S  3.5474587E-02  3.0221302E-02  6.5695912E-02
VAR L1 X,Y,S  2.9836617E-02  2.1311665E-02  5.1148374E-02
VAR H0 X,Y,S  3.2718193E-02  4.4196032E-02  7.6914117E-02
VAR L0 X,Y,S  3.0066125E-02  4.6102658E-02  7.6168917E-02
VAR H3 X,Y,S  2.8940508E-02  1.5458346E-02  4.4398893E-02

INTEGRATED SQUARED DEVIATION FROM DIF SPECTRA
DIF H1 A,C,S  4.8439694E-03  7.8988951E-03  1.2742856E-02
DIF L1 A,C,S  3.9584450E-03  4.5577637E-03  8.5162157E-03
DIF H0 A,C,S  6.3451394E-03  9.9539766E-03  1.6299114E-02
DIF L0 A,C,S  6.9748438E-03  8.6326208E-03  1.5607472E-02
DIF H3 A,C,S  3.6549233E-03  3.2773714E-03  6.9322861E-03

DIF H1 X,Y,S  6.5700652E-03  6.0727964E-03  1.2742856E-02
DIF L1 X,Y,S  4.6290546E-03  3.8871660E-03  8.5162157E-03
DIF H0 X,Y,S  6.0026641E-03  1.0296471E-02  1.6299114E-02
DIF L0 X,Y,S  5.3251460E-03  1.0282330E-02  1.5607472E-02
DIF H3 X,Y,S  3.7413742E-03  3.1909160E-03  6.9322861E-03
```

```
CASE70.DAT

PARAMETERS
 1.200000    3.7500001E-02   64.00000    56789.00
 36.00000    0.0000000E+00   135.0000    64.00000
 53.20000     135.0000       53.20000    9.885000
 1.337000    1.0200000E-09   99999.00    99999.00

MAGNITUDE ARRAY SCALING FACTORS
H1(0,0),HIGH,FACTOR  0.3487161    7.5149625E-03   62.43788
L1(0,0),HIGH,FACTOR  0.3723494    8.3725294E-03   56.04260
H0(0,0),HIGH,FACTOR  0.4540349    5.9766928E-03   78.50802
L0(0,0),HIGH,FACTOR  0.5829871    5.2999984E-03   88.53178
H3(0,0),HIGH,FACTOR  0.3311667    1.4548268E-02   32.25252

INTEGRATED VARIANCE FROM POWER SPECTRA
VAR S0 A,C,S  2.2896348E-02  1.3720991E-02  3.6617409E-02
VAR H1 A,C,S  2.4100667E-02  9.5773051E-03  3.3677969E-02
VAR L1 A,C,S  2.2517534E-02  9.4384765E-03  3.1956017E-02
VAR H0 A,C,S  2.6060198E-02  1.0337407E-02  3.6397602E-02
VAR L0 A,C,S  2.6066361E-02  1.1178694E-02  3.7245091E-02
VAR H3 A,C,S  2.3449168E-02  1.2349859E-02  3.5799056E-02

VAR S0 X,Y,S  1.8308669E-02  1.8308718E-02  3.6617409E-02
VAR H1 X,Y,S  2.1522341E-02  1.2155607E-02  3.3677969E-02
VAR L1 X,Y,S  2.1087047E-02  1.0868950E-02  3.1956017E-02
VAR H0 X,Y,S  2.1889100E-02  1.4508496E-02  3.6397602E-02
VAR L0 X,Y,S  2.1840112E-02  1.5405006E-02  3.7245091E-02
VAR H3 X,Y,S  2.2961054E-02  1.2837982E-02  3.5799056E-02

INTEGRATED SQUARED DEVIATION FROM DIF SPECTRA
DIF H1 A,C,S  1.6505575E-03  2.2827203E-03  3.9332751E-03
DIF L1 A,C,S  1.7935724E-03  2.4376162E-03  4.2311889E-03
DIF H0 A,C,S  1.6220136E-03  1.9154929E-03  3.5375110E-03
DIF L0 A,C,S  1.7085157E-03  1.7636572E-03  3.4721713E-03
DIF H3 A,C,S  2.2449493E-03  2.3219802E-03  4.5669228E-03

DIF H1 X,Y,S  1.3030567E-03  2.6302172E-03  3.9332751E-03
DIF L1 X,Y,S  1.1757435E-03  3.0554512E-03  4.2311889E-03
DIF H0 X,Y,S  1.5603121E-03  1.9771934E-03  3.5375110E-03
DIF L0 X,Y,S  1.7011950E-03  1.7709751E-03  3.4721713E-03
DIF H3 X,Y,S  1.8865734E-03  2.6803578E-03  4.5669228E-03
```

CASE71.DAT

```
PARAMETERS
 1.200000     3.7500001E-02  64.00000     56789.00
 36.00000     0.0000000E+00  135.0000     64.00000
 53.20000     180.0000       53.20000     9.885000
 1.337000     1.0200000E-09  99999.00     99999.00

MAGNITUDE ARRAY SCALING FACTORS
H1(0,0),HIGH,FACTOR  0.4618708    8.4568635E-03  55.48373
L1(0,0),HIGH,FACTOR  0.4800421    9.3807466E-03  50.01929
H0(0,0),HIGH,FACTOR  0.5671896    6.9197142E-03  67.80891
L0(0,0),HIGH,FACTOR  0.6906798    6.3075949E-03  74.38942
H3(0,0),HIGH,FACTOR  0.4499777    1.6611675E-02  28.24630

INTEGRATED VARIANCE FROM POWER SPECTRA
VAR S0 A,C,S  2.2896348E-02  1.3720991E-02  3.6617409E-02
VAR H1 A,C,S  2.3192881E-02  1.6868340E-02  4.0061269E-02
VAR L1 A,C,S  2.2091735E-02  1.5953334E-02  3.8045023E-02
VAR H0 A,C,S  2.4590764E-02  1.8404990E-02  4.2995792E-02
VAR L0 A,C,S  2.4689313E-02  1.8936923E-02  4.3626297E-02
VAR H3 A,C,S  2.3630153E-02  1.6822167E-02  4.0452335E-02

VAR S0 X,Y,S  1.8308669E-02  1.8308718E-02  3.6617409E-02
VAR H1 X,Y,S  2.9178087E-02  1.0883181E-02  4.0061269E-02
VAR L1 X,Y,S  2.7825229E-02  1.0219757E-02  3.8045023E-02
VAR H0 X,Y,S  3.0898277E-02  1.2097485E-02  4.2995792E-02
VAR L0 X,Y,S  3.0966079E-02  1.2660165E-02  4.3626297E-02
VAR H3 X,Y,S  2.7382283E-02  1.3070044E-02  4.0452335E-02

INTEGRATED SQUARED DEVIATION FROM DIF SPECTRA
DIF H1 A,C,S  3.7582247E-03  2.8456589E-03  6.6038906E-03
DIF L1 A,C,S  3.6714089E-03  2.7342150E-03  6.4056213E-03
DIF H0 A,C,S  3.9164852E-03  3.0353272E-03  6.9518303E-03
DIF L0 A,C,S  3.9198939E-03  3.0840728E-03  7.0039663E-03
DIF H3 A,C,S  3.3268870E-03  2.8100666E-03  6.1369473E-03

DIF H1 X,Y,S  2.8968644E-03  3.7070140E-03  6.6038906E-03
DIF L1 X,Y,S  2.5124990E-03  3.8931221E-03  6.4056213E-03
DIF H0 X,Y,S  3.5682137E-03  3.3836088E-03  6.9518303E-03
DIF L0 X,Y,S  3.7646899E-03  3.2392826E-03  7.0039663E-03
DIF H3 X,Y,S  2.9566681E-03  3.1802794E-03  6.1369473E-03
```

CASE72.DAT

```
PARAMETERS
 1.200000     3.7500001E-02  64.00000     56789.00
 36.00000     0.0000000E+00  135.0000     64.00000
 53.20000     0.0000000E+00  53.20000     9.885000
 1.337000     1.0200000E-09  99999.00     99999.00

MAGNITUDE ARRAY SCALING FACTORS
H1(0,0),HIGH,FACTOR  1.462870     2.1951627E-02  21.37510
L1(0,0),HIGH,FACTOR  1.540414     2.4539392E-02  19.12102
H0(0,0),HIGH,FACTOR  1.568188     2.0598857E-02  22.77885
L0(0,0),HIGH,FACTOR  1.751051     2.1810774E-02  21.51314
H3(0,0),HIGH,FACTOR  1.761322     4.0031515E-02  11.72122

INTEGRATED VARIANCE FROM POWER SPECTRA
VAR S0 A,C,S  2.2896348E-02  1.3720991E-02  3.6617409E-02
VAR H1 A,C,S  3.4064941E-02  2.3759818E-02  5.7824850E-02
VAR L1 A,C,S  3.1846914E-02  2.2055427E-02  5.3902365E-02
VAR H0 A,C,S  3.5372987E-02  2.4807891E-02  6.0180854E-02
VAR L0 A,C,S  3.3822011E-02  2.3678033E-02  5.7500102E-02
VAR H3 A,C,S  3.8336053E-02  2.5813524E-02  6.4149491E-02

VAR S0 X,Y,S  1.8308669E-02  1.8308718E-02  3.6617469E-02
VAR H1 X,Y,S  4.0320482E-02  1.7504290E-02  5.7824850E-02
VAR L1 X,Y,S  3.7930399E-02  1.5971845E-02  5.3902365E-02
VAR H0 X,Y,S  4.1672867E-02  1.8507935E-02  6.0180854E-02
VAR L0 X,Y,S  3.9960001E-02  1.7539956E-02  5.7500102E-02
VAR H3 X,Y,S  4.1655004E-02  2.2494484E-02  6.4149491E-02

INTEGRATED SQUARED DEVIATION FROM DIF SPECTRA
DIF H1 A,C,S  5.4429444E-03  4.3215170E-03  9.7644553E-03
DIF L1 A,C,S  4.8988634E-03  3.8808582E-03  8.7797344E-03
DIF H0 A,C,S  5.8019441E-03  4.6035340E-03  1.0405492E-02
DIF L0 A,C,S  5.3944718E-03  4.2622811E-03  9.6567506E-03
DIF H3 A,C,S  5.7735159E-03  4.6678586E-03  1.0441364E-02

DIF H1 X,Y,S  6.6231498E-03  3.1413157E-03  9.7644553E-03
DIF L1 X,Y,S  5.6312727E-03  3.1484521E-03  8.7797344E-03
DIF H0 X,Y,S  7.2277086E-03  3.1777681E-03  1.0405492E-02
DIF L0 X,Y,S  6.5191011E-03  3.1376560E-03  9.6567506E-03
DIF H3 X,Y,S  7.2094752E-03  3.2318889E-03  1.0441364E-02
```

6.3 Appendix III - FORTRAN 77 Code

The input data files, FORTRAN programs, and FORTRAN subroutines that were created in support of this study are listed as follows:

Input Data Files
- PARM.DAT
- V_DATA.DAT

FORTRAN Programs
- SURF.FOR
- LIGHTBLUE.FOR
- LIGHT.FOR
- ANALYS.FOR
- PSVARY.FOR

FORTRAN Subroutines
- ALPHA.FOR
- ALPHAS.FOR
- CHECKERBOARD.FOR
- DARKNESS.FOR
- DEEPBLUE.FOR
- DIST_GEN.FOR
- FFT2D.FOR
- PLT2DFILE.FOR
- PLT2DOUTPUT.FOR
- PLT3DFILE.FOR
- PLT3DINPUT.FOR
- PLT3DOUTPUT.FOR
- PSVARY1.FOR
- PSVARY2.FOR
- RALPH.FOR
- RIMP.FOR
- SEA_SPEC.FOR
- SKYBLUE.FOR
- SKYMAP.FOR
- SPREADVARY.FOR
- WGN_SPEC.FOR
- WGN2D.FOR
- WIND.FOR

Input Data Files

TYPE PARM.DAT

```
        4               4
        1.20            0.0375          64.0            56789.0
        60.0            0.0             135.0           64.0
        53.2            0.0             53.2            9.885
        1.337           1.02E-9         99999.0         99999.0
*
******* PARM.DAT        PARAMETERS ***************************************
*
*       PARM_ROWS       PARM_COLS
*       K_NYQ           DELTA_K         N1(SURF_ARRAY)  ISEED(RANDOMIZER)
*       WIND_V(Z)       Z [CM]          WIND_AZ         N(DOME_ARRAY)
*       THETA(SENSOR)   PHI0(SUN)       THETA0(SUN)     LREF(LSKY(0,0))
*       INDEX_REAL      INDEX_IMAG      UNUSED          UNUSED
*
**************************************************************************
*
* NOTES: LREF = 100.0 FOR THETA0 =  0.0 DEG
*        LREF = 32.65 FOR THETA0 = 26.6 DEG
*        LREF = 9.885 FOR THETA0 = 53.2 DEG
*
**************************************************************************
```

TYPE V_DATA.DAT

9.3570001E-02	5.000000	98.63132	116.0000	118.7493	124.0000
7.1240805E-02	6.000000	122.4473	143.0000	146.5888	153.0000
2.8380003E-02	10.00000	227.0883	262.0000	267.3242	278.0000
1.8863197E-02	12.00000	284.7601	326.0000	333.0432	346.0000
1.0929998E-02	15.00000	376.4139	428.0000	436.7679	453.0000
7.5672008E-03	18.00000	468.2427	530.0000	540.6674	561.0000
7.0200004E-03	20.00000	524.0226	593.0000	604.4945	627.0000
8.8527985E-03	24.00000	614.9089	698.0000	711.4752	738.0000
9.8099969E-03	25.00000	634.1133	721.0000	734.7032	763.0000
1.7019998E-02	30.00000	719.6121	824.0000	840.3198	874.0000
2.7672853E-02	35.00000	797.0169	918.0000	937.8427	977.0000
3.0168798E-02	36.00000	812.0167	937.0000	956.8661	997.0000
4.1279998E-02	40.00000	870.8839	1010.000	1031.828	1075.000
4.7484916E-02	42.00000	899.7244	1045.000	1068.715	1115.000
5 7569999E-02	45.00000	942.3242	1098.000	1123.386	1173.000
6.8561204E-02	48.00000	984.1787	1151.000	1177.311	1231.000
7.6380000E-02	50.00000	1011.687	1185.000	1212.867	1269.000
9.3171470E-02	54.00000	1065.795	1253.000	1283.069	1343.000
9.7606353E-02	55.00000	1079.138	1270.000	1300.435	1362.000
0.1211800	60.00000	1144.791	1353.000	1386.207	1453.000
0.1470531	65.00000	1208.744	1434.000	1470.277	1543.000
0.1525004	66.00000	1221.338	1450.000	1486.895	1562.000
0.1751914	70.00000	1271.084	1514.000	1552.736	1631.000
0.1870752	72.00000	1295.587	1545.000	1585.286	1665.000
0.2055700	75.00000	1331.893	1592.000	1633.663	1717.000
0.2248644	78.00000	1367.675	1638.000	1681.516	1768.000
0.2381700	80.00000	1391.246	1669.000	1713.134	1802.000
0.2658397	84.00000	1437.728	1729.000	1775.710	1869.000
0.2729771	85.00000	1449.214	1744.000	1791.219	1886.000
0.3099800	90.00000	1505.859	1818.000	1867.983	1968.000
0.3491700	95.00000	1561.244	1891.000	1943.485	2049.000
0.3572698	96.00000	1572.174	1905.000	1958.439	2065.000
0.3905400	100.0000	1615.421	1962.000	2017.781	2129.000
0.4076971	102.0000	1636.766	1990.000	2047.173	2161.000
0.4340843	105.0000	1668.444	2032.000	2090.922	2208.000
0.4612525	108.0000	1699.723	2074.000	2134.271	2254.000
0.4797982	110.0000	1720.359	2101.000	2162.954	2285.000
0.5179287	114.0000	1761.123	2156.000	2219.813	2347.000
0.5276778	115.0000	1771.210	2170.000	2233.923	2362.000
0.5777199	120.0000	1821.038	2237.000	2303.869	2437.000
0.6299220	125.0000	1869.881	2303.000	2372.831	2512.000
0.6406213	126.0000	1879.535	2315.000	2386.508	2527.000
0.6842815	130.0000	1917.775	2368.000	2440.843	2585.000
0.7066289	132.0000	1936.674	2354.000	2467.789	2615.000
0.7407966	135.0000	1964.753	2433.000	2507.938	2658.000
0.7757397	138.0000	1992.513	2471.000	2547.769	2701.000

FORTRAN Programs

```
      PROGRAM SURF
*
* CREATE SYNTHETIC WIND-DRIVEN WATERWAVE SURFACE OF TWO SLOPE-COMPONENT
* (X & Y) ARRAYS (+ OPTIONAL ELEVATION ARRAY)
* CONVERT SLOPE-COMPONENT ARRAYS INTO MAXIMUM-SLOPE & SLOPE-AZIMUTH ARRAY
*
* INPUTS:
* WIND_V  = WIND_VELOCITY               [CM/SEC]  [ > 0 ] '
* Z       = HEIGHT OF WIND_V MEASUREMENT [CM]     [ > 0 ] '
* WIND_AZ = WIND_AZIMUTH                [DEG]     [-180..+180] '
* K_NYQ   = MAX_WAVENUMBER              [CY/CM]   [ > 0 ] '
* DELTA_K = DELTA_WAVENUMBER            [CY/CM]   [ > 0 ] '
*
      IMPLICIT NONE
      INTEGER I,I1,I2,J,J1,J2,N,N1,N2,N3,P,P1,P2,Q,Q1,Q2
      PARAMETER(N=64,P=-N/2,Q=N/2-1)
      PARAMETER(N1=64,P1=-N1/2,Q1=N1/2-1)
      INTEGER*4 ISEED
      INTEGER KCOR(P:Q,P:Q)
      REAL ANG0,ANG1,ANG2,ANG3,BIAS1,BIAS2,DELTA_K,K_NYQ,PI,SCALE1,SCALE2
      REAL SLOPE,SUM1,SUM2,TEMP,VAR_UD,VAR_US,VAR_CD,VAR_CS,VAR_SD,VAR_SS
      REAL WGHT,WIND_AZ,WIND_V,X1,Y1,X2,Y2,Z
      REAL F1(P:Q,P:Q),F2(P:Q,P:Q),F3(P:Q,P:Q),F4(P:Q,P:Q),W1(P:Q,P:Q)
      REAL DIST1(P1:Q1,P1:Q1),DIST2(P1:Q1,P1:Q1),FX1(P:Q,P:Q),FY1(P:Q,P:Q)
      REAL XDIST1(P1:Q1,2),XDIST2(P1:Q1,2),YDIST1(P1:Q1,2),YDIST2(P1:Q1,2)
      REAL PARM(-2:1,-2:1),VARY(0:4,0:4)
      REAL RY(P1:Q1,P1:Q1),IY(P1:Q1,P1:Q1),MY(P1:Q1,P1:Q1),PY(P1:Q1,P1:Q1)
***   COMPLEX G1(P:Q,P:Q),G2(P:Q,P:Q)
***   COMPLEX G3(P:Q,P:Q),G4(P:Q,P:Q)
      COMPLEX GX1(P:Q,P:Q),GY1(P:Q,P:Q),GWN(P:Q,P:Q)
      CHARACTER*1 OPT
      CHARACTER*18 FNAME
*
      PI=3.14159
*
      WRITE(*,*) ' '
      WRITE(*,*) 'ENTER FILENAME OF PARAMETERS = PARM'
***   READ(*,300) FNAME
      FNAME='PARM.DAT'
*
      WRITE(*,*) ' '
      WRITE(*,*) 'READING PARM..........'
      CALL PLT3DINPUT(FNAME,PARM,N3,-2,1)
*
      WRITE(*,*) ' '
      DO I=-2,1
      WRITE(*,*) (PARM(I,J),J=-2,1)
      END DO
*
      K_NYQ=PARM(-2,-2)
```

```
      DELTA_K=PARM(-2,-1)
      N2=INT(PARM(-2,0))
      N3=INT(PARM(-1,1))
      ISEED=JINT(PARM(-2,1))
      WIND_V=PARM(-1,-2)
      Z=PARM(-1,-1)
      WIND_AZ=PARM(-1,0)
*
      IF ((N.NE.N2).OR.((K_NYQ/DELTA_K).NE.FLOAT(N/2))) THEN
              WRITE(*,*) 'INCORRECT PARAMETER FILE [N(SURF)]'
              GOTO 5
      ENDIF
*
      IF (N1.NE.N3) THEN
              WRITE(*,*) 'INCORRECT PARAMETER FILE [N1(DOME)]'
              GOTO 5
      ENDIF
*
* CREATE N*N COMPLEX MATRIX GWN(L,M) OF NORMALIZED, FREQUENCY-DOMAIN
* WHITE GAUSSIAN NOISE
*
      CALL WGN_SPEC(W1,GWN,ISEED,N,P,Q)
*
      WIND_AZ=WIND_AZ*(PI/180.0)
*
      CALL SEA_SPEC(WIND_V,Z,WIND_AZ,DELTA_K,F1,F2,F3,F4,FX1,FY1,KCOR,N,P,Q)
*
      WRITE(*,*) ' '
      WRITE(*,*) 'TSLOPE = TOTAL (X+Y) SLOPE SPECTRUM=SQRT[(K^2)*S(L,M)]'
      IF (N.EQ.64) CALL ALPHA(F1,64)
      FNAME='TSLOPE.RAE'
      CALL PLT3DOUTPUT(FNAME,F1,N,P,Q)
***   CALL PLT3DFILE(F1,N)
*
      WRITE(*,*) ' '
      WRITE(*,*) 'HEIGHT = ELEVATION SPECTRUM=SQRT[S(L,M)]'
      IF (N.EQ.64) CALL ALPHA(F2,64)
      FNAME='HEIGHT.RAE'
      CALL PLT3DOUTPUT(FNAME,F2,N,P,Q)
***   CALL PLT3DFILE(F2,N)
*
      WRITE(*,*) ' '
      WRITE(*,*) 'XSLOPE = X-COMPONENT SLOPE SPECTRUM=SQRT[(L^2)*S(L,M)]'
      IF (N.EQ.64) CALL ALPHA(F3,64)
      FNAME='XSLOPE.RAE'
      CALL PLT3DOUTPUT(FNAME,F3,N,P,Q)
***   CALL PLT3DFILE(F3,N2)
*
      WRITE(*,*) ' '
      WRITE(*,*) 'YSLOPE = Y-COMPONENT SLOPE SPECTRUM=SQRT[(M^2)*S(L,M)]'
      IF (N.EQ.64) CALL ALPHA(F4,64)
      FNAME='YSLOPE.RAE'
```

```
      CALL PLT3DOUTPUT(FNAME,F4,N,P,Q)
***   CALL PLT3DFILE(F4,N)
*
* FILTER MATRIX GWN WITH SLOPE-COMPONENT SPECTRUMS FX1 & FY1
* OPTIONAL FILTERING OF TOTAL_SLOPE SPECTRUM G1 & ELEVATION SPECTRUM G2
*
      DO I=P,Q
      DO J=P,Q
*
***           G1(I,J)=CMPLX(0.0,F1(I,J))*GWN(I,J)
***           G2(I,J)=CMPLX(0.0,F2(I,J))*GWN(I,J)
              GX1(I,J)=CMPLX(0.0,FX1(I,J))*GWN(I,J)
              GY1(I,J)=CMPLX(0.0,FY1(I,J))*GWN(I,J)
*
      END DO
      END DO
*
* BACK-FOURIER-TRANSFORM THE FILTERED SLOPE-COMPONENT SPECTRUMS GX1 & GY1
* OPTIONAL BACK-FOURIER-TRANSFORM OF G1 & G2
*
***   CALL FFT2D(G1.N,+1)
***   CALL FFT2D(G2,N,+1)
      CALL FFT2D(GX1,N,+1)
      CALL FFT2D(GY1,N,+1)
*
* OPTIONAL COMPLEX DISPLAY (REAL,IMAG,MAG,PHS) OF G1,G2,GX1 & GX2
*
***   IF (N.EQ.64) THEN
***           CALL RALPH(G1,64,RY,IY,MY,PY)
***           CALL RALPH(G2,64,RY,IY,MY,PY)
***           CALL RALPH(GX1,64,RY,IY,MY,PY)
***           CALL RALPH(GY1,64,RY,IY,MY,PY)
***   ENDIF
*
      SCALE1=FLOAT(Q1)
      SCALE2=FLOAT(Q1)/90.0
      WIND_AZ=WIND_AZ*(180.0/PI)
      WGHT=1.0/FLOAT(N*N)
*
* RESCALE THE TRANSFORMED SLOPE-COMPONENT ARRAYS GX1 & GY1
* CONVERT SLOPE-COMPONENTS INTO MAXIMUM_SLOPE ARRAY=FY1(X,Y) [DEG] [0..+90]
* AND SLOPE AZIMUTH ARRAY=FX1(X,Y) [DEG] [-180..+180]
* CALCULATE ALONG-WIND, CROSS-WIND, & COMBINED VARIANCES
* CREATE SLOPE DISTRIBUTION ARRAYS=DIST(SLOPE,AZIMUTH) [PROBABILITY] [0..1]
*
      DO I=P,Q
      DO J=P,Q
*
              X1=TAN(REAL(GX1(I,J))*DELTA_K)
              Y1=TAN(REAL(GY1(I,J))*DELTA_K)
*
              IF (X1.NE.0.0) THEN
```

```
                FX1(I,J)=ATAN2D(Y1,X1)
            ELSE
                FX1(I,J)=0.0
            ENDIF
*
            SLOPE=SQRT((X1**2)+(Y1**2))
            FY1(I,J)=ATAND(SLOPE)
*
            ANG0=COSD(FX1(I,J))
            ANG1=SIND(FX1(I,J))
*
            X1=ANG0*SLOPE
            Y1=ANG1*SLOPE
*
            X2=ANG0*FY1(I,J)
            Y2=ANG1*FY1(I,J)
*
            ANG2=COSD(WIND_AZ-FX1(I,J))
            ANG3=SIND(WIND_AZ-FX1(I,J))
*
            VAR_UD=VAR_UD+WGHT*(ANG2*FY1(I,J))**2
            VAR_US=VAR_US+WGHT*(ANG2*SLOPE)**2
*
            VAR_CD=VAR_CD+WGHT*(ANG3*FY1(I,J))**2
            VAR_CS=VAR_CS+WGHT*(ANG3*SLOPE)**2
*
            VAR_SD=VAR_SD+WGHT*(FY1(I,J)**2)
            VAR_SS=VAR_SS+WGHT*(SLOPE**2)
*
            I1=INT(X1*SCALE1+SIGN(0.5,ANG0))
            J1=INT(Y1*SCALE1+SIGN(0.5,ANG1))
*
            I2=INT(X2*SCALE2+SIGN(0.5,ANG0))
            J2=INT(Y2*SCALE2+SIGN(0.5,ANG1))
*
            IF (ABS(I1*J1).LE.(Q1**2)) DIST1(I1,J1)=DIST1(I1,J1)+WGHT
            DIST2(I2,J2)=DIST2(I2,J2)+WGHT
*
        END DO
        END DO
*
        WRITE(*,*) ' '
        WRITE(*,*) 'WANT CROSS-SECTION DISTRIBUTIONS FOR PLT2D? [N]'
        READ(*,300) OPT
*
        IF ((OPT.EQ.'Y').OR.(OPT.EQ.'y')) THEN
*
            DO I=P1,Q1
            DO J=P1,Q1
*
                XDIST1(I,1)=FLOAT(I)/SCALE1
                XDIST1(I,2)=DIST1(I,0)
```

```
*
                        YDIST1(J,1)=FLOAT(J)/SCALE1
                        YDIST1(J,2)=DIST1(0,J)
*
                        XDIST2(I,1)=FLOAT(I)/SCALE2
                        XDIST2(I,2)=DIST2(I,0)
*
                        YDIST2(J,1)=FLOAT(J)/SCALE2
                        YDIST2(J,2)=DIST2(0,J)
*
                END DO
                END DO
*
                WRITE(*,*) ' '
                WRITE(*,*) 'CROSS-SECTION DISTRIBUTIONS FOR PLT2D'
                WRITE(*,*) ' '
                WRITE(*,*) 'XDIST1'
                CALL PLT2DFILE(XDIST1,N1)
                WRITE(*,*) ' '
                WRITE(*,*) 'YDIST1'
                CALL PLT2DFILE(YDIST1,N1)
                WRITE(*,*) ' '
                WRITE(*,*) 'XDIST2'
                CALL PLT2DFILE(XDIST2,N1)
                WRITE(*,*) ' '
                WRITE(*,*) 'YDIST2'
                CALL PLT2DFILE(YDIST2,N1)
*
        ENDIF

* BIAS ALL ZERO VALUES IN F3 FOR ALPHASCALE DISPLAY
*
***     BIAS1=0.02/-25.0
***     BIAS2=0.02/-25.0
*
***     DO I=P1,Q1
***     DO J=P1,Q1
***             IF (DIST1(I,J).EQ.0.0) DIST1(I,J)=BIAS1
***             IF (DIST2(I,J).EQ.0.0) DIST2(I,J)=BIAS2
***     END DO
***     END DO
*
        WRITE(*,*) ' '
        WRITE(*,*) 'SLOPE DISTRIBUTION ARRAY=DIST1 [PROB] (SLOPE COORDINATES)'
        IF (N1.EQ.64) CALL ALPHA(DIST1,64)
        FNAME='DIST1.RAE'
        CALL PLT3DOUTPUT(FNAME,DIST1,N1,P1,Q1)
***     CALL PLT3DFILE(DIST1,N1)
*
        WRITE(*,*) ' '
        WRITE(*,*) 'CROSS-WIND SLOPE VAR [SLOPE^2] & DEV= ',VAR_CS,SQRT(VAR_CS)
        WRITE(*,*) 'ALONG-WIND SLOPE VAR [SLOPE^2] & DEV= ',VAR_US,SQRT(VAR_US)
```

```
      WRITE(*,*) 'TOTAL-WIND SLOPE VAR [SLOPE^2] & DEV= ',VAR_SS,SQRT(VAR_SS)
*
      WRITE(*,*) ' '
      WRITE(*,*) 'SLOPE DISTRIBUTION ARRAY=DIST2 [PROB] (FILENAME=DIST.RAY)'
      IF (N1.EQ.64) CALL ALPHA(DIST2,64)
      FNAME='DIST2.RAE'
      CALL PLT3DOUTPUT(FNAME,DIST2,N1,P1,Q1)
***   CALL PLT3DFILE(DIST2,N1)
*
      WRITE(*,*) ' '
      WRITE(*,*) 'CROSS-WIND SLOPE VAR [DEG^2]   & DEV= ',VAR_CD,SQRT(VAR_CD)
      WRITE(*,*) 'ALONG-WIND SLOPE VAR [DEG^2]   & DEV= ',VAR_UD,SQRT(VAR_UD)
      WRITE(*,*) 'TOTAL-WIND SLOPE VAR [DEG^2]   & DEV= ',VAR_SD,SQRT(VAR_SD)
*
      K_NYQ=FLOAT(N/2)*DELTA_K
      CALL PSVARY1(K_NYQ,N,WIND_V,Z,VARY)
*
      WRITE(*,*) ' '
      WRITE(*,*) 'MAXIMUM-SLOPE ARRAY=BETA [DEG] (FILENAME=BETA.RAY)'
      IF (N.EQ.64) CALL ALPHA(FY1,64)
      FNAME='BETA.RAE'
      CALL PLT3DOUTPUT(FNAME,FY1,N,P,Q)
***   CALL PLT3DFILE(FY1,N)
*
      WRITE(*,*) ' '
      WRITE(*,*) 'SLOPE-AZIMUTH ARRAY=ALPH [DEG] (FILENAME=ALPH.RAY)'
      IF (N.EQ.64) CALL ALPHA(FX1,64)
      FNAME='ALPH.RAE'
      CALL PLT3DOUTPUT(FNAME,FX1,N,P,Q)
***   CALL PLT3DFILE(FX1,N)
*
300   FORMAT (A)
*
5     END
```

```
      PROGRAM LIGHTBLUE
*
* CREATE UNPOLARIZED SKYDOME HEMISPHERICAL RADIANCE DISTRIBUTION
* CREATE HORIZONTALLY_ & VERTICALLY_POLARIZED RADIANCE COMPONENTS
*
* MAP SKYDOME RADIANCE DISTRIBUTIONS TO REFLECTED SURFACE COORDINATES
*
* CREATE UNPOLARIZED SUBDOME HEMISPHERICAL RADIANCE DISTRIBUTION
* CREATE HORIZONTALLY_ & VERTICALLY_POLARIZED RADIANCE COMPONENTS
*
* LSUB IS ALREADY LINEARLY MAPPED TO REFRACTED SURFACE COORDINATES
*
* INPUT:
* LREF = REFERENCE RADIANCE MEASURED AT THE ZENITH POINT, LSKY(0,0) [UNIT]
* PHIO = SUN AZIMUTH [DEG] [-180..+180]
* THETA = SENSOR ZENITH ANGLE [DEG] [0..+90]
* ZO   = SOLAR ZENITH ANGLE [DEG] [0..+90]
*
* OUTPUT:
* LSKY = UNPOLARIZED SKYDOME SPATIAL RADIANCE DISTRIBUTION
* HSKY = HORIZONTALLY_POLARIZED LSKY
* VSKY = VERTICALLY_POLARIZED LSKY
*
* LSRF = LSKY MAPPED TO REFLECTED SURFACE COORDINATES (ALPH,BETA)
* HSRF = HSKY MAPPED TO REFLECTED SURFACE COORDINATES (ALPH,BETA)
* VSRF = VSKY MAPPED TO REFLECTED SURFACE COORDINATES (ALPH,BETA)
*
* LSUB = UNPOLARIZED SUBDOME SPATIAL RADIANCE DISTRIBUTION
* HSUB = HORIZONTALLY_POLARIZED LSUB
* VSUB = VERTICALLY_POLARIZED LSUB
*
      IMPLICIT NONE
      INTEGER I,J,N,N1,P,Q
      PARAMETER (N=64,P=-N/2,Q=N/2-1)
      REAL LSKY(P:Q,P:Q),HSKY(P:Q,P:Q),VSKY(P:Q,P:Q)
      REAL LSRF(P:Q,P:Q),HSRF(P:Q,P:Q),VSRF(P:Q,P:Q)
      REAL LSUB(P:Q,P:Q),HSUB(P:Q,P:Q),VSUB(P:Q,P:Q)
      REAL LREF,PHIO,PI,THETA,ZO
      REAL PARM(-2:1,-2:1)
      CHARACTER*18 FNAME
*
      PI=3.14159
*
      WRITE(*,*) 'ENTER FILENAME OF PARAMETERS = PARM'
      FNAME='PARM.DAT'
*
      WRITE(*,*) 'READING PARM..........'
      CALL PLT3DINPUT(FNAME,PARM,N1,-2,1)
*
      DO I=-2,1
      WRITE(*,*) (PARM(I,J),J=-2,1)
      END DO
```

```
*
        N1=INT(PARM(-1,1))
        THETA=PARM(0,-2)
        PHI0=PARM(0,-1)
        Z0=PARM(0,0)
        LREF=PARM(0,1)
*
        IF (N.NE.N1) THEN
                WRITE(*,*) 'INCORRECT PARAMETER FILE'
                GOTO 1
        ENDIF
*
***     WRITE(6,*) 'INPUT LREF [RADIANCE],PHI0 [DEG],Z0 [DEG],THETA [DEG] ='
***     READ(*,*) LREF,PHI0,Z0,THETA
*
        WRITE(*,*) 'LREF,PHI0,Z0,THETA=',LREF,PHI0,Z0,THETA
*
        PHI0=PHI0*(PI/180.0)
        Z0=Z0*(PI/180.0)
*
***     CALL SKYBLUE(LREF,PHI0,Z0,N,P,Q,LSKY,HSKY,VSKY)
*
        CALL SKYMAP(LREF,PHI0,Z0,THETA,N,P,Q,LSRF,HSRF,VSRF)
*
        CALL DEEPBLUE(LREF,Z0,N,P,Q,LSUB,HSUB,VSUB)
*
1       END
```

```
      PROGRAM LIGHT
*
 * CREATES OBJECT SPATIAL RADIANCE DISTRIBUTION IN THE DIRECTION OF SENSOR
 *
 * CALCULATES FORWARD FAST FOURIER TRANSFORMS OF SYNTHETIC IMAGES
 *
       IMPLICIT NONE
       INTEGER I,I1,I2,INV,J,J1,J2,N,N1,N2,NTMP,P,P1,P2,Q,Q1,Q2
*      PARAMETER(N=64,P=-N/2,Q=N/2-1)
*      PARAMETER(N1=64,P1=-N1/2,Q1=N1/2-1)
*      PARAMETER(N2=64,P2=-N2/2,Q2=N2/2-1)
       REAL IV1,IV2,IV3,NV1,NV2,NV3,RV1,RV2,RV3
       REAL D1(P:Q,P:Q),D2(P:Q,P:Q),D3(P:Q,P:Q),D4(P:Q,P:Q)
       REAL DARK1(P:Q,P:O),DARK2(P:Q,P:Q),DELTA
       REAL DST1(P:Q,P:Q),DST2(P:Q,P:Q),DST3(P:Q,P:Q),DST4(P:Q,P:Q)
       REAL GAMH(P:Q,P:Q),GAMS(P:Q,P:Q),GAMV(P:Q,P:Q)
       REAL HRAD(P1:Q1,P1:Q1),LRAD(P1:Q1,P1:Q1),VRAD(P1:Q1,P1:Q1)
       REAL HSKY(P:Q,P:Q),LSKY(P:Q,P:Q),VSKY(P:Q,P:Q)
       REAL HSUB(P:Q,P:Q),LSUB(P:Q,P:Q),VSUB(P:Q,P:Q)
       REAL PARM(-2:1,-2:1),V1250,VARY(0:4,0:4)
       REAL ALPH(P1:Q1,P1:Q1),COSALPHA,SINALPHA
*      REAL BETA(P1:Q1,P1:Q1),COSBETA,SINBETA
       REAL DEVA,DEVC,DEVT
       REAL GAMMAHOR,GAMMASUM,GAMMAVER
       REAL MU,COSMU,SINMU
       REAL NMBR(P:Q,P:Q),REF1,REF2,SWITCH
       REAL NU,COSNU,SINNU,TANNU1,TANNU2
       REAL OMEGA,COSOMEGA,SINOMEGA
*      REAL INDEXI,INDEXR,RHO,RHO1
       REAL THETA,COSTHETA,SINTHETA
       REAL DELTA_K,K_NYQ,PHI,PHI1,PHI2,RADIUS,RANGE,TEMP,WIND_V,WIND_AZ,Z
***    REAL RY(P:Q,P:Q),IY(P:Q,P:Q),MY(P:Q,P:Q),PY(P:Q,P:Q)
       REAL ATH1(P:Q,P:Q),ATS1(P:Q,P:Q),ATV1(P:Q,P:Q)
       REAL ATH2(P:Q,P:Q),ATS2(P:Q,P:Q),ATV2(P:Q,P:Q)
       REAL HMAG0(P1:Q1,P1:Q1),LMAG0(P1:Q1,P1:Q1),VMAG0(P1:Q1,P1:Q1)
       REAL HMAG1(P1:Q1,P1:Q1),LMAG1(P1:Q1,P1:Q1),VMAG1(P1:Q1,P1:Q1)
       REAL HMAG2(P1:Q1,P1:Q1),LMAG2(P1:Q1,P1:Q1),VMAG2(P1:Q1,P1:Q1)
       REAL HMAG3(P1:Q1,P1:Q1)
*      REAL RDH1(P2:Q2,P2:Q2),RDS1(P2:Q2,P2:Q2),RDV1(P2:Q2,P2:Q2)
       REAL RDH2(P:Q,P:Q),RDS2(P:Q,P:Q),RDV2(P:Q,P:Q)
       REAL RFLH(P1:Q1,P1:Q1),RFLS(P1:Q1,P1:Q1),RFLV(P1:Q1,P1:Q1)
       REAL RFLX(P1:Q1,P1:Q1)
       REAL RFRH(P1:Q1,P1:Q1),RFRS(P1:Q1,P1:Q1),RFRV(P1:Q1,P1:Q1)
       REAL HAVG,LAVG,VAVG,HAVG1,LAVG1,VAVG1,HAVG2,LAVG2,VAVG2,XAVG
       COMPLEX GD1(P2:Q2,P2:Q2),GH1(P2:Q2,P2:Q2),GV1(P2:Q2,P2:Q2)
*      COMPLEX GD2(P2:Q2,P2:Q2),GH2(P2:Q2,P2:Q2),GV2(P2:Q2,P2:Q2)
       COMPLEX SH0(P1:Q1,P1:Q1),SL0(P1:Q1,P1:Q1),SV0(P1:Q1,P1:Q1)
*      COMPLEX SH1(P1:Q1,P1:Q1),SL1(P1:Q1,P1:Q1),SV1(P1:Q1,P1:Q1)
       COMPLEX SH2(P1:Q1,P1:Q1),SL2(P1:Q1,P1:Q1),SV2(P1:Q1,P1:Q1)
       COMPLEX SH3(P1:Q1,P1:Q1)
       CHARACTER*18 FNAME0,FNAME1,FNAME2,FNAME3,FNAME4,FNAME5,FNAME6
       CHARACTER*18 FNAME7,FNAME8,FNAME
```

```
*
***      WRITE(*,*) 'ENTER FILENAME OF PARAMETERS = PARM'
***      READ(*,300) FNAME0
         FNAME0='PARM.DAT'
*
***      WRITE(*,*) 'ENTER FILENAME OF MAXIMUM_SLOPE ARRAY = BETA'
***      READ(*,300) FNAME1
         FNAME1='BETA.RAE'
*
***      WRITE(*,*) 'ENTER FILENAME OF SLOPE_AZIMUTH ARRAY = ALPH'
***      READ(*,300) FNAME2
*        FNAME2='ALPH.RAE'
*
***     WRITE(*,*) 'ENTER FILENAME OF SKYDOME_RADIANCE ARRAY = LSRF'
***     READ(*,300) FNAME3
***     FNAME3='LSRF.RAY'
*
***     WRITE(*,*) 'ENTER FILENAME OF HORZ-POLARIZED LSRF = HSRF'
***     READ(*,300) FNAME4
        FNAME4='HSRF.RAY'
*
***     WRITE(*,*) 'ENTER FILENAME OF VERT-POLARIZED LSRF = VSRF'
***     READ(*,300) FNAME5
        FNAME5='VSRF.RAY'
*
***     WRITE(*,*) 'ENTER FILENAME OF SUBDOME_RADIANCE ARRAY = LSUB'
***     READ(*,300) FNAME6
***     FNAME6='LSUB.RAY'
*
***     WRITE(*,*) 'ENTER FILENAME OF HORZ-POLARIZED LSUB = HSUB'
***     READ(*,300) FNAME7
        FNAME7='HSUB.RAY'
*
***     WRITE(*,*) 'ENTER FILENAME OF VERT-POLARIZED LSUB = VSUB'
***     READ(*,300) FNAME8
        FNAME8='VSUB.RAY'
*
        WRITE(*,*) 'READING PARM..........'
        CALL PLT3DINPUT(FNAME0,PARM,NTMP,-2,1)
*
        DO I=-2,1
                WRITE(*,*) (PARM(I,J),J=-2,1)
        END DO
*
        K_NYQ=PARM(-2,-2)
        DELTA_K=PARM(-2,-1)
        NTMP=INT(PARM(-2,0))
*
        IF ((N1.NE.NTMP).OR.((K_NYQ/DELTA_K).NE.FLOAT(NTMP/2))) THEN
                WRITE(*,*) 'INCORRECT PARAMETER FILE [N(SURF)]'
                GOTO 5
        ENDIF
```

```
*
      WIND_V=PARM(-1,-2)
      Z=PARM(-1,-1)
      WIND_AZ=PARM(-1,0)
      NTMP=INT(PARM(-1,1))
*
      IF (N.NE.NTMP) THEN
              WRITE(*,*) 'INCORRECT PARAMETER FILE [N1(DOME)]'
              GOTO 5
      ENDIF
*
      THETA=PARM(0,-2)
      RANGE=PARM(0,-1)
      INDEXR=PARM(1,-2)
      INDEXI=PARM(1,-1)
*
      WRITE(*,*) 'READING ARRAYS.......'
*
***   WRITE(*,*) 'READING BETA.........'
      CALL PLT3DINPUT(FNAME1,BETA,NTMP,P,Q)
*
      IF (N1.NE.NTMP) THEN
              WRITE(*,*) 'BETA & DEFAULT ARRAY SIZES DO NOT MATCH'
              GOTO 5
      ENDIF
*
***   WRITE(*,*) 'READING ALPH.........'
      CALL PLT3DINPUT(FNAME2,ALPH,NTMP,P,Q)
*
      IF (N1.NE.NTMP) THEN
              WRITE(*,*) 'ALPH & DEFAULT ARRAY SIZES DO NOT MATCH'
              GOTO 5
      ' ºIF
*
***     'TE(*,*) 'READING LSKY.........'
***   CALL PLT3DINPUT(FNAME3,LSKY,NTMP,P,Q)
*
***   IF (N.NE.NTMP) THEN
***           WRITE(*,*) 'LSKY & DEFAULT ARRAY SIZES DO NOT MATCH'
***           GOTO 5
***   ENDIF
*
***   WRITE(*,*) 'READING HSKY.........'
      CALL PLT3DINPUT(FNAME4,HSKY,NTMP,P,Q)
*
      IF (N.NE.NTMP) THEN
              WRITE(*,*) 'HSKY & DEFAULT ARRAY SIZES DO NOT MATCH'
              GOTO 5
      ENDIF
*
***   WRITE(*,*) 'READING VSKY.........'
      CALL PLT3DINPUT(FNAME5,VSKY,NTMP,P,Q)
```

```
*
        IF (N.NE.NTMP) THEN
                WRITE(*,*) 'VSKY & DEFAULT ARRAY SIZES DO NOT MATCH'
                GOTO 5
        ENDIF
*
***     WRITE(*,*) 'READING LSUB..........'
***     CALL PLT3DINPUT(FNAME6,LSUB,NTMP,P,Q)
*
***     IF (N.NE.NTMP) THEN
***             WRITE(*,*) 'LSUB & DEFAULT ARRAY SIZES DO NOT MATCH'
***             GOTO 5
***     ENDIF
*
***     WRITE(*,*) 'READING HSUB..........'
        CALL PLT3DINPUT(FNAME7,HSUB,NTMP,P,Q)
*
        IF (N.NE.NTMP) THEN
                WRITE(*,*) 'HSUB & DEFAULT ARRAY SIZES DO NOT MATCH'
                GOTO 5
        ENDIF
*
***     WRITE(*,*) 'READING VSUB..........'
        CALL PLT3DINPUT(FNAME8,VSUB,NTMP,P,Q)
*
        IF (N.NE.NTMP) THEN
                WRITE(*,*) 'VSUB & DEFAULT ARRAY SIZES DO NOT MATCH'
                GOTO 5
        ENDIF
*
***     WRITE(*,*) 'BETA'
***     IF (N1.EQ.64) CALL ALPHA(BETA,64)
*
***     WRITE(*,*) 'ALPH'
***     IF (N1.EQ.64) CALL ALPHA(ALPH,64)
*
***     WRITE(*,*) 'LSKY'
***     IF (N.EQ.64) CALL ALPHA(LSKY,64)
*
***     WRITE(*,*) 'HSKY'
***     IF (N.EQ.64) CALL ALPHA(HSKY,64)
*
***     WRITE(*,*) 'VSKY'
***     IF (N.EQ.64) CALL ALPHA(VSKY,64)
*
***     WRITE(*,*) 'LSUB'
***     IF (N.EQ.64) CALL ALPHA(LSUB,64)
*
***     WRITE(*,*) 'HSUB'
***     IF (N.EQ.64) CALL ALPHA(HSUB,64)
*
***     WRITE(*,*) 'VSUB'
```

```
***     IF (N.EQ.64) CALL ALPHA(VSUB,64)
*
* NOTE: NO SLOPE VARIANCE CALCULATIONS REQUIRED WHEN SURFACE IS FLAT
* IE: IF WIND_V = 0.0 THEN MEAN SLOPE = 0.0 AND SLOPE VARIANCE = 0.0
* SLOPE DISTRIBUTION = DELTA FUNCTION
*
        IF (WIND_V.EQ.0.0) GOTO 1
*
* CALCULATE ALONG-WIND, CROSS-WIND & TOTAL-WIND SLOPE VARIANCES ABOVE, BELOW
* & WITHIN THE SPATIAL (WAVENUMBER) FREQUENCY RANGE OF THE MODEL SURFACE
*
        CALL PSVARY2(K_NYQ,N,WIND_V,Z,V1250,VARY)
*
* CREATE HIGH_K_SLOPE_DISTRIBUTION ARRAY = DST1
* (K_NYQ < K < INF)
*   FOR CORRELATION OF SURFACE_REFLECTED_SKYDOME RADIANCE AND
*   FOR CORRELATION OF SURFACE_REFRACTED_SUBDOME RADIANCE
*
        WRITE(*,*) ' '
        WRITE(*,*) 'CALCULATING HIGH_K_SLOPE_DISTRIBUTIONS'
*
        DEVA=SQRT(VARY(4,3)-VARY(3,3))
        DEVC=SQRT(VARY(4,2)-VARY(3,2))
        WRITE(*,*) 'VAR_C,DEV_C     = ',DEVC**2,DEVC
        WRITE(*,*) 'VAR_A,DEV_A     = ',DEVA**2,DEVA
        DEVT=SQRT((DEVA**2)+(DEVC**2))
        WRITE(*,*) 'VAR_TOT,DEV_TOT = ',DEVT**2,DEVT
*
        CALL DIST_GEN(1,N,P,Q,WIND_AZ,V1250,DEVA,DEVC,D1,D2,D3,D4)
*
        DO I=P,Q
        DO J=P,Q
                IF (D3(I,J).GT.0.0) DST1(I,J)=D3(I,J)
                D1(I,J)=0.0
                D2(I,J)=0.0
                D3(I,J)=0.0
                D4(I,J)=0.0
        END DO
        END DO
*
* CREATE MID_K_SLOPE_DISTRIBUTION ARRAY = DST2
* (DELTA_K < K < INF)
*
***     WRITE(*,*) ' '
***     WRITE(*,*) 'CALCULATING MID_K_SLOPE_DISTRIBUTIONS
*
***     DEVA=SQRT(VARY(4,3)-VARY(2,3))
***     DEVC=SQRT(VARY(4,2)-VARY(2,2))
***     WRITE(*,*) 'VAR_C,DEV_C     = ',DEVC**2,DEVC
***     WRITE(*,*) 'VAR_A,DEV_A     = ',DEVA**2,DEVA
***     DEVT=SQRT((DEVA**2)+(DEVC**2))
***     WRITE(*,*) 'VAR_TOT,DEV_TOT = ',DEVT**2,DEVT
```

```
*
***     CALL DIST_GEN(1,N,P,Q,WIND_AZ,V1250,DEVA,DEVC,D1,D2,D3,D4)
*
***     DO I=P,Q
***     DO J=P,Q
***             IF (D3(I,J).GT.0.0) DST2(I,J)=D3(I,J)
***             D1(I,J)=0.0
***             D2(I,J)=0.0
***             D3(I,J)=0.0
***             D4(I,J)=0.0
***     END DO
***     END DO
*
* CREATE FULL_K_SLOPE_DISTRIBUTION ARRAY = DST3
* (0 < K < INF)
*
***     WRITE(*,*) ' '
***     WRITE(*,*) 'CALCULATING FULL_K_SLOPE_DISTRIBUTIONS
*
***     DEVA=SQRT(VARY(4,3)
***     DEVC=SQRT(VARY(4,2)
***     WRITE(*,*) 'VAR_C,DEV_C      = ',DEVC**2,DEVC
***     WRITE(*,*) 'VAR_A,DEV_A      = ',DEVA**2,DEVA
***     DEVT=SQRT((DEVA**2)+(DEVC**2))
***     WRITE(*,*) 'VAR_TOT,DEV_TO   = ',DEVT**2,DEVT
*
***     CALL DIST_GEN(1,N,P,Q,WIND_AZ,V1250,DEVA,DEVC,D1,D2,D3,D4)
*
***     DO I=P,Q
***     DO J=P,Q
***             IF (D3(I,J).GT.0.0) DST3(I,J)=D3(I,J)
***             D1(I,J)=0.0
***             D2(I,J)=0.0
***             D3(I,J)=0.0
***             D4(I,J)=0.0
***     END DO
***     END DO
*
* CREATE SAMPLE_K_SLOPE_DISTRIBUTION ARRAY = DST4
* (DELTA_K < K < K_NYQ)
*
***     WRITE(*,*) ' '
***     WRITE(*,*) 'CALCULATING SAMPLE_K_SLOPE_DISTRIBUTIONS'
*
***     DEVA=SQRT(VARY(3,3)-VARY(2,3))
***     DEVC=SQRT(VARY(3,2)-VARY(2,2))
***     WRITE(*,*) 'VAR_C,DEV_C       = ',DEVC**2,DEVC
***     WRITE(*,*) 'VAR_A,DEV_A       = ',DEVA**2,DEVA
***     DEVT=SQRT((DEVA**2)+(DEVC**2))
***     WRITE(*,*) 'VAR_TOT,DEV_TOT   = ',DEVT**2,DEVT
*
***     CALL DIST_GEN(1,N,P,Q,WIND_AZ,V1250,DEVA,DEVC,D1,D2,D3,D4)
```

```
*
***     DO I=P,Q
***     DO J=P,Q
***             IF (D3(I,J).GT.0.0) DST4(I,J)=D3(I,J)
***             D1(I,J)=0.0
***             D2(I,J)=0.0
***             D3(I,J)=0.0
***             D4(I,J)=0.0
***     END DO
***     END DO
*
* CALCULATE ANGULAR SURFACE_REFLECTED_SKYDOME_RADIANCE DISTRIBUTIONS:
*
* 1)CREATE ANGULAR POLARIZED (HORZ & VERT) FRESNEL_COEFFICIENT DISTRIBUTION
*   RELATIVE TO SENSOR AND SURFACE COORDINATES
*
*   CREATE ANGULAR SURFACE_PROJECTION_ATTENUATION_COEFFICIENT DISTRIBUTION
*   RELATIVE TO SENSOR AND SURFACE COORDINATES
*
1       CALL DARKNESS(P,Q,THETA,INDEXR,INDEXI,GAMH,GAMV,DARK1)
*
* 2)CREATE ATTENUATED_SKYDOME_RADIANCE DISTRIBUTIONS
*
        DO I=P,Q
        DO J=P,Q
*
        ATH1(I,J)=GAMH(I,J)*DARK1(I,J)*HSKY(I,J)
        ATV1(I,J)=GAMV(I,J)*DARK1(I,J)*VSKY(I,J)
        ATS1(I,J)=ATH1(I,J)+ATV1(I,J)
*
        IF (WIND_V.EQ.0.0) THEN
                RDH1(I,J)=ATH1(I,J)
                RDV1(I,J)=ATV1(I,J)
                RDS1(I,J)=ATS1(I,J)
        ENDIF
*
        END DO
        END DO
*
        IF (WIND_V.EQ.0.0) GOTO 2
*
        WRITE(*,*) 'ATH1 = ATTENUATED HORIZONTAL_SKYDOME_RADIANCE'
***     IF (N.EQ.64) CALL ALPHA(ATH1,64)
***     CALL PLT3DFILE(ATH1,N)
*
        WRITE(*,*) 'ATV1 = ATTENUATED VERTICAL_SKYDOME_RADIANCE'
***     IF (N.EQ.64) CALL ALPHA(ATV1,64)
***     CALL PLT3DFILE(ATV1,N)
*
        WRITE(*,*) 'ATS1 = ATTENTUATED TOTAL_SKYDOME_RADIANCE'
***     IF (N.EQ.64) CALL ALPHA(ATS1,64)
***     CALL PLT3DFILE(ATS1,N)
```

```
*
* 3)CORRELATE SKYDOME BY HIGH_K_WATER_SURFACE_FILTER=DST1 (K > K_NYQ)
*
        WRITE(*,*) 'DST1 = HIGH_K SLOPE PROBABILITY DISTRIBUTION'
***     IF (N.EQ.64) CALL ALPHA(DST1,64)
***     CALL PLT3DFILE(DST1,N)
*
        DO I=P,Q
        DO J=P,Q
                GD1(I,J)=CMPLX(DST1(-I,-J),0.0)
                GH1(I,J)=CMPLX(ATH1(I,J),0.0)
                GV1(I,J)=CMPLX(ATV1(I,J),0.0)
        END DO
        END DO
*
        CALL FFT2D(GD1,N2,-1)
        CALL FFT2D(GH1,N2,-1)
        CALL FFT2D(GV1,N2,-1)
*
        DO I=P2,Q2
        DO J=P2,Q2
                GH1(I,J)=GH1(I,J)*GD1(I,J)
                GV1(I,J)=GV1(I,J)*GD1(I,J)
        END DO
        END DO
*
        CALL FFT2D(GH1,N2,+1)
        CALL FFT2D(GV1,N2,+1)
*
        TEMP=FLOAT(N2*N2)
*
        DO I=P2,Q2
        DO J=P2,Q2
*
        RDH1(I,J)=CABS(GH1(I,J))/TEMP
        RDV1(I,J)=CABS(GV1(I,J))/TEMP
        RDS1(I,J)=RDH1(I,J)+RDV1(I,J)
*
        END DO
        END DO
*
2       WRITE(*,*) 'RDH1 = FILTERED ATH1'
***     IF (N2.EQ.64) CALL ALPHA(RDH1,64)
***     CALL PLT3DFILE(RDH1,N2)
*
        WRITE(*,*) 'RDV1 = FILTERED ATV1'
***     IF (N2.EQ.64) CALL ALPHA(RDV1,64)
***     CALL PLT3DFILE(RDV1,N2)
*
        WRITE(*,*) 'RDS1 = FILTERED ATS1'
***     IF (N2.EQ.64) CALL ALPHA(RDS1,64)
***     CALL PLT3DFILE(RDS1,N2)
```

```
*
* CALCULATE ANGULAR SUBSURFACE_REFRACTED_SUBDOME_RADIANCE DISTRIBUTIONS:
*
* 1)CREATE ANGULAR POLARIZED (HORZ & VERT) UPWELLING_RADIANCE DISTRIBUTION
*   RELATIVE TO SENSOR COORDINATES
*
*   CREATE ANGULAR SUBSURFACE_PROJECTION_ATTENUATION_COEFFICIENT DISTRIBUTION
*   RELATIVE TO SENSOR COORDINATES
*
* 2)CREATE ATTENUATED_SUBDOME_RADIANCE DISTRIBUTIONS
*
      DO I=P,Q
      DO J=P,Q
*
      ATH2(I,J)=DARK1(I,J)*HSUB(I,J)
      ATV2(I,J)=DARK1(I,J)*VSUB(I,J)
      ATS2(I,J)=ATH2(I,J)+ATV2(I,J)
*
***   IF (WIND_V.EQ.0.0) THEN
              RDH2(I,J)=ATH2(I,J)
              RDV2(I,J)=ATV2(I,J)
              RDS2(I,J)=ATS2(I,J)
***   ENDIF
*
      END DO
      END DO
*
      SWITCH = 1
      IF (SWITCH.EQ.1) GOTO 3
*
***   IF (WIND_V.EQ.0.0) GOTO 3
*
      WRITE(*,*) 'ATH2 = ATTENUATED HORZ_POLARIZED_SUBDOME_RADIANCE'
      IF (N.EQ.64) CALL ALPHA(ATH2,64)
      CALL PLT3DFILE(ATH2,N)
*
      WRITE(*,*) 'ATV2 = ATTENUATED VERT_POLARIZED_SUBDOME_RADIANCE'
      IF (N.EQ.64) CALL ALPHA(ATV2,64)
      CALL PLT3DFILE(ATV2,N)
*
      WRITE(*,*) 'ATS2 = ATTENTUATED TOTAL_SUBDOME_RADIANCE'
      IF (N.EQ.64) CALL ALPHA(ATS2,64)
      CALL PLT3DFILE(ATS2,N)
*
* 3)CORRELATE SUBDOME BY HIGH_K_WATER_SURFACE_FILTER=DST1 (K > K_NYQ)
* NOTE:DST1 WAS PREVIOUSLY FORWARD_TRANSORMED BY REFLECTION ALGORITHM
*
      DO I=P,Q
      DO J=P,Q
              GD2(I,J)=CMPLX(DST1(-I,-J),0.0)
              GH2(I,J)=CMPLX(ATH2(I,J),0.0)
              GV2(I,J)=CMPLX(ATV2(I,J),0.0)
```

```
      END DO
      END DO
*
      CALL FFT2D(GD2,N2,-1)
      CALL FFT2D(GH2,N2,-1)
      CALL FFT2D(GV2,N2,-1)
*
      DO I=P2,Q2
      DO J=P2,Q2
              GH2(I,J)=GH2(I,J)*GD2(I,J)
              GV2(I,J)=GV2(I,J)*GD2(I,J)
      END DO
      END DO
*
      CALL FFT2D(GH2,N2,+1)
      CALL FFT2D(GV2,N2,+1)
*
      TEMP=FLOAT(N2*N2)
*
      DO I=P2,Q2
      DO J=P2,Q2
*
      RDH2(I,J)=CABS(GH2(I,J))/TEMP
      RDV2(I,J)=CABS(GV2(I,J))/TEMP
      RDS2(I,J)=RDH2(I,J)+RDV2(I,J)
*
      END DO
      END DO
*
3     WRITE(*,*) 'RDH2 = FILTERED ATH2'
***   IF (N2.EQ.64) CALL ALPHA(RDH2,64)
***   CALL PLT3DFILE(RDH2,N2)
*
      WRITE(*,*) 'RDV2 = FILTERED ATV2'
***   IF (N2.EQ.64) CALL ALPHA(RDV2,64)
***   CALL PLT3DFILE(RDV2,N2)
*
      WRITE(*,*) 'RDS2 = FILTERED ATS2'
***   IF (N2.EQ.64) CALL ALPHA(RDS2,64)
***   CALL PLT3DFILE(RDS2,N2)
*
* CALCULATE REFLECTED & REFRACTED RADIANCE DISTRIBUTIONS IN DIRECTION OF SENSOR
*
      DELTA=90.0/FLOAT(Q)
      COSTHETA=COSD(THETA)
      SINTHETA=SIND(THETA)
*
* IV1,IV2,IV3 ARE THE RESOLVED COMPONENTS OF THE SENSOR COORDINATE VECTOR
*
      IV1=SINTHETA*SIND(180.0)
      IV2=SINTHETA*COSD(180.0)
      IV3=COSTHETA
```

```
*
      DO I=P1,Q1
      DO J=P1,Q1
*
      COSBETA=COSD(BETA(I,J))
      SINBETA=SIND(BETA(I,J))
      COSALPHA=COSD(ALPH(I,J))
      SINALPHA=SIND(ALPH(I,J))
*
* NV1,NV2,NV3 ARE THE RESOLVED COMPONENTS OF THE SURFACE NORMAL VECTOR
*
      NV1=SINBETA*SINALPHA
      NV2=SINBETA*COSALPHA
      NV3=COSBETA
*
* DOT PRODUCT OF IV & NV = |IV||NV|(COSOMEGA) = COSOMEGA
*
      COSOMEGA=(IV1*NV1)+(IV2*NV2)+(IV3*NV3)
      OMEGA=ACOSD(COSOMEGA)
      SINOMEGA=SIND(OMEGA)
*
* RV1,RV2,RV3 ARE THE RESOLVED COMPONENTS OF THE REFLECTED SKYDOME VECTOR
*
      RV1=(NV1*2.0*COSOMEGA)-IV1
      RV2=(NV2*2.0*COSOMEGA)-IV2
      RV3=(NV3*2.0*COSOMEGA)-IV3
*
      COSMU=RV3
      MU=ACOSD(COSMU)
      SINMU=SIND(MU)
*
      IF (MU.GT.0.0) THEN
             NU=ATAN2D(RV1,RV2)
      ELSE
             NU=0.0
      ENDIF
*
      COSNU=COSD(NU)
      SINNU=SIND(NU)
*
      RADIUS=MU/DELTA
      I2=INT(COSNU*(RADIUS+0.5))
      J2=INT(SINNU*(RADIUS+0.5))
*
      I1=INT(COSALPHA*(BETA(I,J)/DELTA)+0.5)
      J1=INT(SINALPHA*(BETA(I,J)/DELTA)+0.5)
*
      RFLH(I,J)=RDH1(I1,J1)
      RFLV(I,J)=RDV1(I1,J1)
      RFLS(I,J)=RFLH(I,J)+RFLV(I,J)
*
      RFRH(I,J)=RDV2(I1,J1)
```

```
      RFRV(I,J)=RDV2(I1,J1)
      RFRS(I,J)=RFRH(I,J)+RFRV(I,J)
*
      HRAD(I,J)=RFLH(I,J)+RFRH(I,J)
      VRAD(I,J)=RFLV(I,J)+RFRV(I,J)
      LRAD(I,J)=HRAD(I,J)+VRAD(I,J)
*
      IF (MU.LE.90.0) THEN
              RFLX(I,J)=ATH1(I1,J1)
              NMBR(I2,J2)=NMBR(I2,J2)+1.0
      ELSEIF (RDS1(I1,J1).GT.0.0) THEN
              REF1=REF1+1.0
              REF2=REF2+1.0
      ELSE
              REF2=REF2+1.0
      ENDIF
*
4     END DO
      END DO
*
      TEMP=FLOAT(N1*N1)
*
      DO I=P1,Q1
      DO J=P1,Q1
*
      SH1(I,J)=CMPLX(RFLH(I,J),0.0)
***   SV1(I,J)=CMPLX(RFLV(I,J),0.0)
      SL1(I,J)=CMPLX(RFLS(I,J),0.0)
*
      HAVG1=HAVG1+RFLH(I,J)/TEMP
      VAVG1=VAVG1+RFLV(I,J)/TEMP
      LAVG1=LAVG1+RFLS(I,J)/TEMP
*
***   SH2(I,J)=CMPLX(RFRH(I,J),0.0)
***   SV2(I,J)=CMPLX(RFRV(I,J),0.0)
***   SL2(I,J)=CMPLX(RFRS(I,J),0.0)
*
      HAVG2=HAVG2+RFRH(I,J)/TEMP
      VAVG2=VAVG2+RFRV(I,J)/TEMP
      LAVG2=LAVG2+RFRS(I,J)/TEMP
*
      SH0(I,J)=CMPLX(HRAD(I,J),0.0)
***   SV0(I,J)=CMPLX(VRAD(I,J),C.0)
      SL0(I,J)=CMPLX(LRAD(I,J),0.0)
*
      HAVG=HAVG+HRAD(I,J)/TEMP
      VAVG=VAVG+VRAD(I,J)/TEMP
      LAVG=LAVG+LRAD(I,J)/TEMP
*
      SH3(I,J)=CMPLX(RFLX(I,J),0.0)
*
      XAVG=XAVG+RFLX(I,J)/TEMP
```

```
*
      END DO
      END DO
*
      WRITE(*,*) ' '
      WRITE(*,*) 'SYNTHETIC RADIANCE IMAGES '
*
      WRITE(*,*) ' '
      WRITE(*,*) 'NMBR=PIXEL COUNTS REFLECTING FROM SKYDOME LOCATION'
***   IF (N.EQ.64) CALL ALPHA(NMBR,64)
***   CALL PLT3DFILE(NMBR,N)
*
      WRITE(*,*) ' '
      WRITE(*,*) 'NMBR OF 2NDARY REFLECTORS & RATIO = ',REF2,REF2/TEMP

      WRITE(*,*) '(IE PIXELS WITH MU > 90.0 DEGREES)'
*
      WRITE(*,*) ' '
      WRITE(*,*) 'NMBR THAT REFLECT SOME SKY & RATIO = ',REF1,REF1/TEMP

      WRITE(*,*) '(IE PIXELS WITH 90.0 DEGREES < MU < MU_MAX)'
*
      WRITE(*,*) ' '
      WRITE(*,*) 'RFLH=REFLECTED HORZ_POLARIZED RADIANCE'
      WRITE(*,*) 'MEAN PIXEL RADIANCE = ',HAVG1
***   IF (N1.EQ.64) CALL ALPHA(RFLH,64)
***   CALL PLT3DFILE(RFLH,N1)
*
      WRITE(*,*) ' '
      WRITE(*,*) 'RFLX=RFLH WITHOUT SUB-RESOLUTION FILTERING'
      WRITE(*,*) 'MEAN PIXEL RADIANCE = ',XAVG
***   IF (N1.EQ.64) CALL ALPHA(RFLX,64)
***   CALL PLT3DFILE(RFLX,N1)
*
      WRITE(*,*) ' '
      WRITE(*,*) 'RFLV=REFLECTED VERT_POLARIZED RADIANCE'
      WRITE(*,*) 'MEAN PIXEL RADIANCE = ',VAVG1
***   IF (N1.EQ.64) CALL ALPHA(RFLV,64)
***   CALL PLT3DFILE(RFLV,N1)
*
      WRITE(*,*) ' '
      WRITE(*,*) 'RFLS=REFLECTED TOTAL RADIANCE'
      WRITE(*,*) 'MEAN PIXEL RADIANCE = ',LAVG1
***   IF (N1.EQ.64) CALL ALPHA(RFLS,64)
***   CALL PLT3DFILE(RFLS,N1)
*
      WRITE(*,*) ' '
      WRITE(*,*) 'RFRH=REFRACTED HORZ_POLARIZED RADIANCE'
      WRITE(*,*) 'MEAN PIXEL RADIANCE = ',HAVG2
***   IF (N1.EQ.64) CALL ALPHA(RFRH,64)
***   CALL PLT3DFILE(RFRH,N1)
*
```

```
      WRITE(*,*) ' '
      WRITE(*,*) 'RFRV=REFRACTED VERT_POLARIZED RADIANCE'
      WRITE(*,*) 'MEAN PIXEL RADIANCE = ',VAVG2
***   IF (N1.EQ.64) CALL ALPHA(RFRV,64)
***   CALL PLT3DFILE(RFRV,N1)
*
      WRITE(*,*) ' '
      WRITE(*,*) 'RFRS=REFRACTED TOTAL RADIANCE'
      WRITE(*,*) 'MEAN PIXEL RADIANCE = ',LAVG2
***   IF (N1.EQ.64) CALL ALPHA(RFRS,64)
***   CALL PLT3DFILE(RFRS,N1)
*
      WRITE(*,*) ' '
      WRITE(*,*) 'HRAD=REFLECTED & REFRACTED HORZ_POLARIZED RADIANCE'
      WRITE(*,*) 'MEAN PIXEL RADIANCE = ',HAVG
***   IF (N1.EQ.64) CALL ALPHA(HRAD,64)
***   CALL PLT3DFILE(HRAD,N1)
*
      WRITE(*,*) ' '
      WRITE(*,*) 'VRAD=REFLECTED & REFRACTED VERT_POLARIZED RADIANCE'
      WRITE(*,*) 'MEAN PIXEL RADIANCE = ',VAVG
***   IF (N1.EQ.64) CALL ALPHA(VRAD,64)
***   CALL PLT3DFILE(VRAD,N1)
*
      WRITE(*,*) ' '
      WRITE(*,*) 'LRAD=REFLECTED & REFRACTED TOTAL RADIANCE'
      WRITE(*,*) 'MEAN PIXEL RADIANCE = ',LAVG
***   IF (N1.EQ.64) CALL ALPHA(LRAD,64)
***   CALL PLT3DFILE(LRAD,N1)
*
      CALL FFT2D(SL1,N1,-1)
      CALL FFT2D(SH1,N1,-1)
***   CALL FFT2D(SV1,N1,-1)
*
***   CALL FFT2D(SL2,N1,-1)
***   CALL FFT2D(SH2,N1,-1)
***   CALL FFT2D(SV2,N1,-1)
*
      CALL FFT2D(SL0,N1,-1)
      CALL FFT2D(SH0,N1,-1)
***   CALL FFT2D(SV0,N1,-1)
*
      CALL FFT2D(SH3,N1,-1)
*
      DO I=P1,Q1
      DO J=P1,Q1
*
      HMAG1(I,J)=CABS(SH1(I,J))/TEMP
***   VMAG1(I,J)=CABS(SV1(I,J))/TEMP
      LMAG1(I,J)=CABS(SL1(I,J))/TEMP
*
***   HMAG2(I,J)=CABS(SH2(I,J))/TEMP
```

```
***     VMAG2(I,J)=CABS(SV2(I,J))/TEMP
***     LMAG2(I,J)=CABS(SL2(I,J))/TEMP
*
        HMAG0(I,J)=CABS(SH0(I,J))/TEMP
***     VMAG0(I,J)=CABS(SV0(I,J))/TEMP
        LMAG0(I,J)=CABS(SL0(I,J))/TEMP
*
        HMAG3(I,J)=CABS(SH3(I,J))/TEMP
*
        END DO
        END DO
*
        WRITE(*,*) ' '
        WRITE(*,*) 'FORWARD TRANSFORMS OF RADIANCE IMAGES'
*
                WRITE(*,*) 'HMAG1= HORZ/REFLECTED RAD MAG SPECTRUM'
                TEMP=HMAG1(0,0)
                WRITE(*,*) 'HMAG1(0,0) = ',HMAG1(0,0)
***             HMAG1(0,0)=0.0
***             IF (N1.EQ.64) CALL ALPHA(HMAG1,64)
***             HMAG1(0,0)=TEMP
                FNAME='HMAG1.RAD'
                CALL PLT3DOUTPUT(FNAME,HMAG1,N1,P1,Q1)
***             CALL PLT3DFILE(HMAG1,N1)
*
                WRITE(*,*) 'HMAG3= HMAG1 WITHOUT SUB-RESOLUTION FILTER'
                TEMP=HMAG3(0,0)
                WRITE(*,*) 'HMAG3(0,0) = ',HMAG3(0,0)
***             HMAG3(0,0)=0.0
***             IF (N1.EQ.64) CALL ALPHA(HMAG3,64)
***             HMAG3(0,0)=TEMP
                FNAME='HMAG3.RAD'
                CALL PLT3DOUTPUT(FNAME,HMAG3,N1,P1,Q1)
***             CALL PLT3DFILE(HMAG3,N1)
*
                WRITE(*,*) 'LMAG1= TOTAL/REFLECTED RAD MAG SPECTRUM'
                TEMP=LMAG1(0,0)
                WRITE(*,*) 'LMAG1(0,0) = ',LMAG1(0,0)
***             LMAG1(0,0)=0.0
***             IF (N1.EQ.64) CALL ALPHA(LMAG1,64)
***             LMAG1(0,0)=TEMP
                FNAME='LMAG1.RAD'
                CALL PLT3DOUTPUT(FNAME,LMAG1,N1,P1,Q1)
***             CALL PLT3DFILE(LMAG1,N1)
*
                WRITE(*,*) 'HMAG0= HORZ/REFL & REFR RAD MAG SPECTRUM'
                TEMP=HMAG0(0,0)
                WRITE(*,*) 'HMAG0(0,0) = ',HMAG0(0,0)
***             HMAG0(0,0)=0.0
***             IF (N1.EQ.64) CALL ALPHA(HMAG0,64)
***             HMAG0(0,0)=TEMP
                FNAME='HMAG0.RAD'
```

```
               CALL PLT3DOUTPUT(FNAME,HMAGO,N1,P1,Q1)
***            CALL PLT3DFILE(HMAGO,N1)
*
               WRITE(*,*) 'LMAGO= TOTAL/REFL & REFR RAD MAG SPECTRUM'
               TEMP=LMAGO(0,0)
               WRITE(*,*) 'LMAGO(0,0) = ',LMAGO(0,0)
***            LMAGO(0,0)=0.0
***            IF (N1.EQ.64) CALL ALPHA(LMAGO,64)
***            LMAGO(0,0)=TEMP
               FNAME='LMAGO.RAD'
               CALL PLT3DOUTPUT(FNAME,LMAGO,N1,P1,Q1)
***            CALL PLT3DFILE(LMAGO,N1)
*
        GOTO 1000
5       WRITE(*,*) 'BAD FILE OPENING'
300     FORMAT (A)
1000    END
```

```
      PROGRAM ANALYS
*
*     ANALYSIS PROGRAM FOR THE GENERATION AND ANALYSIS OF 2D DIFFERENCE
*     SPECTRA
*
      IMPLICIT NONE
      INTEGER I,I1,I2,INV,J,J1,J2,KINT,N,N1,N2,NTMP,P,PHINT,P1,P2,Q,Q1,Q2,R
      PARAMETER(N=64,P=-N/2,Q=N/2-1,R=Q+1)
      PARAMETER(N1=64,P1=-N1/2,Q1=N1/2-1)
      PARAMETER(N2=64,P2=-N2/2,Q2=N2/2-1)
      REAL ANG0,ANG1,COSA1,COSA2,K,L,M,KMAG,DELTA_K,DELTA_PHI,PI,SINA1,SINA2
      REAL DAT1,DAT2,DAT3,DAT4,DAT5
      REAL DATH1,DATL1,DATH0,DATL0,DATH3,DATS0
      REAL DST1(P:Q,P:Q)
      REAL HIGH,LOW,FACTOR
      REAL FACTOR1,FACTOR2,FACTOR3,FACTOR4,FACTOR5
      REAL PARM(-2:1,-2:1),V1250
      REAL K_NYQ,PHI,PHI1,PHI2,RADIUS,RANGE,TEMP,TEMP1,WIND_V,WIND_AZ,Z
      REAL HMAG0(P1:Q1,P1:Q1),LMAG0(P1:Q1,P1:Q1),VMAG0(P1:Q1,P1:Q1)
      REAL HMAG1(P1:Q1,P1:Q1),LMAG1(P1:Q1,P1:Q1),VMAG1(P1:Q1,P1:Q1)
      REAL SLOPE(P1:Q1,P1:Q1),LMAG2(P1:Q1,P1:Q1),VMAG2(P1:Q1,P1:Q1)
      REAL HMAG3(P1:Q1,P1:Q1)
      REAL D1KH1(1:R,2),D1KL1(1:R,2)
      REAL D1KH0(1:R,2),D1KL0(1:R,2)
      REAL D1KH3(1:R,2)
*
      REAL SLP0(-90:90,2)
*
      REAL D1PH1(-90:+90,2),D1PL1(-90:+90,2)
      REAL D1PH0(-90:+90,2),D1PL0(-90:+90,2)
      REAL D1PH3(-90:+90,2)
      REAL D1FH1(-90:+90,2),D1FL1(-90:+90,2)
      REAL D1FH0(-90:+90,2),D1FL0(-90:+90,2)
      REAL D1FH3(-90:+90,2)
      REAL D2H1(P:Q,P:Q),D2L1(P:Q,P:Q)
      REAL D2H0(P:Q,P:Q),D2L0(P:Q,P:Q)
      REAL D2H3(P:Q,P:Q)
      REAL DIFA1,DIFC1,DIFS1
      REAL DIFA2,DIFC2,DIFS2
      REAL DIFA3,DIFC3,DIFS3
      REAL DIFA4,DIFC4,DIFS4
      REAL DIFA5,DIFC5,DIFS5
      REAL DIFX1,DIFY1
      REAL DIFX2,DIFY2
      REAL DIFX3,DIFY3
      REAL DIFX4,DIFY4
      REAL DIFX5,DIFY5
      REAL VARA0,VARC0,VARS0
      REAL VARA1,VARC1,VARS1
      REAL VARA2,VARC2,VARS2
      REAL VARA3,VARC3,VARS3
      REAL VARA4,VARC4,VARS4
```

```
      REAL VARA5,VARC5,VARS5
      REAL VARX0,VARY0
      REAL VARX1,VARY1
      REAL VARX2,VARY2
      REAL VARX3,VARY3
      REAL VARX4,VARY4
      REAL VARX5,VARY5
*
      REAL VARXX
*
      REAL DVRA1,DVRC1,DVRS1
      REAL DVRA2,DVRC2,DVRS2
      REAL DVRA3,DVRC3,DVRS3
      REAL DVRA4,DVRC4,DVRS4
      REAL DVRA5,DVRC5,DVRS5
      COMPLEX GD1(P2:Q2,P2:Q2),GH1(P2:Q2,P2:Q2),GV1(P2:Q2,P2:Q2)
      COMPLEX GD2(P2:Q2,P2:Q2),GH2(P2:Q2,P2:Q2),GV2(P2:Q2,P2:Q2)
      COMPLEX SH0(P1:Q1,P1:Q1),SL0(P1:Q1,P1:Q1),SV0(P1:Q1,P1:Q1)
      COMPLEX SH1(P1:Q1,P1:Q1),SL1(P1:Q1,P1:Q1),SV1(P1:Q1,P1:Q1)
      COMPLEX SH2(P1:Q1,P1:Q1),SL2(P1:Q1,P1:Q1),SV2(P1:Q1,P1:Q1)
      COMPLEX SH3(P1:Q1,P1:Q1)
      CHARACTER*18 FNAME0,FNAME1,FNAME2,FNAME3,FNAME4,FNAME5,FNAME6
      CHARACTER*18 FNAME7,FNAME8,FNAME
*
      PI=3.141593
*
      FNAME0='PARM.DAT'
      FNAME1='HMAG1.RAD'
      FNAME2='LMAG1.RAD'
      FNAME3='HMAG0.RAD'
      FNAME4='LMAG0.RAD'
      FNAME5='HMAG3.RAD'
      FNAME6='TSLOPE.RAE'
*
      CALL PLT3DINPUT(FNAME0,PARM,NTMP,-2,1)
*
      DO I=-2,1
             WRITE(*,*) (PARM(I,J),J=-2,1)
      END DO
*
      K_NYQ=PARM(-2,-2)
      DELTA_K=PARM(-2,-1)
      NTMP=INT(PARM(-2,0))
*
      IF ((N1.NE.NTMP)..OR.((K_NYQ/DELTA_K).NE.FLOAT(NTMP/2))) THEN
             WRITE(*,*) 'INCORRECT PARAMETER FILE [N(SURF)]'
             GOTO 5
      ENDIF
*
      WIND_AZ=PARM(-1,0)
      NTMP=INT(PARM(-1,1))
*
```

```
      IF (N.NE.NTMP) THEN
            WRITE(*,*) 'INCORRECT PARAMETER FILE [N1(DOME)]'
            GOTO 5
      ENDIF
*
      WRITE(*,*) 'READING ARRAYS........'
*
      CALL PLT3DINPUT(FNAME1,HMAG1,NTMP,P,Q)
      CALL PLT3DINPUT(FNAME2,LMAG1,NTMP,P,Q)
      CALL PLT3DINPUT(FNAME3,HMAG0,NTMP,P,Q)
      CALL PLT3DINPUT(FNAME4,LMAG0,NTMP,P,Q)
      CALL PLT3DINPUT(FNAME5,HMAG3,NTMP,P,Q)
      CALL PLT3DINPUT(FNAME6,SLOPE,NTMP,P,Q)
*
      DAT1=HMAG1(0,0)
      DAT2=LMAG1(0,0)
      DAT3=HMAG0(0,0)
      DAT4=LMAG0(0,0)
      DAT5=HMAG3(0,0)
*
      HMAG1(0,0)=0.0
      LMAG1(0,0)=0.0
      HMAG0(0,0)=0.0
      LMAG0(0,0)=0.0
      HMAG3(0,0)=0.0
*
***   WRITE(*,*) 'HMAG1'
***   IF (N1.EQ.64) CALL ALPHA(HMAG1,64)
*
***   WRITE(*,*) 'LMAG1'
***   IF (N1.EQ.64) CALL ALPHA(LMAG1,64)
*
***   WRITE(*,*) 'HMAG0'
***   IF (N.EQ.64) CALL ALPHA(HMAG0,64)
*
***   WRITE(*,*) 'LMAG0'
***   IF (N.EQ.64) CALL ALPHA(LMAG0,64)
*
***   WRITE(*,*) 'HMAG3'
***   IF (N.EQ.64) CALL ALPHA(HMAG3,64)
*
***   WRITE(*,*) 'SLOPE'
***   IF (N.EQ.64) CALL ALPHA(SLOPE,64)
*
      WRITE(*,*) 'HMAG1'
      IF (N1.EQ.64) CALL ALPHAS(HMAG1,64,DATH1,LOW,FACTOR)
*
      WRITE(*,*) 'LMAG1'
      IF (N1.EQ.64) CALL ALPHAS(LMAG1,64,DATL1,LOW,FACTOR)
*
      WRITE(*,*) 'HMAG0'
      IF (N.EQ.64) CALL ALPHAS(HMAG0,64,DATH0,LOW,FACTOR)
```

```
*
      WRITE(*,*) 'LMAG0'
      IF (N.EQ.64) CALL ALPHAS(LMAG0,64,DATL0,LOW,FACTOR)
*
      WRITE(*,*) 'HMAG3'
      IF (N.EQ.64) CALL ALPHAS(HMAG3,64,DATH3,LOW,FACTOR)
*
      WRITE(*,*) 'SLOPE'
      IF (N.EQ.64) CALL ALPHAS(SLOPE,64,DATS0,LOW,FACTOR)
*
      FACTOR1=DATS0/DATH1
      FACTOR2=DATS0/DATL1
      FACTOR3=DATS0/DATH0
      FACTOR4=DATS0/DATL0
      FACTOR5=DATS0/DATH3
*
      DO I=P,Q
      DO J=P,Q
      HMAG1(I,J)=HMAG1(I,J)*FACTOR1
      LMAG1(I,J)=LMAG1(I,J)*FACTOR2
      HMAG0(I,J)=HMAG0(I,J)*FACTOR3
      LMAG0(I,J)=LMAG0(I,J)*FACTOR4
      HMAG3(I,J)=HMAG3(I,J)*FACTOR5
*
      D2H1(I,J)=SLOPE(I,J)-HMAG1(I,J)
      D2L1(I,J)=SLOPE(I,J)-LMAG1(I,J)
      D2H0(I,J)=SLOPE(I,J)-HMAG0(I,J)
      D2L0(I,J)=SLOPE(I,J)-LMAG0(I,J)
      D2H3(I,J)=SLOPE(I,J)-HMAG3(I,J)
      END DO
      END DO
*
      WRITE(*,*) '2D DIFFERENCE SPECTRA'
*
      WRITE(*,*) ' '
      WRITE(*,*) 'D2H1=SLOPE-HMAG1'
      WRITE(*,*) 'MEAN PIXEL RADIANCE = ',DAT1
      WRITE(*,*) 'FACTOR1              = ',FACTOR1
***   IF (N.EQ.64) CALL ALPHA(D2H1,64)
***   CALL PLT3DFILE(D2H1,N)
*
      WRITE(*,*) ' '
      WRITE(*,*) 'D2L1=SLOPE-LMAG1'
      WRITE(*,*) 'MEAN PIXEL RADIANCE = ',DAT2
      WRITE(*,*) 'FACTOR2              = ',FACTOR2
***   IF (N.EQ.64) CALL ALPHA(D2L1,64)
***   CALL PLT3DFILE(D2L1,N)
*
      WRITE(*,*) ' '
      WRITE(*,*) 'D2H0=SLOPE-HMAG0'
      WRITE(*,*) 'MEAN PIXEL RADIANCE = ',DAT3
      WRITE(*,*) 'FACTOR3              = ',FACTOR3
```

```
***     IF (N.EQ.64) CALL ALPHA(D2H0,64)
***     CALL PLT3DFILE(D2H0,N)
*
        WRITE(*,*) ' '
        WRITE(*,*) 'D2L0=SLOPE-LMAG0'
        WRITE(*,*) 'MEAN PIXEL RADIANCE = ',DAT4
        WRITE(*,*) 'FACTOR4             = ',FACTOR4
        IF (N.EQ.64) CALL ALPHA(D2L0,64)
***     CALL PLT3DFILE(D2L0,N)
*
        WRITE(*,*) ' '
        WRITE(*,*) 'D2H3=SLOPE-HMAG3'
        WRITE(*,*) 'MEAN PIXEL RADIANCE = ',DAT5
        WRITE(*,*) 'FACTOR5             = ',FACTOR5
***     IF (N.EQ.64) CALL ALPHA(D2H3,64)
***     CALL PLT3DFILE(D2H3,N)
*
50      DO I=P,Q
        DO J=P,Q
*
        L=FLOAT(I)
        M=FLOAT(J)
        KMAG=SQRT((L**2)+(M**2))
        KINT=INT(KMAG+0.5)
        K=KMAG*DELTA_K
*
        IF ((K.EQ.0.0).OR.(KINT.GT.R)) GOTO 10

        ANG0=ATAN2D(M,L)
        ANG1=WIND_AZ-ANG0
*
        IF (ABS(ANG0).LE.90.0) THEN
                PHINT=INT(ANG0+SIGN(0.5,ANG0))
        ELSE
                PHINT=INT((ANG0-SIGN(180.0,ANG0))-SIGN(0.5,ANG0))
        ENDIF
*
        IF (ABS(PHINT).GT.90.0) WRITE(*,*) 'PHINT.GT.+/- 90.0'
*
        COSA1=COSD(ANG0)**2
        SINA1=SIND(ANG0)**2
        COSA2=COSD(ANG1)**2
        SINA2=SIND(ANG1)**2
*
        TEMP=(SLOPE(I,J)**2)*(DELTA_K**2)
        VARS0=VARS0+TEMP
        VARA0=VARA0+TEMP*COSA2
        VARC0=VARC0+TEMP*SINA2
        VARX0=VARX0+TEMP*COSA1
        VARY0=VARY0+TEMP*SINA1
*
        TEMP=(HMAG1(I,J)**2)*(DELTA_K**2)
```

```
      TEMP1=(D2H1(I,J)**2)*(DELTA_K**2)
      VARS1=VARS1+TEMP
      VARA1=VARA1+TEMP*COSA2
      VARC1=VARC1+TEMP*SINA2
      VARX1=VARX1+TEMP*COSA1
      VARY1=VARY1+TEMP*SINA1
      DIFX1=DIFX1+TEMP1*COSA1
      DIFY1=DIFY1+TEMP1*SINA1
      DIFS1=DIFS1+TEMP1
      DIFA1=DIFA1+TEMP1*COSA2
      DIFC1=DIFC1+TEMP1*SINA2
      D1KH1(KINT,2)=D1KH1(KINT,2)+(TEMP1/DELTA_K)
      D1PH1(PHINT,2)=D1PH1(PHINT,2)+(TEMP1/DELTA_K)
      D1PH1(PHINT,1)=D1PH1(PHINT,1)+1.0
*
      TEMP=(LMAG1(I,J)**2)*(DELTA_K**2)
      TEMP1=(D2L1(I,J)**2)*(DELTA_K**2)
      VARS2=VARS2+TEMP
      VARA2=VARA2+TEMP*COSA2
      VARC2=VARC2+TEMP*SINA2
      VARX2=VARX2+TEMP*COSA1
      VARY2=VARY2+TEMP*SINA1
      DIFX2=DIFX2+TEMP1*COSA1
      DIFY2=DIFY2+TEMP1*SINA1
      DIFS2=DIFS2+TEMP1
      DIFA2=DIFA2+TEMP1*COSA2
      DIFC2=DIFC2+TEMP1*SINA2
***   D1KL1(KINT,2)=D1KL1(KINT,2)+(TEMP1/DELTA_K)
***   D1PL1(PHINT,2)=D1PL1(PHINT,2)+(TEMP1/DELTA_K)
***   D1PL1(PHINT,1)=D1PL1(PHINT,1)+1.0
*
      TEMP=(HMAG0(I,J)**2)*(DELTA_K**2)
      TEMP1=(D2H0(I,J)**2)*(DELTA_K**2)
      VARS3=VARS3+TEMP
      VARA3=VARA3+TEMP*COSA2
      VARC3=VARC3+TEMP*SINA2
      VARX3=VARX3+TEMP*COSA1
      VARY3=VARY3+TEMP*SINA1
      DIFX3=DIFX3+TEMP1*COSA1
      DIFY3=DIFY3+TEMP1*SINA1
      DIFS3=DIFS3+TEMP1
      DIFA3=DIFA3+TEMP1*COSA2
      DIFC3=DIFC3+TEMP1*SINA2
***   D1KH0(KINT,2)=D1KH0(KINT,2)+(TEMP1/DELTA_K)
***   D1PH0(PHINT,2)=D1PH0(PHINT,2)+(TEMP1/DELTA_K)
***   D1PH0(PHINT,1)=D1PH0(PHINT,1)+1.0
*
      TEMP=(LMAG0(I,J)**2)*(DELTA_K**2)
      TEMP1=(D2L0(I,J)**2)*(DELTA_K**2)
      VARS4=VARS4+TEMP
      VARA4=VARA4+TEMP*COSA2
      VARC4=VARC4+TEMP*SINA2
```

```
          VARX4=VARX4+TEMP*COSA1
          VARY4=VARY4+TEMP*SINA1
          DIFX4=DIFX4+TEMP1*COSA1
          DIFY4=DIFY4+TEMP1*SINA1
          DIFS4=DIFS4+TEMP1
          DIFA4=DIFA4+TEMP1*COSA2
          DIFC4=DIFC4+TEMP1*SINA2
          D1KL0(KINT,2)=D1KL0(KINT,2)+(TEMP1/DELTA_K)
          D1PL0(PHINT,2)=D1PL0(PHINT,2)+(TEMP1/DELTA_K)
          D1PL0(PHINT,1)=D1PL0(PHINT,1)+1.0
*
          TEMP=(HMAG3(I,J)**2)*(DELTA_K**2)
          TEMP1=(D2H3(I,J)**2)*(DELTA_K**2)
          VARS5=VARS5+TEMP
          VARA5=VARA5+TEMP*COSA2
          VARC5=VARC5+TEMP*SINA2
          VARX5=VARX5+TEMP*COSA1
          VARY5=VARY5+TEMP*SINA1
          DIFX5=DIFX5+TEMP1*COSA1
          DIFY5=DIFY5+TEMP1*SINA1
          DIFS5=DIFS5+TEMP1
          DIFA5=DIFA5+TEMP1*COSA2
          DIFC5=DIFC5+TEMP1*SINA2
          D1KH3(KINT,2)=D1KH3(KINT,2)+(TEMP1/DELTA_K)
          D1PH3(PHINT,2)=D1PH3(PHINT,2)+(TEMP1/DELTA_K)
          D1PH3(PHINT,1)=D1PH3(PHINT,1)+1.0
*
10        END DO
          END DO
*
          DO I=1,R
                  D1KH1(I,1)=FLOAT(I)*DELTA_K
***               D1KL1(I,1)=FLOAT(I)*DELTA_K
***               D1KH0(I,1)=FLOAT(I)*DELTA_K
                  D1KL0(I,1)=FLOAT(I)*DELTA_K
                  D1KH3(I,1)=FLOAT(I)*DELTA_K
          END DO
*
          DO I=-90,+90
                  D1FH1(I,1)=FLOAT(I)
***               D1FL1(I,1)=FLOAT(I)
***               D1FH0(I,1)=FLOAT(I)
                  D1FL0(I,1)=FLOAT(I)
                  D1FH3(I,1)=FLOAT(I)
*
                  IF (D1PH1(I,1).GT.0.0) D1PH1(I,2)=D1PH1(I,2)/D1PH1(I,1)
***               IF (D1PL1(I,1).GT.0.0) D1PL1(I,2)=D1PL1(I,2)/D1PL1(I,1)
***               IF (D1PH0(I,1).GT.0.0) D1PH0(I,2)=D1PH0(I,2)/D1PH0(I,1)
                  IF (D1PL0(I,1).GT.0.0) D1PL0(I,2)=D1PL0(I,2)/D1PL0(I,1)
                  IF (D1PH3(I,1).GT.0.0) D1PH3(I,2)=D1PH3(I,2)/D1PH3(I,1)
*
          END DO
```

```
*
      DO I=-90,+90
*
      IF ((I.GT.-89).AND.(I.LT.89)) THEN
            D1FH1(I,2)=(D1PH1(I-1,2)+D1PH1(I,2)+D1PH1(I+1,2))/3.0
***         D1FL1(I,2)=(D1PL1(I-1,2)+D1PL1(I,2)+D1PL1(I+1,2))/3.0
***         D1FH0(I,2)=(D1PH0(I-1,2)+D1PH0(I,2)+D1PH0(I+1,2))/3.0
            D1FL0(I,2)=(D1PL0(I-1,2)+D1PL0(I,2)+D1PL0(I+1,2))/3.0
            D1FH3(I,2)=(D1PH3(I-1,2)+D1PH3(I,2)+D1PH3(I+1,2))/3.0
      ELSEIF (I.EQ.-90) THEN
            D1FH1(I,2)=(D1PH1(+89,2)+D1PH1(I,2)+D1PH1(I+1,2))/3.0
***         D1FL1(I,2)=(D1PL1(+89,2)+D1PL1(I,2)+D1PL1(I+1,2))/3.0
***         D1FH0(I,2)=(D1PH0(+89,2)+D1PH0(I,2)+D1PH0(I+1,2))/3.0
            D1FL0(I,2)=(D1PL0(+89,2)+D1PL0(I,2)+D1PL0(I+1,2))/3.0
            D1FH3(I,2)=(D1PH3(+89,2)+D1PH3(I,2)+D1PH3(I+1,2))/3.0
      ELSEIF (I.EQ.+90) THEN
            D1FH1(I,2)=(D1PH1(I-1,2)+D1PH1(I,2)+D1PH1(-89,2))/3.0
***         D1FL1(I,2)=(D1PL1(I-1,2)+D1PL1(I,2)+D1PL1(-89,2))/3.0
***         D1FH0(I,2)=(D1PH0(I-1,2)+D1PH0(I,2)+D1PH0(-89,2))/3.0
            D1FL0(I,2)=(D1PL0(I-1,2)+D1PL0(I,2)+D1PL0(-89,2))/3.0
            D1FH3(I,2)=(D1PH3(I-1,2)+D1PH3(I,2)+D1PH3(-89,2))/3.0
      ENDIF
*
      END DO
*
      WRITE(*,*) '             PARAMETERS'
      WRITE(*,*) '           ',PARM(-2,-2),PARM(-2,-1),PARM(-2,0),PARM(-2,1)

      WRITE(*,*) '           ',PARM(-1,-2),PARM(-1,-1),PARM(-1,0),PARM(-1,1)

      WRITE(*,*) '           ',PARM(+0,-2),PARM(+0,-1),PARM(+0,0),PARM(+0,1)

      WRITE(*,*) '           ',PARM(+1,-2),PARM(+1,-1),PARM(+1,0),PARM(+1,1)
      WRITE(*,*) ' '
*
      WRITE(*,*) '             MAGNITUDE ARRAY SCALING FACTORS'
      WRITE(*,*) '             H1(0,0),HIGH,FACTOR',DAT1,DATH1,FACTOR1
      WRITE(*,*) '             L1(0,0),HIGH,FACTOR',DAT2,DATL1,FACTOR2
      WRITE(*,*) '             H0(0,0),HIGH,FACTOR',DAT3,DATH0,FACTOR3
      WRITE(*,*) '             L0(0,0),HIGH,FACTOR',DAT4,DATL0,FACTOR4
      WRITE(*,*) '             H3(0,0),HIGH,FACTOR',DAT5,DATH3,FACTOR5
      WRITE(*,*) ' '
*
      WRITE(*,*) '             INTEGRATED VARIANCE FROM POWER SPECTRA'
      WRITE(*,*) '             VAR S0 A,C,S',VARA0,VARC0,VARS0
      WRITE(*,*) '             VAR H1 A,C,S',VARA1,VARC1,VARS1
      WRITE(*,*) '             VAR L1 A,C,S',VARA2,VARC2,VARS2
      WRITE(*,*) '             VAR H0 A,C,S',VARA3,VARC3,VARS3
      WRITE(*,*) '             VAR L0 A,C,S',VARA4,VARC4,VARS4
      WRITE(*,*) '             VAR H3 A,C,S',VARA5,VARC5,VARS5
      WRITE(*,*) ' '
*
```

```
      WRITE(*,*) '             VAR S0 X,Y,S',VARX0,VARY0,VARS0
      WRITE(*,*) '             VAR H1 X,Y,S',VARX1,VARY1,VARS1
      WRITE(*,*) '             VAR L1 X,Y,S',VARX2,VARY2,VARS2
      WRITE(*,*) '             VAR H0 X,Y,S',VARX3,VARY3,VARS3
      WRITE(*,*) '             VAR L0 X,Y,S',VARX4,VARY4,VARS4
      WRITE(*,*) '             VAR H3 X,Y,S',VARX5,VARY5,V/ 5
      WRITE(*,*) ' '
*
      WRITE(*,*) '             INTEGRATED SQUARED DEVIATION FROM DIF SPECTRA'
      WRITE(*,*) '             DIF H1 A,C,S',DIFA1,DIFC1,DIFS1
      WRITE(*,*) '             DIF L1 A,C,S',DIFA2,DIFC2,DIFS2
      WRITE(*,*) '             DIF H0 A,C,S',DIFA3,DIFC3,DIFS3
      WRITE(*,*) '             DIF L0 A,C,S',DIFA4,DIFC4,DIFS4
      WRITE(*,*) '             DIF H3 A,C,S',DIFA5,DIFC5,DIFS5
      WRITE(*,*) ' '
*
      WRITE(*,*) '             DIF H1 X,Y,S',DIFX1,DIFY1,DIFS1
      WRITE(*,*) '             DIF L1 X,Y,S',DIFX2,DIFY2,DIFS2
      WRITE(*,*) '             DIF H0 X,Y,S',DIFX3,DIFY3,DIFS3
      WRITE(*,*) '             DIF L0 X,Y,S',DIFX4,DIFY4,DIFS4
      WRITE(*,*) '             DIF H3 X,Y,S',DIFX5,DIFY5,DIFS5
      WRITE(*,*) ' '
*
* WRITE DATA TO FILE
*
      WRITE(*,*) 'ENTER FILENAME TO CONTAIN STATISTICS'
      READ(*,300) FNAME0
      OPEN(1,FILE=FNAME0,STATUS='NEW',ERR=5)
*
      WRITE(1,*) '            ',FNAME0
      WRITE(1,*) ' '
      WRITE(1,*) '             PARAMETERS'
      WRITE(1,*) '           ',PARM(-2,-2),PARM(-2,-1),PARM(-2,0),PARM(-2,1)

      WRITE(1,*) '           ',PARM(-1,-2),PARM(-1,-1),PARM(-1,0),PARM(-1,1)

      WRITE(1,*) '           ',PARM(+0,-2),PARM(+0,-1),PARM(+0,0),PARM(+0,1)

      WRITE(1,*) '           ',PARM(+1,-2),PARM(+1,-1),PARM(+1,0),PARM(+1,1)
      WRITE(1,*) ' '
*
      WRITE(1,*) '             MAGNITUDE ARRAY SCALING FACTORS'
      WRITE(1,*) '             H1(0,0),HIGH,FACTOR',DAT1,DATH1,FACTOR1
      WRITE(1,*) '             L1(0,0),HIGH,FACTOR',DAT2,DATL1,FACTOR2
      WRITE(1,*) '             H0(0,0),HIGH,FACTOR',DAT3,DATH0,FACTOR3
      WRITE(1,*) '             L0(0,0),HIGH,FACTOR',DAT4,DATL0,FACTOR4
      WRITE(1,*) '             H3(0,0),HIGH,FACTOR',DAT5,DATH3,FACTOR5
      WRITE(1,*) ' '
*
      WRITE(1,*) '             INTEGRATED VARIANCE FROM POWER SPECTRA'
      WRITE(1,*) '             VAR S0 A,C,S',VARA0,VARC0,VARS0
      WRITE(1,*) '             VAR H1 A,C,S',VARA1,VARC1,VARS1
```

```
      WRITE(1,*) '            VAR L1 A,C,S',VARA2,VARC2,VARS2
      WRITE(1,*) '            VAR H0 A,C,S',VARA3,VARC3,VARS3
      WRITE(1,*) '            VAR L0 A,C,S',VARA4,VARC4,VARS4
      WRITE(1,*) '            VAR H3 A,C,S',VARA5,VARC5,VARS5
      WRITE(1,*) ' '
*
      WRITE(1,*) '            VAR S0 X,Y,S',VARX0,VARY0,VARS0
      WRITE(1,*) '            VAR H1 X,Y,S',VARX1,VARY1,VARS1
      WRITE(1,*) '            VAR L1 X,Y,S',VARX2,VARY2,VARS2
      WRITE(1,*) '            VAR H0 X,Y,S',VARX3,VARY3,VARS3
      WRITE(1,*) '            VAR L0 X,Y,S',VARX4,VARY4,VARS4
      WRITE(1,*) '            VAR H3 X,Y,S',VARX5,VARY5,VARS5
      WRITE(1,*) ' '
*
      WRITE(1,*) '            INTEGRATED SQUARED DEVIATION FROM DIF SPECTRA'
      WRITE(1,*) '            DIF H1 A,C,S',DIFA1,DIFC1,DIFS1
      WRITE(1,*) '            DIF L1 A,C,S',DIFA2,DIFC2,DIFS2
      WRITE(1,*) '            DIF H0 A,C,S',DIFA3,DIFC3,DIFS3
      WRITE(1,*) '            DIF L0 A,C,S',DIFA4,DIFC4,DIFS4
      WRITE(1,*) '            DIF H3 A,C,S',DIFA5,DIFC5,DIFS5
      WRITE(1,*) ' '
*
      WRITE(1,*) '            DIF H1 X,Y,S',DIFX1,DIFY1,DIFS1
      WRITE(1,*) '            DIF L1 X,Y,S',DIFX2,DIFY2,DIFS2
      WRITE(1,*) '            DIF H0 X,Y,S',DIFX3,DIFY3,DIFS3
      WRITE(1,*) '            DIF L0 X,Y,S',DIFX4,DIFY4,DIFS4
      WRITE(1,*) '            DIF H3 X,Y,S',DIFX5,DIFY5,DIFS5
      WRITE(1,*) ' '
*
      CLOSE(1)
*
      FNAME1='K1.DT'
      FNAME2='K2.DT'
      FNAME3='K3.DT'
      FNAME4='K4.DT'
      FNAME5='K5.DT'
*
*     CALL PLT2DOUTPUT(FNAME1,D1KH1,R)
***   CALL PLT2DOUTPUT(FNAME2,D1KL1,R)
***   CALL PLT2DOUTPUT(FNAME3,D1KH0,R)
*     CALL PLT2DOUTPUT(FNAME4,D1KL0,R)
*     CALL PLT2DOUTPUT(FNAME5,D1KH3,R)
*
      FNAME1='P1.DT'
      FNAME2='P2.DT'
      FNAME3='P3.DT'
      FNAME4='P4.DT'
      FNAME5='P5.DT'
*
      CALL PLT2DOUTPUT(FNAME1,D1FH1,181)
*     CALL PLT2DOUTPUT(FNAME2,D1FL1,181)
*     CALL PLT2DOUTPUT(FNAME3,D1FH0,181)
```

```
      CALL PLT2DOUTPUT(FNAME4,D1FL0,181)
      CALL PLT2DOUTPUT(FNAME5,D1FH3,181)
*
      GOTO 1000
5     WRITE(*,*) 'BAD FILE OPENING'
300   FORMAT (A)
1000  END
```

```
      PROGRAM PSVARY
      IMPLICIT NONE
      INTEGER I,J,N,P,Q
      REAL A,ALPH,BETA,D,DELT,DELTA_K,ENUG,G,K,K_MAX,KNU,K1,K2,K3
      REAL L,M,P2,PI,SPEC
      REAL VAR,VAR1,VAR2,VAR3,VAR4,VAR5,VAR6,VAR7,VAR8,VAR9,VAR10,VAR11
      REAL VAR12,VAR13,VAR14,VAR15,VAR16
      REAL V_FRIC,V_MIN,V250,V1000,V1250,V1950,WIND_V,Z
      REAL F1(-800:400,2),F2(-800:400,2),F3(-800:400,2),F4(-800:400,2)
      REAL F5(-800:400,2)
*
      A=1.0
      ALPH=0.0081
* ALPH=PHILLIPS CONSTANT [ ]
      BETA=0.74
* BETA=    [UNITLESS]
      ENUG=1.473E-4
* ENUG=E/(NU*G) [UNITLESS]
      G=980.0
* G=ACCELERATION OF GRAVITY [CM/SEC^2]
      K2=0.359
* [1/CM]
      K3=0.942
* [1/CM]
      K_MAX=3.63
* [1/CM]
      PI=3.141593
*
      V_MIN=12.0
* V_MIN=MINIMUM FRICTION VELOCITY [CM/SEC]
*
      WRITE(*,*) 'ENTER WIND_V [CM/SEC^2] & Z [CM] '
      READ(*,*) WIND_V,Z
*
* WIND_V=WIND VELOCITY AT HEIGHT Z [CM/SEC^2]
* Z=HEIGHT OF WIND_V MEASUREMENT ABOVE WATER SURFACE [CM]
*
      CALL WIND(WIND_V,Z,V_FRIC,V250,V1000,V1250,V1950)
*
      D=(1.274+(0.0268*V_FRIC)+(6.03E-5*(V_FRIC**2)))**2
      K1=(K2*(V_MIN**2))/(V_FRIC**2)
      KNU=(0.5756*SQRT(V_FRIC)*K_MAX)/(D**0.16667)
      P2=LOG10(D/(V_FRIC/V_MIN))/LOG10(K3/K2)
*
      DELT=0.010
      VAR=0.0
*
      DO I=-800,400
      L=FLOAT(I-200)*DELT
      K=EXP(L)
      F1(I,1)=K
      F2(I,1)=LOG10(K)
```

```
      F3(I,1)=LOG10(K)
      F4(I,1)=LOG10(K)
      F5(I,1)=K
*
      IF ((0.0.LT.K).AND.(K.LE.K1)) THEN
      SPEC=(ALPH/(2.0*(K**3)))*EXP((-1.0*BETA*(G**2))/((V1950**4)*(K**2)))
      GOTO 1
      ENDIF
*
      IF ((K1.LT.K).AND.(K.LE.K2)) THEN
      SPEC=ALPH/(2.0*SQRT(K1)*(K**2.5))
      GOTO 1
      ENDIF
*
      IF ((K2.LT.K).AND.(K.LE.K3)) THEN
      SPEC=(ALPH*D)/(2.0*(K3**P2)*(K**(3.0-P2)))
      GOTO 1
      ENDIF
*
      IF ((K3.LT.K).AND.(K.LE.KNU)) THEN
      SPEC=(ALPH*D)/(2.0*(K**3))
      GOTO 1
      ENDIF
*
      IF (KNU.LT.K) THEN
      SPEC=(ENUG*(V_FRIC**3)*(K_MAX**6))/(K**9)
      ENDIF
*
1     F1(I,2)=(K**2)*SPEC
      F5(I,2)=SQRT((K**2)*SPEC)
      F2(I,2)=(K**3)*SPEC
      F3(I,2)=(K*SPEC)
      F4(I,2)=(K**5)*SPEC
      VAR=VAR+(F2(I,2)*DELT)
*
***   WRITE(*,*) L,K,VAR
*
      IF (EXP(L-DELT).LE.0.0030000) VAR1=VAR
      IF (EXP(L-DELT).LE.0.0046875) VAR2=VAR
      IF (EXP(L-DELT).LE.0.0093750) VAR3=VAR
      IF (EXP(L-DELT).LE.0.0187500) VAR4=VAR
      IF (EXP(L-DELT).LE.0.0375000) VAR5=VAR
      IF (EXP(L-DELT).LE.0.0750000) VAR6=VAR
      IF (EXP(L-DELT).LE.0.1500000) VAR7=VAR
      IF (EXP(L-DELT).LE.0.3000000) VAR8=VAR
      IF (EXP(L-DELT).LE.0.6000000) VAR9=VAR
      IF (EXP(L-DELT).LE.1.2000000) VAR10=VAR
      IF (EXP(L-DELT).LE.2.4000000) VAR11=VAR
      IF (EXP(L-DELT).LE.4.8000000) VAR12=VAR
      IF (EXP(L-DELT).LE.9.6000000) VAR13=VAR
      IF (EXP(L-DELT).LE.19.200000) VAR14=VAR
      IF (EXP(L-DELT).LE.38.200000) VAR15=VAR
```

```
      IF (EXP(L-DELT).LE.300.00000) VAR16=VAR
*
      END DO
*
      WRITE(*,*) 'CUM SLOPE VARIANCE UP TO 0.0030000/CM = ',VAR1
      WRITE(*,*) 'CUM SLOPE VARIANCE UP TO 0.0046875/CM = ',VAR2
      WRITE(*,*) 'CUM SLOPE VARIANCE UP TO 0.0093750/CM = ',VAR3
      WRITE(*,*) 'CUM SLOPE VARIANCE UP TO 0.0187500/CM = ',VAR4
      WRITE(*,*) 'CUM SLOPE VARIANCE UP TO 0.0375000/CM = ',VAR5
      WRITE(*,*) 'CUM SLOPE VARIANCE UP TO 0.0750000/CM = ',VAR6
      WRITE(*,*) 'CUM SLOPE VARIANCE UP TO 0.1500000/CM = ',VAR7,VAR7-VAR2
      WRITE(*,*) 'CUM SLOPE VARIANCE UP TO 0.3000000/CM = ',VAR8,VAR8-VAR3
      WRITE(*,*) 'CUM SLOPE VARIANCE UP TO 0.6000000/CM = ',VAR9,VAR9-VAR4
      WRITE(*,*) 'CUM SLOPE VARIANCE UP TO 1.2000000/CM = ',VAR10,VAR10-VAR5
      WRITE(*,*) 'CUM SLOPE VARIANCE UP TO 2.4000000/CM = ',VAR11,VAR11-VAR6
      WRITE(*,*) 'CUM SLOPE VARIANCE UP TO 4.8000000/CM = ',VAR12,VAR12-VAR7
      WRITE(*,*) 'CUM SLOPE VARIANCE UP TO 9.6000000/CM = ',VAR13,VAR13-VAR8
      WRITE(*,*) 'CUM SLOPE VARIANCE UP TO 19.200000/CM = ',VAR14,VAR14-VAR9
      WRITE(*,*) 'CUM SLOPE VARIANCE UP TO 38.400000/CM = ',VAR15,VAR15-VAR10
      WRITE(*,*) 'CUM SLOPE VARIANCE UP TO 300.00000/CM = ',VAR16
      WRITE(*,*) 'TOTAL SLOPE VARIANCE =                  ',VAR
*
      WRITE(*,*) 'K^2*SPEC VS K'
      CALL PLT2DFILE(F1,1201)
*
      WRITE(*,*) 'K^2*SPEC VS K'
      CALL PLT2DFILE(F5,1201)
*
      WRITE(*,*) 'K^3*SPEC VS LOG10(K)'
      CALL PLT2DFILE(F2,1201)
*
      WRITE(*,*) 'K^1*SPEC VS LOG10(K)'
      CALL PLT2DFILE(F3,1201)
*
      WRITE(*,*) 'K^5*SPEC VS LOG10(K)'
      CALL PLT2DFILE(F4,1201)
*
      END
```

FORTRAN Subroutines

```
      SUBROUTINE ALPHA(MAT1,N)
      IMPLICIT NONE
      INTEGER I,J,K,L,M,N
      REAL MAT1(N,64),LOW,HIGH,FACTOR,Q
      CHARACTER*1 CHOICE,LTR
      CHARACTER*64 A,B,C,D,TEMP,PICS(208)
*
      WRITE(*,*) 'WANT AN ALPHASCALE IMAGE? [N]'
      READ(*,300) CHOICE
      IF (CHOICE.NE.'Y') GOTO 2
*
      LOW=MAT1(1,1)
      HIGH=MAT1(1,1)
      DO I=1,N
              DO J=1,64
                      IF (MAT1(I,J).LT.LOW) LOW=MAT1(I,J)
                      IF (MAT1(I,J).GT.HIGH) HIGH=MAT1(I,J)
              END DO
      END DO
*
      IF (HIGH.LT.0.0) THEN
      HIGH=0.0
      FACTOR=LOW/-26.5
      GOTO 1
      ENDIF
*
      IF (LOW.GT.0.0) THEN
      LOW=0.0
      FACTOR=HIGH/26.5
      GOTO 1
      ENDIF
*
      IF (HIGH.GE.-1.0*LOW) THEN
      FACTOR=HIGH/26.5
      ELSE
      FACTOR=LOW/-26.5
      ENDIF
*
      IF (FACTOR.EQ.0.0) FACTOR=1.0
*
1     WRITE(*,*) 'ALPHASCALE:HIGH,LOW,FACTOR =',HIGH,LOW,FACTOR
*
      DO I=N,1,-1
      M=I-N/2-1
      TEMP=' '
              DO J=1,64
              K=INT((MAT1(I,J))/FACTOR)
              IF (K.GT.0) THEN
                      L=K+64
                      LTR=CHAR(L)
```

```
          ELSEIF (K.LT.0) THEN
                  L=-1*K+96
                  LTR=CHAR(L)
          ELSE
                  LTR=CHAR(32)
          ENDIF
          TEMP=TEMP(1:J-1)//LTR
          END DO
  WRITE(*,*) TEMP,' ',M
  PICS(N-I+1)=TEMP
  END DO
*
  A='                                                                '
  B='------------------------------- ++++++++++++++++++++++++++++++++'
  C='3332222222222111111111100000000000000000001111111111222222222233'
  D='2109876543210987654321098765432101234567890123456789012345678901'

  WRITE(*,*) A
  WRITE(*,*) B
  WRITE(*,*) C
  WRITE(*,*) D
*
  PICS(N+1)=A
  PICS(N+2)=B
  PICS(N+3)=C
  PICS(N+4)=D
*
  CALL PICFILE(PICS,N,HIGH,LOW,FACTOR)
*
2 RETURN
300 FORMAT (A)
  END


  SUBROUTINE ALPHAS(MAT1,N,HIGH,LOW,FACTOR)
  IMPLICIT NONE
  INTEGER I,J,K,L,M,N
  REAL MAT1(N,64),LOW,HIGH,FACTOR,Q
  CHARACTER*1 CHOICE,LTR
  CHARACTER*64 A,B,C,D,TEMP,PICS(208)
*
  LOW=MAT1(1,1)
  HIGH=MAT1(1,1)
  DO I=1,N
          DO J=1,64
                  IF (MAT1(I,J).LT.LOW) LOW=MAT1(I,J)
                  IF (MAT1(I,J).GT.HIGH) HIGH=MAT1(I,J)
          END DO
  END DO
*
  IF (HIGH.LT.0.0) THEN
  HIGH=0.0
```

```
      FACTOR=LOW/-26.5
      GOTO 1
      ENDIF
*
      IF (LOW.GT.0.0) THEN
      LOW=0.0
      FACTOR=HIGH/26.5
      GOTO 1
      ENDIF
*
      IF (HIGH.GE.-1.0*LOW) THEN
      FACTOR=HIGH/26.5
      ELSE
      FACTOR=LOW/-26.5
      ENDIF
*
      IF (FACTOR.EQ.0.0) FACTOR=1.0
*
*
1     WRITE(*,*) 'WANT AN ALPHASCALE IMAGE? [N]'
      READ(*,300) CHOICE
      IF (CHOICE.NE.'Y') GOTO 2
      WRITE(*,*) 'ALPHASCALE:HIGH,LOW,FACTOR =',HIGH,LOW,FACTOR
*
      DO I=N,1,-1
      M=I-N/2-1
      TEMP=' '
              DO J=1,64
              K=INT((MAT1(I,J))/FACTOR).
              IF (K.GT.0) THEN
                      L=K+64
                      LTR=CHAR(L)
              ELSEIF (K.LT.0) THEN
                      L=-1*K+96
                      LTR=CHAR(L)
              ELSE
                      LTR=CHAR(32)
              ENDIF
              TEMP=TEMP(1:J-1)//LTR
              END DO
      WRITE(*,*) TEMP,' ',M
      PICS(N-I+1)=TEMP
      END DO
*
      A=' '
      B='-------------------------------- +++++++++++++++++++++++++++++++'
      C='3332222222222111111111100000000000000000001111111111222222222233'
      D='2109876543210987654321098765432101234567890123456789012345678901'

      WRITE(*,*) A
      WRITE(*,*) B
      WRITE(*,*) C
```

```
      WRITE(*,*) D
*
      PICS(N+1)=A
      PICS(N+2)=B
      PICS(N+3)=C
      PICS(N+4)=D
*
      CALL PICFILE(PICS,N,HIGH,LOW,FACTOR)
*
2     RETURN
300   FORMAT (A)
      END


      SUBROUTINE CHECKERBOARD(X,N)
      IMPLICIT NONE
      INTEGER I,J,N
      COMPLEX X(1:N,1:N)
      DO I=1,N
              DO J=1,N
              X(I,J)=X(I,J)*(-1.0)**((I-1)+(J-1))
              END DO
      END DO
      RETURN
      END


      SUBROUTINE DARKNESS(P,Q,THETA,INDEXR,INDEXI,GAMH,GAMV,DARK)
*
* CREATES POLARIZED (HORZ & VERT) FRESNEL_COEFFICIENT DISTRIBUTIONS
* RELATIVE TO SENSOR AND SURFACE COORDINATES
*
* CREATES SURFACE_PROJECTION_ATTENUATION_COEFFICIENT DISTRIBUTION
* RELATIVE TO SENSOR AND SURFACE COORDINATES
*
      IMPLICIT NONE
      INTEGER I,J,N,P,Q
      REAL I1,I2,I3,N1,N2,N3,R1,R2,R3
      REAL ALPH,COSALPHA,SINALPHA
      REAL BETA,COSBETA,SINBETA,SECBETA
      REAL DELTA,GAMMAHOR,GAMMAPAR,GAMMAPER,GAMMASUM,GAMMAVER
      REAL DARK(P:Q,P:Q),GAMH(P:Q,P:Q),GAMV(P:Q,P:Q)
      REAL DRK1(-32:31,-32:31),DRK2(-32:31,-32:31),GAMS(-32:31,-32:31)
      REAL L,M,MU,COSMU,SINMU
      REAL NU,COSNU,SINNU
      REAL OMEGA,COSOMEGA,COSOMEGA2,SINOMEGA
      REAL INDEXI,INDEXR,RHO,RHO1
      REAL PI,PROJECT,R0,THETA
      REAL PHI,PHI1,PHI2,RADIUS
*
      DELTA=90.0/FLOAT(Q)
      N=Q-P+1
```

```
      PI=3.141593
      RO=(INDEXR-1.0)**2/(INDEXR+1.0)**2
*
      WRITE(*,*) ' '
      WRITE(*,*) 'THETA,INDEXR,INDEXI,RO= ',THETA,INDEXR,INDEXI,RO
*
* I1,I2,I3 ARE THE RESOLVED COMPONENTS OF THE SENSOR COORDINATE VECTOR
*
      I1=SIND(THETA)*COSD(180.0)
      I2=SIND(THETA)*SIND(180.0)
      I3=COSD(THETA)*(+1.0)
*
      DO I=P,Q
      DO J=P,Q
*
      L=INT(I)*DELTA
      M=INT(J)*DELTA
      MU=SQRT((L**2)+(M**2))
*
      IF (MU.GT.FLOAT(Q)*DELTA) GOTO 1
*
      IF (MU.GT.0.0) THEN
              NU=ATAN2D(M,L)
      ELSE
              NU=0.0
      ENDIF
*
* N1,N2,N3 ARE THE RESOLVED COMPONENTS OF THE SURFACE NORMAL VECTOR
*
      N1=SIND(MU)*COSD(NU)
      N2=SIND(MU)*SIND(NU)
      N3=COSD(MU)*(+1.0)
*
* DOT PRODUCT OF I & N = |I||N|(COSOMEGA) = COSOMEGA
*
      COSOMEGA=(I1*N1)+(I2*N2)+(I3*N3)
      OMEGA=ACOSD(COSOMEGA)
      SINOMEGA=SIND(OMEGA)
*
      IF (COSOMEGA.LE.0.0) GOTO 1
*
      BETA=MU
*
      IF (BETA.GT.60.0) BETA=60.0
***   IF (BETA.LT.90.0) THEN
              SECBETA=1.0/(COSD(BETA))
***   ELSE
***           SECBETA=0.0
***   ENDIF
*
      PROJECT=COSOMEGA*SECBETA
      DARK(I,J)=PROJECT
```

```
*
        IF (SINOMEGA.EQ.0.0) THEN
                GAMMAHOR=R0
                GAMMAVER=R0
                GOTO 3
        ENDIF
*
        RHO=ASIND(SINOMEGA/INDEXR)
        GAMMAHOR=(SIND(OMEGA-RHO)**2)/(SIND(OMEGA+RHO)**2)
        GAMMAVER=(TAND(OMEGA-RHO)**2)/(TAND(OMEGA+RHO)**2)
*
3       GAMMASUM=0.5*(GAMMAHOR+GAMMAVER)
*
                GAMH(I,J)=GAMMAHOR
                GAMV(I,J)=GAMMAVER
*
                IF (N.EQ.64) THEN
                        GAMS(I,J)=GAMMASUM
                        DRK1(I,J)=SECBETA
                        DRK2(I,J)=COSOMEGA
                ENDIF
*
1       END DO
        END DO
*
        IF (N.EQ.64) THEN
                WRITE(*,*) 'GAMH= HORZ_POLARIZED FRESNEL COEFF DISTRIBUTION'
***             CALL ALPHA(GAMH,64)
***             CALL PLT3DFILE(GAMH,64)
*
                WRITE(*,*) 'GAMV= VERT_POLARIZED FRESNEL COEFF DISTRIBUTION'
***             CALL ALPHA(GAMV,64)
***             CALL PLT3DFILE(GAMV,64)
*
                WRITE(*,*) 'GAMS= UNPOLARIZED FRESNEL COEFF DISTRIBUTION'
***             CALL ALPHA(GAMS,64)
***             CALL PLT3DFILE(GAMS,64)
*
                WRITE(*,*) 'DRK1= ACTUAL AREA OF SLOPING SURFACE'
***             CALL ALPHA(DRK1,64)
***             CALL PLT3DFILE(DRK1,64)
*
                WRITE(*,*) 'DRK2= PROJECTION OF AREA NORMAL TO INCIDENCE'
***             CALL ALPHA(DRK2,64)
***             CALL PLT3DFILE(DRK2,64)
*
                WRITE(*,*) 'DARK= DRK1*DRK2= SECBETA*COSOMEGA'
***             CALL ALPHA(DARK,64)
***             CALL PLT3DFILE(DARK,64)
        ENDIF
*
        RETURN
```

```
5       WRITE(*,*) 'BAD FILE OPENING'
300     FORMAT (A)
        END


        SUBROUTINE DEEPBLUE(LREF,Z0,N,P,Q,LSUB,HSUB,VSUB)
*
* CREATE UNPOLARIZED SUBDOME HEMISPHERICAL RADIANCE DISTRIBUTION
* RESOLVE HORIZONTALLY & VERTICALLY POLARIZED RADIANCE COMPONENTS
* BASED UPON THE MONTE CARLO RESULTS OF PLASS, KATTAWAR & GUINN [1976]
*
* INPUT:
* LREF = REFERENCE RADIANCE MEASURED AT THE ZENITH POINT, LSKY(0,0) [UNIT]
* Z0   = SOLAR ZENITH ANGLE
*
* OUTPUT:
* LSUB = UNPOLARIZED SUBDOME HEMISPHERICAL RADIANCE DISTRIBUTION
* HSUB = HORIZONTALLY_POLARIZED LSUB
* VSUB = VERTICALLY_POLARIZED LSUB
*
        IMPLICIT NONE
        INTEGER I,J,N,P,Q
        REAL LSUB(P:Q,P:Q),HSUB(P:Q,P:Q),VSUB(P:Q,P:Q)
        REAL A,B,C,COSMU,COSMU2,COSNU,L,LREF,M,MU,PHI,PI,PSI,R0,THETA,Z0
        CHARACTER*18 FNAME
*
        PI=3.14159
*
        DO I=P+1,Q
        DO J=P+1,Q
*
        L=FLOAT(I)
        M=FLOAT(J)
        THETA=(PI/2.0)*(SQRT((L**2)+(M**2))/FLOAT(Q))
                IF (THETA.GT.PI/2.0) THEN
                        LSUB(I,J)=0.0
                        HSUB(I,J)=0.0
                        VSUB(I,J)=0.0
                        GOTO 4
                ENDIF
*
                IF (THETA.GT.0.0) THEN
                        PHI=ATAN2D(M,L)
                ELSE
                        PHI=0.0
                ENDIF
*
        A=COS(Z0)**2
        B=(SIN(1.1*Z0))**SQRT(3.0)
        C=0.32*(10.0**B)
        R0=0.02
        LSUB(I,J)=LREF*R0*C*((1.0+(COS(A*THETA)**2))/2.0)
```

```
*
* CALCULATE HORIZONTALLY_ & VERTICALLY_POLARIZED FRACTIONS
* VIA RANDOM SCATTERING MODEL
*
      HSUB(I,J)=LSUB(I,J)*0.5
      VSUB(I,J)=HSUB(I,J)
*
4     END DO
      END DO
*
***   WRITE(*,*) 'LSUB = UNPOLARIZED SUBDOME RADIANCE DISTRIBUTION'
***   IF (N.EQ.64) CALL ALPHA(LSUB,64)
      FNAME='LSUB.RAY'
***   CALL PLT3DOUTPUT(FNAME,LSUB,N,P,Q)
***   CALL PLT3DFILE(LSUB,N)
*
      WRITE(*,*) 'HSUB = HORIZONTALLY_POLARIZED LSUB'
      IF (N.EQ.64) CALL ALPHA(HSUB,64)
      FNAME='HSUB.RAY'
      CALL PLT3DOUTPUT(FNAME,HSUB,N,P,Q)
***   CALL PLT3DFILE(HSUB,N)
*
      WRITE(*,*) 'VSUB = VERTICALLY_POLARIZED LSUB'
      IF (N.EQ.64) CALL ALPHA(VSUB,64)
      FNAME='VSUB.RAY'
      CALL PLT3DOUTPUT(FNAME,VSUB,N,P,Q)
***   CALL PLT3DFILE(VSUB,N)
*
      RETURN
      END


      SUBROUTINE DIST_GEN(OPT,N1,P,Q,WIND_AZ,V1250,DEVA,DEVC,D1,D2,D3,D4)
*
* CREATES SURFACE SLOPE PROBABILITY DISTRIBUTIONS
*
* OUTPUTS:
* D1      = UNNORMALIZED GAUSSIAN DISTRIBUTION      (MIN PROB < 1/N1^2)
* D2      = UNNORMALIZED GRAM-CHARLIER DISTRIBUTION (MIN PROB < 1/N1^2)
* D3      =   NORMALIZED GAUSSIAN DISTRIBUTION      (MIN PROB = 1/N1^2)
* D4      =   NORMALIZED GRAM-CHARLIER DISTRIBUTION (MIN PROB = 1/N1^2)
*
* INPUTS:
* OPT     = SELECT 1 OF 2 DISTRIBUTION TYPES:
*             1 = SLOPE ANGLE [DEG]
*             2 = SLOPE ANGLE [TAND(DEG)]
* N1      = SPATIAL ARRAY SIZE
* P & Q   = DISTRIBUTION ARRAY DIMENSIONS
* WIND_AZ = AZIMUTH OF WIND DIRECTION
* V1250   = WIND VELOCITY AT 1250 CM ABOVE SURFACE
* DEVA    = ALONG-WIND SLOPE DEVIATION [TAND(DEG)]
* DEVC    = CROSS-WIND SLOPE DEVIATION [TAND(DEG)]
```

```
*
      IMPLICIT NONE
      INTEGER I,J,N1,OPT,P,Q
      REAL ANG,ANG1,DELTA,DEVA,DEVC,C03,C04,C21,C22,C40,GC1,GC2,GC3,GC4 .
      REAL GRAMCHAR,L,L1,M,M1,PI,RAD,SUM1,SUM2,SUM3,SUM4,VAR1,VAR2,VAR3
      REAL VAR4,V1250,WGHT0,WGHT1,WGHT2,WGHT3,WGHT4,WIND_AZ
      REAL D1(P:Q,P:Q),D2(P:Q,P:Q),D3(P:Q,P:Q),D4(P:Q,P:Q)
*
* GRAM-CHARLIER SERIES COEFFICIENTS FROM COX-MUNK STUDY
*
      C03=0.04-0.00033*V1250
      C04=0.23
      C21=0.01-0.000086*V1250
      C22=0.12
      C40=0.40
*
      PI=3.141593
      WIND_AZ=WIND_AZ*(PI/180.0)
*
      IF (OPT.EQ.1) DELTA=90.0/FLOAT(Q)
      IF (OPT.EQ.2) DELTA=1.0/FLOAT(Q)
*
      DO I=P+1,Q
      DO J=P+1,Q
      L=FLOAT(I)*DELTA
      M=FLOAT(J)*DELTA
*
      RAD=SQRT((L**2)+(M**2))
*
      IF (RAD.GE.(FLOAT(Q)*DELTA)) GOTO 1
*
      IF ((M.EQ.0.0).AND.(L.EQ.0.0)) THEN
              L1=0.0
              M1=0.0
              GOTO 2
      ENDIF
*
      ANG=ATAN2(M,L)
      ANG1=WIND_AZ-ANG
*
      IF (OPT.EQ.1) THEN
              L1=(TAND(RAD)/DEVA)*COS(ANG1)
              M1=(TAND(RAD)/DEVC)*SIN(ANG1)
      ENDIF
*
      IF (OPT.EQ.2) THEN
              L1=(RAD/DEVA)*COS(ANG1)
              M1=(RAD/DEVC)*SIN(ANG1)
      ENDIF
*
* CALCULATE GRAM-CHARLIER EXPANSION
*
```

```
 2       GC1=1.0-(0.5*C21*((M1**2)-1.0)*L1)-(C03*((L1**3)-3.0*L1)/6.0)
         GC2=C40*((L1**4)-6.0*(L1**2)+3.0)/24.0
         GC3=C22*((L1**2)-1.0)*((M1**2)-1.0)/4.0
         GC4=C04*((M1**4)-6.0*(M1**2)+3.0)/24.0
         GRAMCHAR=GC1+GC2+GC3+GC4
 *
         D1(I,J)=EXP(-0.5*((L1**2)+(M1**2)))/(2.0*PI*DEVA*DEVC)
         D2(I,J)=GRAMCHAR*D1(I,J)
         SUM1=SUM1+D1(I,J)
         SUM2=SUM2+D2(I,J)
 *
 1       END DO
         END DO
 *
 * BIAS ALL ZERO VALUES IN DIST1 & DIST2 FOR ALPHASCALE DISPLAY
 * CALCULATE VARIANCES OF DIST1 & DIST2
 * NORMALIZE DIST1 & DIST2
 *
         WGHT0=1.0/(FLOAT(N1)**2)
         WGHT1=0.0
         WGHT2=0.0
***      WGHT1=-0.005
***      WGHT2=-0.005
 *
         DO I=P+1,Q
         DO J=P+1,Q
 *
         L=FLOAT(I)*DELTA
         M=FLOAT(J)*DELTA
         RAD=SQRT((L**2)+(M**2))
 *
         IF (RAD.GE.(FLOAT(Q)*DELTA)) GOTO 3
 *
         D1(I,J)=D1(I,J)/SUM1
         D2(I,J)=D2(I,J)/SUM2
 *
         VAR1=VAR1+D1(I,J)*(RAD**2)
         VAR2=VAR2+D2(I,J)*(RAD**2)
 *
         IF (D1(I,J).EQ.0.0) D1(I,J)=WGHT1
 *
         IF (D1(I,J).LT.WGHT0) THEN
                 D3(I,J)=WGHT1
         ELSE
                 D3(I,J)=D1(I,J)
                 SUM3=SUM3+D3(I,J)
         ENDIF
 *
         IF (D2(I,J).EQ.0.0) D2(I,J)=WGHT2
 *
         IF (D2(I,J).LT.WGHT0) THEN
                 D4(I,J)=WGHT2
```

```
        ELSE
                D4(I,J)=D2(I,J)
                SUM4=SUM4+D4(I,J)
        ENDIF
*
3       END DO
        END DO
*
* BIAS ALL ZERO VALUES IN DIST3 & DIST4 FOR ALPHASCALE DISPLAY
* CALCULATE VARIANCES OF DIST3 & DIST4
* NORMALIZE DIST3 & DIST4
*
        WGHT3=0.0
        WGHT4=0.0
***     WGHT3=-0.005
***     WGHT4=-0.005
*
        DO I=P+1,Q
        DO J=P+1,Q
*
        L=FLOAT(I)*DELTA
        M=FLOAT(J)*DELTA
        RAD=SQRT((L**2)+(M**2))
*
        IF (RAD.GE.(FLOAT(Q)*DELTA)) GOTO 4
*
        IF (D3(I,J).GE.WGHT0) THEN
                D3(I,J)=D3(I,J)/SUM3
                VAR3=VAR3+D3(I,J)*(RAD**2)
        ELSE
                D3(I,J)=WGHT3
        ENDIF
*
        IF (D4(I,J).GE.WGHT0) THEN
                D4(I,J)=D4(I,J)/SUM4
                VAR4=VAR4+D4(I,J)*(RAD**2)
        ELSE
                D4(I,J)=WGHT4
        ENDIF
*
4       END DO
        END DO
*
        WRITE(*,*) ' '
        WRITE(*,*) 'SUM1,SUM2= ',SUM1,SUM2
*
        IF (OPT.EQ.1) THEN
                WRITE(*,*) 'DEV1,DEV2= ',TAND(SQRT(VAR1)),TAND(SQRT(VAR2))
        ELSE
                WRITE(*,*) 'DEV1,DEV2= ',SQRT(VAR1),SQRT(VAR2)
        ENDIF
*
```

```
      WRITE(*,*) 'SUM3,SUM4= ',SUM3,SUM4
*
      IF (OPT.EQ.1) THEN
              WRITE(*,*) 'DEV3,DEV4= ',TAND(SQRT(VAR3)),TAND(SQRT(VAR4))
      ELSE
              WRITE(*,*) 'DEV3,DEV4= ',SQRT(VAR3),SQRT(VAR4)
      ENDIF
*
      WRITE(*,*) ' '
*
***   WRITE(*,*) 'UNNORMALIZED GAUSSIAN SLOPE DISTRIBUTION ARRAY'
***   IF (N1.EQ.64) CALL ALPHA(D1,64)
***   CALL PLT3DFILE(D1,N1)
*
***   WRITE(*,*) 'NORMALIZED GAUSSIAN SLOPE DISTRIBUTION ARRAY'
***   IF (N1.EQ.64) CALL ALPHA(D3,64)
***   CALL PLT3DFILE(D3,N1)
*
***   WRITE(*,*) 'UNNORMALIZED GRAM-CHARLIER SLOPE DISTRIBUTION ARRAY'
***   IF (N1.EQ.64) CALL ALPHA(D2,64)
***   CALL PLT3DFILE(D2,N1)
*
***   WRITE(*,*) 'NORMALIZED GRAM-CHARLIER SLOPE DISTRIBUTION ARRAY'
***   IF (N1.EQ.64) CALL ALPHA(D4,64)
***   CALL PLT3DFILE(D4,N1)
*
      RETURN
      END


      SUBROUTINE FFT2D(X,N,INV)
*
*     CALCULATES FORWARD & BACKWARD FAST_FOURIER_TRANSFORM
*
*     OUTPUT:
*     X    = TRANSFORMED COMPLEX SQUARE ARRAY
*
*     INPUT:
*     X    = UNTRANSFORMED SQUARE ARRAY
*     N    = DIMENSION OF X
*     INV  = DIRECTION OF TRANSFORMATION:
*            -1 = FORWARD TRANSFORM
*            +1 = BACKWARD TRANSFORM
*
      IMPLICIT NONE
      REAL ANGLE,PI,RTEM,WPWR
      INTEGER I,INV,IREM,IT,ITER,J,J1,J2,K,L,M,MXP,M1,N,NXP,NXP2,N1,N2
      COMPLEX X(1:N,1:N),W,T
*
      PI=3.141593
      ITER=0
      IREM=N
```

```
*
10      IREM=INT(IREM/2)
*
              IF (IREM.EQ.0) GOTO 20
*
              ITER=ITER+1
              GOTO 10
*
20      CONTINUE
*
        CALL CHECKERBOARD(X,N)
*
        DO 80 M1=1,2
        DO 70 L=1,N
*
        NXP2=N
*
              DO 50 IT=1,ITER
*
              NXP=NXP2
              NXP2=INT(NXP/2)
*
              IF (NXP2.EQ.0) GOTO 50
*
              WPWR=PI/FLOAT(NXP2)
*
                      DO 40 M=1,NXP2
*
                      ANGLE=FLOAT(M-1)*WPWR
                      W=CMPLX(COS(ANGLE),FLOAT(INV)*SIN(ANGLE))
*
                              DO 40 MXP=NXP,N,NXP
*
                              J1=MXP-NXP+M
                              J2=J1+NXP2
*
                              IF (M1.EQ.1) THEN
                                      T=X(J1,L)-X(J2,L)
                                      X(J1,L)=X(J1,L)+X(J2,L)
                                      X(J2,L)=T*W
                              ELSE
                                      T=X(L,J1)-X(L,J2)
                                      X(L,J1)=X(L,J1)+X(L,J2)
                                      X(L,J2)=T*W
                              ENDIF
*
40            CONTINUE
50            CONTINUE
*
              N2=N/2
              N1=N-1
              J=1
```

```
*
                         DO I=1,N1
*
                         IF (I.GE.J) GOTO 55
*
                         IF (M1.EQ.1) THEN
                                T=X(J,L)
                                X(J,L)=X(I,L)
                                X(I,L)=T
                         ELSE
                                T=X(L,J)
                                X(L,J)=X(L,I)
                                X(L,I)=T
                         ENDIF
*
55                       K=N2
*
60                       IF (K.GE.J) GOTO 65
*
                         J=J-K
                         K=K/2
                         GOTO 60
65                       J=J+K
*
                         END DO
70       CONTINUE
80       CONTINUE
*
         CALL CHECKERBOARD(X,N)
*
***      IF (INV.EQ.-1) GOTO 90
*
***      RTEM=FLOAT(N*N)
*
***      DO 90 J=1,N
***      DO 85 I=1,N
*
***             X(I,J)=X(I,J)/RTEM
*
***85    CONTINUE
***90    CONTINUE
*
         RETURN
         END


         SUBROUTINE PICFILE(DATA,N,A,B,C)
         IMPLICIT NONE
         INTEGER I,J,N
         REAL A,B,C
         CHARACTER*64 DATA(204)
         CHARACTER*1 OPT
```

```
      CHARACTER*10 FNAME
*
      WRITE(*,*) 'WANT AN ALPHASCALE PIC FILE? [N] '
      READ(*,300) OPT
      IF (OPT.NE.'Y') GOTO 5
*
      WRITE(*,*) 'ENTER PIC FILENAME => '
      READ(*,300) FNAME
      OPEN(3,FILE=FNAME,STATUS='UNKNOWN',ERR=10)
*
      WRITE(3,*) FNAME,':HIGH,LOW,DELTA =',A,B,C
      DO I=1,N
      WRITE(3,*) DATA(I),N/2-I
      END DO
*
***   DO I=N+1,N+4
***   WRITE(3,*) DATA(I)
***   END DO
*
      CLOSE (3)
      WRITE(*,*) 'FILENAME = ',FNAME,' IS WRITTEN'
5     RETURN
10    WRITE(*,*) 'BAD FILE OPENING'
300   FORMAT (A)
      END



      SUBROUTINE PLT2DFILE(X,N)
      IMPLICIT NONE
      INTEGER I,J,N
      REAL X(N,2),Y,Z
      CHARACTER*1 CHOICE
      CHARACTER*18 FILENAME
      WRITE(*,*) 'WANT A PLT2D OUTPUT FILE? [N] '
      READ(*,300) CHOICE
      IF (CHOICE.NE.'Y') GOTO 1
      WRITE(*,*) 'ENTER PLT2D OUTPUT FILENAME ==>'
      READ(*,300) FILENAME
      OPEN(1,FILE=FILENAME,STATUS='NEW',ERR=5)
      DO I=1,N
      WRITE(1,*)(X(I,J),J=1,2)
      END DO
      CLOSE(1)
      WRITE(*,*) FILENAME,'HAS BEEN WRITTEN AS AN OUTPUT FILE'
1     RETURN
5     WRITE(*,*) 'BAD FILE OPENING'
300   FORMAT (A)
      END


      SUBROUTINE PLT2DOUTPUT(FILENAME,X,N)
```

```
      IMPLICIT NONE
      INTEGER I,J,N
      REAL X(N,2),Y,Z
      CHARACTER*1 CHOICE
      CHARACTER*18 FILENAME
*
      WRITE(*,*) 'WANT A PLT2D OUTPUT FILE? [N] FILE =',FILENAME
*
      READ(*,300) CHOICE
      IF (CHOICE.NE.'Y') GOTO 1
***   WRITE(*,*) 'ENTER PLT2D OUTPUT FILENAME ==>'
***   READ(*,300) FILENAME
      OPEN(1,FILE=FILENAME,STATUS='NEW',ERR=5)
      DO I=1,N
      WRITE(1,*)(X(I,J),J=1,2)
      END DO
      CLOSE(1)
      WRITE(*,*) FILENAME,'HAS BEEN WRITTEN AS AN OUTPUT FILE'
1     RETURN
5     WRITE(*,*) 'BAD FILE OPENING'
300   FORMAT (A)
      END


      SUBROUTINE PLT3DFILE(X,N)
      IMPLICIT NONE
      INTEGER I,J,N
      REAL X(N,N),Y,Z
      CHARACTER*1 CHOICE
      CHARACTER*18 FILENAME
      WRITE(*,*) 'WANT A PLT3D OUTPUT FILE? [N] '
      READ(*,300) CHOICE
      IF (CHOICE.NE.'Y') GOTO 1
      WRITE(*,*) 'ENTER PLT3D OUTPUT FILENAME ==>'
      READ(*,300) FILENAME
      OPEN(1,FILE=FILENAME,STATUS='NEW',ERR=5)
      WRITE(1,*) N,N
      DO I=1,N
      WRITE(1,*)(X(I,J),J=1,N)
      END DO
      CLOSE(1)
      WRITE(*,*) FILENAME,'HAS BEEN WRITTEN AS AN OUTPUT FILE'
1     RETURN
5     WRITE(*,*) 'BAD FILE OPENING'
300   FORMAT (A)
      END


      SUBROUTINE PLT3DINPUT(FILENAME,X,N,P,Q)
      IMPLICIT NONE
      INTEGER I,J,N,P,P1,Q,Q1
      REAL X(N,P:Q)
```

```
      CHARACTER*18 FILENAME
*
***   WRITE(*,*) 'ENTER PLT3D INPUT FILENAME ==>'
***   READ(*,300) FILENAME
*
      OPEN(1,FILE=FILENAME,STATUS='OLD',ERR=5)
      READ(1,*) N,N
      P1=-N/2
      Q1=N/2-1
*
      DO I=P1,Q1
      READ(1,*)(X(I,J),J=P1,Q1)
      END DO
*
      CLOSE(1)
      WRITE(*,*) FILENAME,'HAS BEEN INPUT'
1     RETURN
5     WRITE(*,*) 'BAD FILE OPENING'
300   FORMAT (A)
      END


      SUBROUTINE PLT3DOUTPUT(FILENAME,X,N,P,Q)
      IMPLICIT NONE
      INTEGER I,J,N,P,P1,Q,Q1
      REAL X(P:Q,P:Q)
      CHARACTER*1 CHOICE
      CHARACTER*18 FILENAME
*
      WRITE(*,*) 'WANT A PLT3D OUTPUT FILE? [N] FILE= ',FILENAME
*
      READ(*,300) CHOICE
      IF (CHOICE.NE.'Y') GOTO 1
*
***   WRITE(*,*) 'ENTER PLT3D OUTPUT FILENAME ==>'
***   READ(*,300) FILENAME
*
      OPEN(1,FILE=FILENAME,STATUS='NEW',ERR=5)
      WRITE(1,*) N,N
      P1=-N/2
      Q1=N/2-1
      DO I=P1,Q1
      WRITE(1,*)(X(I,J),J=P1,Q1)
      END DO
      CLOSE(1)
      WRITE(*,*) FILENAME,'HAS BEEN OUTPUT'
1     RETURN
5     WRITE(*,*) 'BAD FILE OPENING'
300   FORMAT (A)
      END
```

```
      SUBROUTINE PSVARY1(KNYQ,N,WIND_V,Z,VARY)
*
* CALCULATES ALONG-WIND, CROSS-WIND AND TOTAL VARIANCE OF SLOPE DISTRIBUTION
* FOR THREE SPECTRAL REGIONS: 1) BELOW LOWEST SAMPLE FREQUENCY, 2) WITHIN
* SAMPLED SPECTRAL REGION, & 3) ABOVE HIGHEST SAMPLE FREQUENCY
*
      IMPLICIT NONE
      INTEGER I,J,N,P,Q
      REAL A,ALPH,ANG,BETA,D,DELT,DELTA,ENUG,G,K,K_MAX,KNU,KNYQ
      REAL K1,K2,K3,L,M,P2,PI,SPEC,SPREAD_TOT,TEMP
      REAL VAR_S,VAR_X,VAR_Y,VAR1_S,VAR1_X,VAR1_Y,VAR2_S,VAR2_X,VAR2_Y
      REAL V_FRIC,V_MIN,V250,V1000,V1250,V1950,WIND_V,Z
      'EAL LNSPEC(-800:400,2),SPREAD(0:179),VARY(0:4,0:4)
      CHARACTER*1 OPT
*
** WIND_V=WIND VELOCITY AT HEIGHT Z [CM/SEC^2]
** Z=HEIGHT OF WIND_V MEASUREMENT ABOVE WATER SURFACE [CM]
*
      A=1.0
      ALPH=0.0081
** ALPH=PHILLIPS CONSTANT [ ]
      BETA=0.74
** BETA=    [UNITLESS]
      ENUG=1.473E-4
** ENUG=E/(NU*G) [UNITLESS]
      G=980.0
** G=ACCELERATION OF GRAVITY [CM/SEC^2]
      K2=0.359
** [1/CM]
      K3=0.942
** [1/CM]
      K_MAX=3.63
** '' ^M]
       'I=3.141593
*
      V_MIN=1 0
** V_MIN=MINIMUM FRICTION VELOCITY [CM/SEC]
*
      WRITE(*,*) 'WANT FULL-SPECTRUM STATISTICS? [N] '
       .EAD(*,300) OPT
      IF (OPT.NE.'Y') GOTO 2
*
      WRITE(*,*) 'CALCULATING FULL-SPECTRUM STATISTICS..........'
*
      CALL WIND(WIND_V,Z,V_FRIC,V250,V1000,V1250,V1950)
*
      D=(1.274+(0.0268*V_FRIC)+(6.03E-5*(V_FRIC**2)))**2
      K1=(K2*(V_MIN**2))/(V_FRIC**2)
      KNU=(0.5756*SQRT(V_FRIC)*K_MAX)/(D**0.16667)
      P2=LOG10(D/(V_FRIC/V_MIN))/LOG10(K3/K2)
*
      DELT=0.01
```

```
      DELTA=PI/180.0
      VAR_S=0.0
      VAR_X=0.0
      VAR_Y=0.0
      VARY(0,2)=0.0
      VARY(0,3)=0.0
      VARY(0,4)=0.0
*
      DO I=-800,400
      L=FLOAT(I)*DELT
      K=EXP(L)
      LNSPEC(I,1)=LOG10(K)
*
      CALL SPREADVARY(K,V1950,SPREAD,SPREAD_TOT)
*
      IF ((0.0.LT.K).AND.(K.LE.K1)) THEN
      SPEC=(ALPH/(2.0*(K**3)))*EXP((-1.0*BETA*(G**2))/((V1950**4)*(K**2)))
      GOTO 1
      ENDIF
*
      IF ((K1.LT.K).AND.(K.LE.K2)) THEN
      SPEC=ALPH/(2.0*SQRT(K1)*(K**2.5))
      GOTO 1
      ENDIF
*
      IF ((K2.LT.K).AND.(K.LE.K3)) THEN
      SPEC=(ALPH*D)/(2.0*(K3**P2)*(K**(3.0-P2)))
      GOTO 1
      ENDIF
*
      IF ((K3.LT.K).AND.(K.LE.KNU)) THEN
      SPEC=(ALPH*D)/(2.0*(K**3))
      GOTO 1
      ENDIF
*
      IF (KNU.LT.K) THEN
      SPEC=(ENUG*(V_FRIC**3)*(K_MAX**6))/(K**9)
      ENDIF
*
1     LNSPEC(I,2)=(K**3)*SPEC
*
      DO J=0,179
      ANG=FLOAT(J)*DELTA
      TEMP=(SPREAD(J)*LNSPEC(I,2)*DELT*DELTA)
      VAR_S=VAR_S+TEMP
      VAR_X=VAR_X+((COS(ANG)**2)*TEMP)
      VAR_Y=VAR_Y+((SIN(ANG)**2)*TEMP)
      END DO
*
***   WRITE(*,*) L,K,VAR
*
      IF (EXP(L-DELT).LE.0.003) THEN
```

```
              VARY(1,1)=0.003
              VARY(1,2)=VAR_X
              VARY(1,3)=VAR_Y
              VARY(1,4)=VAR_S
        ENDIF
*
        IF (EXP(L-DELT).LE.(KNYQ/FLOAT(N/2))) THEN
              VARY(2,1)=KNYQ/FLOAT(N/2)
              VARY(2,2)=VAR_Y
              VARY(2,3)=VAR_X
              VARY(2,4)=VAR_S
        ENDIF
*
        IF (EXP(L-DELT).LE.KNYQ) THEN
              VARY(3,1)=KNYQ
              VARY(3,2)=VAR_Y
              VARY(3,3)=VAR_X
              VARY(3,4)=VAR_S
        ENDIF
*
        IF (EXP(L-DELT).LE.300.0) THEN
              VARY(4,1)=300.0
              VARY(4,2)=VAR_Y
              VARY(4,3)=VAR_X
              VARY(4,4)=VAR_S
        ENDIF
*
        END DO
*
        WRITE(*,*) 'RESULTS OF PSVARY1'
***     WRITE(*,*) 'SPREAD_TOT = ',SPREAD_TOT
        WRITE(*,*) ' '
*
        DO I=1,4
        WRITE(*,*) 'WAVE SLOPE VARIANCE UP TO ',VARY(I,1),' CY/CM & DIFFER'
        WRITE(*,*) 'CUM CROSS-WIND VARIANCE = ',VARY(I,2),VARY(I,2)-VARY(I-1,2)

        WRITE(*,*) 'CUM ALONG-WIND VARIANCE = ',VARY(I,3),VARY(I,3)-VARY(I-1,3)
        WRITE(*,*) 'CUM COMBINED   VARIANCE = ',VARY(I,4),VARY(I,4)-VARY(I-1,4)
        WRITE(*,*) ' '
        END DO
*
2       RETURN
300     FORMAT (A)
        END


        SUBROUTINE PSVARY2(KNYQ,N,WIND_V,Z,V1250,VARY)
*
* CALCULATES ALONG-WIND, CROSS-WIND AND TOTAL VARIANCE OF SLOPE DISTRIBUTION
* FOR THREE SPECTRAL REGIONS: 1) BELOW LOWEST SAMPLE FREQUENCY, 2) WITHIN
* SAMPLED SPECTRAL REGION, & 3) ABOVE HIGHEST SAMPLE FREQUENCY
```

```
*
      IMPLICIT NONE
      INTEGER I,J,N,P,Q
      REAL A,ALPH,ANG,BETA,D,DELT,DELTA,ENUG,G,K,K_MAX,KNU,KNYQ
      REAL K1,K2,K3,L,M,P2,PI,SPEC,SPREAD_TOT,TEMP
      REAL VAR_S,VAR_X,VAR_Y,VAR1_S,VAR1_X,VAR1_Y,VAR2_S,VAR2_X,VAR2_Y
      REAL V_FRIC,V_MIN,V250,V1000,V1250,V1950,WIND_V,Z
      REAL LNSPEC(-800:400,2),SPREAD(0:179),VARY(0:4,0:4)
      CHARACTER*1 OPT
*
** WIND_V=WIND VELOCITY AT HEIGHT Z [CM/SEC^2]
** Z=HEIGHT OF WIND_V MEASUREMENT ABOVE WATER SURFACE [CM]
*
      A=1.0
      ALPH=0.0081
** ALPH=PHILLIPS CONSTANT [ ]
      BETA=0.74
** BETA=    [UNITLESS]
      ENUG=1.473E-4
** ENUG=E/(NU*G) [UNITLESS]
      G=980.0
** G=ACCELERATION OF GRAVITY [CM/SEC^2]
      K2=0.359
** [1/CM]
      K3=0.942
** [1/CM]
      K_MAX=3.63
** [1/CM]
      PI=3.141593
**
      V_MIN=12.0
** V_MIN=MINIMUM FRICTION VELOCITY [CM/SEC]
*
***   WRITE(*,*) 'WANT FULL-SPECTRUM STATISTICS? [N] '
***   READ(*,300) OPT
***   IF ((OPT.NE.'Y').OR.(OPT.NE.'y')) GOTO 2
*
      WRITE(*,*) 'CALCULATING FULL-SPECTRUM STATISTICS..........'
*
      CALL WIND(WIND_V,Z,V_FRIC,V250,V1000,V1250,V1950)
*
      D=(1.274+(0.0268*V_FRIC)+(6.03E-5*(V_FRIC**2)))**2
      K1=(K2*(V_MIN**2))/(V_FRIC**2)
      KNU=(0.5756*SQRT(V_FRIC)*K_MAX)/(D**0.16667)
      P2=LOG10(D/(V_FRIC/V_MIN))/LOG10(K3/K2)
*
      DELT=0.01
      DELTA=PI/180.0
      VAR_S=0.0
      VAR_X=0.0
      VAR_Y=0.0
      VARY(0,2)=0.0
```

```
      VARY(0,3)=0.0
      VARY(0,4)=0.0
*
      DO I=-800,400
      L=FLOAT(I)*DELT
      K=EXP(L)
      LNSPEC(I,1)=LOG10(K)
*
      CALL SPREADVARY(K,V1950,SPREAD,SPREAD_TOT)
*
      IF ((0.0.LT.K).AND.(K.LE.K1)) THEN
      SPEC=(ALPH/(2.0*(K**3)))*EXP((-1.0*BETA*(G**2))/((V1950**4)*(K**2)))
      GOTO 1
      ENDIF
*
      IF ((K1.LT.K).AND.(K.LE.K2)) THEN
      SPEC=ALPH/(2.0*SQRT(K1)*(K**2.5))
      GOTO 1
      ENDIF
*
      IF ((K2.LT.K).AND.(K.LE.K3)) THEN
      SPEC=(ALPH*D)/(2.0*(K3**P2)*(K**(3.0-P2)))
      GOTO 1
      ENDIF
*
      IF ((K3.LT.K).AND.(K.LE.KNU)) THEN
      SPEC=(ALPH*D)/(2.0*(K**3))
      GOTO 1
      ENDIF
*
      IF (KNU.LT.K) THEN
      SPEC=(ENUG*(V_FRIC**3)*(K_MAX**6))/(K**9)
      ENDIF
*
1     LNSPEC(I,2)=(K**3)*SPEC
*
      DO J=0,179
      ANG=FLOAT(J)*DELTA
      TEMP=(SPREAD(J)*LNSPEC(I,2)*DELT*DELTA)
      VAR_S=VAR_S+TEMP
      VAR_X=VAR_X+((COS(ANG)**2)*TEMP)
      VAR_Y=VAR_Y+((SIN(ANG)**2)*TEMP)
      END DO
*
***   WRITE(*,*) L,K,VAR
*
      IF (EXP(L-DELT).LE.0.003) THEN
              VARY(1,1)=0.003
              VARY(1,2)=VAR_X
              VARY(1,3)=VAR_Y
              VARY(1,4)=VAR_S
      ENDIF
```

```
*
      IF (EXP(L-DELT).LE.(KNYQ/FLOAT(N/2))) THEN
            VARY(2,1)=KNYQ/FLOAT(N/2)
            VARY(2,2)=VAR_Y
            VARY(2,3)=VAR_X
            VARY(2,4)=VAR_S
      ENDIF
*
      IF (EXP(L-DELT).LE.KNYQ) THEN
            VARY(3,1)=KNYQ
            VARY(3,2)=VAR_Y
            VARY(3,3)=VAR_X
            VARY(3,4)=VAR_S
      ENDIF
*
      IF (EXP(L-DELT).LE.300.0) THEN
            VARY(4,1)=300.0
            VARY(4,2)=VAR_Y
            VARY(4,3)=VAR_X
            VARY(4,4)=VAR_S
      ENDIF
*
      END DO
*
      WRITE(*,*) 'RESULTS OF PSVARY1'
***   WRITE(*,*) 'SPREAD_TOT = ',SPREAD_TOT
      WRITE(*,*) ' '
*
      DO I=1,4
      WRITE(*,*) 'WAVE SLOPE VARIANCE UP TO ',VARY(I,1),' CY/CM & DIFFER'
      WRITE(*,*) 'CUM CROSS-WIND VARIANCE = ',VARY(I,2),VARY(I,2)-VARY(I-1,2)

      WRITE(*,*) 'CUM ALONG-WIND VARIANCE = ',VARY(I,3),VARY(I,3)-VARY(I-1,3)
      WRITE(*,*) 'CUM COMBINED   VARIANCE = ',VARY(I,4),VARY(I,4)-VARY(I-1,4)
      WRITE(*,*) ' '
      END DO
*
2     RETURN
300   FORMAT (A)
      END



      SUBROUTINE RALPH(X,N,RY,IY,MY,PY)
*
* COMPOSITE SUBROUTINE TO DISPLAY COMPLEX ARRAY AS REAL, IMAGINARY,
* MAGNITUDE, AND PHASE COMPONENTS
*
* INPUT:
* COMPLEX ARRAY X(N,N)
*
```

```
* OUTPUTS:
* REAL ARRAY      RY(N,N)
* IMAGINARY ARRAY IY(N,N)
* MAGNITUDE ARRAY MY(N,N)
* PHASE ARRAY     PY(N,N)
*
        IMPLICIT NONE
        INTEGER N
        COMPLEX X(N,N)
        REAL RY(N,N),IY(N,N),MY(N,N),PY(N,N)
*
        CALL RIMP(X,N,RY,IY,MY,PY)
*
        WRITE(*,*) 'REAL COMPONENT OF COMPLEX ARRAY'
        CALL ALPHA(RY,N)
*
        WRITE(*,*) 'IMAGINARY COMPONENT OF COMPLEX ARRAY'
        CALL ALPHA(IY,N)
*
        WRITE(*,*) 'MAGNITUDE COMPONENT OF COMPLEX ARRAY'
        CALL ALPHA(MY,N)
*
        WRITE(*,*) 'PHASE COMPONENT OF COMPLEX ARRAY'
        CALL ALPHA(PY,N)
*
        RETURN
        END


        SUBROUTINE RIMP(X,N,RY,IY,MY,PY)
        IMPLICIT NONE
        INTEGER I,J,N
        COMPLEX X(N,N)
        REAL RY(N,N),IY(N,N),MY(N,N),PY(N,N),HALFPI
*
        HALFPI=3.141593/2.0
*
        DO I=1,N
                DO J=1,N
                        RY(I,J)=REAL(X(I,J))
                        IY(I,J)=AIMAG(X(I,J))
                        MY(I,J)=CABS(X(I,J))
                        IF ((RY(I,J).EQ.0.0).AND.(IY(I,J).EQ.0.0)) THEN
                        PY(I,J)=0.0
                        ELSEIF (IY(I,J).EQ.0.0) THEN
                        PY(I,J)=SIGN(HALFPI,RY(I,J))
                        ELSE
                        PY(I,J)=ATAN2(IY(I,J),RY(I,J))
                        ENDIF
                END DO
        END DO
        RETURN
```

```
      END


      SUBROUTINE SEA_SPEC(W_V,Z,W_AZ,DELTA_K,F1,F2,F3,F4,FX1,FY1,KCOR,N,P,Q)
*
* GENERATES PIERSON-STACY 2D SLOPE & ELEVATION SPECTRA IN RECT COORDINATES [L,M]

* CALCULATES VARIANCE OF SPECTRA FROM 1*DELTA_K TO (N/2-1)*DELTA_K
*
* INPUTS:
* W_V     = WIND_VELOCITY MEASUREMENT AT HEIGHT Z ABOVE WATER SURFACE [CM/SEC]
* Z       = HEIGHT OF WIND_VELOCITY MEASUREMENT                       [CM]
* W_AZ    = AZIMUTHAL DIRECTION OF WIND RELATIVE TO SENSOR            [RAD]
* DELTA_K = DELTA SPATIAL FREQUENCY                                   [CY/CM]
*
* OUTPUTS:
* F1      = ABS( TOTAL (X+Y) SLOPE SPECTRUM)                          [ ]
* F2      = ABS(ELEVATION SPECTRUM)                                   [CM]
* F3      = ABS(X-COMPONENT SLOPE SPECTRUM)                           [ ]
* F4      = ABS(Y-COMPONENT SLOPE SPECTRUM)                           [ ]
* FX1     = X-COMPONENT SLOPE SPECTRUM                                [ ]
* FY1     = Y-COMPONENT SLOPE SPECTRUM                                [ ]
* KCOR    = INTEGER(K+OFF) POINTER ARRAY TO POLAR-RECTANGULAR CORRECTION FACTOR
*
      IMPLICIT NONE
      INTEGER I,J,N,P,Q
      INTEGER KCOR(P:Q,P:Q)
      REAL A,ALPH,ANG0,ANG1,BETA,D,DELTA_K,ENUG,G,K,KINT,KMAG,K_MAX,KNU
      REAL K1,K2,K3,L,M,P2,PI,SPANG,SPEC,SPREAD,SPRED0,SPRED1,SPRED2,SPRED3
      REAL TEMP,VAR_X,VAR_Y,VAR_ELV,VAR_TOT,V_FRIC,V_MIN,V250,V1000,V1250
      REAL V1950,W_AZ,W_V,X2,Y2,Z
      REAL F1(P:Q,P:Q),F2(P:Q,P:Q),F3(P:Q,P:Q),F4(P:Q,P:Q)
      REAL FX1(P:Q,P:Q),FY1(P:Q,P:Q),SPRDCOR(0:4096)
      REAL CSPAN(0:512),SPANGCOR(0:512),SPECCOR(0:512,1:2)
*
      A=1.0
      ALPH=0.0081
* ALPH=PHILLIPS CONSTANT [UNITLESS]
      BETA=0.74
* BETA=    [ ]
      ENUG=1.473E-4
* ENUG=E/(NU*G) [ ]
      G=980.0
* G=ACCELERATION OF GRAVITY [CM/SEC^2]
      K2=0.359
* [CY/CM]
      K3=0.942
* [CY/CM]
      K_MAX=3.63
* [CY/CM]
      PI=3.141593
*
```

```
      V_MIN=12.0
* V_MIN=MINIMUM FRICTION VELOCITY [CM/SEC]
*
      CALL WIND(W_V,Z,V_FRIC,V250,V1000,V1250,V1950)
*
      D=(1.274+(0.0268*V_FRIC)+(6.03E-5*(V_FRIC**2)))**2
      K1=(K2*(V_MIN**2))/(V_FRIC**2)
      KNU=((0.5756*SQRT(V_FRIC)*K_MAX)/(D**(0.16667)))
      P2=LOG10(D/(V_FRIC/V_MIN))/LOG10(K3/K2)
*
      DO I=P,Q
      DO J=P,Q
      L=FLOAT(I)
      M=FLOAT(J)
      KMAG=SQRT((L**2)+(M**2))
      K=KMAG*DELTA_K
              IF((K.EQ.0.0).OR.(K.GE.(FLOAT(-P)*DELTA_K))) THEN
              SPANG=0.0
              GOTO 2
              ENDIF
      ANG0=ATAN2(M,L)
      ANG1=W_AZ-ANG0
*
* CALCULATE 2D DIRECTIONAL SPREADING FUNCTION
*
      SPRED0=COS(ANG1)**2
      SPRED1=(8.0/(3.0*PI))*(SPRED0**2)
      SPRED2=EXP((-1.0*(G**2))/(2.0*(K**2)*(V1950**4)))
      SPRED3=(1.0-(A/2.0)+(A*SPRED0))/PI
      SPREAD=((SPRED1*(1.0-SPRED2))+(SPRED3*SPRED2))
*
* CALCULATE POLAR-TO-RECTANGULAR CORRECTION FACTORS
*
      KINT=4*INT(KMAG-0.25)
      SPRDCOR(KINT)=SPRDCOR(KINT)+SPREAD
      KCOR(I,J)=KINT
*
* CALCULATE 1D ELEVATION POWER SPECTRUM
*
      IF ((0.0.LT.K).AND.(K.LE.K1)) THEN
      SPEC=(ALPH/(2.0*(K**3)))*EXP((-1.0*BETA*(G**2))/((V1950**4)*(K**2)))
      GOTO 1
      ENDIF
*
      IF ((K1.LT.K).AND.(K.LE.K2)) THEN
      SPEC=ALPH/(2.0*SQRT(K1)*(K**2.5))
      GOTO 1
      ENDIF
*
      IF ((K2.LT.K).AND.(K.LE.K3)) THEN
      SPEC=(ALPH*D)/(2.0*(K3**P2)*(K**(3.0-P2)))
      GOTO 1
```

```
      ENDIF
*
      IF ((K3.LT.K).AND.(K.LE.KNU)) THEN
      SPEC=(ALPH*D)/(2.0*(K**3))
      GOTO 1
      ENDIF
*
      IF (KNU.LT.K) THEN
      SPEC=(ENUG*(V_FRIC**3)*(K_MAX**6))/(K**9)
      ENDIF
*
* CALCULATE UNCORRECTED 2D SLOPE & ELEVATION SPECTRA
*
1     SPANG=SQRT(SPREAD*SPEC)
      X2=(L*DELTA_K)
      Y2=(M*DELTA_K)
*
2     F1(I,J)=K*SPANG
      F2(I,J)=SPANG
      FX1(I,J)=X2*SPANG
      FY1(I,J)=Y2*SPANG
      F3(I,J)=ABS(X2*SPANG)
      F4(I,J)=ABS(Y2*SPANG)
*
* OPTION: CALCULATE POLAR-RECTANGULAR CORRECTION DATA
*
***   SPECCOR(KINT,1)=SPECCOR(KINT,1)+((K**2)*SPEC)
***   SPECCOR(KINT,2)=SPECCOR(KINT,2)+1.0
***   SPANGCOR(KINT)=SPANGCOR(KINT)+F1(I,J)**2
*
      END DO
      END DO
*
* CORRECT SPECTRA FOR POLAR-TO-RECTANGULAR CONVERSION
* CALCULATE CUMULATIVE VARIANCES
*
      DO I=P,Q
      DO J=P,Q
*
      KMAG=SQRT(FLOAT(I)**2+FLOAT(J)**2)
*
      KINT=KCOR(I,J)
      IF (KINT.EQ.0) GOTO 3
*
      TEMP=SQRT(SPRDCOR(KINT)*DELTA_K)
*
      F1(I,J)=F1(I,J)/TEMP
      VAR_TOT=VAR_TOT+(F1(I,J)**2)*(DELTA_K**2)
      CSPAN(KINT)=CSPAN(KINT)+F1(I,J)**2
      F2(I,J)=F2(I,J)/TEMP
      VAR_ELV=VAR_ELV+(F2(I,J)**2)*(DELTA_K**2)
      FX1(I,J)=FX1(I,J)/TEMP
```

```
      VAR_X=VAR_X+(FX1(I,J)**2)*(DELTA_K**2)
      FY1(I,J)=FY1(I,J)/TEMP
      VAR_Y=VAR_Y+(FY1(I,J)**2)*(DELTA_K**2)
      F3(I,J)=F3(I,J)/TEMP
      F4(I,J)=F4(I,J)/TEMP
*
* ADDITIONAL VARIANCE FOR DOUBLY-SAMPLED NYQUIST FREQUENCY
*
      IF (KMAG.GT.FLOAT(Q)) THEN
            VAR_TOT=VAR_TOT+(F1(I,J)**2)*(DELTA_K**2)
            VAR_ELV=VAR_ELV+(F2(I,J)**2)*(DELTA_K**2)
            VAR_X=VAR_X+(FX1(I,J)**2)*(DELTA_K**2)
            VAR_Y=VAR_Y+(FY1(I,J)**2)*(DELTA_K**2)
      ENDIF
*
3     END DO
      END DO
*
* OPTION: WRITE OUT POLAR-RECTANGULAR CORRECTION PARAMETERS
*
***   WRITE(*,*) 'K,SPANGCOR,SPRDCOR,CSPAN'
***   DO I=1,Q+1
***   K=FLOAT(I)*DELTA_K
***   WRITE(*,*) K,SPANGCOR(I),SPRDCOR(I),CSPAN(I)
***   END DO
*
      WRITE(*,*) 'TOTAL SLOPE VARIANCE OF THE Y-COMPONENTS = ',VAR_Y
      WRITE(*,*) 'TOTAL SLOPE VARIANCE OF THE X-COMPONENTS = ',VAR_X
      WRITE(*,*) 'TOTAL SLOPE COMBINED VARIANCE            = ',VAR_TOT
      WRITE(*,*) 'TOTAL ELEVATION VARIANCE     [CM^2]      = ',VAR_ELV
*
      RETURN
      END


      SUBROUTINE SKYBLUE(LREF,PHI0,Z0,N,P,Q,LSKY,HSKY,VSKY)
*
* CREATE UNPOLARIZED SKYDOME HEMISPHERICAL RADIANCE DISTRIBUTION
* RESOLVE HORIZONTALLY_ & VERTICALLY_POLARIZED RADIANCE COMPONENTS
*
* INPUT:
* LREF = REFERENCE RADIANCE MEASURED AT THE ZENITH POINT, LSKY(0,0) [UNIT]
* PHI0 = SUN AZIMUTH [DEG] [-180..+180]
* Z0   = SUN DECLINATION
*
* OUTPUT:
* LSKY = UNPOLARIZED SKYDOME ANGULAR RADIANCE DISTRIBUTION
* HSKY = HORIZONTALLY_POLARIZED LSKY
* VSKY = VERTICALLY_POLARIZED LSKY
*
      IMPLICIT NONE
      INTEGER I,J,N,P,Q
```

```
      REAL LSKY(P:Q,P:Q),HSKY(P:Q,P:Q),VSKY(P:Q,P:Q)
      REAL A,B,C,COSMU,COSMU2,COSNU,H,L,LREF,M,MU,PHI,PHI0,PI,PSI,THETA,Z0
      CHARACTER*18 FNAME
*
      PI=3.14159
*
      DO I=P+1,Q
      DO J=P+1,Q
*
      L=FLOAT(I)
      M=FLOAT(J)
      THETA=(PI/2.0)*(SQRT((L**2)+(M**2))/FLOAT(Q))
*
              IF (THETA.GT.PI/2.0) THEN
                      LSKY(I,J)=0.0
                      HSKY(I,J)=0.0
                      VSKY(I,J)=0.0
                      GOTO 4
              ENDIF
*
              IF (THETA.EQ.0.0) THEN
                      PHI=0.0
                      GOTO 1
              ENDIF
*
      PHI=ATAN2(M,L)
*
1     COSMU=COS(Z0)*COS(THETA)+SIN(Z0)*SIN(THETA)*COS(PHI-PHI0)
      MU=ACOS(COSMU)
      A=0.91+10.0*EXP(-3.0*MU)+0.45*(COSMU**2.0)
              IF (THETA.GE.1.57) THEN
                      B=1.0
                      GOTO 2
              ENDIF
      B=1.0-EXP(-0.32/COS(THETA))
2     C=0.274*(0.91+10.0*EXP(-3.0*Z0)+0.45*((COS(Z0))**2.0))
      LSKY(I,J)=LREF*A*B/C
*
* CALCULATE HORIZONTALLY & VERTICALLY POLARIZED FRACTIONS
* VIA PURE RAYLEIGH SCATTERING MODEL
*
      IF (MU.EQ.0.0) THEN
              PSI=0.0
              GOTO 3
      ENDIF
*
      COSMU2=COSMU**2
      COSNU=(SIN(THETA)*COS(Z0)-SIN(Z0)*COS(THETA)*COS(PHI-PHI0))/SIN(MU)
      PSI=0.94*((1.0-COSMU2)/(1.0+COSMU2))
3     H=(0.5*(1.0-PSI))+(PSI*(COSNU**2))
      HSKY(I,J)=LSKY(I,J)*H
      VSKY(I,J)=LSKY(I,J)*(1.0-H)
```

```
*
4       END DO
        END DO
*
        WRITE(*,*) 'LSKY = UNPOLARIZED SKYDOME ANGULAR RADIANCE DISTRIBUTION'
        IF (N.EQ.64) CALL ALPHA(LSKY,64)
        FNAME='LSKY.RAY'
        CALL PLT3DOUTPUT(FNAME,LSKY,N,P,Q)
***     CALL PLT3DFILE(LSKY,N)
*
        WRITE(*,*) 'HSKY = HORIZONTALLY_POLARIZED LSKY'
        IF (N.EQ.64) CALL ALPHA(HSKY,64)
        FNAME='HSKY.RAY'
        CALL PLT3DOUTPUT(FNAME,HSKY,N,P,Q)
***     CALL PLT3DFILE(HSKY,N)
*
        WRITE(*,*) 'VSKY = VERTICALLY_POLARIZED LSKY'
        IF (N.EQ.64) CALL ALPHA(VSKY,64)
        FNAME='VSKY.RAY'
        CALL PLT3DOUTPUT(FNAME,VSKY,N,P,Q)
***     CALL PLT3DFILE(VSKY,N)
*
        RETURN
        END


        SUBROUTINE SKYMAP(LREF,PHI0,Z0,THETA,N,P,Q,LSRF,HSRF,VSRF)
*
* CREATE UNPOLARIZED SKYDOME HEMISPHERICAL RADIANCE DISTRIBUTION
* IN SURFACE SLOPE COORDINATES (BETA,ALPHA) RELATIVE TO SENSOR
* RESOLVE HORIZONTALLY_ & VERTICALLY_POLARIZED RADIANCE COMPONENTS
*
* INPUT:
* LREF = REFERENCE RADIANCE MEASURED AT THE ZENITH POINT, LSKY(0,0) [UNIT]
* PHI0 = SUN AZIMUTH [DEG] [-180..+180]
* THETA = SENSOR AZIMUTH ANGLE [DEG] [0..+90]
* Z0   = SUN AZIMUTH ANGLE [DEG] [0..+90]
*
* OUTPUT:
* LSRF = LINEAR MAP OF LSKY TO SURFACE COORDINATES (ALPH,BETA)
* HSRF = LINEAR MAP OF HSKY TO SURFACE COORDINATES (ALPH,BETA)
* VSRF = LINEAR MAP OF VSKY TO SURFACE COORDINATES (ALPH,BETA)
*
        IMPLICIT NONE
        INTEGER I,J,N,P,Q
        REAL ALPH,BETA,COSOMEGA,DELTA,IV1,IV2,IV3,NV1,NV2,NV3,RV1,RV2,RV3,THET
        REAL LSRF(P:Q,P:Q),HSRF(P:Q,P:Q),VSRF(P:Q,P:Q)
        REAL A,B,C,COSMU,COSMU2,COSNU,H,L,LREF,M,MU,PHI,PHI0,PI,PSI,THETA,Z0
        CHARACTER*18 FNAME
*
        PI=3.14159
        DELTA=90.0/FLOAT(Q)
```

```
*
* IV1,IV2,IV3 ARE THE RESOLVED COMPONENTS OF THE SENSOR COORDINATE VECTOR
*
      IV1=SIND(THETA)*SIND(180.0)
      IV2=SIND(THETA)*COSD(180.0)
      IV3=COSD(THETA)
*
      DO I=P+1,Q
      DO J=P+1,Q
*
      L=FLOAT(I)*DELTA
      M=FLOAT(J)*DELTA
*
      BETA=SQRT((L**2)+(M**2))
*
      IF (BETA.GE.90.0) GOTO 4
*
      IF (BETA.GT.0.0) THEN
              ALPH=ATAN2D(M,L)
      ELSE
              ALPH=0.0
      ENDIF
*
*     NV1,NV2,NV3 ARE THE RESOLVED COMPONENTS OF THE SURFACE NORMAL VECTOR
*
      NV1=SIND(BETA)*SIND(ALPH)
      NV2=SIND(BETA)*COSD(ALPH)
      NV3=COSD(BETA)
*
* DOT PRODUCT OF IV & NV = |IV||NV|(COSOMEGA) = COSOMEGA
*
      COSOMEGA=(IV1*NV1)+(IV2*NV2)+(IV3*NV3)
*
* RV1,RV2,RV3 ARE THE RESOLVED COMPONENTS OF THE REFLECTED SKYDOME VECTOR
*
      RV1=(NV1*2.0*COSOMEGA)-IV1
      RV2=(NV2*2.0*COSOMEGA)-IV2
      RV3=(NV3*2.0*COSOMEGA)-IV3
*
      THET=ACOS(RV3)
*
      IF (THET.GT.0.0) THEN
              PHI=ATAN2(RV1,RV2)
      ELSE
              PHI=0.0
      ENDIF
*
              IF (THET.GT.PI/2.0) THEN
                      LSRF(I,J)=0.0
                      HSRF(I,J)=0.0
                      VSRF(I,J)=0.0
                      GOTO 4
```

```
                ENDIF
*
1           COSMU=COS(Z0)*COS(THET)+SIN(Z0)*SIN(THET)*COS(PHI-PHI0)
            MU=ACOS(COSMU)
            A=0.91+10.0*EXP(-3.0*MU)+0.45*(COSMU**2.0)
                IF (THET.GE.1.57) THEN
                    B=1.0
                    GOTO 2
                ENDIF
            B=1 0-EXP(-0.32/COS(THET))
2           C=0.274*(0.91+10.0*EXP(-3.0*Z0)+0.45*((COS(Z0))**2.0))
            LSRF(I,J)=LREF*A*B/C
*
* CALCULATE HORIZONTALLY & VERTICALLY POLARIZFD FRACTIONS
* VIA PURE RAYLEIGH SCATTERING MODEL
*
            IF (MU.EQ.0.0) THEN
                PSI=0.0
                GOTO 3
            ENDIF
*
            COSMU2=COSMU**2
            COSNU=(SIN(THET)*COS(Z0)-SIN(Z0)*COS(THET)*COS(PHI-PHI0))/SIN(MU)
            PSI=0.94*((1.0-COSMU2)/(1.0+COSMU2))
3           H=(0.5*(1.0-PSI))+(PSI*(COSNU**2))
            HSRF(I,J)=LSRF(I,J)*H
            VSRF(I,J)=LSRF(I,J)*(1.0-H)
*
4           END DO
            END DO
*
***         WRITE(*,*) 'LSRF = LSKY MAPPED TO SURFACE COORDINATES'
***         IF (N.EQ.64) CALL ALPHA(LSRF,64)
            FNAME='LSRF.RAY'
***         CALL PLT3DOUTPUT(FNAME,LSRF,N,P,Q)
***         CALL PLT3DFILE(LSRF,N)
*
            WRITE(*,*) 'HSRF = HSKY MAPPED TO SURFACE COORDINATES'
            IF (N.EQ.64) CALL ALPHA(HSRF,64)
            FNAME='HSRF.RAY'
            CALL PLT3DOUTPUT(FNAME,HSRF,N,P,Q)
***         CALL PLT3DFILE(HSRF,N)
*
            WRITE(*,*) 'VSRF = VSKY MAPPED TO SURFACE COORDINATES'
            IF (N.EQ.64) CALL ALPHA(VSRF,64)
            FNAME='VSRF.RAY'
            CALL PLT3DOUTPUT(FNAME,VSRF,N,P,Q)
***         CALL PLT3DFILE(VSRF,N)
*
            RETURN
            END
```

```
      SUBROUTINE SPREADVARY(K,V1950,F3,SPREAD_TOT)
      IMPLICIT NONE
      INTEGER I,J,N,P,Q
      REAL A,ANG1,DELTA,G,K
      REAL PI,SPREAD,SPRED0,SPRED1,SPRED2,SPRED3
      REAL SPREAD_TOT,V_FRIC,V_MIN,V1950,X2,Y2,Z
      REAL F3(0:179)
*
      A=1.0
      G=980.0
      PI=3.141593
      DELTA=PI/180.0
      SPREAD_TOT=0.0
*
      DO I=0,179
              ANG1=FLOAT(I)*DELTA
              SPRED0=COS(ANG1)**2
              SPRED1=(8.0/(3.0*PI))*(SPRED0**2)
              SPRED2=EXP((-1.0*(G**2))/(2.0*(K**2)*(V1950**4)))
              SPRED3=(1.0-(A/2.0)+(A*(SPRED0)))/PI
              SPREAD=(SPRED1*(1.0-SPRED2))+(SPRED3*SPRED2)
              SPREAD_TOT=SPREAD_TOT+SPREAD*DELTA
              F3(I)=SPREAD
      END DO
*
      RETURN
      END


      SUBROUTINE WGN_SPEC(W1,GWN,ISEED,N,P,Q)
*
* CREATE FREQUENCY DOMAIN REPRESENTATION OF WHITE GAUSSIAN NOISE
* OUTPUT:
* N*N COMPLEX MATRIX GWN(P:Q,P:Q) WHERE:
*       P=-N/2 AND Q=N/2-1
*       REAL(WGN(I,J)) VARIES FROM -1.0 TO +1.0
*       IMAG(WGN(I,J)) VARIES FROM -1.0 TO +1.0
*       MAG (WGN(I,J)  EQUALS +1.0 EVERYWHERE
*       PHS (WGN(I,J)  VARIES FROM -PI TO +PI
*
      IMPLICIT NONE
      INTEGER I,J,N,P,Q
      INTEGER*4 ISEED
      REAL VAR,X1,X2,Y1,Y2
      REAL W1(P:Q,P:Q)
      COMPLEX GWN(P:Q,P:Q)
*
      VAR=FLOAT(N*N)
*
* CREATE N*N REAL MATRIX W1(P:Q,P:Q) OF PSEUDORANDOM VALUES
*
```

```
      CALL WGN2D(N,VAR,ISEED,W1)
*
* INSERT W1 VALUES INTO REAL COMPONENTS OF N*N COMPLEX MATRIX GWN(P:Q,P:Q)
*
      DO I=P,Q
              DO J=P,Q
              GWN(I,J)=CMPLX(W1(I,J),0.0)
              END DO
      END DO
*
* FORWARD-FFT THE COMPLEX MATRIX GWN(P:Q,P:Q) INTO THE FREQUENCY DOMAIN
*
      CALL FFT2D(GWN,N,-1)
*
* NORMALIZE THE MAGNITUDE OF GWN(P:Q,P:Q)
*
      DO I=P,Q
              DO J=P,Q
              GWN(I,J)=GWN(I,J)/CABS(GWN(I,J))
              END DO
      END DO
*
      RETURN
      END


      SUBROUTINE WGN2D(N,VAR,ISEED,WAY)
      REAL WAY(N,N),VAR,SUM,TEMP,TVAR
      INTEGER I,J,K,N
      INTEGER*4 ISEED
*
      TVAR=SQRT(VAR)*1.414159
*
      DO I=1,N
              DO J=1,N
              SUM=0.0
                      DO K=1,6
                      TEMP = RAN (ISEED)
                      SUM = SUM + TEMP
                      END DO
              WAY(I,J)=TVAR*(SUM-3.0)
              END DO
      END DO
      RETURN
      END


      SUBROUTINE WIND(WIND_V,Z,V_FRIC,V250,V1000,V1250,V1950)
*
* OUTPUTS WIND VELOCITIES AT HEIGHTS 0 CM, 250 CM, 1250 CM, & 1950 CM
* ABOVE WATER SURFACE BASED ON INPUT WIND_VELOCITY MEASUREMENT AND MEASUREMENT
* HEIGHT ABOVE WATER SURFACE. AN HOMOGENEOUS WIND PROFILE IS ASSUMED.
```

```
*
* INPUTS:
* WIND_V = INPUT WIND_VELOCITY MEASUREMENT        [CM/SEC]
* Z      = MEASUREMENT HEIGHT ABOVE WATER SURFACE [CM]
* OUTPUTS:
* V_FRIC = WIND VELOCITY AT    0 CM               [CM/SEC]
* V250   = WIND VELOCITY AT  250 CM               [CM/SEC]
* V1000  = WIND VELOCITY AT 1000 CM               [CM/SEC]
* V1250  = WIND VELOCITY AT 1250 CM               [CM/SEC]
* V1950  = WIND VELOCITY AT 1950 CM               [CM/SEC]
*
      IMPLICIT NONE
      INTEGER I,J,N
      REAL RATIO,WIND_V,V_FRIC,V250,V1000,V1250,V1950,X(46,6),Y,Z,Z0
*
      OPEN(1,FILE='V_DATA.DAT',STATUS='OLD',ERR=5)
      DO I=1,46
      READ(1,*) (X(I,J),J=1,6)
      END DO
      CLOSE(1)
*
      IF (Z.EQ.1950.0) J=6
      IF (Z.EQ.1250.0) J=5
      IF (Z.EQ.1000.0) J=4
      IF (Z.EQ.250.0) J=3
      IF (Z.EQ.0.0) J=2
*
      DO I=1,46
      IF (X(I,J).GT.WIND_V) THEN
              RATIO=(WIND_V-X(I-1,J))/(X(I,J)-X(I-1,J))
              V_FRIC=X(I-1,2)+(RATIO*(X(I,2)-X(I-1,2)))
              GOTO 1
      ENDIF
      END DO
*
1     Z0=(0.684/V_FRIC)+(4.28E-5*(V_FRIC**2))-0.0443
      V250=(V_FRIC/0.4)*LOG(250.0/Z0)
      V1000=(V_FRIC/0.4)*LOG(1000.0/Z0)
      V1250=(V_FRIC/0.4)*LOG(1250.0/Z0)
      V1950=(V_FRIC/0.4)*LOG(1950.0/Z0)
*
      WRITE(*,*) 'V_FRIC = ',V_FRIC
      WRITE(*,*) 'V250   = ',V250
      WRITE(*,*) 'V1000  = ',V1000
      WRITE(*,*) 'V1250  = ',V1250
      WRITE(*,*) 'V1950  = ',V1950
*

      RETURN
5     WRITE(*,*) 'BAD FILE OPENING FOR V_DATA.DAT'
      END
```

[redacted]

Bibliography of key primary and secondary sources (extracted from 101 total references):

Primary Sources

Chapman, R.D. & G.B. Irani, "Errors in estimating slope spectra from wave images", in Applied Optics, 20(20), pp 3645-3652, 1981.

Kasevich, R.S., "Directional wave spectra from daylight scattering", in Journal of Geophysical Research, 80 (33), pp 4535-4541, 1975.

Pierson, W.J., Jr. & R.A. Stacy, "The elevation, slope, and curvature spectra of a wind roughened sea surface", NASA Contractor Report 2247, 1973.

Stilwell, D., Jr., "Directional energy spectra of the sea from photographs", in Journal of Geophysical Research, 74(8), pp 1974-1986, 1969.

Secondary Sources

CIE Technical Committee 4.2, "Standardization of luminance distribution on clear skies", in CIE Publication #22, Comission International de l'Eclairaze, Paris, 1973.

Cox, C.S. & W.H. Munk, "Measurement of the roughness of the sea surface from photographs of the sun's glitter", in Journal of the Optical Society of America, 44(11), pp 838-850, 1954a.

Cox, C.S. & W.H. Munk, "Statistics of the sea surface derived from sun glitter", in Journal of Marine Research, 13(2), pp 198-227, 1954b.

Goodell, J.B., "The appearance of the sea reflected sky", in Applied Optics, 10, pp 223-225, 1971.

Kinsman, B., Wind Waves: their generation and propagation on the ocean surface, Prentice Hall, Englewood Cliffs NJ, 1965.

Maul, G.A., Introduction To Satellite Oceanography, Martinus Nijhoff Publishers, Dordrecht Netherlands, 1985.

Plass, G.N., G.W. Kattawar & J.A. Guinn, Jr., "Radiance distribution over a ruffled sea: contributions from glitter, sky, and ocean", in Applied Optics, 15(12), pp 3161-3165, 1976.

Saunders, P.M., "Shadowing on the ocean and the existence of the horizon", in Journal of Geophysical Research, 72 (18), pp 4643-4649, 1967.

Stilwell, D., Jr. & R.D. Pilon, "Directional spectra of surface waves from photographs", in Journal of Geophysical Research, 79(9), pp 1277-1284, 1974.